UNIVERSITAT ROVIRA I VIRGILI
TEMPERATURE MODULATED GENOSENSOR FOR DETECTION OF CYSTIC FIBROSIS MUTATIONS
Hany Abdel Hady Abdel Rahman Nasef
ISBN:978-84-693-3386-0/DL:T.1002-2010

DOCTORAL THESIS

Hany Abdel Hady Abdel Rahman Nasef

Temperature Modulated Genosensor for Detection of Cystic Fibrosis mutations

Universitat Rovira I Virgili

Department of Chemical Engineering

UNIVERSITAT ROVIRA I VIRGILI
TEMPERATURE MODULATED GENOSENSOR FOR DETECTION OF CYSTIC FIBROSIS MUTATIONS
Hany Abdel Hady Abdel Rahman Nasef
ISBN:978-84-693-3386-0/DL:T.1002-2010

UNIVERSITAT ROVIRA I VIRGILI
TEMPERATURE MODULATED GENOSENSOR FOR DETECTION OF CYSTIC FIBROSIS MUTATIONS
Hany Abdel Hady Abdel Rahman Nasef
ISBN:978-84-693-3386-0/DL:T.1002-2010

Hany Abdel Hady Abdel Rahman Nasef

Temperature Modulated Genosensor for Detection of Cystic Fibrosis Mutations

DOCTORAL THESIS

Supervised by

Dr. Ciara K. O´Sullivan & Dr. Valerio Beni

Department of Chemical Engineering

UNIVERSITAT ROVIRA I VIRGILI

Tarragona

2010

UNIVERSITAT ROVIRA I VIRGILI
TEMPERATURE MODULATED GENOSENSOR FOR DETECTION OF CYSTIC FIBROSIS MUTATIONS
Hany Abdel Hady Abdel Rahman Nasef
ISBN:978-84-693-3386-0/DL:T.1002-2010

Department of Chemical Engineering
University of Rovira I Virgili,
Avinguda Països Catalans, 26
43007, Tarragona, Spain.
Tel: +34-977-558740/8722
Fax: +34-977-559621/8205

Dra. Ciara K. O´Sullivan i Dr. Valerio Beni,

CERTIFICO:

Que el present treball, titulat “Temperature Modulated Genosensor for Detection of Cystic Fibrosis mutations”, que presenta Hany Abdel Hady Abdel Rahman Nasef per a l’obtenció del títol de Doctor, ha estat realitzat sota la meva direcció al Departament Enginyeria Química d’aquesta universitat.

Tarragona,

Dra. Ciara K. O´Sullivan Dr. Valerio Beni

UNIVERSITAT ROVIRA I VIRGILI
TEMPERATURE MODULATED GENOSENSOR FOR DETECTION OF CYSTIC FIBROSIS MUTATIONS
Hany Abdel Hady Abdel Rahman Nasef
ISBN:978-84-693-3386-0/DL:T.1002-2010

Department of Chemical Engineering
University of Rovira i Virgili,
Avinguda Països Catalans, 26
43007, Tarragona, Spain.
Tel: +34-977-558740/8579
Fax: +34-977-559621/8205

Dr. Ciara K. O´Sullivan and Dr. Valerio Beni

Certify that:

The present work entitled with "Temperature Modulated Genosensor for Detection of Cystic Fibrosis mutations", presented by Hany Abdel Hady Abdel Rahman Nasef to obtain the degree of doctor by the University Rovira i Virgili, has been carried out under my supervision at the Chemical Engineering Departament.

Tarragona,

Dr. Ciara K. O´Sullivan Dr. Valerio Beni

UNIVERSITAT ROVIRA I VIRGILI
TEMPERATURE MODULATED GENOSENSOR FOR DETECTION OF CYSTIC FIBROSIS MUTATIONS
Hany Abdel Hady Abdel Rahman Nasef
ISBN:978-84-693-3386-0/DL:T.1002-2010

Acknowledgement

Al Hamdu to **ALLAH** in the beginning and end.

I would like to thank **Dr. Ciara K. O´Sullivan**, for suggesting the point of research, valuable and expert supervision and continuous advice. Also I would like to express my appreciation to **Dr.Valerio Beni** for his supervision and encouragement during the experimental work and preparation of the thesis.

I would like to thank **Dr.Cengiz Ozlap** and **Dr. Enric Llaudet** for their supervision and efforts during the early stages of the experimental work.

Also I will not forget to thank Ms. Barbara Vastenavond, Ms. Sira Duran and Ms. Nuria Juanpere for their sustenance in all administrative works.

Finally, I would like to thank **my wife; my kids** who have tolerate and provided much over the years including love and support to me. I would like also to thank **my family, specially my mother** for their support. I also extend my thanks and gratitude to the spirit of **my Father** who died during my work in my thesis and I hope God will make us together in heaven.

Special thanks to **NBG** and **BBG** group members, and all staff members of the department of chemical engineering, university of Rovira i Virgili, for their unique help and support. I would like to thank **URV** for the financial support (BRDI scholarship). And also the financial support from the Commission of the European Communities, specific RTD program ‘Isolation of fetal cells from maternal blood, SAFER, NEST-ADVENTURE 04977’.

Hany Nasef

UNIVERSITAT ROVIRA I VIRGILI
TEMPERATURE MODULATED GENOSENSOR FOR DETECTION OF CYSTIC FIBROSIS MUTATIONS
Hany Abdel Hady Abdel Rahman Nasef
ISBN:978-84-693-3386-0/DL:T.1002-2010

Resumen

La memoria de la tesis está organizada en 8 capítulos. Un resumen de cada capítulo se detalla a continuación.

El **Capítulo 1** es una Introducción, en la que se presenta el estado del arte así como los objetivos de la tesis.

En el **Capítulo 2** se describe el uso de la impedancia electroquímica a diferentes temperaturas para la discriminación de la mutación DF508 con respecto a la secuencia normal sin mutación. Las sondas de DNA (de 15 y 21 bases de longitud) fueron inmovilizadas en la superficie de los electrodos de oro y de la variación de la resistencia a la transferencia de carga (R_{ct}) fue medida en función de la hibridación. Para la detección se han utilizado dos tipos de secuencias diana: secuencias sintéticas 15 mer y dos análogos sintéticos de productos de PCR de 82 (mutante) y 85 (normal) bases. La hibridación con la secuencia corta resulto en una variaciones de R_{ct} muy específicas a la secuencia estudiada, con un factor de discriminación a temperatura ambiente de 5 veces cuando se comparó la respuesta obtenida con la secuencia totalmente complementaria con respecto a las no coincidentes. Sin embargo, en el caso de los productos de PCR sintéticos de cadena sencilla el factor de discriminación fue menor (1.5 veces). Por ellos, el efecto de la temperatura fue investigado como vía para mejorar la discriminación. El uso de lavados post-hibridación a temperatura elevada dio lugar a una mejora de 5 veces en el factor de discriminación. De esta manera, utilizando *array*s de electrodos inmovilizadas con sondas selectivas a las secuencias de tipo mutante y normal, se logró una detección inequívoca de la mutación DF508.

En el **Capítulo 3** se describe el uso del azul de metileno como indicador electroquímico en la discriminación de la mutación DF508 de fibrosis quística de secuencias normales en productos de PCR. En condiciones experimentales óptimas se obtuvo un factor de discriminación de 1.5 entre el tipo mutante y el normal. El ensayo propuesto es cuantitativo y lineal en el rango de 10 - 100 nM, exhibiendo un límite de detección (LOD) de 2.64 nM. Estudios electroquímicos en distintas condiciones de fuerza iónica permitió elucidar el mecanismo de la interacción de azul de metileno con

ISBN:978-84-693-3386-0/DL:T.1002-2010

el DNA y, al parecer, este es el primer reporte sobre la detección de hibridación a través de la interacción guanina específica del MB con de DNA, a diferencia de la interacción electrostática como quedó demostrado en el estudio de la fuerza iónica. La introducción de formamida en el tampón de hibridación para mejorar la discriminación también fue investigada. Por último, a una concentración de 10 nM, la secuencia mutante fue efectivamente discriminada respecto de la normal ajustando los parámetros de configuración de un multi-sensor.

El **Capítulo 4** presenta un biosensor electroquímico basado en la discriminación de la mutación DF508 de fibrosis quística de secuencias normales en productos de PCR sintéticos. Para ello se empleo una sonda tipo faro molecular de 34 pares de bases complementaria a la mutación DF508 inmovilizada en la superficie de un electrodo de oro y azul de metileno como indicador electroquímico, el cual interacciona con el extremo 5' del faro molecular. La inmovilización del faro molecular en la superficie del electrodo de oro se logró a través un derivado tiolado en el extremo 3' para formar un enlace S-Au en la superficie del electrodo. El efecto de diferentes tipos de tampón (PBS, PBS-T, CSE, HEPES y Trizma) fue investigado. Dos mecanismos de inmovilización fueron examinados en este trabajo: co-inmovilización e inmovilización en dos etapas ("*backfilling*") con el objetivo de determinar el procedimiento que más tarde sería mejor para la estabilidad de la sonda. También se estudió la temperatura de fusión de la sonda obteniéndose un valor de 31.5ºC, lo cual asegura la estabilidad de la sonda a temperatura ambiente. El tiempo optimo del proceso de hibridación fue de 20 minutos, lo cual segura un ensayo rápido. En condiciones experimentales óptimas se obtuvo un factor de discriminación de 2.5 entre la secuencia mutante y la normal.

En el **Capítulo 5** se presenta un método para la determinación precisa de la temperatura de fusión (T_m) de secuencias de DNA de doble hebra inmovilizadas que explota las propiedades de extinción de fluorescencia de superficies de oro. Para ello se empleo una sonda de DNA de cadena simple tiolada quimisorbida en la superficie de oro que se híbrida a una secuencia complementaria marcada con un fluoróforo. Tras la formación del dúplex, la fluorescencia de la etiqueta se extingue de manera efectiva por la superficie de oro. Al aumentar la temperatura y deshibridarse el dúplex, el fluoróforo se mueve lejos de la superficie del oro y la señal de fluorescencia se recupera de nuevo. De esta manera el aumento de la fluorescencia se mide cuando temperatura se eleva

ISBN:978-84-693-3386-0/DL:T.1002-2010

progresivamente y graficando la primera derivada de la variación e fluorescencia con respecto a la temperatura se determina T_m. Para demostrar este el enfoque, los valores de T_m de secuencias relacionadas a la mutación DF508 se determinaron en tres formatos: en disolución, inmovilizados en nanopartículas de oro (Au-NPs) y en chips de oro (Au-chips).

En el **Capítulo 6** se introduce una propuesta de discriminación de la mutación DF508 basada en la modificación del DNA a determinar con la etiqueta redox. Para ello se preparó un conjugado de ferroceno con la secuencia mutante (Mut-Fc) que se hibrida con dos posibles secuencias complementarias inmovilizadas en una superficie de oro, una con complementaridad total y otra conteniendo 3 bases no coincidentes. Las diferencias en las señales del ferroceno entre los dos métodos de hibridación se han mejorado estudiando las variaciones de la temperatura de fusión, obteniéndose alrededor de 8 ºC de diferencia en los valores de T_m entre ambas secuencias. La mejor discriminación se obtuvo a 40 ºC, en la que la sonda respecto a la secuencia normal dio una respuesta cercana a cero. Este resultado indica que es posible etiquetar las sondas de PCR con ferroceno con el fin de obtener muestras de DNA real marcadas, lo cual haría posible distinguir entre secuencias mutantes y normales mediante medidas de la temperatura de fusión.

En **Capítulo 7** se discute un ensayo basado en mediciones de temperatura de fusión empleando azul de metileno como indicador electroquímico en la discriminación de la mutación DF508 de fibrosis quística de secuencias normales en productos de PCR sintéticos. La sonda complementaria mutante inmovilizada en la superficie de electrodos de oro resultó ser térmicamente estable hasta 70 ºC. La influencia de la fuerza iónica sobre la estabilidad del sistema también se estudió, siendo 0.5 M la concentración de NaCl óptima. El factor de discriminación entre las secuencias de tipo mutante y normal mejoró de 1.1 a 27 ºC hasta 4.26 a 55 ºC. El valor calculado de la temperatura de fusión del dúplex mutante con la secuencia complementaria inmovilizada sobre la superficie del electrodo de oro estuvo de acuerdo con la ecuación de Wallace. El efecto en la estabilidad de dúplex en términos de temperatura de fusión de secuencias laterales situadas en el mutante también fue investigado.

UNIVERSITAT ROVIRA I VIRGILI
TEMPERATURE MODULATED GENOSENSOR FOR DETECTION OF CYSTIC FIBROSIS MUTATIONS
Hany Abdel Hady Abdel Rahman Nasef
ISBN:978-84-693-3386-0/DL:T.1002-2010

Finalmente, en el **Capítulo 8** se presentan las conclusiones principales del trabajo de esta tesis y el trabajo futuro.

UNIVERSITAT ROVIRA I VIRGILI
TEMPERATURE MODULATED GENOSENSOR FOR DETECTION OF CYSTIC FIBROSIS MUTATIONS
Hany Abdel Hady Abdel Rahman Nasef
ISBN:978-84-693-3386-0/DL:T.1002-2010

Summary

Specifically outlining the work achieved in this PhD thesis, the work is organised into separated chapters.

Chapter 1 is an introduction, in which the state of the art and objectives are presented.

In **Chapter 2**, the use of temperature assisted electrochemical impedance spectroscopy for the discrimination of the DF508 mutation from the wild type sequence is illustrated. DNA probe (15 and 21 bases long) were immobilised onto the surface of gold electrodes and the variation of the charge-transfer resistance (R_{CT}) monitored as a function of the hybridisation. Two sets of targets have been used in this work: synthetic 15 mer sequences and two single stranded synthetic analogues of PCR products of 82 (Mutant) and 85 (Wild type) bases long. Hybridisation with short targets resulted in a sequence specific charge-transfer resistance variation with a discrimination factor at room temperature, between fully complementary and mismatched sequence, of ca. 5-fold. However in the case of the single stranded synthetic PCR product analogues a lower discrimination factor was recorded (1.5 fold). Temperature was investigated to improve discrimination; the use of a post-hybridisation wash at elevated temperature resulted in a 5-fold improvement in the discrimination factor. Using an electrode array with probes immobilised against each of mutant and wild type sequences, an unequivocal detection of the DF508 mutation was achieved.

In **Chapter 3**, the use of methylene blue as an electrochemical reporting agent, in the discrimination of synthetic PCR analogue of the DF508 cystic fibrosis mutation (Mut) from the wild type (Wt) is reported. Using optimum experimental conditions a discrimination factor, between mutant and wild type of ca. 1.5 fold was found. The proposed assay was quantitative and linear in the range of 10 – 100 nM, exhibiting a limit of detection (LOD) of 2.64 nM. Electrochemical studies at variable ionic strength conditions allowed further elucidation of the mechanism of the methylene blue-DNA interaction. To the best of our knowledge, this is the first report of detection of hybridisation specifically through the guanine specific MB-DNA interaction

ISBN:978-84-693-3386-0/DL:T.1002-2010

simultaneously in MB solution, eliminating electrostatic interaction as was demonstrated in the ionic strength study. The introduction of formamide in the hybridization buffer, to improve discrimination, was also investigated. Finally mutant versus wild type discrimination was demonstrated, at 10 nM concentration, with the use of a multi-electrode sensor setup.

In **Chapter 4** we present an electrochemical based biosensor for the discrimination between synthetic PCR analogue cystic fibrosis DF508 mutant and the corresponding wild type based on the use of molecular beacons. A 34 bp molecular beacon probe, complementary to the DF508 mutant sequences in 18 bp length of the loop region of the beacon, was immobilized on a gold electrode surface. The electrochemical reporter employed in this work is methylene blue which attached in the 5`-end of the molecular beacon. The immobilization of the beacon probe on the gold electrode surface was achieved via the thiolated 3`-end to form S-Au bond. The effect of different buffer types (PBS, PBS-T, SSC, HEPES and Trizma) was investigated. Two immobilization mechanisms were examined in this work namely “backfilling” and “co-immobilization”, where the latter procedure was demonstrated to be better for the probe stability and reported signal on the electrode surface. Furthermore, the melting temperature was studied for the immobilized beacon probe and a value of 31.5ºC was obtained, assuring the probe stability at room temperature. The hybridisation process was found to be achieved in a relatively short time (20 minutes), and a good discrimination factor of ca. 2.5 was achieved for the differentiation between Df508 mutant and the corresponding wild type amplicons.

In **Chapter 5**, a method for the accurate determination of the melting temperature (Tm) of surface immobilised DNA duplexes, which exploits the fluorescence quenching properties of gold, is reported. A thiolated ssDNA probe is chemisorbed onto a gold surface, and then hybridized to a fluorophore labelled complementary sequence. Upon formation of the duplex, the fluorescence of the label is effectively quenched by the gold surface. As the temperature is increased and the duplex dehybridises, the fluorophore label moves away from the gold surface and the fluorescence signal is again observed. The increase in fluorescence is measured as the temperature is ramped and using first derivative plots, the Tm determined. To demonstrate the approach, the Tm of the Cystic Fibrosis DF508 mutation is determined

ISBN:978-84-693-3386-0/DL:T.1002-2010

in free solution and on two gold surface formats - gold nanoparticles (Au-NPs) and planar thin-film gold chips (Au-chips).

In **Chapter 6**, an approach for the discrimination of mutant from wild type using electrochemical melting curve analysis is presented. An oligonucleotide-ferrocene conjugate (Mut-Fc) was hybridised in optimum solution conditions to an immobilized complementary (or 3 mismatched, representing the wild type complementary) probe on the gold electrode surface. Electrochemical melting curve analysis elucidated an 8 degrees difference in Tm values between mutant (Fc)-mutant probe and mutant (Fc)-wild type probe three mismatched duplexes. A better discrimination was demonstrated at 40 ºC where the wild type probe duplex signal was nearly zero. Using this approach, primers used in PCR amplification can be labelled with ferrocene, facilitating a facile approach for differentiation between wild type and mutant targets.

In **Chapter 7**, electrochemical melting curve analysis employing methylene blue as an electroactive indicator for the discrimination of synthetic PCR analogues of the DF508 cystic fibrosis mutation (Mut) from the wild type (Wt) is discussed. The immobilized mutant complementary probe on the gold electrode surface was shown to be thermally stable up to 70 ºC. The ionic strength influence on the system stability was also investigated and 0.5 M NaCl was demonstrated to be the optimum salt concentration. The discrimination between mutant and wild type amplicons was improved via increasing in temperature, from ca. 1.1 at 27 ºC up to 4.26 at 55ºC. The calculated melting temperature value of the mutant amplicon duplex with a complementary probe on the gold electrode surface was in agreement with Wallace equation.

Chapter 8 outlines the main discussion and conclusions of the thesis work.

ISBN:978-84-693-3386-0/DL:T.1002-2010

List of Publications:

A- Journal papers:

1- " Methylene blue as an electrochemical indicator for DF508 cystic fibrosis mutation detection"
Hany Nasef, V. Beni, C.K. O'Sullivan, Analytical and Bioanalytical Chemistry, DOI 10.1007/s00216-009-3369-5 (2009).

2- "Cystic Fibrosis: a label-free detection approach based on thermally modulated Electrochemical Impedance Spectroscopy"
Hany Nasef, V. Beni, Vali C. Ozlap, C.K. O'Sullivan, Analytical and Bioanalytical Chemistry, DOI: 10.1007/s00216-010-3489-y (2010).

3- " Melting Temperature of Surface-tethered DNA"
Hany Nasef, Vali C. Ozlap, C.K. O'Sullivan, Analytical Biochemistry, Submitted.

4- " Electrochemical Melting Curve Analysis "
Hany Nasef , V. Beni, C.K. O'Sullivan, Analytical letters, Submitted.

5- " Labelless Electrochemical Melting Curve Analysis for Rapid Detection of Mutations"
Hany Nasef, V. Beni, C.K. O'Sullivan, Analytical Methods, Submitted.

6- " Electrochemical molecular beacon based DNA biosensor for the discrimination of Cystic fibrosis mutations"
Hany Nasef, V. Beni, C.K. O'Sullivan, under preparation.

B- Conferences:

1- "Biosensor for cystic fibrosis mutant determination" - 5th PhD Poster Exhibition day, Tarragona, Spain, 20th Oct.,2006.

2- "Electrochemical Impedance: possible tool for cystic fibrosis pre-natal screening" - 1st International Symposium on Electrochemistry, July 2008, University of the Western Cape, Bellville, South Africa.

3- "Cystic Fibrosis: development of an Electrochemical Impedance Spectroscopy based screening tool" - The 59th Annual Meeting of the International Society of Electrochemistry, September 2008, Seville, Spain.

4- " Methylene blue as an Indicator for Electrochemical Quantification of DF508 Cystic Fibrosis mutation on gold electrodes" -7th PhD Poster Exhibition day, Tarragona, Spain, 21th Abril.,2009.

5- "DF508 Cystic fibrosis Determination via Methylene blue Electrochemistry" -XIV Trobada Transferontera on SENSORS and BIOSENSORS, Banyuls Sur Mer-France 24-25 septembre /setembre 2009

UNIVERSITAT ROVIRA I VIRGILI
TEMPERATURE MODULATED GENOSENSOR FOR DETECTION OF CYSTIC FIBROSIS MUTATIONS
Hany Abdel Hady Abdel Rahman Nasef
ISBN:978-84-693-3386-0/DL:T.1002-2010

List of figures

ISBN:978-84-693-3386-0/DL:T.1002-2010

UNIVERSITAT ROVIRA I VIRGILI
TEMPERATURE MODULATED GENOSENSOR FOR DETECTION OF CYSTIC FIBROSIS MUTATIONS
Hany Abdel Hady Abdel Rahman Nasef
ISBN:978-84-693-3386-0/DL:T.1002-2010

List of Tables

ISBN:978-84-693-3386-0/DL:T.1002-2010

List of Abbreviations:

A: Adenine.
C: Cytosine.
CF: cystic fibrosis.
CFTR: cystic fibrosis transmembrane conductance regulator.
(CG%): Cytosine and Guanine content.
CV: Cyclic voltammetry.
DNA: Deoxyribonucleic acid.
DPV: Differential pulse voltammetry.
dsDNA: Double strand DNA.
EIS: Electrochemical impedance spectroscopy.
G: Guanine.
$\mathbf{I_{mut\ (or\ wt)}}$**:** the current peak height of the surface duplex of mutant (or wild type)
$\mathbf{I_{reg}}$**:** the current peak height corresponding to the regenerated electrode surface.
LOD: limit of detection.
MAPH: Multiplex amplification and probe hybridisation.
MB: methylene blue.
MCH: mercaptohexanol.
Mut ampl: DF508 Cystic fibrosis mutation amplicon.
Mut-Fc: Mutant ferrocene conjugate.
PBS: Phosphate buffer saline.
PBS-T: Phosphate buffer saline - Tween.
PCR: polymerase chain reaction.
Pt: Platinum wire, counter electrode.
Rct: Charge transfer resistance.
RU: Resonance unites.
SAM: Self assembly monolayer.
SPR: Surface plasmon resonance.
SSC: Saline Sodium citrate buffer.
ssDNA: Single strand DNA.
T: Thymine.
Tm: Melting temperature.
Wt ampl: cystic fibrosis wild type amplicon.

UNIVERSITAT ROVIRA I VIRGILI
TEMPERATURE MODULATED GENOSENSOR FOR DETECTION OF CYSTIC FIBROSIS MUTATIONS
Hany Abdel Hady Abdel Rahman Nasef
ISBN:978-84-693-3386-0/DL:T.1002-2010

Table of Contents

UNIVERSITAT ROVIRA I VIRGILI
TEMPERATURE MODULATED GENOSENSOR FOR DETECTION OF CYSTIC FIBROSIS MUTATIONS
Hany Abdel Hady Abdel Rahman Nasef
ISBN:978-84-693-3386-0/DL:T.1002-2010

CHAPTER 1:

General Introduction

UNIVERSITAT ROVIRA I VIRGILI
TEMPERATURE MODULATED GENOSENSOR FOR DETECTION OF CYSTIC FIBROSIS MUTATIONS
Hany Abdel Hady Abdel Rahman Nasef
ISBN:978-84-693-3386-0/DL:T.1002-2010

1. Introduction

1.1. DNA:

In 1953, Watson and Crick discovered the structure of the deoxyribonucleic acid, commonly known as DNA [1]. DNA is a chemical polymer present in living cells and contains the genetic instructions (genes) responsible for the development and functioning of living organisms [2]. DNA is a strand consisting of repetitive building blocks called nucleotides [3,4]. Each nucleotide consists of a ribose sugar and phosphate, which represent the strand backbone, and one of four different nitrogenous base units (Figure 1) [3]. These bases are adenine (A), guanine (G), thymine (T) and cytosine (C), and based on the chemical structure, they can be classified into purines (double heterocyclic rings) including A and G bases, and pyrimidines (single heterocyclic ring) including T and C bases [5]. The double stranded DNA (dsDNA) is formed via hydrogen bonds between two bases, one in each of the double strands, where adenine always combines with thymine and guanine with cytosine [6,7]. The dsDNA length, which is as long as 220 million base pairs within the largest human chromosome, chromosome number 1 [8], could be a reason for the structural stability of the double strands, taking into consideration that hydrogen bonding is quite a weak bond as compared to covalent bonding.

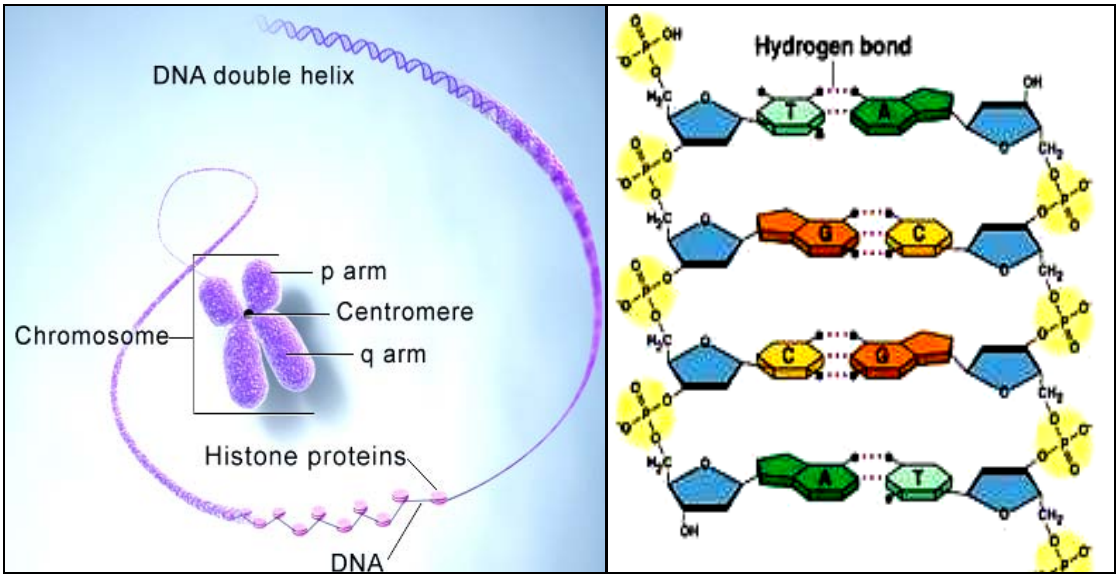

Figure 1.1 DNA location in chromosome (right) and the DNA, double stranded structure, illustrating the different bases combined via H-bonding (left). (ref [9])

ISBN:978-84-693-3386-0/DL:T.1002-2010

1.1.1. The Central Dogma of Molecular Biology

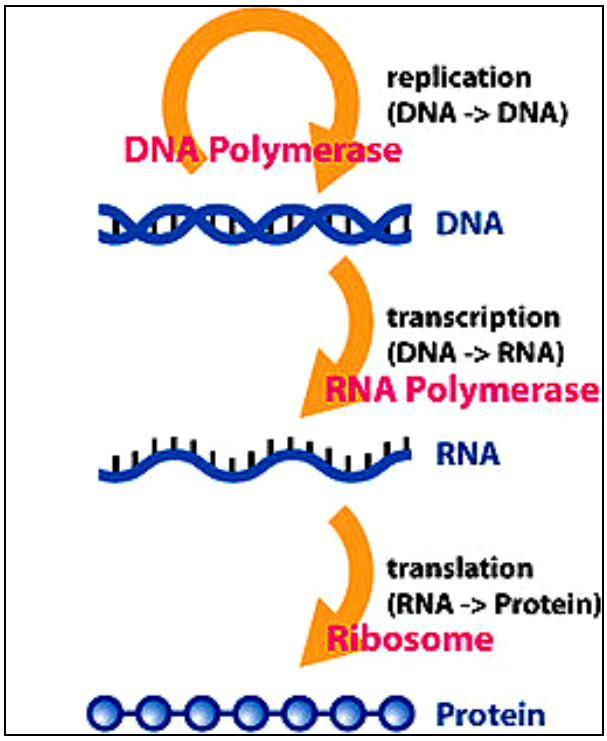

Figure 1.2. Central Dogma of molecular biology. (ref [10])

The most important function of DNA is the production of proteins through a cycle discovered known as the central dogma of molecular biology. In this process, segments of DNA transcribes to consecutive segments of messenger ribonucleic acid (m-RNA) via certain enzymes, and the mRNA is later translated into protein [11] as illustrated in Figure 1.2. RNA is similar to DNA except the thymine bases are replaced by uracil bases in the RNA strands; additionally RNA is single stranded and does not form the double stranded helical structure like DNA.

1.1.2. DNA mutations

Every three base (codon) transcript in DNA, corresponds to one amino acid in the translated polypeptide (protein). Any change (mutation) in the DNA sequence will be reflected as a change in the translated protein and may be manifested as a disease. Ultraviolet and X-rays, as well as some oxidizing and alkylating agents can damage (mutate) DNA [12-15].

ISBN:978-84-693-3386-0/DL:T.1002-2010

There are many types of DNA mutations, such as [16-18]: (1) Missense mutation: an exchange of a single nucleotide for another, (2) Insertion mutation: an addition of one or more extra nucleotides into the DNA sequence, (3) Deletion mutation: due to failure of the replication process or other genetic damage, resulting in the removal of one or more nucleotides from the DNA sequence, (4) Duplication mutation: caused through replication errors, where a gene or group of genes may be copied more than one time within a chromosome and (5) Inversion mutation: in which, segments of DNA are released from a chromosome and then re-inserted in the opposite orientation.

There are many diseases resulting from the DNA mutation. For example, sickle-cell disease is common in Africa and Mediterranean area and resulting from a missense mutation by the replacement of A by T in the haemoglobin beta chain gene which produces a polypeptide chain containing a valine amino acid instead of glutamic acid in the corresponding translated codon [19]. When both parents are carriers for one mutated gene the possibility to have a child with sickle-cell disease is one to four [19]. The spherical shape of nearly half of the circulating red blood cells are changed into a sickle shape resulting in invasive infections, acute chest syndrome, and severely affect the spleen and also results in other painful complications [20]. Another example is Huntington`s disease, produced by an unstable expansion in the CAG repeats number in the IT15 gene, which is responsible for the production of Huntingtin protein [21]. The resulting abnormal protein is responsible for the increase in the p53 protein levels in brain cells and their death by apoptosis.

1.1.3. Polymerase chain reaction (PCR) and (MAPH):

The polymerase chain reaction is the well known process for the amplification of minute amounts of DNA. Since its discovery by Kerry Mullis in 1983 [22], PCR has been commonly employed method for in vitro selective amplification of particular DNA or RNA sequences. RNA is amplified through synthesis of a DNA copy employing the enzyme reverse transcriptase prior to PCR [23]. Through PCR it is possible to obtain more than 100 billions copies of a single DNA sequence from less than 10ng of starting material in a short time [22]. PCR is an enzyme dependent technique, in which the enzyme Taq polymerase is employed in building the DNA molecule bases in a specific area, defined via attachment of specific primers to the DNA strand.

ISBN:978-84-693-3386-0/DL:T.1002-2010

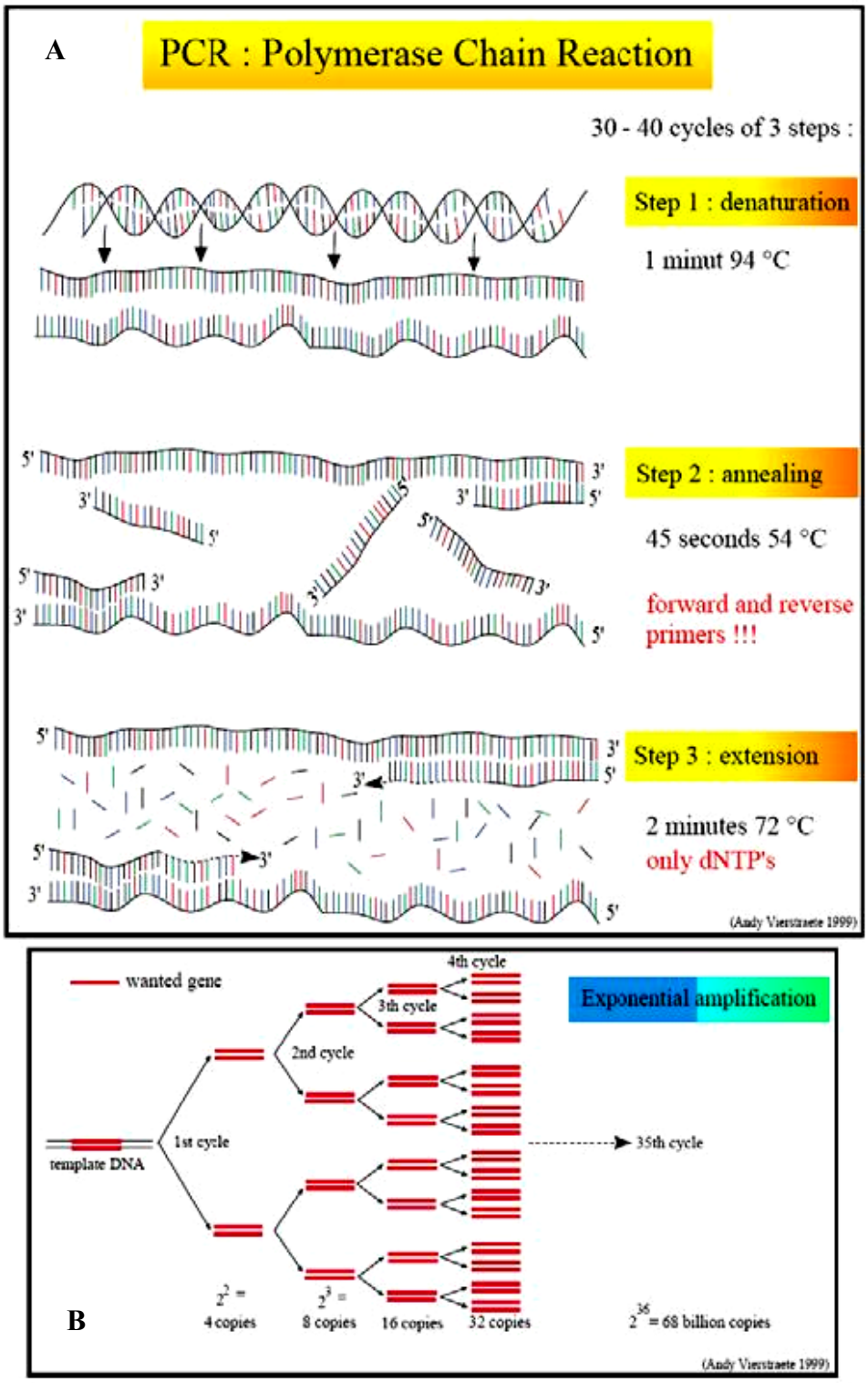

Figure 1.3. Polymerase chain reaction protocol (A) and the exponential amplification of DNA molecule (B). (Ref.[24])

ISBN:978-84-693-3386-0/DL:T.1002-2010

As illustrated in Figure 1.3, PCR consists of three main steps in each amplification cycle: (1) denaturation of the double stranded DNA in to two single strands by heating the sample mixture to 95-100 ºC, (2) primers annealing, where primers are short single stranded nucleotides (oligonucleotides) complementary to specific regions in the original DNA strand and (3) sequence extension, using the Taq polymerase enzyme to continue building the new strand starting from the primer attachment end position. This cycle is repeated including the new produced DNA strands resulting in exponential amplification of the original DNA template.

A new amplification PCR based technique was introduced by John Armour el al., in 2000 for the multiplexed amplification of several DNA targets in one single amplification reaction, namely *multiplex amplifiable probe hybridization (MAPH).* As illustrated in Figure 1.4, this method consists of three main steps [25,26]: (1) hybridisation between certain selective prepared probes (to the target sequences under investigation) and a genomic DNA fixed to a membrane and left overnight in order to assure complete hybridisation (2) the membrane is then washed carefully and vigorously to remove all the unbound probes, and the bound DNA is stripped from the membrane and (3) PCR amplification is carried out on this DNA, and the products are separated via electrophoresis.

The advantage of MAPH over conventional PCR is the possibility of the simultaneous analysis of a large number of loci. On the other hand, the washing step employed in the MAPH procedure could be a source of contamination [25].

ISBN:978-84-693-3386-0/DL:T.1002-2010

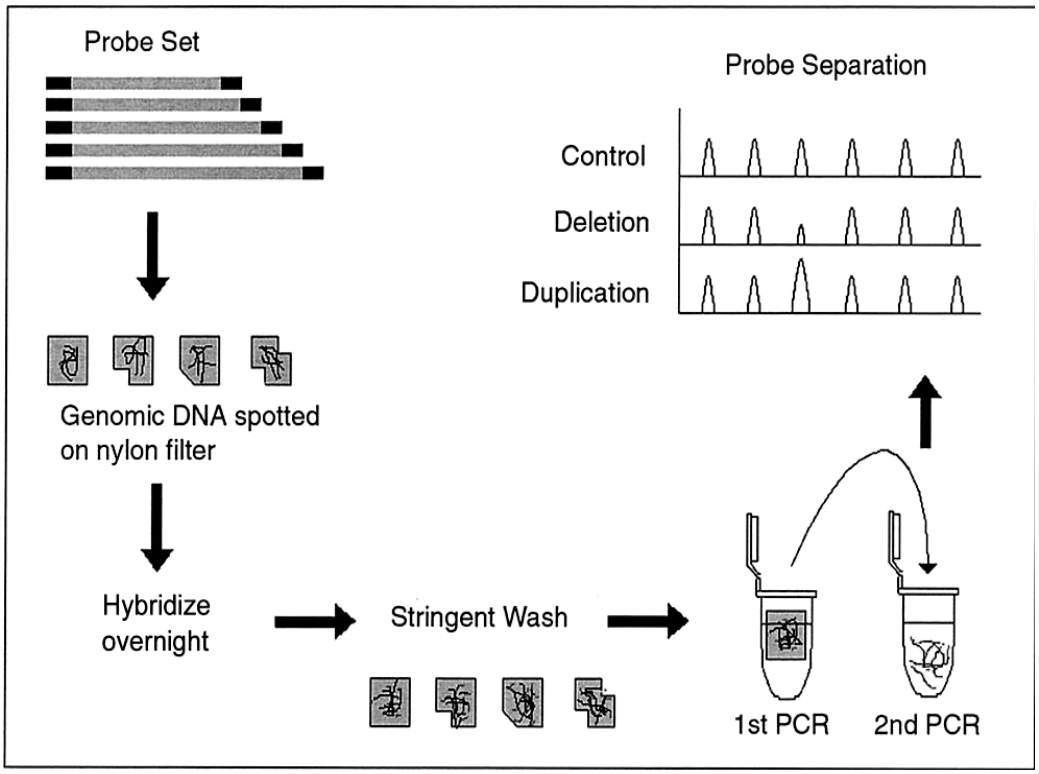

Figure 1.4. General principle of MAPH. Probes are prepared such that all can be amplified with one primer pair. After overnight hybridization to immobilized genomic DNA, stringent washing was applied to eliminate unbound DNA. Changes in peak heights correspond to copy-number changes (i.e., deletions and duplications). (ref.[25])

1.2. Cystic Fibrosis:

Cystic fibrosis (CF) is an inherited disease that affects most of the entire human body organs and results in an early death in most cases. This disease was discovered by Dorothy Andersen in 1938 [27], where she studied the pancreatic, lungs and intestine symptoms and characteristics. Andersen was the first to establish that CF is a recessive disease [27]. The sweat test, which is a routine test for diagnosis of CF was initially highlighted by Agnese in 1952 [28]. Riordan et al., discovered the DF508 cystic fibrosis mutation and also the gene responsible for the disease [29].

CF is the most common genetic disorder existing in the European population [29-35], where one in twenty-two persons have one affected gene with CF, and in all Caucasians, one in 2500 live births are affected. In North America, specifically in USA, the ratio of CF incidence is one in 3900 born infants, and CF carriers represent 4% of the population.

ISBN:978-84-693-3386-0/DL:T.1002-2010

1.2.1. Cystic fibrosis symptoms:

As outlined previously, cystic fibrosis is a disease responsible for a defect in chloride transport in the epithelium, and as a result it causes damage in the lung, pancreas and other concerning organs, resulting in early death in most cases [29-36]. Figure 1.5 depicts the organs could be affected by CF. The CF symptoms developed in the lungs are due to the thick mucus accumulation in the airways which cause inflammation. This media is suitable for the growth of bacteria and inflammation may result in pneumonia and coughing up of blood. Due to these serious problems with the lungs, it is hard to supply the body with sufficient oxygen, resulting in hypoxia. Additional respiratory supports, such as bi-level positive airway pressure machines or ventilators, are essential in the development stages of the lung damage [37]. In severe cases, lung transplantation may be necessary.

As a consequence, the lung disorder has an impact on thickening the pancreatic juice, which contains the necessary enzymes, supplied to the small intestine through the duodenum, for food digestion. The retardation in the movement of the pancreatic juice due to its high viscosity often leads to an onset of pancreatitis, which is an inflammation in pancreas [38]. Other complications as a result of the deficiency of the digested nutrients include malabsorption and poor growth. Individuals with such conditions require external supplementary vitamins and essential nutrients. Patients could develop weakened bones as a result of vitamin D deficiency due to malabsorption and be more prone to fractures [39]. Certain type of diabetes are also related to CF, namely, Cystic Fibrosis Related Diabetes (CFRD), which results from pancreas damage leading to a deficiency in insulin hormone levels, which is secreted from the islets of Langerhans located in pancreas [40].

Similarly, the liver is affected by the formation of the thick bile secretions, which can block the bile ducts and cause liver damage [41,42]. The development of liver cirrhoses will affect the important functions of the liver, critical to correct body functioning, such as detoxification and blood proteins production.

ISBN:978-84-693-3386-0/DL:T.1002-2010

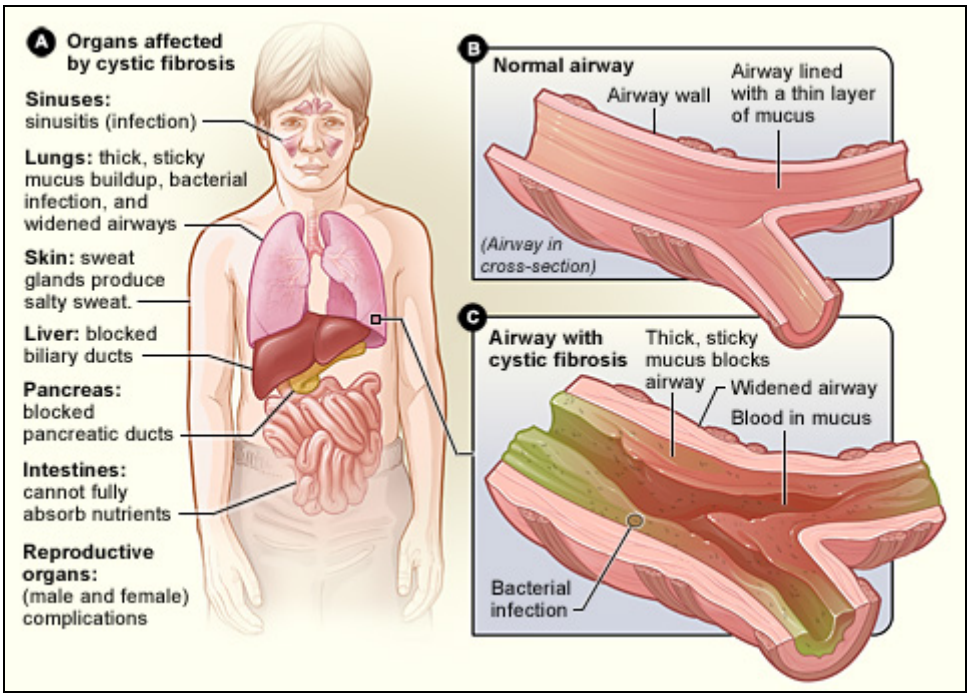

Figure 1.5. The organs affected by Cystic fibrosis (A), a cross section in a normal airway (B) and a cross section in an airway affected with cystic fibrosis. (ref.[43])

1.2.2. Cystic fibrosis mutations:

Cystic fibrosis is expressed when both genes are mutated [27] in chromosome 7, and CF is thus considered an autosomal recessive disease (Figure 1.6). The CF gene susceptible to mutation is called the Cystic fibrosis transmembrane conductance regulator gene (CFTR). The translated protein is responsible for the formation of the chloride channel (Figure 1.7), which is necessary for chloride ion transportation to many organs such as pancreas, lungs, sweat glands, intestine and kidneys [29,33].

In Figure 1.7, the structure of the chloride ion channel (translated 1480 amino acid protein from CFTR gene) is illustrated [44,45]. This channel consists of two symmetrical halves, where in each half, there are six membrane-spanning segments and a nucleotide-binding domain and both halves are joined together via a cytoplasmic regulatory domain (R-domain) [32]. The protein mass distributed within the cell membrane in away that 77% of the protein is in the cytoplasm, 19% in membrane spanning segments, and 4% in extracellular loops [44].

ISBN:978-84-693-3386-0/DL:T.1002-2010

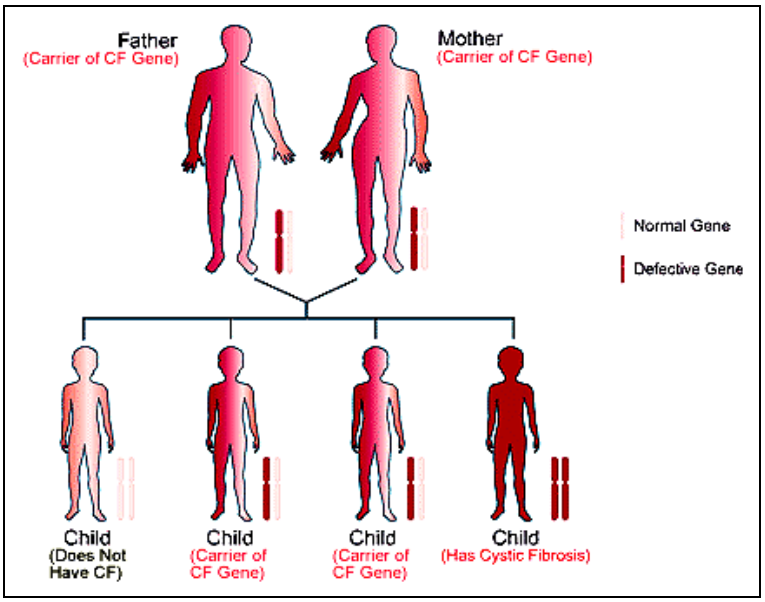

Figure1.6. The inheritance of Cystic fibrosis. (ref.[46])

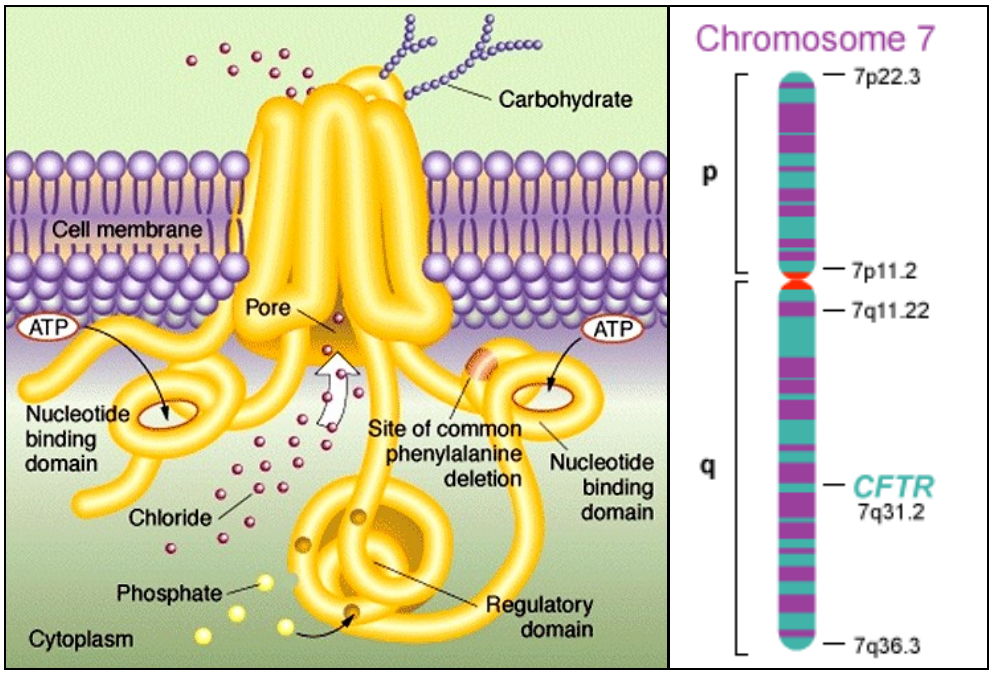

Figure 1.7. The cystic fibrosis transmembrane conductance regulator gene (right) and the produced CFTR protein (left). (ref.[47]

More than 1,000 mutations have been identified in the CF gene, but a few common mutations cause disease in most patients (figure 1.8). Mutations have been divided into six classes based mainly on the molecular fate of CFTR [31]. DF508 is the most common

ISBN:978-84-693-3386-0/DL:T.1002-2010

mutation in which there is a deletion of phenylalanine at position 508 in the amino acid sequence of CFTR (DF508). However, its frequency varies between ethnic groups, accounting for 70 per cent of all cystic fibrosis mutations in the white populations of Britain and US but fewer than 50 per cent in southern European populations. CFTR mutations are correlated with disease severity [48].

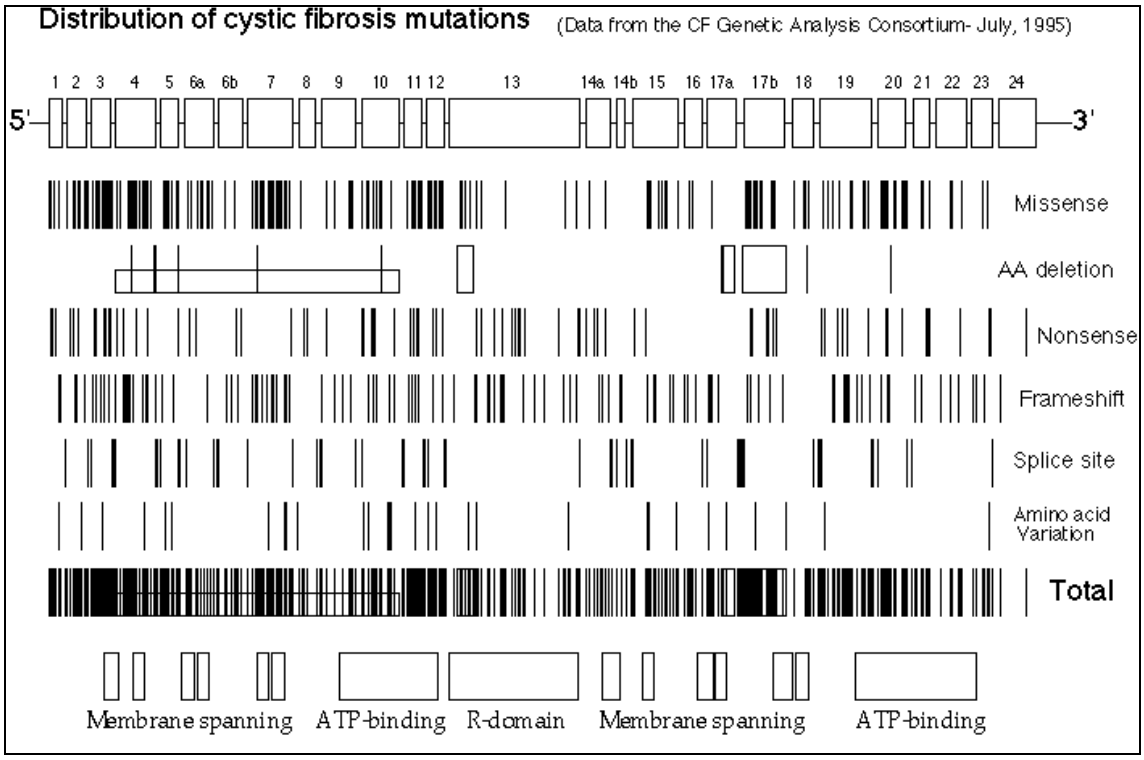

Figure 1.8. Different types of genetic mutations included in cystic fibrosis (ref.[49])

1.2.3. Cystic fibrosis diagnosis and treatment:

Since the discovery of the distinguishable salty character of the skin sweat belonging to individuals suffering from CF [28], it has been employed as a routine test for diagnosis of CF disease [50]. Another specific diagnosis method is the chemical analysis of immunoreactive trypsinogen compound [51], which has high blood levels in the newborn babies suffering from CF. This analysis is achieved through blood test screening in the sixth day after birth. Other important technique is genetic testing [52] where genetic analysis is applied to some blood cells or cells scraped from the internal cheek. The advantage of this test is that it could be used for screening of carrier persons, who do

ISBN:978-84-693-3386-0/DL:T.1002-2010

not express the disease but are susceptible to have CF affected children. Thus, this test is essential couples with a family history of the cystic fibrosis.

Many efforts have been made to developed methods for CF treatment [53-57], including gene therapy [58-62] and supplement of proteins, which are scarce with the CF patients [63]. Unfortunately, to date, these kinds of treatment failed to cure CF. The best available option for CF patients is to take antibiotics and an external supplement of nutrients and vitamins. Patients can also employ some devices to clear the lung mucus. These treatments aim to suppress the progressive inflammations and to minimize the disease symptoms. Within the development of the CF treatment, patients could live to 30 years [64], which was not observed 20 years ago, when individuals suffering from CF normally died in childhood.

1.3. Biosensors:

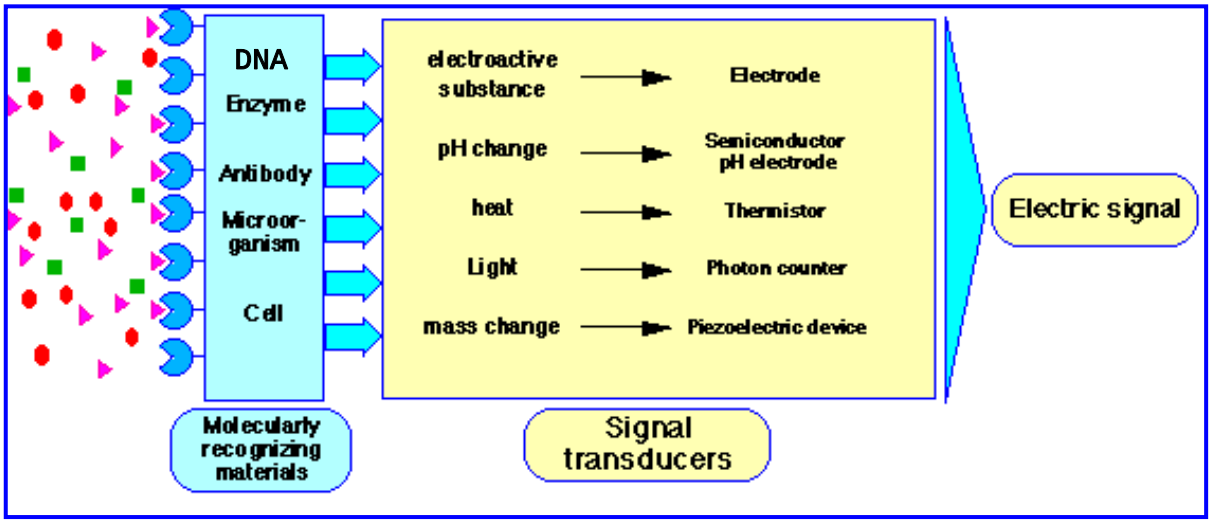

Figure 1.9. Schematic diagram of biosensor main components including molecular recognition components, signal transducers and readout. (ref.[65])

A biosensor, as illustrated in Figure 1.9, is an integrated device consisting of two main parts, the molecular recognizing material, and the signal transducer, where the latter converts the reaction/interaction of the recognizing material with the sample analyte targets into read out data. Hence, the selectivity and sensitivity of the biosensor is mainly determined by the bio-recognition element and the transducer, respectively. The

ISBN:978-84-693-3386-0/DL:T.1002-2010

bio-recognizing material could be either biocatalytic, such as an enzyme, micro-organism or tissue material, or affinity based, like antibodies and nucleic acids [66]. Typical transducers include electrochemical, optical or thermal based detectors.

Since the completion of the human genome project in 2003 [67], there has been an increased interest in DNA diagnostics and a great surge in molecular biology and biotechnology studies towards this goal has been observed. Hence, an increasing number of genes and mutations responsible for causing diseases are being identified, thus resulting in a requirement for simple, cost/effective and easy-to-use tools for the detection of these identified mutations for disease diagnosis. DNA hybridisation based analysis has been commonly applied in diagnostic laboratories due to its simplicity [68]. Biosensors exploiting DNA hybridisation are coined genosensors, where the bio-recognizing material is a DNA probe attached to the sensor surface, capable of selectively interacting with a target sequence to form a DNA duplex, overcoming any possible interference coming from the other non-complementary DNA target sequences. Genosensors, in which their transducers are optically based (e.g.. surface plasmon resonance), mass based (e.g. quartz-crystal microbalance, cantilever) and electrochemically based detectors have been widely reported for DNA analysis.

1.3.1. Optical based biosensors:

Optical biosensors are biosensors employing optically based transducers for the read-out of the selective reaction between the bio-recognizing material and the sample analyte. Based on the change in the optical character before and after the detection step, optical genosensors can detect the hybridised target DNA using fluorescence [69-71], surface plasmon resonance (SPR) [72-74], chemiluminescence [75-82], colorimetry [83-87], interferometry [88-90] surface-enhanced Raman scattering (SERS) spectroscopy [91-97] or, as more recently reported, by employing semiconductor crystals known as quantum dots (QDs) [98-109].

1.3.1.1. Surface plasmon resonance:

Surface plasmon resonance (SPR) results from the resonance energy transfer between evanescent wave and surface plasmons which exists when a complete reflection of the incident monochromatic light occurs on the gold thin layer interface between two phase glass and water [110]. SPR signals are expressed in resonance units and give an indication

ISBN:978-84-693-3386-0/DL:T.1002-2010

of the mass concentration on the gold surface. The linear relation between the SPR response and the mass concentration on the gold interface surface has allowed the extensive use of this technique for the determination of bio-molecules such as proteins and DNA. Furthermore, kinetic data can be calculated by the monitoring of association and dissociation processes [110,111]. Figure 1.10 illustrates this technique, where the incident polarized light is completely reflected on the gold interface and by small tuning in the incident angle, a drop in the intensity of the reflecting light is observed when the SPR is developed. This could be seen in the intensity vs. angle relation. When there is a change in the composition of the gold surface, a shift in this angle is consequently observed and is correlated with the concentrated mass on the gold interface [112].

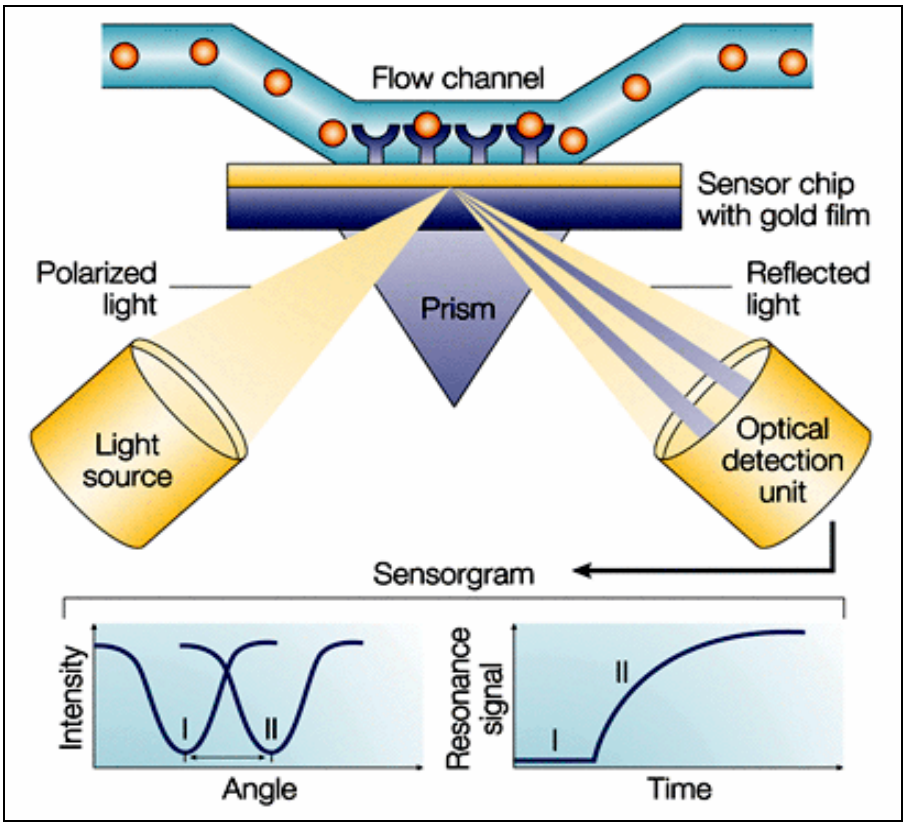

Figure 1.10. Surface plasmon resonance detection unit and the corresponding sensograms. (ref.[113])

SPR has successfully been applied as a biosensing platform since 1983 [114-131], and is an attractive label free method. Different types of molecules and molecular interactions can be determined using SPR, such as protein-protein [132-135], protein-DNA [136-141], DNA-DNA interactions [142-145], as well as being able to follow conformational changes in

ISBN:978-84-693-3386-0/DL:T.1002-2010

proteins [146]. The introduction of the commercially successful Biacore instrument has had an enormous impact on the employment of SPR in the biosensing field [147-149]. Surface plasmon resonance imaging (SPRi) was introduced by Yeatman and Ash in 1987 [150], where the gold thin layer was replaced with a micro-array, allowing hundreds of simultaneous biomolecular reactions to be monitored, whilst also studying the kinetics of the interaction [151]. Fiche et al., employed the SPRi technique accompanied with temperature control to detect DNA point mutations [152]. A series of different probe lengths (14-16 bp) were employed in this study together with fully and single base mismatched complementary targets. Both numerical and experimental data were in a good agreement to be employed for the detection of single base mismatching [152]. A microfluidic system with a four channels SPR microchip was introduced by Springer et al., to rapidly detect very low concentrations of 20 bp oligonucleotides [153]. A core-shell structured nanoparticle localized surface plasmon resonance (LSPR) was developed recently by Endo et al. and employed in the DNA investigated in aqueous conditions [154]. The measured changes in the LSPR optical characteristics were employed in detection of different DNA solution conditions, including DNA length, concentration and aspect (ssDNA or dsDNA). This procedure could detect DNA with different lengths (100–5000 bp), with a concentration of 1×10^7 DNA molecules/mL for DNA with 400 bp length [154].

1.3.1.2 Fluorescence based biosensors:

Optical biosensors based on fluorescence transducers have found widespread application in the biosensors field [69-71,155-165] [166,167]. An early work achieved by Krull et al., demonstrated the possibility for DNA detection via hybridisation with ssDNA probes immobilized on the surface of quartz optical fibres, where the reporter for the fluorescence response was ethidium bromide [168] Taira et al, [169] prepared a DNA-conjugated polymer to be immobilized onto a gold surface while the DNA targets were labelled with fluorescein isothiocyanate as a fluorophore label. This method succeeded in the discrimination between the fully complementary target and a target containing a single nucleotide polymorphism (SNP), where the latter expressed a fluorescent signal lower by 15 % than the former one. Zhao et al, proposed a bioconjugated nanoparticle-based sandwich assay for DNA analysis [170]. The fluorescence signal of the organic dye-doped silica nanoparticles was demonstrated to achieve an improvement in the limit of

ISBN:978-84-693-3386-0/DL:T.1002-2010

detection to reach to 0.8fM. A similar level of the limit of detection was achieved by the procedure introduced by Ali et al., in which DNA probes were immobilized onto porous microbeads via biotin/avidin interaction and the fluorescence signal was measured after hybridisation with the fluorophore labelled DNA targets [156]. Recently, Touahir et al., proposed a DNA biosensor, where they designed a new surface consisting of a thin layer of hydrogenated amorphous silicon–carbon alloy deposited on an aluminium back reflector [171]. The thickness of this layer was adjusted to match with the optimum fluorescence intensity of the labelled DNA targets with cyanine fluorophore (Cy5). An alternative approach was reported by Niu et al., based on enzyme-enhanced fluorescence [172]. The DNA probes were attached to a fibre support via streptavidin-biotin chemistry and hybridised to the target sequences. After careful washing with buffer solution, a HRP-streptavidin enzyme conjugate was attached to the hybrid duplex, and 4-hydroxyphenylacetic acid substrate was converted to the fluorescent product, bi-p,p`-4-hydroxyphenylacetic acid. The sensor showed specificity towards the complementary targets, with 1 pM limit of detection.

An alternative strategy in fluorescence based biosensors is the employment of molecular beacons, which are easily synthesised, target specific and are not affected by modifications such as labelling [173-180]. The molecular beacon format, as illustrated in Figure 1.11, is an oligonucleotide consisting of two main elements namely, the stem and loop parts. The stem part contains complementary bases to each other and is located in the two ends of the oligonucleotide strand, and their function is maintaining the hairpin structure (in the absence of targets) in which both a fluorophore label at one end and a quencher label in the other end are kept in close proximity, effectively quenching the fluorescence signal.. Meanwhile, the loop part contains the complementary bases for the target, and the beacon is designed so that it is energetically more favourable for the loop to bind its target than for the stem to remain hybridised. Thus, when the molecular beacon hybridises to is complementary (analyte target), the hairpin structure undergoes a conformational change and is opened resulting in an emission of the fluorescent signal due to the displacement of the quencher away from the fluorophore moiety [181].

Lui et al., reported a DNA sensor employing a fluorescence based molecular beacon [182], with tetramethylrhodamine as the fluorophore and DABCYL as the quencher, which was immobilized on an optical fibre via avidin-biotin binding. The discrimination of a

ISBN:978-84-693-3386-0/DL:T.1002-2010

single base mismatch was achieved with a detection limit of 0.3nM and 10nM for a 105 µm sensor, and submicrometer sensor, respectively. The breast cancer gene BRCA1 was analysed by Culha et al., via a designed biochip and based on a molecular beacon detection scheme [183]. The molecular beacon quencher was DABCYL and the fluorophore label was Cy5 and the achieved limit of detection was 70 nM.

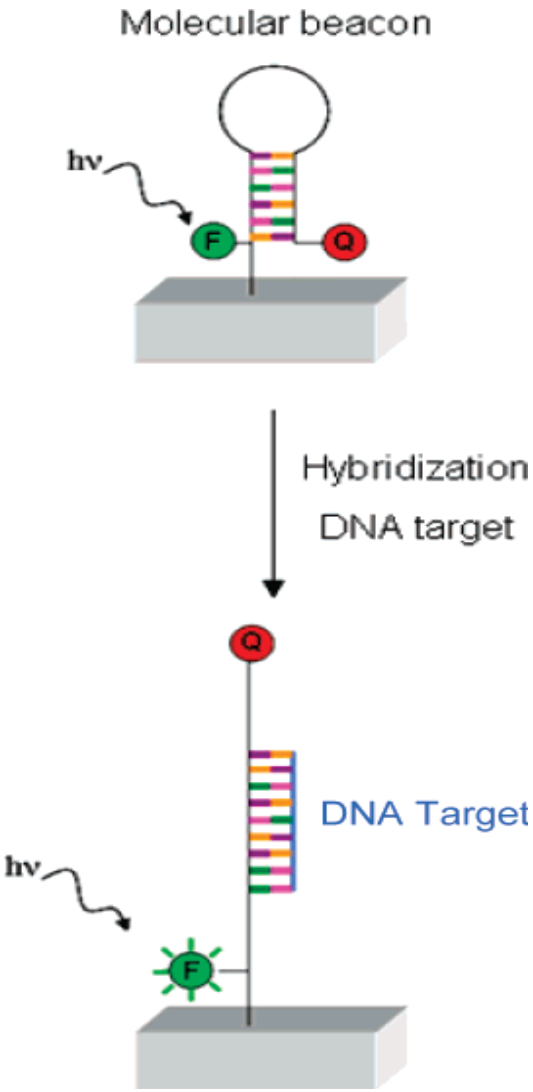

Figure 1.11 Fluorescent DNA biosensor based on the molecular beacon principle (ref.[181]).

One of the most important commercial examples of fluorescence based microarrays for DNA analysis are the Affymetrix gene chips [184-186], where the arrays consist of hundreds of thousands of immobilized DNA probes in which the genetic analysis for a

ISBN:978-84-693-3386-0/DL:T.1002-2010

wide sector of human genes could be achieved [187]. ¨Affymetrix Genome-Wide Human SNP Array 6.0¨ is an example of the commercial Affymetrix gene chips, which can detect more than 906,600 single nucleotide polymorphisms (SNPs) and more than 946,000 probes for the detection of copy number [188]. Figure 1.12 illustrates the Genome-Wide Human SNP Array 6.0 assay and the accompanying kits, which is employed for the sample preparation prior to the detection step via the gene chip. Affymetrix gene chip probe immobilization has been achieved using photolithography, which has been patented [188].

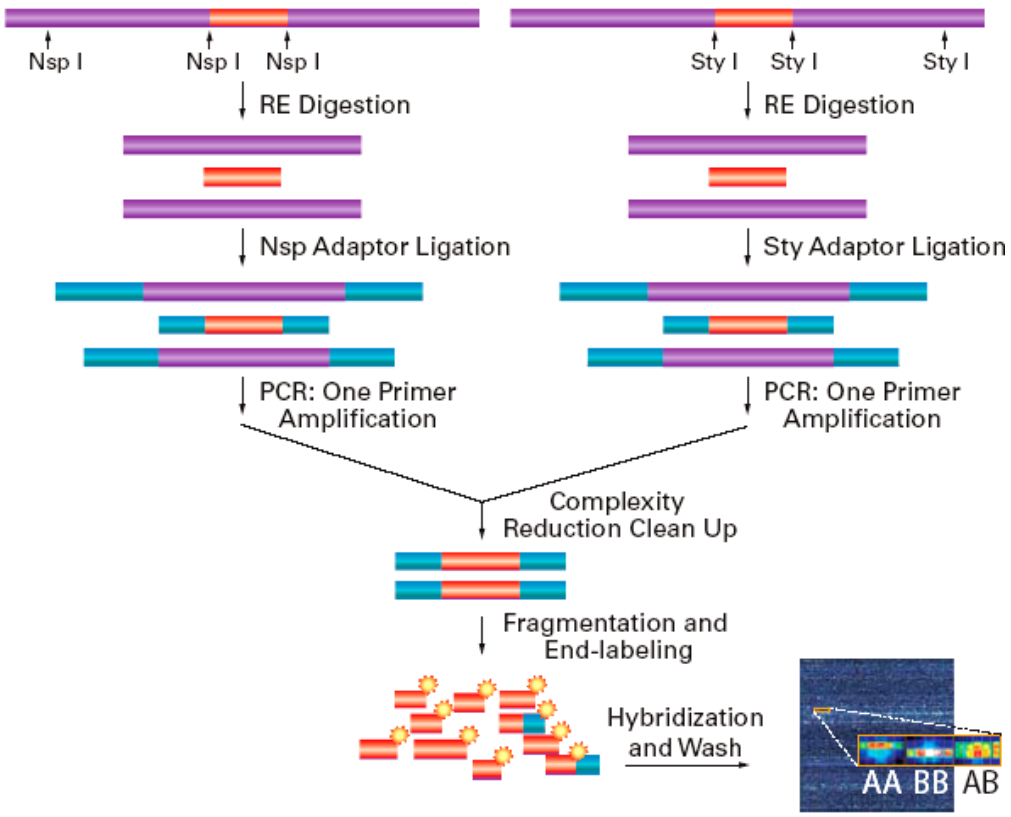

Figure 1.12 Schematic representation of the Affymetrix Genome-Wide Human SNP Array 6.0 (ref.[188])

Although the optical based biosensors have shown great application for DNA analysis, they are time consuming, not easy to use and expensive, which has resulted in a hurdle for the possible usage of these devices in hospital (point of care) or by patients in a home environment. Thus, the need for other alternatives to overcome these

ISBN:978-84-693-3386-0/DL:T.1002-2010

disadvantages is a defined requirement. Electrochemical biosensors offer advantages to overcome the drawbacks of the high/density microarrays and have great promise due to their high sensitivity and selectivity, portable size, rapid and low-cost [189-191].

1.3.2. Electrochemical Biosensors:

Since electrochemical methods are characterised by obvious advantages including high sensitivity, avoidance of potential interferences from sample solution turbidity, compatibility with microfabrication and small portable devices and its comparable low cost, they have been widely employed in biosensing field [189,190,192,193]. In 1960, Palecek [194] introduced an early application for electrochemical DNA sensing depending on the oxidation-reduction of DNA at a mercury electrode, where the amount reduced was concentration dependant and was also employed to discriminate single stranded DNA (ssDNA) from double stranded DNA (dsDNA). Later, an alternative strategy was proposed [195,196], in which the purine bases of DNA were oxidized via adsorption stripping voltammetry technique employing different electrode metals coated surfaces.

The electrochemical genosensors based on hybridisation detection can be classified into two main classes - labelled and label free electrochemical genosensors.

1.3.2.1. DNA probe Immobilisation on gold surfaces:

Attachment of the DNA strand which represents the molecular recognizing layer in the genosensor, is preferred to be through one end of the DNA strand in order to facilitate easy accessibility for the sample DNA targets [197-199]. Self-assembly methods have been widely applied for biosensors, where the electrode surfaces are well organised [200-202]. In one approach, an alkanethiol self-assembled monolayer with a functional head group is chemisorbed and subsequently cross-linked to the DNA probe via carbodimide covalent coupling [203-206]. Zhao et al., [203] reported on carbodiimide covalent coupling with three different thiols terminated with hydroxyl, amino and carboxyl groups employing X-ray photoelectron spectroscopy (XPS) and cyclic voltammetry (CV). They found the hydroxyl-terminated SAM was more suitable for the covalent attachment of DNA. Johansson et al., [204] employed the same technique for assembling oligonucleotides on an immobilised cyteamine monolayer. Furthermore, 3-mercaptopropionic acid self-assembled monolayer was used for carbodiimide covalent coupling with oligonucleotide probes by Ozsos et al., [206]. An alternative approach employed for the self assembly on

ISBN:978-84-693-3386-0/DL:T.1002-2010

gold electrodes exploits phosphorothioester-modified probes [207]. Ihara et al. [207-211] modified an oligonucleotide probe with five successive phosphothioate bonds prepared in 5`-end in order to be self assembled on to the gold surface. The introduction of multi-phosphothioate bonds was to achieve better stability on the gold surfaces.

1.3.2.1.1. Direct self-assembly of thiolated probes

In 1983, Nuzzo et al., studied the self assembly of different thiolated compounds and demonstrated that they form a stable monolayer with different metal surfaces (silver, platinum, copper and gold) [212]. Thiolated DNA monolayers were employed in electrochemical DNA detection [213-215] and proved to be more stable than long chain alkanethiols in a potential window of −0.7 to +0.7V versus SCE [216]. Moreover, a self assembly technique was employed recently to protect gold nanoparticles patterned on to glassy carbon electrodes [217].

Herne et al. [218-220] intensively studied the chemisorption of thiolated labelled DNA probes on gold surfaces. They characterised this phenomena by employing X-ray photoelectron spectroscopy (XPS), ellipsometry, ^{32}P-radiolabeling, neutron reflectivity and electrochemical methods. The investigated immobilisation time was 3 hrs to obtain a full gold surface coverage with thiolated DNA. The ionic strength of the immobilisation solution was demonstrated to have a strong effect on the immobilisation stability and affinity, with the immobilisation (building the self assembled monolayer) of the thiolated DNA showing a great enhancement in chemisorption at high salt concentration. The role of high salt concentration in the immobilisation process was explained to neutralise the charges of DNA strands leading to minimisation of the repulsions between the neighbouring thiolated strands, easing their accessibility to the gold surface. DNA thiolated probes could interact non-specifically with the gold electrode surface through DNA nitrogen-containing bases and not through the S-Au bond, which affects the accessibility of the immobilised probes to hybridise successfully with the DNA targets in the sample solutions.

.

ISBN:978-84-693-3386-0/DL:T.1002-2010

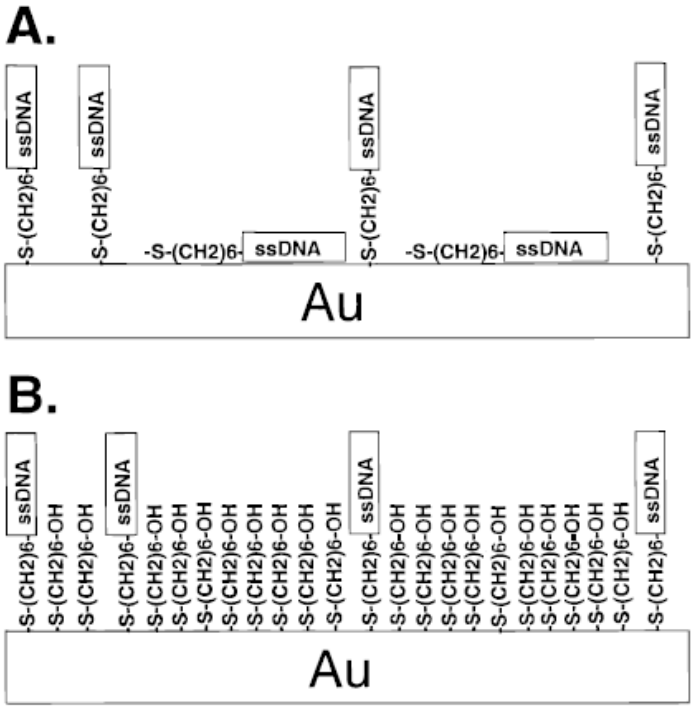

Figure 1.13. A scheme depicts a gold surface immobilised with thiolated DNA (A) and with mixed monolayers of both thiolated DNA and meraptohexanol (B), ref.[218]

The authors [218] suggested an innovative solution to eliminate these non-specifically adsorbed thiolated DNA probes by application of two steps of mixed monolayers procedure, firstly, by immobilisation of the thiolated DNA probes, followed by exposure of the immobilised gold surface to a suitable concentration of mercaptohexanol (MCH) (Figure 1.13). The role of MCH was shown to not only minimise the non-specifically adsorbed thiolated DNA but also to minimize the steric hindrance of the highly packed immobilised thiolated DNA and enhance the hybridisation efficiency. This mixed self assembled monolayers technique has been detailed in many reports [214,221-224]. The electrochemical redox couple $[Fe(CN)_6]^{3-}$ /$[Fe(CN)_6]^{4-}$ has been widely used to investigate the surface coverage of the DNA probe via cyclic voltammetry [207,213,216,220,225], and the peak to peak separation was observed to increase after DNA immobilisation compared to the bare clean gold electrodes. This was explained based on the electrostatic repulsion between the negatively charged couple and the negatively charged backbone of the immobilised DNA probes [226].

ISBN:978-84-693-3386-0/DL:T.1002-2010

1.3.2.2 Labelled approaches in electrochemical biosensors:

1.3.2.2.1 Enzyme Label

Enzyme labelling has been extensively reported in biosensors applications [208,225,227-243], where the target DNA, or a reporter DNA used in a sandwich/type assay format, are commonly labelled with redox-active enzymes.

Azek et al. employed the horseradish peroxidase (HRP) enzyme to detect DNA sequences related to the human cytomegalovirus (HCMV) [229]. On a screen printed carbon electrode the amplified DNA was adsorbed on the surface and subjected to hybridisation with biotinylated complementary targets, and the formed duplexes were subsequently interacted via avidin-biotin interaction with streptavidin conjugated horseradish peroxidase, which, in turn converted the o-phenylenediamine (OPD) substrate into 2,2`- diaminobenzene (DAA), an electroactive molecule [229]. The limit of detection achieved via this procedure was 0.6 amol/ml for HCMV-amplified DNA fragment. Jin Pan prepared a disposable DNA sensor as illustrated in Figure 1.14 [230]. The formation of the dsDNA duplex was found to suppress the activity of the immobilised HRP as an indication of the DNA target concentration as measured via differential pulse voltammetry. A lower target DNA concentration linear range was obtained in the range of 1.5×10^{-10} to 9.5×10^{-9}M with a detection limit of 5.0×10^{-11}M.

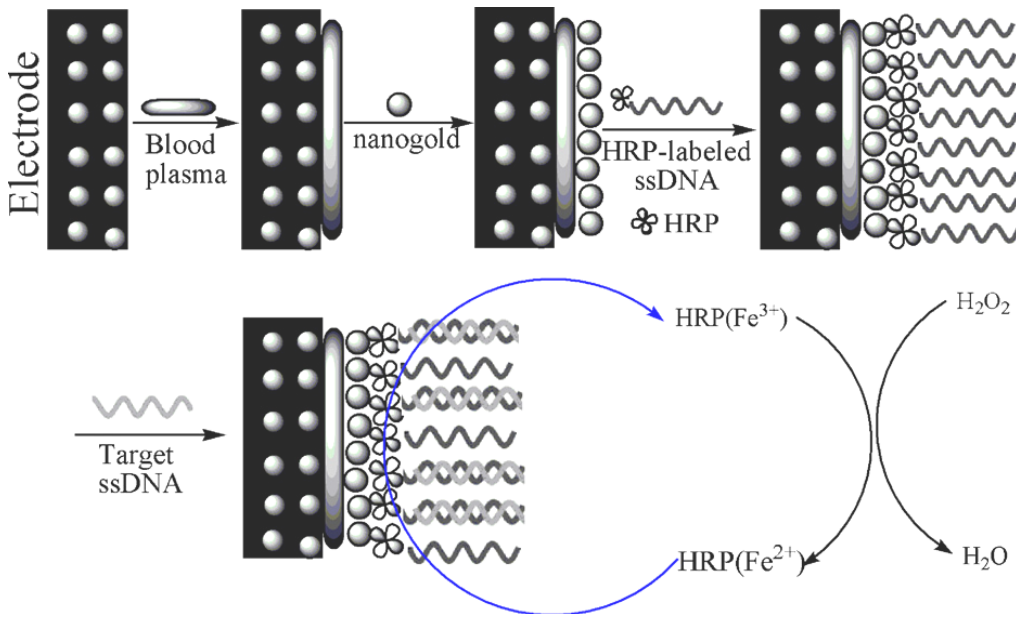

Figure 1.14 Sensor preparation and the mechanism of the HRP reaction (ref. [230])

Carpini et al, employed a disposable screen printed gold electrode for the determination of DNA via enzyme amplification [244]. The surface immobilised thiolated DNA probes were achieved via mixed self assembled monolayer with MCH. The biotinylated DNA targets were bound after hybridisation on the electrode surface to streptavidin-alkaline phosphatase conjugate, while the hybridisation efficiency was indicated via the hydrolysis of α-naphthyl phosphate to the electroactive product, α-naphthol, achieving a limit of detection of 1nM. Lucarelli et al., immobilised thiolated DNA on a screen printed gold electrode for enzyme-label based biosensor application [238]. The hybridisation efficiency was indicated after coupling with a streptavidin–alkaline phosphatase conjugate (sandwich assay) with the hybridised targets and bio-catalysed precipitation of an insoluble and insulating product onto the electrode. The impedimetric measurement was proportional to the DNA target concentration with a limit of detection of 1.2 pM. Xie et al, took advantage of the strong interaction between cationic redox polymers containing osmium-bipyridine complexes and glucose oxidase enzyme to be utilized in DNA biosensors [233]. The gold electrode surface was functionalised via a self assembly of a mixed monolayer of the thiolated DNA and mercaptohexadecanoic acid. The glucose oxidase was brought to the electrode surface via sandwich assay and coated with the anionic redox polymer. The enzyme was activated by the formation of this bi-layer to oxidise glucose present in the solution and this oxidation was measured amperometrically, with a resulting limit of detection of 1 fM.

1.3.2.2.2. Some redox labels examples in electrochemical biosensors:

1.3.2.2.2.1. Ferrocene:

Ferrocene labelled DNA had been utilized in many biosensor applications [245-250]. A number of procedures have been applied for the preparation of this conjugate, including covalent linkage of a ferrocenyl group to the 5`-aminohexyl-terminated synthetic oligonucleotides [251] or to label the 5`-iodouridine terminated oligonucleotides with FC by solid phase coupling [252].

ISBN:978-84-693-3386-0/DL:T.1002-2010

Takenaka et al., biofunctionalised a gold electrode surface with thiolated DNA probes [221,253]. The complementary DNA targets were labelled with ferrocene via a naphthalene diimide threading intercalator and the signal was determined by differential pulse voltammetry. The limit of detection obtained with this procedure was 1fmole of the target DNA. Xu et al., prepared a ferrocene conjugate for a PCR amplified 256 bp DNA fragment employing 1-ethyl-3-(3-dimethylaminopropyl) carbodiimide (EDC) for the first time [250]. The electrode surface was biofunctionalised with ssDNA on a chitosan modified glassy carbon electrode. The sensitivity of this procedure was high with a limit of detection of 2nM.

Recently, a novel electrochemical DNA (E-DNA) biosensor based on the proximity-dependent surface hybridisation assay was introduced [254]. Zhang et al., biofunctionalised the gold electrode surface via self-assembly of 3′ short thiolated capture probe. DNA detection was realized by recording the redox current of the 5′ ferrocene (Fc) tail labelled probe. Upon hybridisation, the DNA target was complementary to the 5′ Fc labelled probe at the one-half-segment and complementary to the 3′ short thiolated capture probe at the other half-segment, resulting in the formation of a stable duplex complex. The observed faradic current indicated a low detection limit and an extensive linear range from 1 fM to 1 nM. A recent comparison of the differences in signalling and stability of electrochemical DNA sensors (E-DNA sensors) fabricated using either ferrocene or methylene blue as the signalling redox moiety was reported [255], where, both tags support efficient E-DNA signalling, but ferrocene produces a slightly improved signal gain and target affinity. These small advantages, however, come at a potentially significant price: the ferrocene-based sensors are far less stable than their methylene blue counterparts, particularly with regards to stability to long term storage, repeated electrochemical interrogations, repeated sensing/regeneration iterations, and employment in complex sample matrices such as blood serum [255].

Electrochemical biosensors based molecular beacons labelled with ferrocene could produce other alternatives for biosensing [163,256]. For example, a molecular beacon labelled with ferrocene in one end of the stem region was immobilised on a gold electrode surface as shown in Figure 1.15. Due to the proximity to the surface, the ferrocene moiety could easily exchange current with the electrode surface in the absence

ISBN:978-84-693-3386-0/DL:T.1002-2010

of the complementary DNA target. Hybridisation caused a complete conformational change and distortion in the molecular beacon hairpin shape to stand up resulting in increasing the distance between the ferrocene and the electrode surface, leading to an obvious retardation in the current exchange. The proposed system permitted a detection of a 27 bp DNA target with low concentrations (10 x 10^{-12} M) [256].

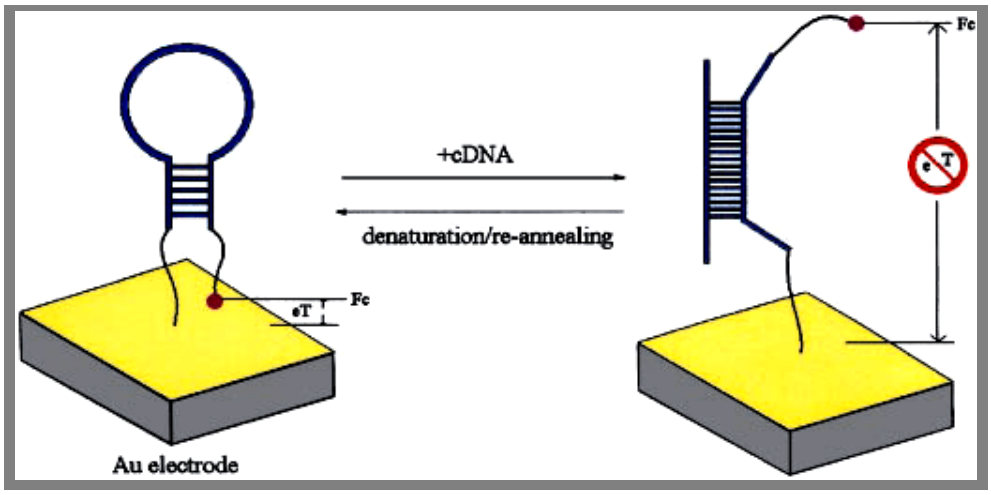

Figure 1.15 A stem–loop oligonucleotide possessing terminal thiol and a ferrocene group is immobilised at a gold electrode through self-assembly. In the absence of target, the stem–loop structure holds the ferrocene tag into close proximity with the electrode surface, thus ensuring rapid electron transfer and efficient redox of the ferrocene label. On hybridisation with the target sequence, a large change in redox currents is observed, presumably because the ferrocene label is separated from the electrode surface (ref.[163]).

1.3.2.2.2.2. Methylene blue

Methylene blue (MB) is an organic dye (Figure 1.16) that has been extensively reported as an electrochemical reporter in biosensing applications [257-260] [216,223,261-263]. The well known interaction between MB and the free guanine bases in the single stranded DNA has been utilized in many electrochemical biosensor applications [206,264] [257-259]. The switch off MB signal was employed as an indicator for the hybridisation efficiency and differentiation of a single base mismatch [257,258] [259]. Wang et al., [260] proposed a new biosensor base on the self assembly of carbon nanotubes onto a gold electrode surface (Figure 1.17). The immobilised nanotubes were functionalised with DNA probes via the

ISBN:978-84-693-3386-0/DL:T.1002-2010

interaction between the nanotubes surface carboxylic groups and the DNA terminated amino groups. The MB signal was shown to decrease after hybridisation with the DNA targets and showed different responses according to the target sequence mismatching. The authors demonstrated that the self-assembled nanotubes were much better than random ones. Lin et al., reported an assay for the detection of 18 bp DNA analogues to the Chronic Myelogenous Leukemia gene sequences [265]. The DNA probes were immobilised onto a glassy carbon electrode surface via covalent binding and subjected to hybridisation with the complementary DNA target to be detected through the MB voltammograms with a detection limit of 5.9×10−8 M.

(a)

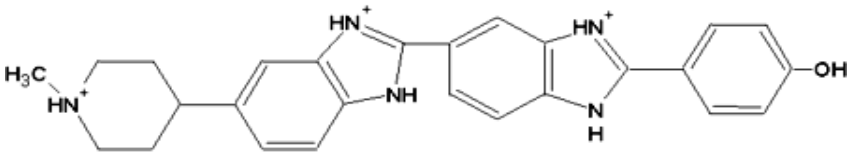

(b)

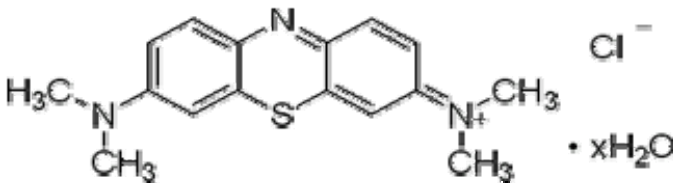

Figure 1.16 Chemical structures of Hoechst 33258 dye (a) and Methylene blue dye (b)

ISBN:978-84-693-3386-0/DL:T.1002-2010

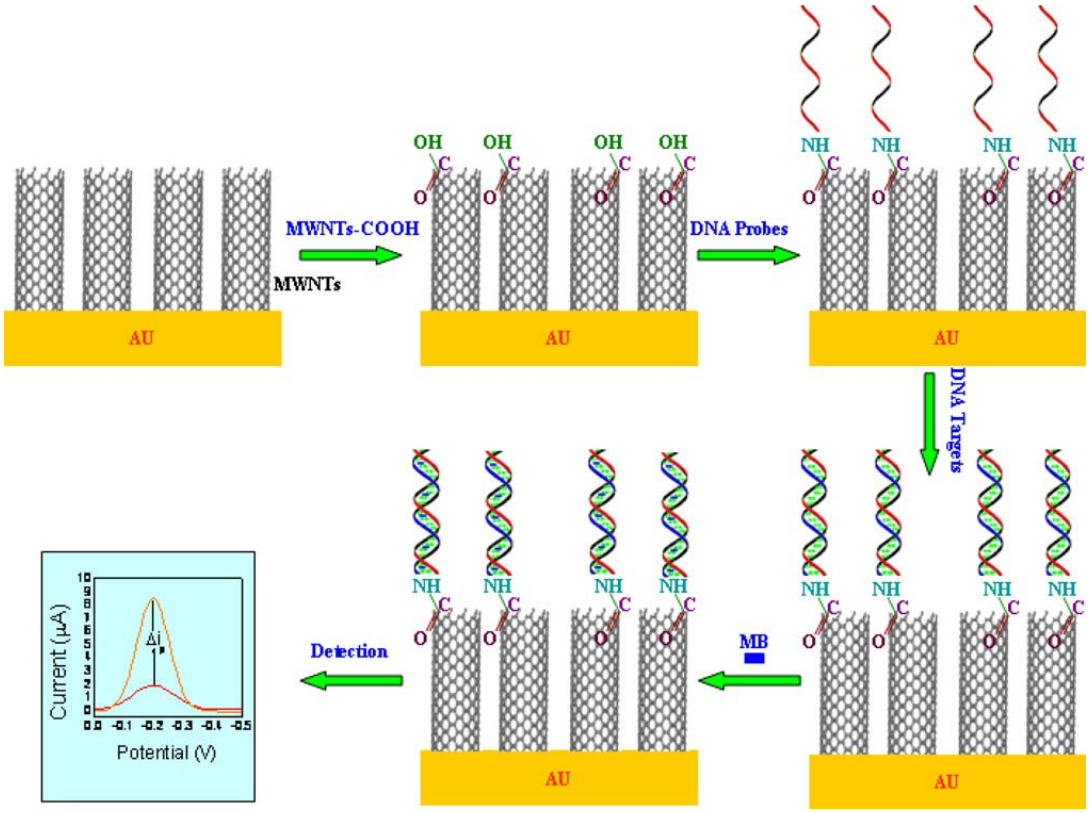

Figure 1.17. Carbon nanotubes based sensor preparation and hybridisation detection via MB. (ref.[260])

Recently, Henry et al, developed a DNA biosensor employing methylene blue as an electrochemical indicator [266], where thiolated DNA probes of 20 base length complementary to gene LTA (107 bp) target were immobilised on to an array of 15 gold electrodes via S-Au bond. After hybridisation with the DNA targets the differential pulse signals of methylene blue was notably enhanced due to the interaction with the free non hybridised 25 guanine bases of the complementary target DNA. The assay showed a linear calibration in the range of 6.25–50nM target DNA with LOD of 17.5 nM and capability of discrimination between the complementary and non complementary targets [266]. Xiao and co-workers [267] developed a DNA sensor consists of triple-stem structured immobilised DNA probes onto gold electrode surface. The immobilised probes were labelled with methylene blue as an electrochemical reporter. Post hybridisation with the fully complementary DNA targets, a conformational change resulted in the original probe triple-stem structured and allowed the methylene blue moieties to be near to the surface, thus the methylene blue alternating current voltammograms were significantly enhanced [267]. The sensor showed capability for the

ISBN:978-84-693-3386-0/DL:T.1002-2010

discrimination between the fully complementary and single nucleotide polymorphism DNA targets with 5 nM (250 ng/μL) limit of detection. Other biosensors based on the immobilisation of peptide nucleic acid (PNA) probe on to gold electrode surface was proposed by Hejazi and co-workers [268]. The 14 base probe sequences were related to the hepatitis C virus genotype 3a (pHCV3a) core/E1 region. Via three sequential steps for the determination with methylene blue, namely incubation, washing and differential pulse voltammetry determination, it was possible to detect the formation of the double strands on to the electrode surface, achieving a limit of detection of 5.7×10^{-11} M. Siddiquee and co-workers [269] proposed a genosensor for the detection of 20 bp DNA targets analogous to Trichoderma harzianum species. They immobilised a thiolated complementary DNA probe on the gold electrode surface and the hybridisation efficiency was investigated via methylene blue as an electrochemical indicator through three steps (incubation, washing, measuring), was and demonstrated that it was possible to discriminate between complementary and non complementary target sequences via the differential pulse voltammograms of methylene blue. This assay showed a linear correlation between the methylene blue redox current and the DNA target concentration between 1 and 20 ppm [269].

1.3.2.2.2.3. Other electroactive substances:

The oxidation of guanine by $Ru(bpy)_3^{3+}$ was utilized by Napier et al, to develop an assay for DNA detection [270]. After hybridisation and in the presence of Ru complex, a notable increase in the signal was recorded du to electrostatic binding and provided an indication for the hybridisation efficiency. Garcia et al, successfully deposited gold nanoparticles onto a gold electrode surface [271]. As a case study, a thiolated capture probe sequence from Helicobacter pylori was immobilised onto the gold nanoparticle-modified surface. The hybridisation was monitored via the pentaamine ruthenium [3-(2-phenanthren-9-yl-vinyl)-pyridine] complex ($Ru(NH_3)_5L$), which is an intercalator whose electroactivity was measured by means of differential pulse voltammetry. The proposed method was valid for the detection of Helicobacter pylori complementary target sequences over the range of 40–800 pmol with a detection limit of 25±2 pmol in what volume. Cobalt complexes were also employed in biosensing applications [272,273]. Hoechst 33258 (Figure 1.16), which has a characteristic recognition of adenine/thymine in DNA strands was employed for biosensor applications [274-280]. Due to the aggregation

ISBN:978-84-693-3386-0/DL:T.1002-2010

with DNA strands, the decrease in Hoechst 33258 linear sweep voltammograms was utilized for the detection of DNA in solution, employing glassy carbon electrode as a working electrode [281]. The aggregation of DNA–Hoechst 33258 complex was proportional to the quantity of DNA in a wide linear range between 1.5 and 25 mg/l. Detection of DNA sequences related to *Salmonella enteritidis*, *Streptococcus sobrinus*, and hepatitis B virus (HBV) were achieved using this system. Choi et al., employed an array of gold electrodes that were functionalised with thiolated DNA probes, and hybridisation was detected via signal enhancement of Hoechst 33258 reporter using linear sweep voltammetry [277-279]. In an alternative approach, anthraquinone derivatives, which are anionic DNA intercalators, were employed [282-285]. A gold electrode surface functionalised with a mixed self-assembled monolayer of synthetic thiolated single-stranded DNA (ss-DNA) and 6-mercapto-1-hexanol (MCH) was prepared and the hybridisation was measured via the electrochemical activity of anthraquinone derivatives by Elicia et al. [283,284]. The sensor showed a clear discrimination of a single base mismatch as compared to a fully complementary target.

1.3.2.2.3. Labelless detection in electrochemical genosensors:

The direct oxidation of DNA guanine bases represents a labelless detection method for biosensor applications [194,286-288]. Erdem et al. [288], developed a biosensor based on label-free electrochemical detection using magneto-composite electrodes. In order to achieve a selective hybridisation, the biotinylated inosine-substituted capture DNA probes were immobilised onto streptavidin coated magnetic beads. The rationale for the substitution of the guanine bases with the inosine ones in the DNA probes is to have a distinct voltammetric signal of the guanine bases belonging to the DNA targets as an indication of hybridisation efficiency. Kagan et al., reported an electrochemical labelless method based on DNA guanine oxidation [289], where the activated carbon paste electrodes were separately, functionalised with peptide nucleic acid (PNA) and DNA probes. The voltammetric guanine signal suppression after hybridisation was correlated to the DNA target concentration in the measurement samples. Single base mismatch detection was achieved via this procedure and the estimated limit of detection was 2.7×10^{-10} M for the complementary 14 bp DNA targets.

ISBN:978-84-693-3386-0/DL:T.1002-2010

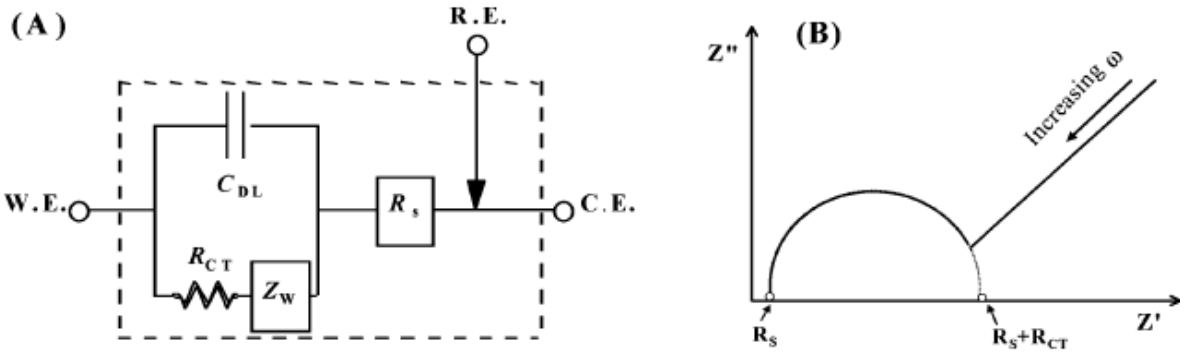

Figure 1.18. (A) The Randles circuit model for a modified gold electrode in an electrolyte. WE, CE, and RE denote working electrode, counter electrode, and reference electrode, respectively. RCT and RS are interfacial charge transport resistance and uncompensated solution resistance, respectively, while CDL is capacitance associated with the charge double layer at the modified electrode. Z_W is the Warburg impedance describing depletion of the redox species in the interfacial region as described in the text. (B) Typical Nyquist plot of reactive (Z``) versus resistive (Z`) part of the complex impedance $Z(\omega) = Z' + jZ''$ (where $j = (-1)^{1/2}$) expected for a reversible electrochemical reaction that is diffusion controlled at low ac modulation frequency ö and electron-transfer controlled at high modulation frequency ω. (ref. [290]).

Electrochemical impedance spectroscopy represents a possible tool for the labelless detection of DNA [290-293]. The impedimetric measurements could be represented as illustrated in Figure 1.18, with Nyquist plots in which the charge transfer spectra (R_{ct}) was taken an indication for any changes occurred to electrode surface.

Pan and Rothberg reported a label free DNA detection proposal using impedance [290], exploiting a mixed self assembled monolayer of 2-mercaptoethanol and 11-mercaptoundecanoic acid, which were immobilised on to gold electrode surface, with the latter being used for anchoring of DNA probes via avidin-biotin interaction. After hybridisation with the complementary DNA target, the impedimetric response decreased and almost no change was observed in the impedance spectra after incubation with a non-complementary DNA target. The loss in the impedance signal after hybridisation was due to the rigidity in the structure of the formed hybrids which increase the cavities between adjacent hybrids to facilitate the movement of the redox species to reach the electrode surface. Recently, Zebda et al., reported the influence of electrical resistivity of bio-modified transparent and conductive oxide (TCO) electrodes on the sensitivity of DNA hybridisation in terms of impedance variation [292]. They deposited pure cadmium

ISBN:978-84-693-3386-0/DL:T.1002-2010

indate ($CdIn_2O_4$) film electrodes on glass substrates by aerosol pyrolysis. Using electrochemical impedance spectroscopy (EIS), they showed that the behaviour of bare films is typical of a semiconductor electrode with flat band potentials depending on the film resistivity. The impedance variation due to DNA hybridisation was particularly studied in the low frequency range where large and significant increases were observed. Simon et al., [294] optimized the surface density of the immobilised thiolated DNA probes via co-immobilisation with mercaptohexanol. Both probe density and hybridisation were impedimetrically observed via the charge transfer resistance with the negatively charged ferri/ferrocyanide redox couple. The optimum probe surface density was $5.4\times10^{12}/cm^2$ and it was achieved by co-immobilisation of oligonucleotide probes and mercaptohexanol with a DNA mole fraction of 20% in order to have the maximum hybridisation response.

1.3.3 Melting temperature:

The melting temperature of a DNA duplex can be defined as temperature at which, under a given set of conditions, 50 % of the double-stranded DNA (dsDNA) is denatured to single-stranded DNA (ssDNA). The denaturation (separation) usually occurs firstly in the AT rich sequences regions of the dsDNA due to the lower number of hydrogen bonds (two) as compared to CG sequences (three H-bonds) [295].

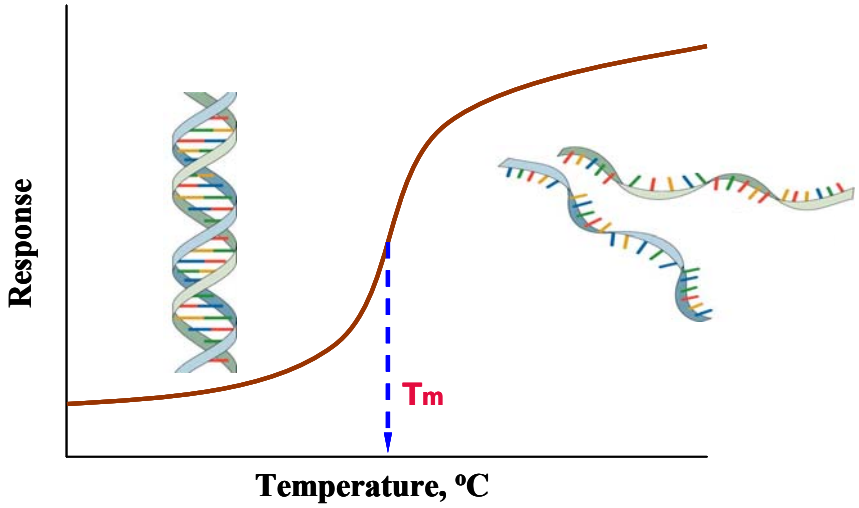

Figure 1.19. DNA melting curve and the allocation of melting temperature value.

ISBN:978-84-693-3386-0/DL:T.1002-2010

Figure (1.19) elucidate the DNA melting curve in which the at lower temperature the DNA presents as dsDNA and by heating a denaturising is developed between the DNA strands form finally the ssDNA. The midway point corresponds to the melting temperature [295].

1.3.3.1 Melting temperature calculations:

One of the commonly applied equations for the oligonucleotides melting temperature calculation is called the nearest neighbour method, as represented in equation 1[296]:

$$\mathbf{Tm = (1000\Delta H)/A + \Delta S + R\ ln(C/4) - 273.15 + 16.6\ log[Na+]} \qquad \mathbf{(1)}$$

Where, ΔH and ΔS are the sum of the nearest-neighbour enthalpy and entropy changes for hybrids, respectively, A is constant containing corrections for helix initiation, R is the Gas Constant and C is the oligo concentration. The Tm values depend on the quantity of salt in the solution [296].

Another equation applied for membrane based calculations is called the Wallace rule, represented in equation 2 [297]:

$$\mathbf{Tm = 2(aA + tT) + 4(cC + gG)} \qquad \mathbf{(2)}$$

where a, t, c, and g are the number of the corresponding nucleotide in the oligo sequence. The salt concentration employed for this equation was 0.9 M NaCl.

Another way to obtain the melting temperature value is through melting temperature curve analysis, simply by representing the melting temperature curve with the first derivative form, where the peak maximum represents the melting temperature value [298].

1.3.3.2 Biosensors DNA melting applications:

DNA melting has a clear impact in biosensing applications. DNA duplexes have different melting temperature values (Tm) according to the length, GC content and the presence of sequence mismatching, and the DNA melting temperature can thus be

ISBN:978-84-693-3386-0/DL:T.1002-2010

exploited as a good tool for the detection of DNA mutations. As previously described, biosensors commonly consist of solid support surfaces for the immobilisation of the molecular recognizing material (e.g. DNA), and it is thus important to determine the Tm of immobilised DNA hybrids. To this end there have been reports of the determination of the melting temperature of surface immobilised DNA duplexes employing SPR [299], and fluorescence based assays[300,301] . Peterlinz et al., reported the Tm value is less by about 5ºC in case of immobilized duplexes than in bulk solution employing SPR technique[299]. Other reports concluded the difference to be around 10 ºC lower in the case of immobilized DNA duplexes then in bulk solution [302,303]. Piunno et al., [300] explained the lower values corresponding to surface Tm compared to that in bulk solution where both cases has the same ionic strength conditions, could be due to the difference in the dielectric constant between immobilized and bulk solution duplexes. Thus a reduction in the dielectric constant associated with the immobilised hybrids resulted in reduction in effective ionic strength associated with immobilisation media and hence affect the DNA melting behaviour[300]. Using gold interdigitated microelectrodes (GIME), Brewood et al., studied the melting temperature via capacitance, impedance, dissipation factor and phase angle in a temperature range from 25ºC to 80ºC. Furthermore, the solution melting temperature was achieved via differential scanning calorimetry (DSC) and UV absorbance spectroscopy and a similar conclusion that the surface melting temperature values are lower than in bulk solution case was reached[304].

DNA melting temperature has also been employed in mismatching (mutation) scoring. In one example, an optical readout system for hybridization detection based on fluorescent-labelled microarrays was developed by Lehr et al. A temperature range of 20-80 ºC was applied in this study for the study of the DNA melting behaviour for 140-mer PCR product which was subjected to hybridisation with 15 and 17 mer immobilized complementary oligonucleotides. This assay showed the possibility to detect single nucleotide polymorphisms[301]. Pröll et al., employed reflectometric interference spectroscopy (RIfS) for the study of the melting of DNA duplexes[305]. Three different complementary immobilised probes were examined, namely, DNA, peptide nucleic acid (PNA) and locked nucleic acid (LNA), where the latter was demonstrated to have a higher melting temperature and was hence more stable. This assay showed a clear differentiation between fully complementary targets and targets containing one and two

ISBN:978-84-693-3386-0/DL:T.1002-2010

single nucleotide polymorphisms[305]. Wang et al., [306] reported the melting behaviour of the complementary duplexes with solid phase covalently linked synthesis DNA probes on fused silica optical fibers via thiazole orange dyes derivatives with different linker lengths of ethylene glycol. The fluorescent signal corresponding to hybridisation with complementary and single base mismatched complementary were highly distinguished applying this method[306]. Utilizing DNA targets labelled with osmium tetraoxide-bipyridine, it was possible for Surkus et al., to electrochemically monitor the melting behaviour with immobilized complementary probes on the gold electrode surface. Different mismatched targets were studied and a distinct variation of Tm values was demonstrated[307]. A fluorescence based assay for scoring of single nucleotide polymorphisms (SNPs) in a method termed Dynamic allele-specific hybridization (DASH) was introduced by Howell et al.[308].

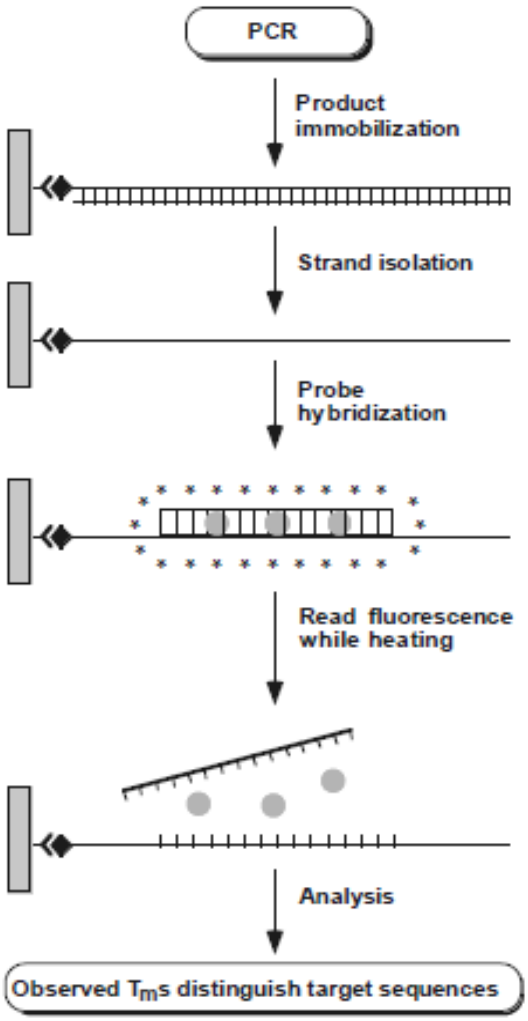

Figure 1.20. A schematic illustration of DASH assay. A monitoring of the Probe-Target denaturising was achieved via fluorescent reported over wide range of temperature (Ref[308]).

ISBN:978-84-693-3386-0/DL:T.1002-2010

As illustrated in figure 1.20, the principle steps of this method consists of the immobilization of biotinylated amplified PCR DNA via employing biotinylated primer and after washing, only the biotinylated ssDNA is bound to streptavidin-coated microtiter plate well. The immobilised DNA is then subjected to hybridisation with specific probes and then heated, where the dsDNA denaturation is monitored via fluorescence signal depletion of an intercalator dye (Syber Green I dye). By applying this method, it was possible to detect single nucleotide polymorphism as the melting temperature value showed a clear difference as compared to the complementary case[308].

ISBN:978-84-693-3386-0/DL:T.1002-2010

1.4. State of Art and Objectives:

As previously described, cystic fibrosis is a well known and abundant disease, caused by different mutations in the cystic fibrosis conductance regulator gene. This disease affects many organs in the human body and results in an early death in most cases. The DF508 mutation represents the most abundant mutation (70 %) above all other mutations in Northern European Caucasian populations. Thus a rapid, accurate and low cost DNA analysis for the determination of the CF associated gene mutations, especially the DF508 mutation, is of high importance. The well known genetic analysis devices currently available, such as Affymetrix biochips, mainly depend on optical detection which are not suitable to be handled at the point of care, due to their cost and lengthy analysis time

Electrochemical genosensors address the need to analyse DNA for clinical diagnostics as they are of low cost, are highly sensitive, compatible with micro-fabrication techniques and can be powered by small portable devices with low power requirements. Thus the objective of this thesis was the development of electrochemical array based genosensors for the multiplexed differentiation between cystic fibrosis mutant and wild types (wild type corresponding to the normal gene).

In order to achieve this objective, a numbers of sub-objectives were designed, namely:

1- Evaluation of different electrochemical techniques for the detection of cystic fibrosis mutations. Namely; electrochemical impedance spectroscopy, differential pulse voltammetry employing methylene blue as electrochemical reporter and electrochemical molecular beacon.

2- Applying a temperature modulating systems for those techniques to improve the discrimination factor between mutant and the corresponding wild type.

3- Utilising the melting curve analysis in the discrimination between mutant and wild type targets to be applied for the electrochemical multiplexing detection.

ISBN:978-84-693-3386-0/DL:T.1002-2010

5. References:

(1) Watson, J.; Crick, F. *Nature* **1953**, *171*, 737.
(2) Bostick, M.; Kim, J. K.; Esteve, P.-O.; Clark, A.; Pradhan, S.; Jacobsen, S. E. *Science* **2007**, *317*, 1760.
(3) Saenger, W. *Principles of Nucleic Acid Structure*; Springer-Verlag: New York, 1984.
(4) Alberts, B.; Johnson, A.; Lewis, J.; Raff, M.; Roberts, K.; Walters, P. *Molecular Biology of the Cell*, 4 ed.; Garland Science: New York and London, 2002.
(5) Berg, J.; Tymoczko, J.; Stryer, L. *biochemistry*, 5 ed.; W. H. Freeman and Company 2002.
(6) Chalikian, T. V.; Jens, V.; Plum, G. E.; Breslauer, K. J. *Proceedings of the National Academy of Sciences of the United States of America* **1999**, *96*, 7853.
(7) Pieter, L. d.; John, D. H. *Molecular Microbiology* **1995**, *16*, 817.
(8) Gregory, S. G.; Barlow, K. F.; McLay, K. E.; Kaul, R.; Swarbreck, D.; Dunham, A.; Scott, C. E.; Howe, K. L.; al., e. *Nature* **2006**, *441*, 315.
(9) http://ghr.nlm.nih.gov.
(10) http://en.wikipedia.org.
(11) Crick, F. *Nature* **1970**, *227*, 561.
(12) Narendra, P. S.; Michael, T. M.; Raymond, R. T.; Edward, L. S. *Experimental Cell Research* **1988**, *175*, 184.
(13) Douki, T.; Reynaud-Angelin, A.; Cadet, J.; Sage, E. *Biochemistry* **2003**, *42*, 9221.
(14) Cadet, J.; Delatour, T.; Douki, T.; Gasparutto, D.; Pouget, J.; Ravanat, J.; Sauvaigo, S. *Mutat Res.* **1999**, *424*, 9.
(15) Beckman, K. B.; Ames, B. N. *Journal of Biological Chemistry* **1997**, *272*, 19633.
(16) Freese, E. *Proceedings of the National Academy of Sciences of the United States of America* **1959**, *45*, 622.
(17) Eyre-Walker, A.; Keightley, P. D. *Nat Rev Genet* **2007**, *8*, 610.
(18) Pfeifer, G. P. *Technologies for detection of DNA damage and mutations* Plenum press: New York, 1996.
(19) Serjeant, G. R. *Lancet* **1997**, *350*, 725–30.
(20) Gomes de Alvarenga, P.; Zanetti, M. V.; H., E. *Progress in Neuro-Psychopharmacology and Biological Psychiatry* **2008**, *32*, 301.
(21) Hickey, M. A.; Franc, M.; Chesselet, O. *Progress in Neuro-Psychopharmacology & Biological Psychiatry* **2003**, *27*, 255– 265.
(22) Mullis, K. *Scientific American* **1990**, 56.
(23) Gerald, S.; Chin-Yih, O.; Wanda, K. J. *The Journal of Infectious Diseases* **1988**, *158*, 1154.
(24) http://users.ugent.be.
(25) Loryn, N. S.; Graham, R. T. *Human Mutation* **2004**, *23*, 413.
(26) Armour, J. A. L.; Sismani, C.; Patsalis, P. C.; Cross, G. *Nucl. Acids Res.* **2000**, *28*, 605.
(27) Andersen, D. H. *Am. J. Dis. Child.* **1938**, *56*, 344–399.
(28) Di Stagnese, P. A.; Darling, R. C.; Perera, G. A.; Shea, E. *Pediatrics* **1953**, *12*, 549.
(29) Rommens, J. M.; Iannuzzi, M. C.; Kerem, B. S.; Drumm, M. L.; Melmer, G.; Dean, M.; et. al. *Science* **1989**, *245*, 1059–65.

(30) Dodge, J. A.; Morison, S.; Lewis, P. A.; Coles, E. C.; Geddes, D.; Russell, G.; Littlewood, J. M.; Scott, M. T. *Arch. Dis. Child.* **1997**, *77*, 493

(31) Ratjen, F.; Döring, G. *The Lancet* **2003**, *361*, 681.

(32) Riordan, J. R.; Rommens, J. M.; Kerem, B. S.; Alon, N.; Rozmahel, R.; Grzelczak, Z.; and et.al. *Science* **1989**, *245*, 1066–73.

(33) Kerem, B. S.; Rommens, J. M.; Buchanan, J. A.; Markiewicz, D.; Cox, T. K.; Chakravarti, A.; et. al. *Science* **1989**, *245*, 1073–80.

(34) Kevin, W. S.; Anne, M.; Rodney, P.; Georges, T.; Luisa, Z.; Jeannette, D.-R.; Carlo, C. *Journal of cystic fibrosis : official journal of the European Cystic Fibrosis Society* **2007**, *6*, 57.

(35) *Cystic fibrosis*; 6th ed.; Boat, T.; Welsh, M.; Beaudet, A. L., Eds.; McGraw Hill: New York, (1989), pp 2649.

(36) Erts, D.; Polyakov, B.; Olin, H.; Tuite, E. *The Journal of Physical Chemistry B* **2003**, *107*, 3591.

(37) Rowe, S.; Miller, S.; Sorscher, E. *N Engl J Med.* **2005**, *352*, 1992.

(38) Cohn, J.; Friedman, K.; Noone, P.; Knowles, M.; Silverman, L.; Jowell, P. *N Engl J Med.* **1998**, *339*, 653.

(39) Haworth, C.; Selby, P.; Webb, A.; Dodd, M.; Musson, H.; McL Niven, R.; Economou, G.; Horrocks, A.; Freemont, A.; Mawer, E.; Adams, J. *Thorax.* **1999**, *54*, 961.

(40) Alves Cde, A.; Aguiar, R.; Alves, A.; Santana, M. *J Bras Pneumol* **2007**, *33*, 213.

(41) Williams, S.; Westaby, D.; Tanner, M.; Mowat, A. *Br Med Bull.* **1992**, *48*, 877.

(42) Colombo, C.; Russo, M.; Zazzeron, L.; Romano, G. *J Pediatr Gastroenterol Nutr.* **2006**, *43*, 549.

(43) www.nhlbi.nih.gov/health.

(44) Akabas, M. H. *Journal of Biological Chemistry* **2000**, *275*, 3729.

(45) Ratbi, I.; Legendre, M.; Niel, F.; Martin, J.; Soufir, J.-C.; Izard, V.; Costes, B.; Costa, C.; Goossens, M.; Girodon, E. *Hum. Reprod.* **2007**, *22*, 1285.

(46) www.daviddarling.info.

(47) http://prometheus.mse.uiuc.edu.

(48) The Cystic Fibrosis Genotype-Phenotype, C. *N Engl J Med* **1993**, *329*, 1308.

(49) http://student.biology.arizona.edu.

(50) Gibson, L. E.; Cooke, R. E. *Pediatrics* **1959**, *23*, 545.

(51) Davies, J. C.; Alton, E. W. F. W.; Bush, A. *BMJ* **2007**, *335*, 1255.

(52) Rosenstein, B. J.; Cutting, G. R. *The Journal of Pediatrics* **1998**, *132*, 589.

(53) Equi, A.; Balfour-Lynn, I. M.; Bush, A.; Rosenthal, M. *The Lancet* **2002**, *360*, 978.

(54) Hassett, D. J.; Cuppoletti, J.; Trapnell, B.; Lymar, S. V.; Rowe, J. J.; Sun Yoon, S.; Hilliard, G. M.; Parvatiyar, K.; Kamani, M. C.; Wozniak, D. J.; Hwang, S.-H.; McDermott, T. R.; Ochsner, U. A. *Advanced Drug Delivery Reviews* **2002**, *54*, 1425.

(55) Konstan, M. W.; Byard, P. J.; Hoppel, C. L.; Davis, P. B. *N Engl J Med* **1995**, *332*, 848.

(56) Ramsey, B. W. *N Engl J Med* **1996**, *335*, 179.

(57) Banerjee, D.; Stableforth, D. *Drugs* **2000**, *60*, 1053.

(58) Colledge, W. H.; Evans, M. J. *Br Med Bull* **1995**, *51*, 82.

(59) Ferrari, S.; Moro, E.; Pettenazzo, A.; Behr, J.; Zacchello, F.; Scarpa, M. *Gene Therapy* **1997**, *4*, 1100.

(60) Yiping, Y.; Frederick, A. N.; Klara, B.; Eva, G.; John, F. E.; James, M. W. *Nature Genetics* **1994**, *7*, 362.

(61) Caplen, N. J.; Alton, E. W. F. W.; Mddleton, P. G.; Dorin, J. R.; Stevenson, B. J.; Gao, X.; Durham, S. R.; Jeffery, P. K.; Hodson, M. E.; Coutelle, C.; Huang, L.; Porteous, D. J.; Williamson, R.; Geddes, D. M. *Nat Med* **1995**, *1*, 39.

(62) Fisher, K. J.; Choi, H.; Burda, J.; Chen, S.-J.; Wilson, J. M. *Virology* **1996**, *217*, 11.

(63) Phillipson, G. T. M.; Petrucco, O. M.; Matthews, C. D. *Hum. Reprod.* **2000**, *15*, 431.

(64) Cystic Fibrosis Foundation Patient Registry
Annual Data Report 2006.

(65) http://www.jaist.ac.jp.

(66) Arnold, M. A.; Meyerhoff, M. E. *CRC Crit. Revs. Anal. Chem.* **1988**, *20*, 149.

(67) Francis, S. C.; Michael, M.; Aristides, P. *Science* **2003**, *300*, 286.

(68) Pividori, M. I.; Merkoçi, A.; Alegret, S. *Biosensors and Bioelectronics* **2000**, *15*, 291.

(69) Abel, A. P.; Weller, M. G.; Duveneck, G. L.; Ehrat, M.; Widmer, H. M. *Analytical Chemistry* **1996**, *68*, 2905.

(70) Fang, X.; Liu, X.; Schuster, S.; Tan, W. *Journal of the American Chemical Society* **1999**, *121*, 2921.

(71) Zhi, Z.-L.; Morita, Y.; Yamamura, S.; Tamiya, E. *Chem. Commun.* **2005**, *19*, 2448.

(72) Ligler, F. S.; Taitt, C. R. *Optical Biosensors: Present and future.*; Elsevier: Amsterdam, 2002.

(73) Homola, J. *Analytical and Bioanalytical Chemistry* **2003**, *377*, 528.

(74) Lechuga, L. M.; Calle, A.; Prieto, F. *Quim. Anal.* **2000**, *19*, 54.

(75) Pavlov, V.; Xiao, Y.; Gill, R.; Dishon, A.; Kotler, M.; Willner, I. *Analytical Chemistry* **2004**, *76*, 2152.

(76) Niazov, T.; Pavlov, V.; Xiao, Y.; Gill, R.; Willner, I. *Nano Letters* **2004**, *4*, 1683.

(77) Marquette, C. A.; Blum, L. J. *Analytica Chimica Acta* **2004**, *506*, 127.

(78) Mallard, F.; Marchand, G.; Ginot, F.; Campagnolo, R. *Biosensors and Bioelectronics* **2005**, *20*, 1813.

(79) Marquette, C.; Thomas, D.; Degiuli, A.; Blum, L. *Analytical and Bioanalytical Chemistry* **2003**, *377*, 922.

(80) Xu, D. K.; Ma, L. R.; Liu, Y. Q.; Jiang, Z. H.; Liu, Z. H. *Analyst* **1999**, *124*, 533

(81) Yang, M. L.; Liu, C. Z.; Qian, K. J.; He, P. G.; Fang, Y. Z. *Analyst* **2002**, *127*, 1267

(82) Marquette, C. A.; Blum, L. J. *Biosensors and Bioelectronics* **2004**, *20*, 197.

(83) Elghanian, R.; Storhoff, J. J.; Mucic, R. C.; Letsinger, R. L.; Mirkin, C. A. *Science* **1997**, *277*, 1078.

(84) Cao, Y. C.; Jin, R.; Thaxton, C. S.; Mirkin, C. A. *Talanta* **2005**, *67*, 449.

(85) Storhoff, J. J.; Lazarides, A. A.; Mucic, R. C.; Mirkin, C. A.; Letsinger, R. L.; Schatz, G. C. *Journal of the American Chemical Society* **2000**, *122*, 4640.

(86) Charrier, A.; Candoni, N.; Liachenko, N.; Thibaudau, F. *Biosensors and Bioelectronics* **2007**, *22*, 1881.
(87) Taton, T. A.; Lu, G.; Mirkin, C. A. *Journal of the American Chemical Society* **2001**, *123*, 5164.
(88) Graham, H. C.; Andrew, R.; Stuart, B.; Marcus, J. S.; Louise, L. P.; Neville, J. F.; Jian, R. L. *Journal of Physics D: Applied Physics* **2004**, 74.
(89) Cross, G. H.; Reeves, A. A.; Brand, S.; Popplewell, J. F.; Peel, L. L.; Swann, M. J.; Freeman, N. J. *Biosensors and Bioelectronics* **2003**, *19*, 383.
(90) Berney, H.; Oliver, K. *Biosensors and Bioelectronics* **2005**, *21*, 618.
(91) Cao, Y. C.; Jin, R.; Mirkin, C. A. *Science* **2002**, *297*, 1536.
(92) Isola, N. R.; Stokes, D. L.; Vo-Dinh, T. *Analytical Chemistry* **1998**, *70*, 1352.
(93) Vo-Dinh, T.; Stokes, D. L.; Griffin, G. D.; Volkan, M.; Kim, U. J.; Simon, M. I. *Journal of Raman Spectroscopy* **1999**, *30*, 785.
(94) Fabris, L.; Dante, M.; Braun, G.; Lee, S. J.; Reich, N. O.; Moskovits, M.; Nguyen, T.-Q.; Bazan, G. C. *Journal of the American Chemical Society* **2007**, *129*, 6086.
(95) Vo-Dinh, T.; Houck, K.; Stokes, D. L. *Analytical Chemistry* **2002**, *66*, 3379.
(96) Culha, M.; Stokes, D.; Allain, L. R.; Vo-Dinh, T. *Analytical Chemistry* **2003**, *75*, 6196.
(97) Allain, L. R.; Vo-Dinh, T. *Analytica Chimica Acta* **2002**, *469*, 149.
(98) Sungchul, H.; Taekjip, H. *ChemPhysChem* **2005**, *6*, 956.
(99) Willard, D. M.; Van Orden, A. *Nat. Mater.* **2003**, *2*, 275.
(100) Wang, Y.; Zou, J.; Zhao, Z. M.; Hao, Z.; Wang, K. L. *Nanotechnology* **2009**, 305301.
(101) Sun, J.; Wang, L.-W.; Buhro, W. E. *Journal of the American Chemical Society* **2008**, *130*, 7997.
(102) Mee Hyang, K.; Soonhag, K.; Won Jun, K.; Jung Hwan, L.; Hyungu, K.; Sung Hwan, M.; Do Won, H.; Hae Young, K.; Dong Soo, L. *Small* **2009**, *5*, 1207.
(103) Stopa, M.; Marcus, C. M. *Nano Letters* **2008**, *8*, 1778.
(104) Dayal, S.; Burda, C. *Journal of the American Chemical Society* **2008**, *130*, 2890.
(105) Lu, S.; Madhukar, A. *Nano Letters* **2007**, *7*, 3443.
(106) Wang, C. H.; Chen, T. T.; Tan, K. W.; Chen, Y. F.; Cheng, C. T.; Chou, P. T. *Journal of Applied Physics* **2006**, *99*, 123521.
(107) Sören, D. *Small* **2007**, *3*, 1856.
(108) Duan, H.; Nie, S. *Journal of the American Chemical Society* **2007**, *129*, 3333.
(109) Gopar, V. A.; Mendez-Bermudez, J. A.; Aly, A. H. *Phys. Rev. B* **2009**, *79*, 245412.
(110) Homola, J.; Yee, S. S.; Gauglitz, G. *Sensors and Actuators B: Chemical* **1999**, *54*, 3.
(111) http://www.uksaf.org.
(112) Schasfoort, R. B. M.; Tudos, A. J. *Handbook of Surface Plasmon Resonance*; RSC publishing: Cambridge, UK, 2008.
(113) http://www.nature.com/nrd/journal/v1/n7/fig_tab/nrd838_F2.html.
(114) Liedberg, B.; Nylander, C.; Lunström, I. *Sensors and Actuators* **1983**, *4*, 299.

(115) Kooyman, R. P. H.; Kolkman, H.; Van Gent, J.; Greve, J. *Analytica Chimica Acta* **1988**, *213*, 35.

(116) Flanagan, M. T.; Pantell, R. H. *Electronics Letters* **1984**, *20*, 968.

(117) Lundström, I. *Biosensors and Bioelectronics* **1994**, *9*, 725.

(118) Severs, A. H.; Schasfoort, R. B. M.; Salden, M. H. L. *Biosensors and Bioelectronics* **1993**, *8*, 185.

(119) Brecht, A.; Gauglitz, G. *Analytica Chimica Acta* **1997**, *347*, 219.

(120) Jürgen, D.; Jürgen, K.; Oliver, M. *European Journal of Biochemistry* **1998**, *253*, 591.

(121) Regnault, V.; Arvieux, J.; Vallar, L.; Lecompte, T. *Journal of Immunological Methods* **1998**, *211*, 191.

(122) Koh, S. S.; Ansari, A. Z.; Ptashne, M.; Young, R. A. *Molecular Cell* **1998**, *1*, 895.

(123) Chapple, D. S.; Mason, D. J.; Joannou, C. L.; Odell, E. W.; Gant, V.; Evans, R. W. *Infect. Immun.* **1998**, *66*, 2434.

(124) Hanin, V.; Déry, O.; Boquet, D.; Sagot, M.-A.; Christophe, C.; Couraud, J.-Y.; Grassi, J. *Molecular Immunology*, *34*, 829.

(125) Adamczyk, M.; Johnson, D. D.; Mattingly, P. G.; Moore, J. A.; Pan, Y. *Bioconjugate Chemistry* **1998**, *9*, 23.

(126) Jwu-Sheng, T.; Juan, G.; Craig, T. P.; George, M. *Journal of Pharmaceutical Sciences* **1998**, *87*, 76.

(127) Kim, E.; DeMarco, S. J.; Marfatia, S. M.; Chishti, A. H.; Sheng, M.; Strehler, E. E. *Journal of Biological Chemistry* **1998**, *273*, 1591.

(128) Garcia, K. C.; Tallquist, M. D.; Pease, L. R.; Brunmark, A.; Scott, C. A.; Degano, M.; Stura, E. A.; Peterson, P. A.; Wilson, I. A.; Teyton, L. *Proceedings of the National Academy of Sciences of the United States of America* **1997**, *94*, 13838.

(129) Sibille, P.; Strosberg, A. D. *Immunology Letters* **1997**, *59*, 133.

(130) Nakamura, F.; Ito, E.; Hayashi, T.; Hara, M. *Colloids and Surfaces A: Physicochemical and Engineering Aspects* **2006**, *284-285*, 495.

(131) Nakamura, F.; Ito, E.; Sakao, Y.; Ueno, N.; Gatuna, I. N.; Ohuchi, F. S.; Hara, M. *Nano Letters* **2003**, *3*, 1083.

(132) Khilko, S. N.; Corr, M.; Boyd, L. F.; Lees, A.; Inman, J. K.; Margulies, D. H. *J. Biol. Chem.* **1993**, *268*, 15425.

(133) Lofas, S.; Malmquist, M.; Ronnberg, I.; Stenberg, E.; Liedberg, B.; Lundstrom, I. *Sens. Actuators B* **1991**, *5*, 79.

(134) Jung, L. S.; Shumaker-Parry, J. S.; Campbell, C. T.; Yee, S. S.; Gelb, M. H. *j. Am. Chem. Soc.* **2000**, *122*, 4177.

(135) Wink, T.; van Zuilen, S. J.; Bult, A.; van Bennekom, W. P. *Anal. chem.* **1998**, *70*, 827.

(136) Mernagh, D. R.; Janscak, P.; Firman, K.; Kneale, G. G. *Biol.Chem.* **1998**, *379*, 497.

(137) Brockman, J. M.; Frutos, A. G.; Corn, R. M. *J. Am. Chem. Soc.* **1999**, *121*, 8044.

(138) Frutos, A. G.; Brockman, J. M.; Corn, R. M. *Langmuir* **2000**, *16*, 2192.

(139) Bondeson, K.; Frostellkarlsson, A.; Fagerstam, L.; Magnusson, G. *Anal. Biochem.* **1993**, *214*, 245.

(140) Babic, I.; Andrew, S. E.; Jirik, F. R. *Mutat. Res.* **1996**, *372*, 87.

(141) Lin, S.; Long, S.; Ramirez, S. M.; Cotter, R. J.; Woods, A. S. *Anal. Chem.* **2000**, *72*, 2635.

(142) Jordan, C. E.; Frutos, A. G.; Thiel, A. J.; Corn, R. M. *Anal. Chem.* **1997**, *69*, 4939.

(143) Peterlinz, K. A.; Georgiadis, R. M. J. *Anal. Chem.* **1997**, *119*, 3401.

(144) He, L.; Musick, M. D.; Nicewarner, S. R.; Salinas, F. G.; Benkovic, S. J.; Natan, M. J.; Keating, C. D. *J. Am. Chem. Soc.* **2000**, *122*, 9071.

(145) Kai, E.; Sawata, S.; Ikebukuro, K.; Iida, T.; Honda, T.; Karube, I. *Anal. Chem.* **1999**, *71*, 796.

(146) Sota, H.; Hasegawa, Y.; Iwakura, M. *Analytical Chemistry* **1998**, *70*, 2019.

(147) Lofas, S.; Malmqvist, M.; Ronnberg, I.; Stenberg, E.; Liedberg, B.; Lundstrom, I. *Sens. Actuators B* **1991**, *5*, 79.

(148) Bates, P. J.; Dosanjh, H. S.; Kumar, S.; Jenkins, T. C.; Laughton, C. A.; Neidle, S. *Nucleic Acids Res.* **1995**, *23*, 3627.

(149) Nilsson, P.; Persson, B.; Uhlen, M.; Nygren, P. A. *Anal. Biochem.* **1995**, *224*, 400.

(150) Yeatman, E.; Ash, E. A. *Electronics Letters* **1987**, *23*, 1091–1092.

(151) Spadavecchia, J.; Manera, M. G.; Quaranta, F.; Siciliano, P.; Rella, R. *Biosensors and Bioelectronics* **2005**, *21*, 894.

(152) Fiche, J. B.; Fuchs, J.; Buhot, A.; Calemczuk, R.; Livache, T. *Anal. Chem.* **2008**, *80*, 1049–1057.

(153) *T.Springer, et al., Surface plasmon resonance sensor with dispersionless microfluidics for direct detection of nucleic acids at the low femtomole level, Sens. Actuators B: Chem. 2009, doi:10.1016/j.snb.2009.11.018*.

(154) *T. Endo, D. Ikeda, Y. Yanagida, T. Hatsuzawa, Fabrication of core-shell structured nanoparticle layer substrate for excitation of localized surface plasmon resonance and its optical response for DNA in aqueous conditions, Analytica Chimica Acta (2008), doi:10.1016/j.aca.2009.12.022*.

(155) Healey, B. G.; Matson, R. S.; Walt, D. R. *Analytical Biochemistry* **1997**, *251*, 270.

(156) Ali, M. F.; Kirby, R.; Goodey, A. P.; Rodriguez, M. D.; Ellington, A. D.; Neikirk, D. P.; McDevitt, J. T. *Analytical Chemistry* **2003**, *75*, 4732.

(157) Livache, T.; Maillart, E.; Lassalle, N.; Mailley, P.; Corso, B.; Guedon, P.; Roget, A.; Levy, Y. *Journal of Pharmaceutical and Biomedical Analysis* **2003**, *32*, 687.

(158) Ferguson, J. A.; Boles, T. C.; Adams, C. P.; Walt, D. R. *Nature Biotechnology* **1996**, *14*, 1681.

(159) Song, L.; Ahn, S.; Walt, D. R. *Analytical Chemistry* **2006**, *78*, 1023.

(160) Bowden, M.; Song, L.; Walt, D. R. *Analytical Chemistry* **2005**, *77*, 5583.

(161) Zhou, X.; Zhou, J. *Analytical Chemistry* **2004**, *76*, 5302.

(162) Li, J.; Tan, W. H.; Wang, K. M.; Xiao, D.; Yang, X. H.; He, X. X.; Tang, Z. Q. *Analytical Sciences* **2001**, *17*, 1149.

(163) Fan, C.; Plaxco, K. W.; Heeger, A. J. *Proceedings of the National Academy of Sciences of the United States of America* **2003**, *100*, 9134.

(164) Liu, X.; Tan, W. *Analytical Chemistry* **1999**, *71*, 5054.

(165) Guo, Q.; Yang, X.; Wang, K.; Tan, W.; Li, W.; Tang, H.; Li, H. *Nucl. Acids Res.* **2009**, gkn1024.

(166) Yan, J.; Estévez, M. C.; Smith, J. E.; Wang, K.; He, X.; Wang, L.; Tan, W. *Nano Today* **2007**, *2*, 44.

(167) Proudnikov, D.; Timofeev, E.; Mirzabekov, A. *Analytical Biochemistry* **1998**, *259*, 34.

(168) Piunno, P. A. E.; Krull, U. J.; Hudson, R. H. E.; Damha, M. J.; Cohen, H. *Analytical Chemistry* **2002**, *67*, 2635.

(169) Taira, S.; Yokoyama, K. *Biotechnology and Bioengineering* **2004**, *88*, 35.

(170) Zhao, X.; Tapec-Dytioco, R.; Tan, W. *Journal of the American Chemical Society* **2003**, *125*, 11474.

(171) Touahir, L.; Moraillon, A.; Allongue, P.; Chazalviel, J.-N.; Henry de Villeneuve, C.; Ozanam, F.; Solomon, I.; Gouget-Laemmel, A. C. *Biosensors and Bioelectronics* **2009**, *25*, 952.

(172) Shu-yan Niu, Q.-y. L., Rui Ren, Shu-sheng Zhang. *Biosensors and Bioelectronics* **2009**, *24*, 2943.

(173) Silverman, A. P.; Kool, E. T. *Trends in Biotechnology* **2005**, *23*, 225.

(174) Tyagi, S.; Kramer, F. R. *Nat Biotech* **1996**, *14*, 303.

(175) Tyagi, S.; Marras, S. A. E.; Kramer, F. R. *Nat Biotech* **2000**, *18*, 1191.

(176) Campàs, M.; Katakis, I. *TrAC Trends in Analytical Chemistry* **2004**, *23*, 49.

(177) Marras, S. A. E.; Tyagi, S.; Kramer, F. R. *Clinica Chimica Acta* **2006**, *363*, 48.

(178) Leung, Y. F.; Cavalieri, D. *Trends in Genetics* **2003**, *19*, 649.

(179) Hanai, T.; Hamada, H.; Okamoto, M. *Journal of Bioscience and Bioengineering* **2006**, *101*, 377.

(180) Beckers, G. J. M.; Conrath, U. *Trends in Plant Science* **2006**, *11*, 322.

(181) Sassolas, A.; Leca-Bouvier, B. D.; Blum, L. J. *Chemical Reviews* **2008**, *108*, 109.

(182) Xiaojing, L.; William, F.; Sheldon, S.; Weihong, T. *Analytical Biochemistry* **2000**, *283*, 56.

(183) Mustafa, C.; David, L. S.; Guy, D. G.; Tuan, V. *Biosensors and Bioelectronics* **2004**, *19*, 1007.

(184) Tu, Y.; Stolovitzky, G.; Klein, U. *Proceedings of the National Academy of Sciences of the United States of America* **2002**, *99*, 14031.

(185) Kaderali, L.; Schliep, A. *Bioinformatics* **2002**, *18*, 1340.

(186) Vikalo, H.; Hassibi, B.; Hassibi, A. *IEEE Trans. Signal Process.* **2006**, *54*, 2444.

(187) Vallone, M.; Jakupciak, J. P.; Coble, M. D. *Forensic Science International: Genetics* **2007**, *1*, 196.

(188) http://www.affymetrix.com.

(189) Drummond, T. G.; Hill, M. G.; Barton, J. K. *Nat Biotech* **2003**, *21*, 1192.

(190) Gooding, J. J. *Electroanalysis* **2002**, *14*, 1149.

(191) Bakker, E.; Telting-Diaz, M. *Analytical Chemistry* **2002**, *74*, 2781.

(192) Edman, C. F.; Raymond, D. E.; Wu, D. J.; Tu, E.; Sosnowski, R. G.; Butler, W. F.; Nerenberg, M.; Heller, M. J. *Nucl. Acids Res.* **1997**, *25*, 4907.

(193) Sosnowski, R. G.; Tu, E.; Butler, W. F.; Connell, J. P.; Heller, M. J. *Proceedings of the National Academy of Sciences of the United States of America* **1997**, *94*, 1119.

(194) Palecek, E. *Nature* **1960**, *188*, 656.

(195) Palecek, E. *Analytical Biochemistry* **1988**, *170*, 421.

(196) Singhal, P.; Kuhr, W. G. *Analytical Chemistry* **1997**, *69*, 4828.

(197) Lucarelli, F.; Marrazza, G.; Turner, A. P. F.; Mascini, M. *Biosensors and Bioelectronics* **2004**, *19*, 515.

(198) Yang, M.; McGovern, M. E.; Thompson, M. *Analytica Chimica Acta* **1997**, *346*, 259.

(199) Palek, E.; Fojta, M. *Analytical Chemistry* **2001**, *73*, 74 A.
(200) Chidsey, C. E. D.; Loiacono, D. N. *Langmuir* **2002**, *6*, 682.
(201) Wink, T.; van Zuilen, S. J.; Bult, A.; van Bennkom, W. P. *Analyst* **1997**, *122*, 43R
(202) Chaki, N. K.; Vijayamohanan, K. *Biosensors and Bioelectronics* **2002**, *17*, 1.
(203) Zhao, Y.-D.; Pang, D.-W.; Hu, S.; Wang, Z.-L.; Cheng, J.-K.; Dai, H.-P. *Talanta* **1999**, *49*, 751.
(204) Christine, B.; Per, S.; Jan, B.; Gillis, J. *Electroanalysis* **1999**, *11*, 156.
(205) Sun, X.; He, P.; Liu, S.; Ye, J.; Fang, Y. *Talanta* **1998**, *47*, 487.
(206) Kerman, K.; Ozkan, D.; Kara, P.; Meric, B.; Gooding, J. J.; Ozsoz, M. *Analytica Chimica Acta* **2002**, *462*, 39.
(207) Nakayama, M.; Ihara, T.; Nakano, K.; Maeda, M. *Talanta* **2002**, *56*, 857.
(208) Patolsky, F.; Katz, E.; Bardea, A.; Willner, I. *Langmuir* **1999**, *15*, 3703.
(209) Bardea, A.; Patolsky, F.; Dagan, A.; Willner, I. *Chem. Commun.* **1999**, 21.
(210) Alfonta, L.; Bardea, A.; Khersonsky, O.; Katz, E.; Willner, I. *Biosensors and Bioelectronics* **2001**, *16*, 675.
(211) Hianik, T.; Gajdos, V.; Krivanek, R.; Oretskaya, T.; Metelev, V.; Volkov, E.; Vadgama, P. *Bioelectrochemistry* **2001**, *53*, 199.
(212) Nuzzo, R. G.; Allara, D. L. *Journal of the American Chemical Society* **1983**, *105*, 4481.
(213) Hashimoto, K.; Ito, K.; Ishimori, Y. *Analytical Chemistry* **1994**, *66*, 3830.
(214) Hiroshi, A.; Philippe, B.; Yoshio, U. *Electroanalysis* **2000**, *12*, 1272.
(215) Boon, E. M.; Salas, J. E.; Barton, J. K. *Nat Biotech* **2002**, *20*, 282.
(216) Kelley, S. O.; Barton, J. K.; Jackson, N. M.; Hill, M. G. *Bioconjugate Chemistry* **1997**, *8*, 31.
(217) Tesfaye, R. S.; S., J.; Ciara, K. O. S. *Chem. Phys. Chem.* **2008**, *9*, 920 – 927.
(218) Herne, T. M.; Tarlov, M. J. *Journal of the American Chemical Society* **1997**, *119*, 8916.
(219) Levicky, R.; Herne, T. M.; Tarlov, M. J.; Satija, S. K. *Journal of the American Chemical Society* **1998**, *120*, 9787.
(220) Steel, A. B.; Herne, T. M.; Tarlov, M. J. *Analytical Chemistry* **1998**, *70*, 4670.
(221) Takenaka, S.; Yamashita, K.; Takagi, M.; Uto, Y.; Kondo, H. *Analytical Chemistry* **2000**, *72*, 1334.
(222) Kertesz, V.; Whittemore, N. A.; Chambers, J. Q.; McKinney, M. S.; Baker, D. C. *Journal of Electroanalytical Chemistry* **2000**, *493*, 28.
(223) Kelley, S. O.; Boon, E. M.; Barton, J. K.; Jackson, N. M.; Hill, M. G. *Nucl. Acids Res.* **1999**, *27*, 4830.
(224) Umek, R. M.; Lin, S. W.; Vielmetter, J.; Terbrueggen, R. H.; Irvine, B.; Yu, C. J.; Kayyem, J. F.; Yowanto, H.; Blackburn, G. F.; Farkas, D. H.; Chen, Y.-P. *J Mol Diagn* **2001**, *3*, 74.
(225) Danke, X.; Kai, H.; Zhihong, L.; Yaoqing, L.; Liren, M. *Electroanalysis* **2001**, *13*, 882.
(226) Yang, M.; Yau, H. C. M.; Chan, H. L. *Langmuir* **1998**, *14*, 6121.
(227) Gao, Z.; Rafea, S.; Lim, L. H. *Advanced Materials* **2007**, *19*, 602.

(228) He, W.; Yang, Q. J.; Liu, Z. H.; Yu, X. B.; Xu, D. K. *ANal. lett.* **2005**, *38*, 2567.

(229) Azek, F.; Grossiord, C.; Joannes, M.; Limoges, B.; Brossier, P. *Analytical Biochemistry* **2000**, *284*, 107.

(230) Pan, J. *Biochemical Engineering Journal* **2007**, *35*, 183.

(231) Alfonta, L.; Singh, A. K.; Willner, I. *Analytical Chemistry* **2000**, *73*, 91.

(232) Dominguez, E.; Rincon, O.; Narvaez, A. *Analytical Chemistry* **2004**, *76*, 3132.

(233) Xie, H.; Zhang, C.; Gao, Z. *Analytical Chemistry* **2004**, *76*, 1611.

(234) Kavanagh, P.; Leech, D. *Analytical Chemistry* **2006**, *78*, 2710.

(235) Del Giallo, M. L.; Ariksoysal, D. O.; Marrazza, G.; Mascini, M. *Anal. lett.* **2005**, *38*, 2509.

(236) Miranda-Castro, R.; de-los-Santos-Alvarez, P.; Lobo-Castanon, M. J.; Miranda-Ordieres, A. J. *Analytical Chemistry* **2007**, *79*, 4050.

(237) Carpini, G.; Lucarelli, F.; Marrazza, G.; Mascini, M. *Biosensors and Bioelectronics* **2004**, *20*, 167.

(238) Lucarelli, F.; Marrazza, G.; Mascini, M. *Biosensors and Bioelectronics* **2005**, *20*, 2001.

(239) Aguilar, Z. P.; Fritsch, I. *Analytical Chemistry* **2003**, *75*, 3890.

(240) Hernandez-Santos, D.; Diaz-Gonzalez, M.; Gonzalez-Garcia, M. B.; Costa-Garcia, A. *Analytical Chemistry* **2004**, *76*, 6887.

(241) Suye, S.; Matsuura, T.; Kimura, T.; Zheng, H.; Hori, T.; Amano, Y.; Katayama, H. *Microelectronic Engineering* **2005**, *81*, 441.

(242) Ikebukuro, K.; Kohiki, Y.; Sode, K. *Biosensors and Bioelectronics* **2002**, *17*, 1075.

(243) Fortin, E.; Mailley, P.; Lacroix, L.; Szunerits, S. *Analyst* **2006**, *131*, 186.

(244) Guido, C.; Fausto, L.; Giovanna, M.; Marco, M. *Biosensors and Bioelectronics* **2004**, *20*, 167.

(245) Wang, J.; Li, J.; Baca, A. J.; Hu, J.; Zhou, F.; Yan, W.; Pang, D.-W. *Analytical Chemistry* **2003**, *75*, 3941.

(246) Alfred , J. B.; Feimeng, Z.; Jun, W.; Jingbo, H.; Jinhua, L.; Jianxiu, W.; Zarui , S. C. *Electroanalysis* **2004**, *16*, 73.

(247) Le Floch, F.; Ho, H. A.; Harding-Lepage, P.; Bedard, M.; Neagu-Plesu, R.; Leclerc, M. *Advanced Materials* **2005**, *17*, 1251.

(248) Zai-Sheng, W.; Jian-Hui, J.; Guo-Li, S.; Ru-Qin, Y. *Human Mutation* **2007**, *28*, 630.

(249) Cai, H.; Xu, C.; He, P.; Fang, Y. *Journal of Electroanalytical Chemistry* **2001**, *510*, 78.

(250) Xu, C.; Cai, H.; He, P. G.; Fang, Y. Z. *Analyst* **2001**, *126*, 62.

(251) Ihara, T.; Maruo, Y.; Takenaka, S.; Takagi, M. *Nucl. Acids Res.* **1996**, *24*, 4273.

(252) Beilstein, A. E.; Grinstaff, M. W. *Chem. Commun.* **2000**, 509.

(253) Takenaka, S.; Uto, Y.; Saita, H.; Yokoyama, M.; Kondo, H.; Wilson, W. D. *Chem. Commun.* **1998**, 1111.

(254) Zhang, Y.; Wang, Y.; Wang, H.; Jiang, J.-H.; Shen, G.-L.; Yu, R.-Q.; Li, J. *Analytical Chemistry* **2009**, *81*, 1982.

(255) Kang, D.; Zuo, X.; Yang, R.; Xia, F.; Plaxco, K. W.; White, R. J. *Analytical Chemistry* **2009**, *81*, 9109.

(256) Holden Thorp, H. *Trends in Biotechnology* **2003**, *21*, 522.

(257) Erdem, A.; Kerman, K.; Meric, B.; Akarca, U. S.; Ozsoz, M. *Analytica Chimica Acta* **2000**, *422*, 139.

(258) Meric, B.; Kerman, K.; Ozkan, D.; Kara, P.; Erensoy, S.; Akarca, U. S.; Mascini, M.; Ozsoz, M. *Talanta* **2002**, *56*, 837.

(259) Teh, H. F.; Gong, H.; Dong, X.-D.; Zeng, X.; Lai Kuan Tan, A.; Yang, X.; Tan, S. N. *Analytica Chimica Acta* **2005**, *551*, 23.

(260) Wang, S. G.; Wang, R.; Sellin, P. J.; Zhang, Q. *Biochemical and Biophysical Research Communications* **2004**, *325*, 1433.

(261) Boon, E. M.; Barton, J. K.; Bhagat, V.; Nersissian, M.; Wang, W.; Hill, M. G. *Langmuir* **2003**, *19*, 9255.

(262) Boon, E. M.; Ceres, D. M.; Drummond, T. G.; Hill, M. G.; Barton, J. K. *Nat Biotech* **2000**, *18*, 1318.

(263) Boal, A. K.; Barton, J. K. *Bioconjugate Chemistry* **2005**, *16*, 312.

(264) Arzum, E.; Kagan, K.; Burcu, M.; Mehmet, O. *Electroanalysis* **2001**, *13*, 219.

(265) Lin, X.-H.; Wu, P.; Chen, W.; Zhang, Y.-F.; Xia, X.-H. *Talanta* **2007**, *72*, 468.

(266) Henry, O. Y. F.; Acero Sanchez, J. L.; Latta, D.; O'Sullivan, C. K. *Biosensors and Bioelectronics* **2009**, *24*, 2064.

(267) Xiao, Y.; Lou, X.; Uzawa, T.; Plakos, K. J. I.; Plaxco, K. W.; Soh, H. T. *Journal of the American Chemical Society* **2009**, *131*, 15311.

(268) Hejazi, M. S.; Pournaghi-Azar, M. H.; Ahour, F. *Analytical Biochemistry*, *In Press, Accepted Manuscript*.

(269) Siddiquee, S.; Yusof, N. A.; Salleh, A. B.; Bakar, F. A.; Heng, L. Y. *Bioelectrochemistry*, *In Press, Corrected Proof*.

(270) Napier, M. E.; Loomis, C. R.; Sistare, M. F.; Kim, J.; Eckhardt, A. E.; Thorp, H. H. *Bioconjugate Chemistry* **1997**, *8*, 906.

(271) García, T.; Casero, E.; Revenga-Parra, M.; Martín-Benito, J.; Pariente, F.; Vázquez, L.; Lorenzo, E. *Biosensors and Bioelectronics* **2008**, *24*, 184.

(272) Millan, K. M.; Mikkelsen, S. R. *Analytical Chemistry* **2002**, *65*, 2317.

(273) Kelly, M. M.; Aleksandrs, J. S.; Susan, R. M. *Electroanalysis* **1992**, *4*, 929.

(274) Pjura, P. E.; Grzeskowiak, K.; Dickerson, R. E. *Journal of Molecular Biology* **1987**, *197*, 257.

(275) Ito, K.; Hashimoto, K.; Ishimori, Y. *Analytica Chimica Acta* **1996**, *327*, 29.

(276) Hashimoto, K.; Ito, K.; Ishimori, Y. *Analytical Chemistry* **2002**, *66*, 3830.

(277) Choi, Y.-S.; Lee, K.-S.; Park, D.-H. *Current Applied Physics* **2006**, *6*, 777.

(278) Yong-Sung, C.; Kyung-Sup, L.; Dae-Hee, P. *Journal of Micromechanics and Microengineering* **2005**, *15*, 1938.

(279) Choi, Y.-S.; Park, D. H. *J. Korean Phys. Soc.* **2004**, *44*, 1556.

(280) Toshiba: Press Releases 20 June 2003. http://www.toshiba.co.jp/about/press/2003_06/pr2001.htm.

(281) Masaaki, K.; Takashi, K.; Masato, S.; Sakiko, K.; Miyuki, O.; Shinichiro, I.; Yasutaka, M.; Quamrul, H.; Eiichi, T. *Electrochemistry Communications* **2004**, *6*, 337.

(282) Wong, E. L. S.; Gooding, J. J. *Analytical Chemistry* **2003**, *75*, 3845.

(283) Wong, E. L. S.; Mearns, F. J.; Gooding, J. J. *Sensors and Actuators B: Chemical* **2005**, *111-112*, 515.

(284) Wong, E. L. S.; Erohkin, P.; Gooding, J. J. *Electrochemistry Communications* **2004**, *6*, 648.

(285) Liu, S.; Ye, J.; He, P.; Fang, Y. *Analytica Chimica Acta* **1996**, *335*, 239.

(286) Wang, J.; Rivas, G.; Fernandes, J. R.; Lopez Paz, J. L.; Jiang, M.; Waymire, R. *Analytica Chimica Acta* **1998**, *375*, 197.

(287) Wang, J.; Kawde, A.-N. *Analytica Chimica Acta* **2001**, *431*, 219.

(288) Erdem, A.; Pividori, M. I.; Lermo, A.; Bonanni, A.; Valle, M. d.; Alegret, S. *Sensors and Actuators B: Chemical* **2006**, *114*, 591.

(289) Kagan, K.; Dilsat, O.; Pinar, K.; Arzum, E.; Burcu, M.; Peter , E. N.; Mehmet, O. *Electroanalysis* **2003**, *15*, 667.

(290) Pan, S.; Rothberg, L. *Langmuir* **2005**, *21*, 1022.

(291) Travas-Sejdic, J.; Peng, H.; Kilmaitin, P. A.; Cannell, M. B.; Bowmaker, G. A.; Cooney, R. P.; Soeller, C. *Synthetic Metals* **2005**, *152*, 37.

(292) Zebda, A.; Labeau, M.; Diard, J. P.; Lavalley, V.; Stambouli, V. *Sensors and Actuators B: Chemical*, *In Press, Accepted Manuscript*.

(293) Guan, J.; Miao, Y.; Zhang, Q. *Journal of Bioscience and Bioengineering* **2004**, *97*, 219.

(294) Simon, D. K.; Peng, L.; Pedro, E.; Piero, M. *Biosensors and Bioelectronics* **2008**, *23*, 1291.

(295) Clark, D. P. *Molecular biology*; Elsevier: UK, 2005.

(296) Breslauer, K., J.; Frank, R.; Blocker, H.; Marky, L. A. *Proc. Natl. Acad. Sci. USA* **1986**, *83*, 3746.

(297) Wallace, R. B.; Shaffer, J.; Murphy, R. F.; Bonner, J.; Hirose, T.; Itakura, K. *Nucl. Acids Res.* **1979**, *6*, 3543.

(298) Oweczarzy, R. *Biophysical chemistry* **2005**, *117*, 207.

(299) Peterlinz, K. A.; Georgiadis, R. M.; Herne, T. M.; Tarlov, M. J. *Journal of the American Chemical Society* **1997**, *119*, 3401.

(300) Piunno, P. A. E.; Watterson, J.; Wust, C. C.; Krull, U. J. *Analytica Chimica Acta* **1999**, *400*, 73.

(301) Lehr, H. P.; Reimann, M.; Brandenburg, A.; Sulz, G.; Klapproth, H. *Analytical Chemistry* **2003**, *75*, 2414.

(302) Finot, E.; Bourillot, E.; Meunier-Prest, R.; Lacroute, Y.; Legay, G.; Cherkaoui-Malki, M.; Latruffe, N.; Siri, O.; Braunstein, P.; Dereux, A. *Ultramicroscopy*, *97*, 441.

(303) Meunier-Prest, R.; Raveau, S.; Finot, E.; Legay, G.; Cherkaoui-Malki, M.; Latruffe, N. *Nucl. Acids Res.* **2003**, *31*, e150.

(304) Brewood, G. P.; Rangineni, Y.; Fish, D. J.; Bhandiwad, A. S.; Evans, D. R.; Solanki, R.; Benight, A. S. *Nucl. Acids Res.* **2008**, *36*, e98.

(305) Proll, F.; Mohrle, B.; Kumpf, M.; Gauglitz, G. *Anal.Bional.Chem.* **2005**, *382*, 1889.

(306) Wang, X.; Krull, U. J. *Bioorganic & Medicinal Chemistry Letters* **2005**, *15*, 1725.

(307) Annette-Enrica, S.; Gerd-Uwe, F. *Electroanalysis* **2009**, *21*, 1119.

(308) Howell, W. M.; Jobs, M.; Gyllensten, U.; Brookes, A. J. *Nat Biotech* **1999**, *17*, 87.

ISBN:978-84-693-3386-0/DL:T.1002-2010

CHAPTER 2 (Art.1):

Cystic Fibrosis: a label-free detection approach based on temperature assisted Electrochemical Impedance Spectroscopy

UNIVERSITAT ROVIRA I VIRGILI
TEMPERATURE MODULATED GENOSENSOR FOR DETECTION OF CYSTIC FIBROSIS MUTATIONS
Hany Abdel Hady Abdel Rahman Nasef
ISBN:978-84-693-3386-0/DL:T.1002-2010

Cystic Fibrosis: a label-free detection approach based on thermally modulated Electrochemical Impedance Spectroscopy.

Hany Nasef[1], Valerio Beni[1], Veli C. Őzalp[1] and Ciara K. O'Sullivan*[1,2]

[1] *Nanobiotechnology & Bioanalysis Group, Department of Chemical Engineering, Universitat Rovira i Virgili, Avinguda Països Catalans, 26, 43007 Tarragona, Spain*

[2] *Institucio Catalana de Recerca i Estudis Avançats, Passeig Lluis Companys 23, 08010, Barcelona, Spain*

Corresponding Authors: Ciara.osullivan@urv.cat; Valerio.beni@urv.cat

Fax: 0034-977-558205

Abstract

Cystic fibrosis is one of the most common genetically inherited diseases in Northern Europe, with the DF508 mutation being the most common, among the Caucasian population being responsible for almost the 70 % of the cases.

In this work, we report on the use of thermally modulated electrochemical impedance spectroscopy for the discrimination of the DF508 mutation from the wild type sequence. DNA probe (15 and 21 bases long) were immobilised on the surface of gold electrodes and the variation of the charge-transfer resistance (R_{CT}) monitored as a function of hybridisation. Two sets of targets have been used in this work: synthetic 15 mer sequences and two single stranded synthetic analogues of PCR products of 82 (Mutant) and 85 (Wild type) bases long

Hybridisation with short targets resulted in very sequence specific charge-transfer resistance variation with a discrimination factor at room temperature, between fully complementary and mismatched sequence, of ca. 5-fold. However in the case of the single stranded synthetic PCR product analogues a lower discrimination factor was recorded (1.5 fold). Temperature was investigated to improve discrimination and the use of a post-hybridisation wash at elevated temperature resulted in a 5-fold improvement in the discrimination factor. Using an electrode array with probes immobilised against

ISBN:978-84-693-3386-0/DL:T.1002-2010

each of mutant and wild type sequences, an unequivocal detection of the DF508 mutation was achieved.

Keywords: Electrochemical Impedance Spectroscopy; Cystic Fibrosis; label-less detection; DNA sensor; DF508.

1. Introduction:

Cystic fibrosis (CF) is one of the most common life-shortening, childhood-onset inherited diseases, which manifests itself as an inherited defect of chloride transport in the epithelium, resulting in damage to lung, sweat glands and the pancreatic glands, causing progressive disability, and, for most, early death [1-5]. The incidence of CF is 1 in 2,500 live births in the Caucasian population [2, 3]. Moreover, CF is the most common genetic disease among the population of European descent; 1 in 22 people carry one gene for CF [6]. CF is caused by mutations in a gene called the *cystic fibrosis transmembrane conductance regulator* (CFTR). The CFTR protein is a transport protein that functions as an ion channel and is involved in the regulation of the production of sweat, digestive juices and mucus. Although most people without CF have two functional copies of the CFTR gene, only one is needed to prevent cystic fibrosis; CF develops when neither gene works normally. Therefore, CF is classified as an autosomal recessive disease. The name cystic fibrosis refers to the characteristic 'fibrosis' (tissue scarring) of the biliary tract ("cystic" being a generic term for all that is related to the biliary vesicle and/or the bladder), and was first thus named in the 1930s [1, 5, 6].

Almost 1,000 mutations, divided into six classes based mainly on the molecular fate of CFTR [4], have been identified in the CF gene. The majority of the cases can, however, be related to the presence of a limited number of mutations, of which DF508 is the most common, consisting of the deletion of the phenylalanine at position 508 of the amino acid sequence of CFTR (DF508). Its frequency varies between ethnic groups, for example it is responsible for the 70% of the cases in the white populations of Britain and US, and approximately 50% in southern European populations.

ISBN:978-84-693-3386-0/DL:T.1002-2010

Surface plasmon resonance (SPR) and biosensor technologies have been reported for CF detection. Giordana et al. [7] reported on the use of SPR for the detection of DF508 PCR product, and Mannelli et al. reported the development of a surface plasmon resonance imaging (SPRI) approach, based DNA microarray affinity sensors, to detect in parallel several mutations causing cystic fibrosis DF508, DI507, M470V, Q493X, V520F and 1716 G>A [8].

Nucleic acid detection is one of the challenges of modern biotechnology and current medical diagnostics. Genosensors or sequence-selective DNA biosensors, have received much attention in recent years [9-13]. The transduction of the hybridisation event in these sensors can be performed with the use of, for example, fluorescent or chemiluminescent labels [14-16], or in a label-less format, using surface plasmon resonance, piezoelectric techniques or atomic force microscopy [17-20]. Although widely used and sensitive, these methods are lengthy and costly. An attractive alternative is the use of electrochemical transduction [21-27], which offers the advantages of being rapid, cost-effective, easy to use and implementable in miniaturised devices. Millan et al. [28] reported on the use of modified carbon paste electrode, combined with the use of electroactive DNA intercalators, for the voltammetric detection of the DF508 mutation; more recently Marin and Gan [29, 30] reported the use of nanoparticle based electrochemical sensor for the detection of CF. Mir et al, had demonstrated an electrochemical biosensor for the detection of cystic fibrosis based on sub-optimum displacement [31].

Impedance spectroscopy is a powerful tool for the analysis of surface phenomena and changes of bulk properties [23, 32, 33]. Impedimetric based biosensors are bioelectronic devices that make use of the interactions of biomolecules with a conductive (or semiconducting) transducer surface. Detection involves the formation of a recognition complex between the sensing biomolecule and the analyte at the interface of the electronic transducer, which alters the electrical properties of the recognition surface [34-38], which can be subsequently converted into a quantifiable signal.

Melting temperature is a particular characteristic of dsDNA and is a function of the duplex composition and of the number of mismatches present in the duplex, And

ISBN:978-84-693-3386-0/DL:T.1002-2010

temperature control has been used as a tool to modulate/control the hybridisation event [22]-[28].

In this work we propose, to the best of our knowledge, for the first time the use of a thermally modulated electrochemical impedance spectroscopy approach for the label-less detection of real length PCR analogues. In the reported work it is clearly shown that the use of EIS, in combination with a temperature controlled post-hybridisation wash facilitated a rapid and effective discrimination of DF508 cystic fibrosis mutant and wild type sequences.

2. Experimental

2.1 Chemicals, probes and targets

All chemicals and reagents: Trizma base (Sigma), Potassium hexacyanoferrate (III), $K_3Fe(CN)_6$ (Sigma), hydrochloric acid (6M, Scharlau), potassium dihydrogen phosphate KH_2PO_4 (Scharlau), sodium chloride NaCl (Scharlau), sodium hydroxide NaOH pellets (Panreac), sulphuric acid H_2SO_4 (Sigma) mercaptohexanol, MCH, (Fluka) and potassium hexacyanoferrate (II) $K_4Fe(CN)_6$ (Fluka), Phosphate Buffered Saline, pH 7.4, with Tween 20, PBS-T (Sigma) and methylene blue, MB, (Fluka) were of analytical grade. Alumina powder (1, 0.3, 0.05 micron) was provided by (CHI Instrument, U.K.). MilliQ water (18 MΩ.cm) was obtained using a "Simplicity Water Purification System" (Millipore, France).

Oligonucleotides were provided by the VBC-Biotech Company (Service GmbH Campus Vienna, Austria) and Eurogentec (Eurogentec, Spain). Sequences were selected according to those reported by Riordan et al. [39].

The sequences of the oligonucleotides employed in this work are listed below:

- Short mutant target (**Mut_{short}**): 5' AATATCATTGGTGTT 3'
- Short wild type target (**WT_{short}**): 5' TATCAT**<u>CTT</u>** TGGTGT 3'
- Single stranded analogue of mutant PCR product (**Mut_{long}**): 5'GCCGCGAATTCACTAGTGTGGCACCATTAAAGAAAATATCATTGGT GTTTCCTATGATGAATATAATCGAATTCCCGCGGCC 3'

ISBN:978-84-693-3386-0/DL:T.1002-2010

- Single stranded analogue of wild type PCR product (**WT_{long}**): 5'GCCGCGAATTCACTAGTGTGGCACCATTAAAGAAAATATCAT**CTT**T GGTGTTTCCTATGATGAATATAATCGAATTCCCGCGGCC 3'
- 15 mer probe (**$Mut_{15probe}$**): 5' AACACCAATGATATT-(C6)-SH 3'
- 21 mer probe (**$Mut_{21probe}$**): 5' GGAAACACCAATGATATTTTC-(C6)-SH 3'
- 21 mer probe (**$WT_{21probe}$**): 5' GAAACACCAAAGATGATATTT-(C6)-SH 3'

The mutation site found in the CF DF508 mutant is highlighted in bold in the listed WT sequences.

2.2 Instrumentation

Electrochemical studies were carried out using an Autolab model PGSTAT 12 potentiostat/galvanostat controlled with the General Purpose Electrochemical System (GPES) software (Eco Chemie B.V., The Netherlands), equipped with a FRA2 module for electrochemical impedance spectroscopy. All the electrochemical measurements, if not otherwise specified, were performed at room temperature.

A set of commercially available Au disk (2 mm diameter) electrodes (CHI Instruments) were used as working electrode, an Ag/AgCl was used as reference electrode (CHI Instruments) and a Pt wire (Sigma) was used as counter electrode.

SPR measurements were performed using a Biacore 3000 and the sensograms were analyzed using Biaevaluation software (Biacore). Experiments at controlled temperature were performed using the Biacore implemented temperature controller module.

In the impedimetric experiments, sensor heating was performed using a Thermomixer compact (Eppendorf Iberica, Spain); this was performed by immersing the sensor in an Eppendorf containing 500 µl of the buffer previously stabilised to the desired temperature.

2.3 Procedures

2.3.1 Electrochemical sensor preparation

Previous to surface functionalising the working electrodes were thoroughly cleaned using a two-step protocol: (i) mechanical, followed by (ii) electrochemical cleaning.

ISBN:978-84-693-3386-0/DL:T.1002-2010

The mechanical cleaning consisted of polishing the gold working electrode surface with alumina (using three different sizes: 1, 0.3, 0.05 micron) aqueous slurry, to a mirror finish. After rinsing with MilliQ water the electrode was electrochemically cleaned by cycling it ca. 40 times (scan rate 100 mVs^{-1}) between -0.2 and 1.6 V vs. Ag/AgCl reference electrode in sulphuric acid 0.5 M. The number of cycles was not fixed: the gold electrode was considered clean when, in a cyclic voltammetric experiment with a ferro\ferri equimolar solution, a peak to peak separation below 80 mV was recorded.

Following electrochemical cleaning, immobilisation of the probe was performed. Surface functionalisation was achieved using the well-known backfilling approach where the a thiolated DNA probe (is primarily chemisorbed followed by the chemisorption of a short chain alkanethiol [40], and allowed to self-assemble to form a mixed SAM.

Briefly: 50 µLs of a 4 µM solution of the thiolated probe, freshly prepared in 1 M KH_2PO_4, were spotted onto the electrode surface and chemisorbed for 3 hours [40] in an humidified chamber to prevent evaporation.

Following this step the electrode was washed with Milli-Q water and then back-filled by spotting 50 µl of a 0.01M aqueous solution of mercaptohexanol (MCH) for 30 minutes [40]. Finally the electrode was thoroughly washed by sequential immersion in 0.1 M NaOH, MilliQ water, 0.1 M HCl and MilliQ water in order to remove physisorbed probes, leaving an organized mixed SAM of chemisorbed DNA probe and MCH.

2.3.2 Hybridisation

Hybridisation was carried out via the addition of 50µL of 2µM of unlabelled target (mutant or wild type) in 10 mM Trizma pH 7.4 in the presence of 0.5M NaCl to the surface of the electrode modified as described previously, and incubating for 1 hour in a humidity chamber. The electrode was then washed with an aliquot of 10 mM Trizma pH 7.4 containing 0.5M NaCl and hybridisation levels probed using cyclic voltammetry (CV) (100 mVs^{-1} scan rate) and electrochemical impedance spectroscopy (EIS).

ISBN:978-84-693-3386-0/DL:T.1002-2010

In the case of the thermally modulated EIS experiments, the sensors (after hybridisation) were washed for 10 minutes in an aliquot of the hybridisation buffer set at 40 ºC prior to transfer of the electrode to the measuring cell.

2.3.3 Electrochemical Impedance spectroscopy (EIS)

The EIS measurements were performed by sweeping the frequency between 10000 and 0.1 Hz with a pulse amplitude of 5 mV. The fixed potential used in the different experiments was the "open circuit potential" calculated automatically by the potentiostat. The redox couple $[Fe(CN)_6]^{3-/4-}$, in an equimolar concentration of 2 (1 +1) mM, in Trizma buffer 10 mM + 0.5 M NaCl pH 7.4 was used as redox marker.

2.3.4 Differential Pulse Voltammetry (DPV)

The DPV experiments were performed by immersing the sensor in a solution of 20 µM methylene blue (MB) in Trizma buffer 10 mM + 0.5 M NaCl pH 7.4 for 5 minutes, and subsequently carrying out DPV analysis (potential between 0 and -0.6 V vs. Ag/AgCl). Electrode regeneration (removal of the MB) was performed by immersion for 2 minutes in 100 mM NaOH solution [41].

2.3.5 Surface Plasmon Resonance (SPR) Analysis:

SPR was used as supporting technique to confirm EIS results and to study the effect of the temperature on the on surface hybridisation process. Gold SPR chips were modified as following: thiolated probes 15 ($Mut_{15probe}$) or 21 ($Mut_{21probe}$ or $WT_{21probe}$) bases long, were immobilised on gold surfaces (Biacore Au chip) by injecting (injection rate 5 $\mu l.min^{-1}$) 20 µl of a 4 µM solution in 1 M KH_2PO_4 at room temperature (ca. 21 ºC). The injection was repeated twice. Approximately 1000 resonance unit (RU) immobilisation levels was achieved for each probe, equivalent to ca. 15 $pmolcm^{-2}$ of immobilised probe. Following probe immobilisation backfilling was performed by injection of 20 µl of a 10 mM solution of MCH in water (injection rate 5 $\mu l.min^{-1}$).

Hybridisation was performed by injecting (injection rate 5 $\mu l.min^{-1}$) 20 µl of a solution 0.5 µM of the two synthetic PCR analogous (Mut_{long} or WT_{long}) in PBS-T buffer.

ISBN:978-84-693-3386-0/DL:T.1002-2010

Between two consecutive hybridisation experiments the sensor surface was regenerated by injecting (injection rate 15 µl.min^{-1}) 50 µl of a solution 100 mM of NaOH. The Au chip was heated through the Biacore built-in thermostatting system to reach a maximum of 40 ºC. Once the Biacore signal plateaus for each desired temperature, this limit was taken as the RU value corresponding to the measured temperature.

3. Results and Discussion

3.1 Sensor preparation and characterisation

Schematic illustrations of the sensor surface preparation and EIS measurements are depicted in Figure 1A. In Figure 1B the electrochemical impedance spectra and the cyclic voltammetric responses (inset), obtained during the different steps of the sensor surface preparation (as from Figure 1A) are presented. As expected, the self-assembling of the thiol modified DNA probes was associated with a strong increase of the charge-transfer component (R_{ct}) of the EIS response ("probe immobilisation" curve in Figure 1B). This was reflected in cyclic voltammetry in a decrease of the reduction/oxidation peaks and in an increase in peak to peak separation (Curves "a" and "b" of the inset in Figure 1B). This change is related to the increased impedance/blocking of the redox marker to reach the electrode surface as a result of the sterical and electrostatic "blockages" introduced by the presence of the oligonucleotide chains on the electrode surface. A decrease of the R_{ct} was recorded after self assembling of the back-filler on the transducer surface. Herne et al., [40] explained this behaviour with the fact that, following backfilling with MCH, the HS-ssDNA molecules that previously were interacting with the Au surface through both the nitrogen-containing nucleotide bases and the thiol group where forced to change their spatial organization and to interact with the surface only via the thiol group. This surface reorganization results, in the macroscopic world, in a decrease of the charge-transfer component in the impedance spectra ("after back-filling" curve in Figure 1B) and a gain in the peak definition in the CV (curve "c" of the inset in Figure 1B).

UNIVERSITAT ROVIRA I VIRGILI
TEMPERATURE MODULATED GENOSENSOR FOR DETECTION OF CYSTIC FIBROSIS MUTATIONS
Hany Abdel Hady Abdel Rahman Nasef
ISBN:978-84-693-3386-0/DL:T.1002-2010

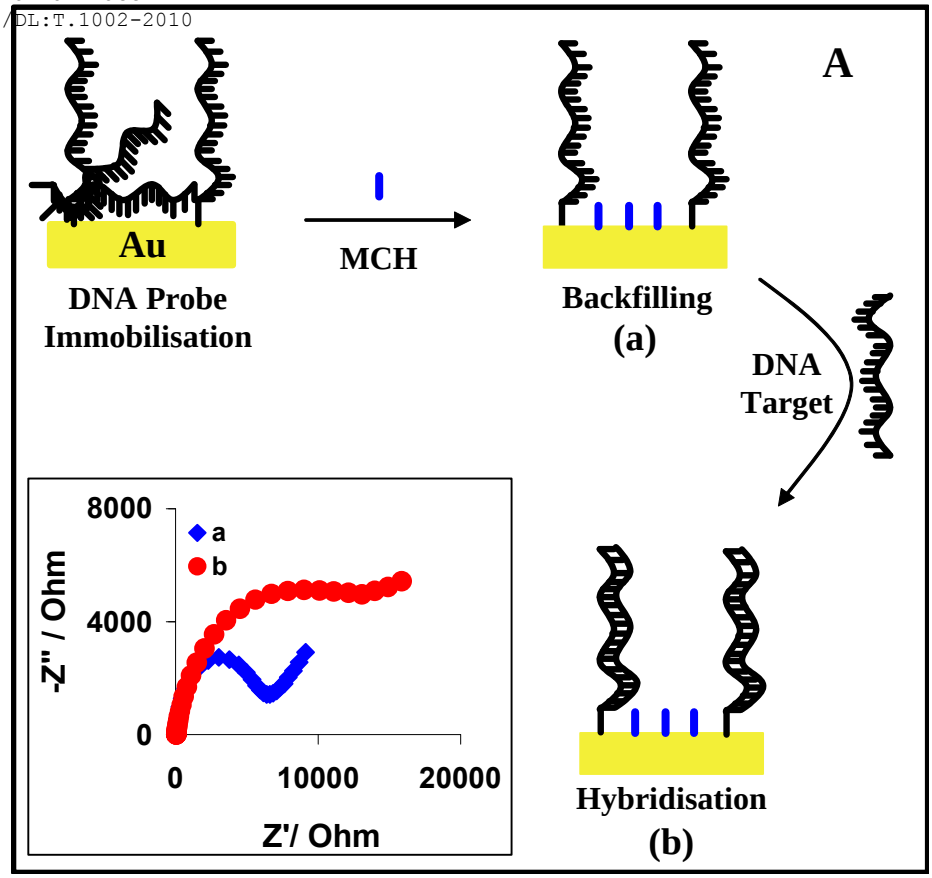

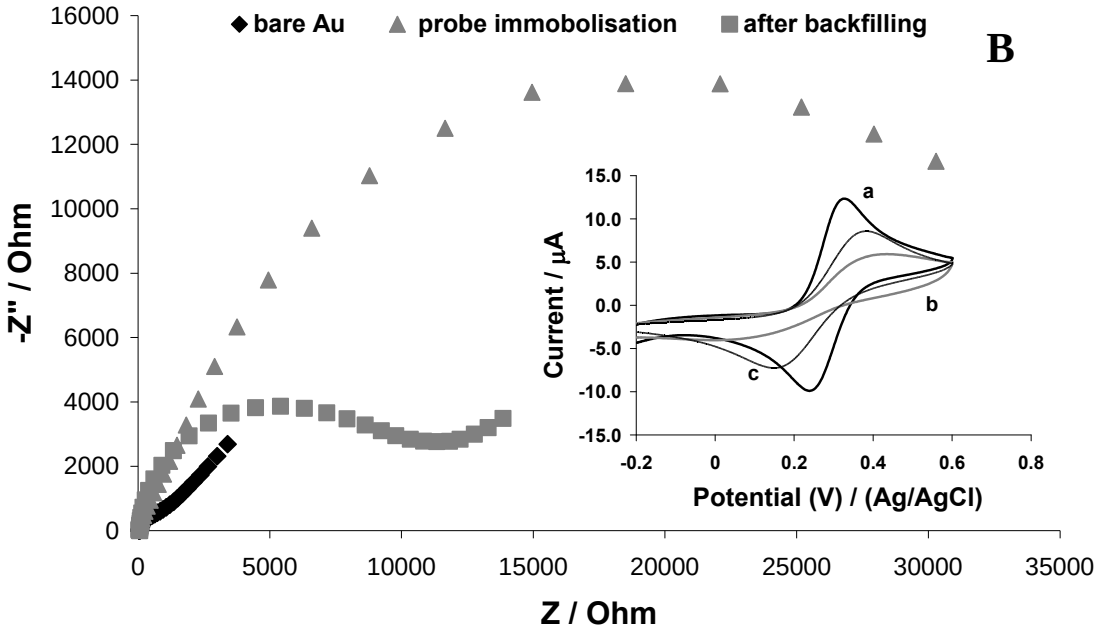

Figure 1: A Schematic representation of sensor preparation and determination using electrochemical impedance spectroscopy detection of DNA. Inset: Impedance spectra of mutant target captured on the electrode surface immobilized with mutant complementary probes. B: Electrochemical Impedance Spectroscopy and Cyclic Voltammetry (inset) of the sensor preparation according to the described protocol. EIS and CV (scan rate 100 mVs^{-1}) experiments have performed in a $[Fe(CN)_6^{3-/4-}]$ equimolar solution 2 (1 +1) mM in Trizma buffer 10 mM + 0.5 M NaCl pH 7.4. Frequency investigated between 10000 and 0.1 Hz.

ISBN:978-84-693-3386-0/DL:T.1002-2010

The surface of the sensors, prepared according to the protocol presented in section 2.3.1, was found to be very stable with no significant variation in the impedimetric spectra recorded before and after storage of the electrode for 24 hours at 4 ºC in Trizma buffer 10 mM with 500 mM NaCl, pH 7.4 (data not shown).

In Figure 2-A the responses obtained when an electrode, modified with a 15 mer probe ($Mut_{15probe}$), was exposed to the two different short targets: "mutant" (Mut_{short}) and "wild type" (WT_{short}) at a concentration of 2 μM, are shown. After hybridisation with the fully complementary target a clear increase in the R_{ct} component was recorded . This increase in the R_{ct} can be associated to the fact that, as a result of the duplex formation (dsDNA), an increase in the total negative charge, present on the electrode surface, is achieved [42]. This increase in surface charge has the effect of increasing the electrostatic repulsion towards the negatively charged ferri/ferrocyanide redox marker [42]. Following specific hybridisation the ability to regenerate the sensor surface, by immersion for 60 seconds in a 100 mM NaOH solution, was evaluated. As can be seen from Figure 2-A after regeneration the impedance response returned to its original value indicating that complete denaturation of the duplex had occurred, leaving the single stranded probe available for subsequent hybridisation. The regenerated sensor was then used to perform hybridisation with the wild type sequence (WT_{short}) target. In this case no significant variation of the impedimetric diagram was recorded. Similar experiments were also carried out by first hybridising to the wild type (WT_{short}), followed by regeneration and hybridisation with mutant target (Mut_{short}), and again, in this case significant R_{ct} variations were recorded only when hybridisation was performed with the mutant target, confirming the fact that R_{ct} variation can be specifically associated to the hybridisation with the fully complementary target (Mut_{short}) and that no loss in sensor surface performances were associated with the regeneration process. In Figure 2-B a summary of the results obtained in this series of experiments are presented.

ISBN:978-84-693-3386-0/DL:T.1002-2010

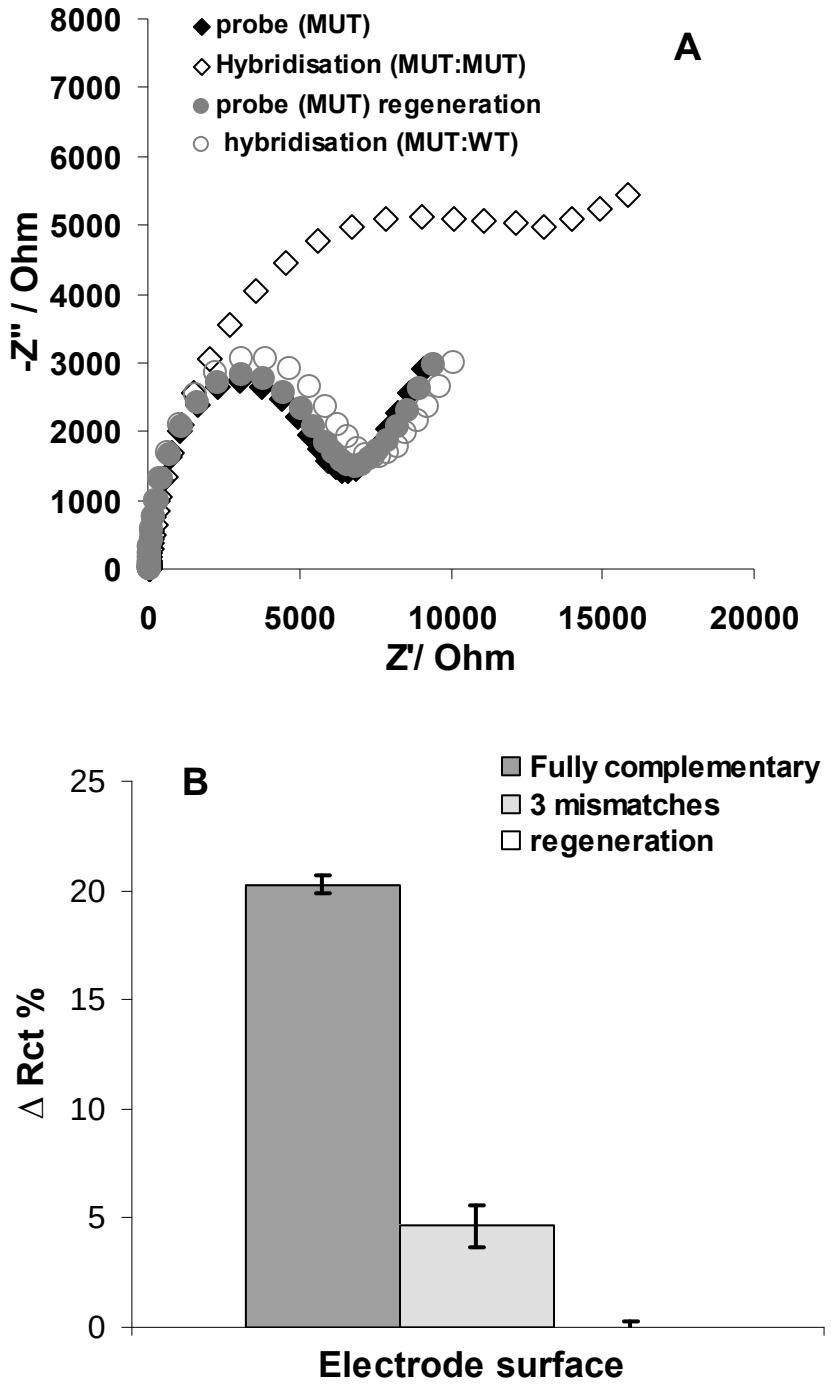

Figure 2: A) Impedimetric spectra of the sensor prepared with $Mut_{15probe,}$ according to the described protocol, before ["probe (MUT)" and "probe (MUT) regeneration"] and after hybridisation with fully complementary (Mut_{short}) and three mismatches (WT_{short}) sequences [respectively "Hybridisation (MUT:MUT)" and "Hybridisation (MUT:WT)"]. B) Summary of the EIS experiment reported as ΔR_{ct}% obtained with the use of a sensor prepared with $Mut_{15probe}$ and the short models ((Mut_{short} and WT_{short} as from experimental section) as targets. Working solution: $[Fe(CN)_6^{3-/4-}]$ equimolar solution 2 (1 +1) mM in Trizma buffer 10 mM + 0.5 M NaCl pH 7.4. Frequency investigated between 10000 and 0.1 Hz.

ISBN:978-84-693-3386-0/DL:T.1002-2010

Due to the variability that can be recorded between different electrodes, attributed to different immobilization levels (due to slightly different surfaces, where minute defects can affect SAM formation), the data are reported as percentage variation of the R_{ct} (ΔR_{ct}%). This value has been calculated as following:

$$\Delta R_{ct}\% = 100 \times [(R_{ct\ after.} - R_{ct\ in.}) / R_{ct\ in}] \qquad \text{Eq.1}$$

where:

$R_{ct\ after.}$ is the value of R_{ct} after hybridisation or regeneration

$R_{ct\ in}$ is the value of R_{ct} before the hybridisation step or the value after electrode preparation in the case of the regeneration.

As clearly shown in Figure 2-B when the hybridisation was performed with the fully complementary target (Mut_{short}) a large R_{ct} variation (average value of ΔR_{ct}% for 6 measurements: 20.3 ± 0.419 (2.06%)) was recorded. On the contrary, when the hybridisation was performed with the target carrying three mismatches (WT_{short}) a much lower variation of the R_{ct} was recorded, with a higher standard deviation (average value of ΔR_{ct}% for 6 measurements: 4.6± 0.968 (21.01%)).

Having demonstrated that it was possible to distinguish between Mutant and wild type sequences using EIS and the short model sequences the detection of ssDNA synthetic PCR analogues, using the same approach, was explored.

3.2 Synthetic PCR analogue detection via EIS

The sequences of the two PCR product analogue for an amplicon (i) containing and (ii) not containing the D508 mutation, were defined according to a reported *Multiplex Amplifiable probe Hybridisation (MAPH) strategy* routinely used for multiplex amplification of Cystic Fibrosis associated genes. [43], where the forward primer was: 5’ GCCGCGAATTCACTAGTG**TGGCACCATTAAAGAAAA** 3’ and the reverse primer was 5’ **GGCCGCGGGAATTCGATTA**TATATTCATCAT AGGAAAC 3’; which would result in double stranded PCR amplicons, the single stranded analogues of which are used in this work, as detailed in Section 2.1.

ISBN:978-84-693-3386-0/DL:T.1002-2010

When detection/discrimination of the two synthetic analogues was attempted, using an electrode modified with the $Mut_{15probe}$ probe, no significant or reproducible R_{ct} variations could be recorded (results not shown).

In order to understand the differences in results recorded in the detection of the short and long sequences, a detailed evaluation of the probe capturing efficiency was performed using SPR. Moreover SPR was used as reference technique in the comparison of the 15 mer probe ($Mut_{15probe}$) with a 21 mer probe ($Mut_{21probe}$).

In order to perform this evaluation solutions containing 0.5 µM of the investigated target sequence were flowed in the channels of an SPR gold chip, previously modified with the probes, according to the modification procedure described in the experimental section (section 2.3.5). In the case of the 15 bases long probe SPR results confirmed the trend recorded with EIS; clearly hybridisation with short target sequences was possible (results not shown) but on the other end no significant hybridisation was recorded in the case of the PCR analogues (curve "PBS-T; probe 15" in Figure 3).

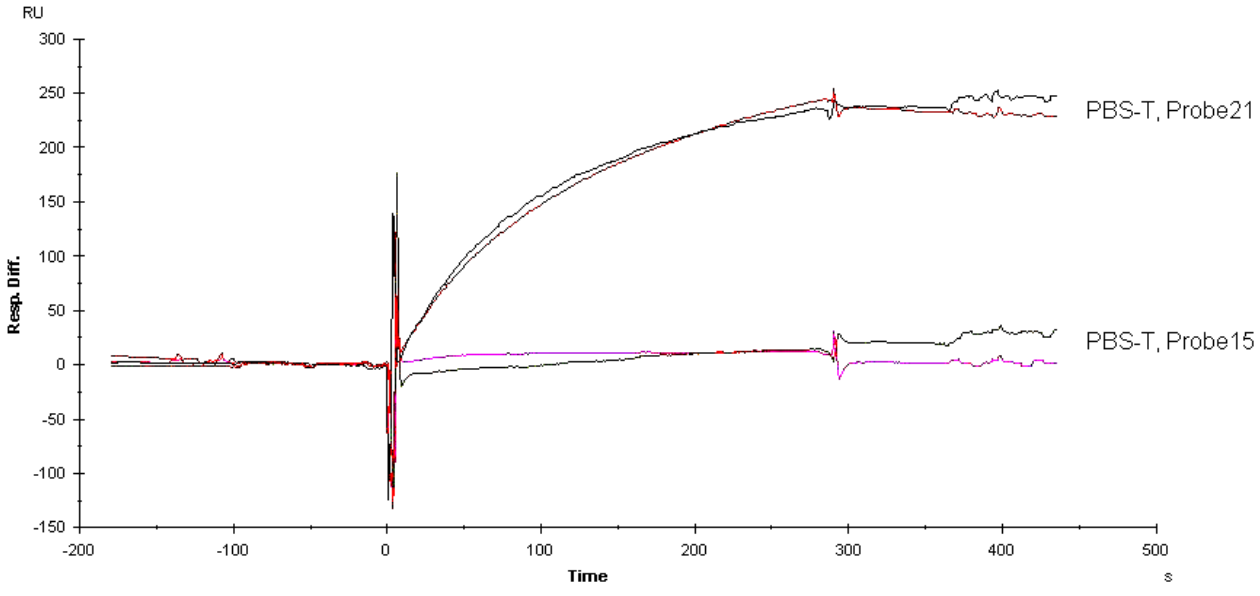

Figure 3: SPR evaluation of the 15 ($Mut_{15probe}$) and 21 ($Mut_{21probe}$) mer probes. Hybridisation experiment performed with a 0.5 µM solution of the fully complementary synthetic PCR analogue target (Mut_{long}) in PBS-T buffer, the repetition of the experiment is highlighted by red and pink lines.

ISBN:978-84-693-3386-0/DL:T.1002-2010

Looking at the effect of the probe length, SPR results showed that the 21mer probe ($Mut_{21probe}$) clearly allowed capture of the PCR analogue (curve "PBS-T; 21 probe" in Figure 3). As previously reported by Del Giallo et al. and Bettazzi et al. [44, 45] in the hybridisation of real PCR product or their synthetic analogous an important rule is played by the sterical hindrance and by the secondary structure present in the oligonucleotide. These have been reported to limit the accessibility to sequences of the amplicon especially if they are located in the centre of the targeted sequences. In our case theoretical calculation of the possible folding of the synthetic PCR analogues (using Mfold Webserver software) highlighted the presence of a stable secondary structure in the capture region. The presence of this secondary structure, together with the position of the recognition sequence, can explain why a longer probe, resulting in a thermodynamically more stable duplex, is required to allow efficient capture of the synthetic PCR analogue.

Based on these results, further electrochemical experiments, for the detection/discrimination of the PCR analogues, were thus carried out using electrodes modified with the $Mut_{21probe}$ probe.

In Figure 4 the percentage variations of R_{ct} recorded in the case of the capture of the synthetic PCR analogue using a sensor prepared with the $Mut_{21probe}$ probe are presented. In the case of the fully complementary sequence (Mut_{long}) ΔR_{ct}% values (average values 18.6±0.49 with n=4) similar to those previously obtained in the case of the short targets were recorded; on the other end in the case of the mismatched sequence (WT_{long}) significant ΔR_{ct}% (average values 11.0±0.68 with n=4) was observed, resulting in a clear loss in specificity (specific signal ca. 1.5 fold that of the unspecific one). Despite this decreased specificity differentiation between the two different targets was possible. This result was expected because the increase in length of the probes has the effect of improve not only the stability of the fully complementary duplex but also to improve those with the mismatched sequence by reducing the effect of the present mismatches.

ISBN:978-84-693-3386-0/DL:T.1002-2010

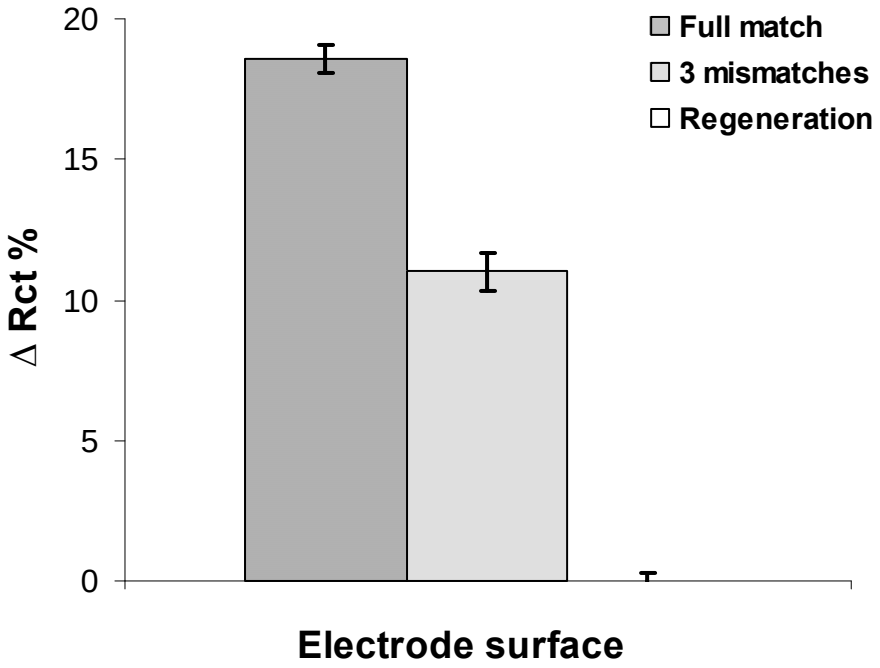

Figure 4: Summary of the EIS, experiment reported as ΔR_{ct}%, obtained with the use of a sensor prepared with $Mut_{21probe}$ and the Synthetic PRC analogues; (Mut_{long} and WT_{long} as from experimental section) as targets. Working solution: $[Fe(CN)_6^{3-/4-}]$ equimolar solution 2 (1 +1) mM in Trizma buffer 10 mM + 0.5 M NaCl pH 7.4.

3.3 Synthetic PCR analogue detection via thermal modulated EIS

Melting temperature is a characteristic of a DNA duplex and a function of the duplex length and composition being strongly influenced by the presence of mismatches [22, 28, 46-48].

In this work we exploited this property as a route to improve the specificity of the assay, in the case of the synthetic PCR analogues. SPR measurements at controlled temperature, in the range between 25 and 40 ºC, were used to evaluate the effect of temperature on duplex formation/stability and subsequently to define the most appropriate temperature to adopt in the following thermally modulated EIS experiments. Each of two SPR gold chips were modified, according to the protocol presented in section 2.3.5, with a 21 mer Mut probe ($Mut_{21probe}$) and with a 21 mer WT probe ($WT_{21probe}$). Hybridisation experiments, at controlled temperature, were performed at the two chips using 500 nM solutions of a fully complementary target, or of the three mismatches target in PBS-T buffer. The results obtained are presented in Table 1. For both probes ($Mut_{21probe}$ and $WT_{21probe}$) similar trends of the response with temperature,

ISBN:978-84-693-3386-0/DL:T.1002-2010

were recorded. In the case of the hybridisation with fully complementary sequences the RU variation increased with temperature indicating an improvement in hybridisation whilst in the case of the three-mismatch sequences the RU variations decreased with increasing temperature. From Table 1, it can be noted, at values over 35 ºC the system demonstrates a clear distinction in stability between fully complementary and 3 mismatched hybrids, with the mutant probe forming more stable hybrids in comparison to the wild type probe, which could be explained by the different GC content of the two probes (33.3% and 28% for $Mut_{21probe}$ and $WT_{21probe}$, respectively)[49-51]. SPR results suggested that 40 ºC is the best temperature to use for in the thermal modulated EIS experiments.

The stability of the immobilised probes as a function of the temperature was performed using an electroactive base-specific label, methylene blue (MB) [41].

	$Mut_{21probe}$		**$WT_{21probe}$**	
	Response difference RU		**Response difference RU**	
Temp. ºC	Mut ampl.	Wt ampl.	Mut ampl.	Wt ampl.
25	137.3	10.1	7.8	143.4
30	156.6	15.2	5.2	213.4
35	179.3	20.7	0.2	235.3
40	194.1	3.2	0.1	166.7

Table 1: SPR evaluation of the effect of the temperature on the PCR analouges/probes duplexes stability. Probe immobilised on the surface: $Mut_{21probe}$ and $Wt_{21probe}$; target concentration used: 500 nM; temperature investigated 25, 30, 35 and 40 ºC. Hybridisation in PBS-T buffer.

This approach was chosen as MB has the ability to specifically address the presence of probes on the electrode surface allowing a precise monitoring of the possible desorption of the probes from the transducer surface.

This evaluation was performed as following: (i) a sensor, prepared as described in section 2.3.1 using the $Mut_{21probe}$ probe, was immersed in an aliquot of the buffer, at a controlled temperature for 10 minutes, (ii) following this incubation the sensor was

ISBN:978-84-693-3386-0/DL:T.1002-2010

transferred to an aliquot of buffer at room temperature and left to cool down for ca. 5 minutes and (iii) finally the sensor was transferred to a solution containing the MB and DPV measurement recorded according to procedure described in section 2.3.4. A thermomixer was used to control the temperature of the buffer during the first step of the experiment, by introducing the eppendorf containing the buffer in the thermostatted block of the thermomixer. Prior to sensor incubation the temperature of the buffer in the eppendorf was checked with a thermometer. In Table 2 the results of this evaluation are reported and are reported as percentage (average of 3 measurements) of those recorded at 24 ºC (reference value). As can be seen from Table 2 no loss of the probe, in the temperature range investigated, was recorded. These results are in agreement with previous reports [52-55] where DNA-SAMs on Au were demonstrated to be stable to at least 55 ºC.

The discrimination of the mutant and wild type synthetic PCR analogues was then evaluated using thermally modulated EIS measurements. In order to obtain an unambiguous discrimination using three different sensors, with one electrode specific for the mutant sequence (sensor prepared with $Mut_{21probe}$ probe), one specific for the wild type sequence (sensor prepared with $WT_{21probe}$ probe) and finally the third electrode modified with MCH only (to monitor unspecific adsorption of the synthetic oligonucleotides) as depicted from the inset of Figure 5.

Temperature ºC	Signal %
24	100 ± 3.4
30	96.1 ± 2.1
40	100 ± 4.8
50	97.7 ± 3.7
60	96.1 ± 1

Table 2: Evaluation of sensor surface stability with the temperature. Signal reported as percentage of the signal at 24 ºC. Evaluation via DPV using MB as reporting molecule. Measurement solution: Trizma buffer 10 mM + 0.5 M NaCl pH 7.4 with 20 μM of MB.

ISBN:978-84-693-3386-0/DL:T.1002-2010

The three sensors, following hybridisation with a different aliquot of the same sample, were washed, for 10 minutes, with hybridisation buffer at 40 °C. Following this washing step the electrodes were transferred to the measurement solution thermostatted at 25 °C and allowed to equilibrate for 5 minutes, and the EIS measurements then recorded. Calculation of the ΔR_{ct}% was achieved employing eq.1 for each sensor, where $Rct_{in.}$ is obtained after regeneration of the sensor surface by immersion in NaOH 0.1 M for 60 seconds.

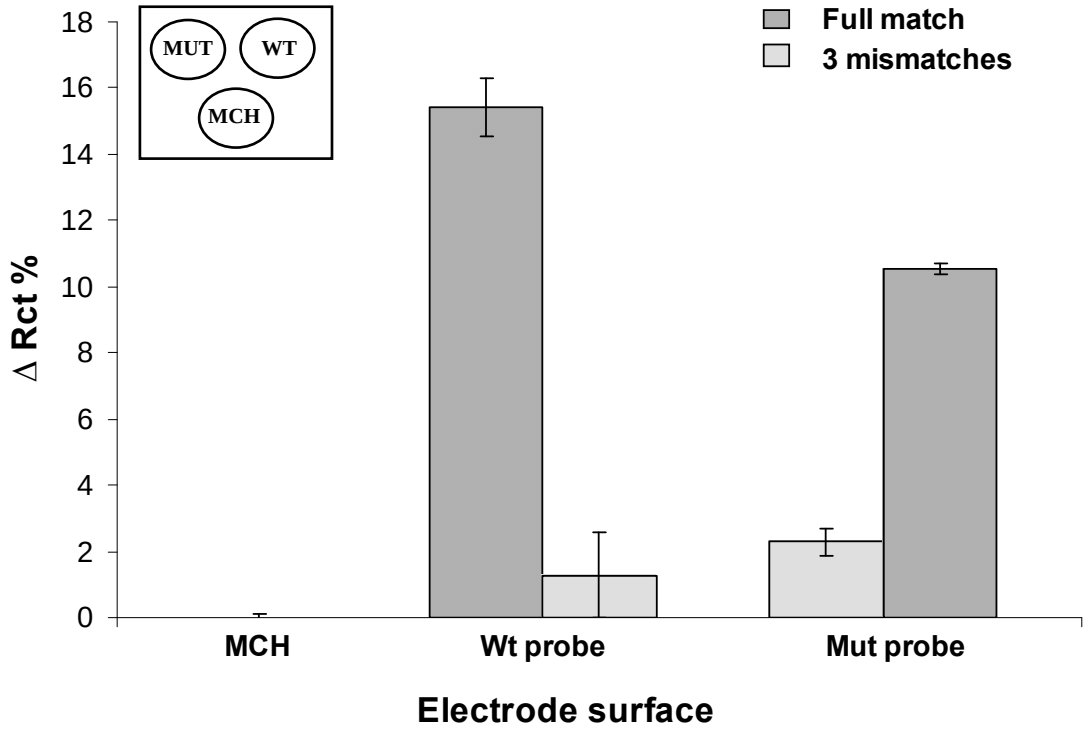

Figure 5: Summary of the EIS experiments, reported as ΔR_{ct}%, obtained with a multiple-parameters detection platform based on three sensors [a Mut sensor (prepared with the $Mut_{21probe}$) a WT sensor (prepared with the$WT_{21probe}$) and a control sensor (no probes)] for the hybridisation of the synthetic PCR analogues (Mut_{long} and WT_{long} as from experimental section). Working solution: $[Fe(CN)_6^{3-/4-}]$ equimolar solution 2 (1 +1) mM in Trizma buffer 10 mM + 0.5 M NaCl pH 7.4. Electrode washed for 10 minutes in hybridisation buffer between at 40 ºC before measurement.

As can be observed in Figure 5 with the use of the wash at 40 ºC a loss in the absolute value of ΔR_{ct}%, for the specific duplex, was recorded as compared to those previously obtained at room temperature (Figure 4). As results obtained at the control electrode demonstrate that the loss in signal is not related to changes in the surface chemistry of

ISBN:978-84-693-3386-0/DL:T.1002-2010

the sensors; it can be concluded that the loss in signal is due to the loss of weakly interacting target oligonucleotides. Although there was a decrease in absolute response the use of the thermally modulated EIS resulted in a significant improvement of the selectivity of the sensors. For both sensors the signal related to the hybridisation of the specific target was between 5 and 8 fold those of the unspecific target.

The reported results clearly demonstrate that the proposed sensing approach, based on the simultaneous use of three sensors (a control sensor, a sensor for the Mut and one for the WT), combined with thermally modulated EIS, allowed an unambiguous discrimination between mutant and wild type synthetic PCR analogues. The proposed sensing approach shows excellent potential for the qualitative discrimination of sequences in clinical analysis.

4. Conclusion

In the reported work a detection platform, based on the use of thermally modulated Electrochemical Impedance Spectroscopy, for unambiguous qualitative analysis of DF508 mutation of CF has been presented. The assessment of the possibility of discriminating between “wild type” and “mutant” sequences has been performed using short models and synthetic PCR analogues. It was clearly illustrated that despite the fact that the 15 bases long probe was able to provide good selectivity for the short models, a longer probe was required for the longer PCR products.

The influence of the temperature on the selectivity of the probes was evaluated using SPR showing that 40 ºC allowed the best discrimination. The stability of the sensor surface chemistry at this elevated temperature was investigated, and finally the use of thermal modulation using EIS detection, clearly resulted in a considerable improvement of the selectivity. Finally, the use of a multi-sensor detection platform facilitated a clear and definitive discrimination between the mutant and wild types of cystic fibrosis associated genes.

ISBN:978-84-693-3386-0/DL:T.1002-2010

5. Acknowledgements

This work has been carried out with partial financial support from the Commission of the European Communities, specific RTD program 'Isolation of fetal cells from maternal blood, SAFER, NEST-ADVENTURE 04977'. Dr. Valerio Beni acknowledges the European Community's, Seventh Framework Programme (FP7/2007-2013) under grant agreement nº (PIGF-GA-2008-220928) for financial support.

ISBN:978-84-693-3386-0/DL:T.1002-2010

6. References:

1 Anderson DH (1938) Cystic fibrosis of the pancreas and its relation to celiac disease: A clinical and pathological study. Am J Dis Child 56:344–399.

2 Boat T, Welsh M, Beaudet AL (1989) Cystic fibrosis, ed 6th. New York, McGraw Hill, pp 2649-2680.

3 Dodge JA, Morison S, Lewis PA, Coles EC, Geddes D, Russell G, Littlewood JM, Scott MT (1997) Incidence, population, and survival of cystic fibrosis in the uk, 1968-95. Arch Dis Child 77: 493 - 496.

4 Ratjen F, Rietschel E, Kasel D, Schwiertz R, Starke K, Beier H, van Koningsbruggen S, Grasemann H (2006) Pharmacokinetics of inhaled colistin in patients with cystic fibrosis. J Antimicrob Chemother 57:306-311.

5 Kerem BS, Rommens JM, Buchanan JA, Markiewicz D, Cox TK, Chakravarti A, et. al.(1989) Identification of the cystic fibrosis gene: Genetic analysis. Science 245:1073–1080.

6 Rommens JM, Iannuzzi MC, Kerem BS, Drumm ML, Melmer G, Dean M, et. al.(1989) Identification of the cystic fibrosis gene: Chromosome walking and jumping. Science 245:1059–1065.

7 Giordana F, Marco L, Nicoletta B, Carlo M, Roberto G (1999) Detection of the df508 (f508del) mutation of the cystic fibrosis gene by surface plasmon resonance and biosensor technology.Human mutation. 13:390 - 400.

8 Mannelli I, Lecerf L, Guerrouache M, Goossens M, Millot M-C, Canva M (2007) DNA immobilisation procedures for surface plasmon resonance imaging (spri) based microarray systems. Biosensors and Bioelectronics 22:803-809.

9 Ferguson JA, Boles TC, Adams CP, Walt DR (1996) A fiber-optic DNA biosensor microarray for the analysis of gene expression. Nature Biotechnology 14:1681 - 1684

10 Venter J, Adams M, Sutton G, Kerlavage A, Smith H, Hunkapiller M (1998) Shotgun sequencing of the human genome. Science 280:1540-1542.

11 Liu X, Tan W (1999) A fiber-optic evanescent wave DNA biosensor based on novel molecular beacons. Analytical Chemistry 71:5054-5059.

12 Bontidean I, Kumar A, Csoeregi E, Galaev IY, Mattiasson B (2001) Highly sensitive novel biosensor based on an immobilized lac repressor. Angewandte Chemie International Edition 40:2676-2678.

13 Willner I (2002) Bioelectronics: Biomaterials for sensors, fuel cells, and circuitry. Science 298:2407-2408.

14 Xu X-H, Bard AJ (1995) Immobilization and hybridization of DNA on an aluminum(iii) alkanebisphosphonate thin film with electrogenerated chemiluminescent detection. Journal of the American Chemical Society 117:2627-2631.

15 Epstein JR, Biran I, Walt DR (2002) Fluorescence-based nucleic acid detection and microarrays. Analytica Chimica Acta 469:3-36.

16 Calvo-Muñoz ML, Dupont-Filliard A, Billon M, Guillerez S, Bidan G, Marquette C, Blum L (2005) Detection of DNA hybridization by abei electrochemiluminescence in DNA-chip compatible assembly. Bioelectrochemistry 66:139-143.

17 Heaton RJ, Peterson AW, Georgiadis RM (2001) Electrostatic surface plasmon resonance: Direct electric field-induced hybridization and denaturation in monolayer nucleic acid films and label-free discrimination of base mismatches. Proceedings of the National Academy of Sciences of the United States of America 98:3701-3704.

18 Livache T, Guedon P, Brakha C, Roget A, Levy Y, Bidan G (2001) Polypyrrole electrospotting for the construction of oligonucleotide arrays compatible with a surface plasmon resonance hybridization detection. Synthetic Metals 121:1443-1444.

19 Towery RB, Fawcett NC, Zhang P, Evans JA (2001) Genomic DNA hybridizes with the same rate constant on the qcm biosensor as in homogeneous solution. Biosensors and Bioelectronics 16:1-8.
20 Wang J, Bard AJ (2001) Monitoring DNA immobilization and hybridization on surfaces by atomic force microscopy force measurements. Analytical Chemistry 73:2207-2212.
21 Palecek E (1988) Adsorptive transfer stripping voltammetry: Determination of nanogram quantities of DNA immobilized at the electrode surface. Analytical Biochemistry 170:421-431.
22 Millan KM, Mikkelsen SR (1993) Sequence-selective biosensor for DNA based on electroactive hybridization indicators. Analytical Chemistry 65:2317-2323.
23 Souteyrand E, Cloarec JP, Martin JR, Wilson C, Lawrence I, Mikkelsen S, Lawrence MF (1997) Direct detection of the hybridization of synthetic homo-oligomer DNA sequences by field effect. The Journal of Physical Chemistry B 101:2980-2985.
24 Marrazza G, Chianella I, Mascini M (1999) Disposable DNA electrochemical sensor for hybridization detection. Biosensors and Bioelectronics 14:43-51.
25 Ozkan D, Erdem A, Kara P, Kerman K, Meric B, Hassmann J, Ozsoz M (2002) Allele-specific genotype detection of factor v leiden mutation from polymerase chain reaction amplicons based on label-free electrochemical genosensor. Analytical Chemistry 74:5931-5936.
26 Dominguez E, Rincon O, Narvaez A (2004) Electrochemical DNA sensors based on enzyme dendritic architectures: an approach for enhanced sensitivity. Analytical Chemistry 76:3132-3138.
27 Wang J (2005) Nanomaterial-based electrochemical biosensors. Analyst 130:421–426.
28 Millan K, Saraullo A, Mikkelsen S (1994) Anal Chem 66(18):2943-2948.
29 Marin S, Merkoçi A (2009) Direct electrochemical stripping detection of cystic-fibrosis-related DNA linked through cadmium sulfide quantum dots. Nanotechnology 20:1-6.
30 Mei G, Honglan Q, Qiang G, Chengxiao Z (2008) Electrochemical detection of DNA hybridization based on the probe labeled with carbon-nanotubes loaded with silver nanoparticles. Electroanalysis 20:123-130.
31 Mir M, Katakis I (2008) Target label-free, reagentless electrochemical DNA biosensor based on sub-optimum displacement. Talanta 75:432-441.
32 Cloarec JP, Martin JR, Polychronakos C, Lawrence I, Lawrence MF, Souteyrand E (1999) Functionalization of si/sio2 substrates with homooligonucleotides for a DNA biosensor. Sensors and Actuators B: Chemical 58:394-398.
33 Berney H, West J, Haefele E, Alderman J, Lane W, Collins JK (2000) A DNA diagnostic biosensor: Development, characterisation and performance. Sensors and Actuators B: Chemical 68:100-108.
34 Fu Y, Yuan R, Xu L, Chai Y, Zhong X, Tang D (2005) Indicator free DNA hybridization detection via eis based on self-assembled gold nanoparticles and bilayer two-dimensional 3-mercaptopropyltrimethoxysilane onto a gold substrate. Biochemical Engineering Journal 23:37-44.
35 Ying X, Lin Y, Xiaoyan Y, Pingang H, Yuzhi F (2006) Impedance-based DNA biosensor employing molecular beacon DNA as probe and thionine as charge neutralizer. Electroanalysis 18:873-881.
36 Long Y-T, Li C-Z, Sutherland TC, Kraatz H-B, Lee JS (2004) Electrochemical detection of single-nucleotide mismatches: application of m-DNA. Analytical Chemistry 76:4059-4065.

37 Degefa TH, Kwak J (2008) Electrochemical impedance sensing of DNA at pna self assembled monolayer. Journal of Electroanalytical Chemistry 612:37-41.
38 Lisdat F, Schäfer D (2008) The use of electrochemical impedance spectroscopy for biosensing. Analytical and Bioanalytical Chemistry 391:1555-1567.
39 Riordan JR, Rommens JM, Kerem BS, Alon N, Rozmahel R, Grzelczak Z, and et.al. (1989) Identification of the cystic fibrosis gene: Cloning and characterization of complementary DNA. Science 245:1066–1073.
40 Herne TM, Tarlov MJ (1997) Characterization of DNA probes immobilized on gold surfaces. Journal of the American Chemical Society 119:8916-8920.
41 Henry OYF, Acero Sanchez JL, Latta D, O'Sullivan CK (2009) Electrochemical quantification of DNA amplicons via the detection of non-hybridised guanine bases on low-density electrode arrays. Biosensors and Bioelectronics 24:2064-2070.
42 Bardea A, Patolsky F, Dagan A, Willner I (1999) Sensing and amplification of oligonucleotide-DNA interactions by means of impedance spectroscopy: A route to a tay–sachs sensor. Chem Commun 1:21-22.
43 Sismani C, Kousoulidou L, Patsalis PC (2000) Multiplex amplifiable probe hybridization (maph) in Walker JM, Rapley R (eds): Molecular biomethods handbook. Totowa, NJ,, Humana Press, pp 179-193.
44 Del Giallo ML, Lucarelli F, Cosulich E, Pistarino E, Santamaria B, Marrazza G, Mascini M (2005) Steric factors controlling the surface hybridization of pcr amplified sequences. Analytical Chemistry 77:6324-6330.
45 Bettazzi F, Lucarelli F, Palchetti I, Berti F, Marrazza G, Mascini M (2008) Disposable electrochemical DNA-array for pcr amplified detection of hazelnut allergens in foodstuffs. Analytica Chimica Acta 614:93-102.
46 Xiaoteng L, Hsing IM (2009) Real time electrochemical monitoring of DNA/pna dissociation by melting curve analysis. Electroanalysis 21:1557-1561.
47 Annette-Enrica S, Gerd-Uwe F (2009) Electrochemical detection of DNA melting curves by means of heated biosensors. Electroanalysis 21:1119-1123.
48 Meunier-Prest R, Raveau S, Finot E, Legay G, Cherkaoui-Malki M, Latruffe N (2003) Direct measurement of the melting temperature of supported DNA by electrochemical method. Nucl Acids Res 31:e150-.
49 Owczarzy R (2005) Melting temperatures of nucleic acids: Discrepancies in analysis. Biophysical Chemistry 117:207-215.
50 Owczarzy R, Moreira BG, You Y, Behlke MA, Walder JA (2008) Predicting stability of DNA duplexes in solutions containing magnesium and monovalent cations. Biochemistry 47:5336-5353.
51 Wallace RB, Shaffer J, Murphy RF, Bonner J, Hirose T, Itakura K (1979) Hybridization of synthetic oligodeoxyribonucleotides to {phi}x 174 DNA: The effect of single base pair mismatch. Nucl Acids Res 6:3543-3558.
52 Storhoff JJ, Mirkin CA (1999) Programmed materials synthesis with DNA. Chemical Reviews 99:1849-1862.
53 Peterlinz KA, Georgiadis RM, Herne TM, Tarlov MJ (1997) Observation of hybridization and dehybridization of thiol-tethered DNA using two-color surface plasmon resonance spectroscopy. Journal of the American Chemical Society 119:3401-3402.
54 Flechsig G-U, Peter J, Hartwich G, Wang J, Grundler P (2005) DNA hybridization detection at heated electrodes. Langmuir 21:7848-7853.
55 Shana OK, Nicole MJ, Michael GH, Jacqueline KB (1999) Long-range electron transfer through DNA films. Angewandte Chemie International Edition 38:941-945.

UNIVERSITAT ROVIRA I VIRGILI
TEMPERATURE MODULATED GENOSENSOR FOR DETECTION OF CYSTIC FIBROSIS MUTATIONS
Hany Abdel Hady Abdel Rahman Nasef
ISBN:978-84-693-3386-0/DL:T.1002-2010

CHAPTER 3 (Art 2):

Methylene blue as an electrochemical indicator for DF508 Cystic Fibrosis mutation detection.

UNIVERSITAT ROVIRA I VIRGILI
TEMPERATURE MODULATED GENOSENSOR FOR DETECTION OF CYSTIC FIBROSIS MUTATIONS
Hany Abdel Hady Abdel Rahman Nasef
ISBN:978-84-693-3386-0/DL:T.1002-2010

Methylene blue as an electrochemical indicator for DF508 Cystic Fibrosis mutation detection.

Hany Nasef[1], Valerio Beni[1] and Ciara K. O'Sullivan*[1,2]

[1] *Nanobiotechnology & Bioanalysis Group, Department of Chemical Engineering, Universitat Rovira i Virgili, Avinguda Països Catalans, 26, 43007 Tarragona, Spain*
E-mail: ciara.osullivan@urv.cat; Fax: +34 977 55 96 21; Tel.+ 34 977 55 8740
[2] *Institucio Catalana de Recerca i Estudis Avançats, Passeig Lluis Companys 23, 08010, Barcelona, Spain*

Abstract

Cystic fibrosis (CF) is one of the most common life-shortening, childhood-onset inherited diseases. Among the 1000 known cystic fibrosis related mutations, DF508 is the most common, with a frequency varying between 50%-70%, according to geographical areas and population typology. In this work, we report the use of methylene blue as an electrochemical reporting agent, in the discrimination of synthetic PCR analogue of the DF508 cystic fibrosis mutation (Mut) from the wild type (Wt). At optimum experimental condition a discrimination factor, between mutant and wild type of ca. 1.5 fold was found. The proposed assay was quantitative and linear in the range of 10 – 100 nM, exhibiting a limit of detection (LOD) of 2.64 nM. Electrochemical studies at variable ionic strength conditions allowed further elucidation of the mechanism of the methylene blue-DNA interaction. At the best of our knowledge, this is the first report of detection of hybridisation solely via guanine specific MB-DNA interaction simultaneously in MB solution, independent of electrostatic interaction as demonstrated in the ionic strength study. The introduction of formamide in the hybridization buffer, to improve discrimination, was also investigated. Finally mutant wild type discrimination was demonstrated, at 10 nM concentration, with the use of a multi-sensor setup.

Keywords: Methylene blue; Cystic Fibrosis; DF508; DNA sensor, electrochemistry.

UNIVERSITAT ROVIRA I VIRGILI
TEMPERATURE MODULATED GENOSENSOR FOR DETECTION OF CYSTIC FIBROSIS MUTATIONS
Hany Abdel Hady Abdel Rahman Nasef
ISBN:978-84-693-3386-0/DL:T.1002-2010

List of abbreviations:

MB : methylene blue.

MCH: mercaptohexanol.

CF: cystic fibrosis.

CFTR: cystic fibrosis transmembrane conductance regulator

PCR: polymerase chain reaction.

MAPH: Multiplex amplification and probe hybridisation.

Mut ampl: DF508 Cystic fibrosis mutation amplicon.

Wt ampl: cystic fibrosis wild type amplicon.

LOD: limit of detection.

UNIVERSITAT ROVIRA I VIRGILI
TEMPERATURE MODULATED GENOSENSOR FOR DETECTION OF CYSTIC FIBROSIS MUTATIONS
Hany Abdel Hady Abdel Rahman Nasef
ISBN:978-84-693-3386-0/DL:T.1002-2010

1. Introduction

Cystic fibrosis (CF), an autosomal recessive disease, is one of the most common life-shortening, childhood-onset inherited diseases. The disease is caused by mutations in a gene called the *cystic fibrosis transmembrane conductance regulator* (CFTR) which has the function to code a chlorine ion channel protein involved in secretion of sweat, digestive juices, and mucus [1],[2]. The incidence of CF in Caucasians is approximately 1 in 2,500 live births and 4% of the populations are carriers [3],[4].

Almost 1,000 mutations have been identified in the CF gene, but only a few common mutations can be identified as a cause of the disease in the majority of cases. Among these, DF508 is the most common mutation with frequencies varying, according to the ethnic group, between 50% (centre and southern Europe) and 70% (Britain and U.S.). This mutation consists of a three (3) base deletion in the coding sequence that result sin the suppression of the phenylalanine at position 508 in the amino acid sequence of the CFTR [1] protein.

CF phenotyping is currently performed by a variety of approaches, including the polymerase chain reaction (PCR), allele-specific oligonucleotides (ASO), dot-blot and reverse dot-blot hybridisation or SPR [5].These methods, used as in-house testing procedures or as commercially available kits (Innogenetics, Zeneca Diagnostics and PE Applied Biosystems) all have disadvantages [6], such as variations in the number and type of mutations detected or in the ability to distinguish between homozygote and heterozygote genotype.

In recent years the demand for simple and reliable methods for genetic analysis has risen considerably and in this context electrochemical platforms, due to their high sensitivity, small dimensions, rapidity, low cost and suitability for miniaturisation, have resulted in considerable growth in DNA biosensors (genosensors) development [7],[8]. Despite the fact that label-less approaches, based on impedimetric measurements[9, 10], present the majority of the works reported in this area, the introduction of labels to amplify the recognition event has also been reported. Enzymes, such as alkaline phosphatase and horseradish peroxidase [11-13], electroactive tags, like ferrocene, methylene blue [14] and anthraquinone [15, 16], liposomes [17] and redox molecules have been investigated as labels. The use of redox molecules, including metallic

ISBN:978-84-693-3386-0/DL:T.1002-2010

complexes of Ru(II), Os(II), Cd(II) or Co(III) or organic dyes, is particularly interesting due to their simplicity and sensitivity [18-21]. Methylene blue (MB), an organic dye belonging to the phenothiazine family, is an example of a redox active non-metal molecule characterised by having a high affinity for nucleic acids. Three different mechanisms of MB-DNA interaction have been recognised: (i) electrostatic interaction with the negatively charged DNA backbone [22], (ii) intercalation within the DNA double helix [23] and (iii) preferential binding to free guanine bases present on single stranded DNA (ss DNA) [24, 25]. Several reports on the use of MB as a reporting element in electrochemical genosensors can be found in the literature [24-28]. Erdem et al. [24] reported the use of MB voltammetry as a discrimination tool between ssDNA and dsDNA. Current methodologies for DNA biosensing, based on the electrochemical detection of methylene blue (MB), suffer from time consuming incubation and washing steps [29-32]. Zhu et al. [33] reported on the use of a DNA biosenors based on MB and zirconia thin film modified gold electrode, where the zirconia was used to immobilise the DNA probe due to its affinity with the phosphoric group at the 5' terminal of the DNA probe. A detection limit of 1pM was achieved. Pänke et al. [34] offered a different approach where them immobilised probes onto a thin gold film based electrodes, and using targets of equal length to the probe (18 bases) were able to demonstrate single base mismatches. Lin et al. [35] covalently attached DNA probes through their amine moieties to a glassy carbon electrode using EDC-NHS chemistry using MB as an electrochemical indicator of hybridisation with an 18 base target, achieving a detection limit of 0.59nM. Jin et al. [36] exploited the use of a thiolated hairpin probe immobilised on a gold electrode for the detection of 15 base target sequences demonstrating differentiation between fully complementary targets and those containing single mismatches, with a detection limit of 0.2nM. Loiaza et al. [37] describe the immobilisation of a 25 base probe on screen printed gold electrodes using methylene blue as an electrochemical indicator, with MB-DNA interaction detected using square-wave voltammetry achieveing a 2mg/L detection limit. It should be emphasised that all the above reports detect short target sequences of between 18 and 25 bases and at NaCl concentrations ranging between 20 and 100mM, thus (i) not truly reflecting a real application of the genosensor to the detection of PCR amplicons, which can vary in length from 70 to 200 bases and (ii) both electrostatic and bases specific interaction are involved in the MB signal generated. Henry et al. [38] reported the use of MB voltammetry for the development of a rapid microfluidic based device for

ISBN:978-84-693-3386-0/DL:T.1002-2010

clinical analysis. Moreover charge transfer through DNA films was exploited for the electrochemical detection of single-base mismatches [39] where the presence of mismatches was detected by the reduction in the electron transfer that they generated in a dsDNA film immobilised onto a Au electrode and having MB intercalated.

In the work presented here, we report on the use of MB-DNA interaction as an effective approach for the quantitative electrochemical detection of the DF508 mutation and its discrimination toward the wild type using, as target models, two synthetic PCR analogues of 85 and 82 bases long, respectively. A further understanding of the MB-DNA interaction mechanism at high ionic strength is also presented. The results of the attempt of using formamide as route to improve the discrimination between complementary target and mismatched target are also discussed. Electrochemical and spectrofluorimetric experiments suggested that guanine specific interaction of MB occurs principally at high ionic strength; and furthermore it was demonstrated that the use of formamide as destabilising agent is not compatible with the use of MB as an electrochemical reporter of hybridisation.

2. Experimental

2.1. Chemicals, probes and targets

All chemicals and reagents: Trizma base (Sigma), Potassium hexacyanoferrate (III), $K_3Fe(CN)_6$ (Sigma) hydrochloric acid (6M, Scharlau), potassium dihydrogen phosphate KH_2PO_4 (Scharlau), sodium chloride NaCl (Scharlau), sodium hydroxide NaOH pellets (Panreac), sulphuric acid H_2SO_4 (Sigma), 6-mercaptohexanol, MCH (Fluka), formamide (Acros Organics), potassium hexacyanoferrate (II) $K_4Fe(CN)_6$ (Fluka) and Methylene blue (Fluka) were of analytical grade and used without further purification. .Alumina powder (1, 0.3, 0.05 micron) was provided by CHI Instruments (USA). All solutions were prepared in ultra pure water (18 MΩ.cm) obtained using a “Simplicity Water Purification System” (Millipore, France).

Oligonucleotides, listed in Table 1, were provided by Eurogentec (Eurogentec, Spain). Sequences of the probes, mutant and wild type, have been selected according to the work reported by Riordan et al. [40]

ISBN:978-84-693-3386-0/DL:T.1002-2010

Mutant target amplicon (82 mer)	**5' GCC GCG AAT TCA CTA GTG TGG CAC CAT TAA AGA AAA TAT CAT TGG TGT TTC CTA TGA TGA ATA TAA TCG AAT TCC CGC GGC C 3'**
Control Amplicon (82 mer)	**5' TCC ACT AAT TCA CTA ATT TAT CAC CAT TAA AGA AAA TAT CAT TGG TGT TTC CTA TAA TTA ATA TAA TCA AAT TCC CTC AAC C 3'**
Wild type target amplicon (85 mer)	**5' GCC GCG AAT TCA CTA GTG TGG CAC CAT TAA AGA AAA TAT CAT CTT TGG TGT TTC CTA TGA TGA ATA TAA TCG AAT TCC CGC GGC C 3'**
Mutant probe (21 mer)	**5' GGA AAC ACC AAT GAT ATT TTC-C6-SH 3'**
Wt type probe (21 mer)	**5' AAC ACC AAA GAT GAT ATT TTC-C6-SH 3'**

Table 1: Sequences of the oligonucleotides and synthesised amplicons used in this work.

The oligonucleotides, used in this work, are analogues to the PCR products obtained using an amplification protocol, based on a "Multiplex Amplifiable probe Hybridization (MAPH)" strategy [28]. The two primers, specific for the DF508 mutation region and carrying specific MAPH tails, were: 5' GCCGC GAATTCACTAGTG**TGGCACCATTAAAGAAAA** 3' (forward) and 5' **GGCCGCG GGAATTCGATTA**TATATTC ATCAT AGGAAAC 3' (reverse), where the regions specific for the probe are indicated in bold and those for the MAPH tags are underlined. As a result of the amplification process two possible amplicons could be generated: an 82 bases long amplicon in the case of the mutant and an 85 bases long sequence for the wild type. The full sequences of the synthetic PCR analogues are listed in Table 1.

2.2. Instrumentation and measurements

The electrochemical studies were carried out using an Autolab model PGSTAT 12 potentiostat/galvanostat controlled with the General Purpose Electrochemical System (GPES) software (Eco Chemie B.V., The Netherlands). A classical three electrode cell was used. A set of commercially available polycrystalline Au disk (2 mm diameter) electrodes (CHI Instruments) were used as working electrode, a Ag/AgCl (KCl 3 M) was used as reference electrode (CHI Instruments) and a Pt wire (Sigma) used as counter electrode. Working electrodes were cleaned using a two-step protocol: (i) mechanical cleaning followed by (ii) electrochemical cleaning. Firstly they were mechanical cleaned with alumina (using three different sizes: 1, 0.3, 0.05 micron)

ISBN:978-84-693-3386-0/DL:T.1002-2010

aqueous slurry, to a mirror finish. After rinsing with ultra pure water the electrodes were electrochemically cleaned by cycling it ca. 40 times (scan rate 100 mVs^{-1}) between -0.2 and 1.6 V in sulphuric acid 0.5 M. The number of cycles was not fixed: the Au electrodes were considered clean when, in a cyclic voltammetric experiment with a ferro\ferri equimolar solution, a peak to peak separation below 80 mV was recorded. Following the cleaning step, the sensor surface was prepared by the well-approach of back filling [36]. Thiolated probe (Mut or Wt) was self assembled, via spotting of 50 µl of a 4 µM solution, freshly prepared in 1 M KH_2PO_4, onto the electrode surface and left to assemble for 3 hours. Following probe self-assembling the sensor surface was washed with ultra pure water and subsequently back-filled by spotting 50 µl of a 0.01M aqueous solution of mercaptohexanol onto the electrode surface and let to incubate for 30 minutes. This step was performed in order to improve the organization of the sensing surface by reorienting the probes for optimal and efficient hybridisation and by removing those unspecifically physisorbed onto the surface. The sensor was then thoroughly washed by sequential immersion in 0.1 M NaOH, MilliQ water, 0.1 M HCl and MilliQ water, leaving an organized mixed SAM of chemisorbed DNA probe and MCH. In Figure 1-A a schematic representation of the sensor surface preparation is presented.

Targets hybridization was carried out via a 1 hour incubation of 50µL of the desired target (Mut or Wt synthetic PCR analogues) in 20 mM Trizma buffer (pH 7.4) in the presence of 0.5 M NaCl. The sensor was then washed with 20 mM Trizma buffer (pH 7.4) containing 0.5 M NaCl and the hybridization levels were monitored by evaluating the reduction response of the MB. The evaluation of the hybridisation level was based on the monitoring of the electrochemical reduction of the MB selectively interacting with the single stranded part of the on-surface captured synthetic oligonucleotides. A schematic of the detection process is presented in Figure 1-B.The MB capture and the electrochemical evaluation were performed according to a variation of the protocol presented recently by Henry et al. [38].

The sensor, following hybridisation, was immersed in an aliquot of a 20mM Trizma (pH 7.4), 0.5M NaCl buffer containing 20 µM methylene blue and left to interact for 5 minutes. Following this incubation a differential pulse voltammogram (DPV) was recorded. The parameters employed in the DPV experiments were: potential window

ISBN:978-84-693-3386-0/DL:T.1002-2010

between 0 and -0.6 V (vs. Ag/AgCl, KCl 3 M) , step potential 10 mV, modulation amplitude 10 mV, modulation time 0.015 s and interval time 0.1 s. A typical DPV result is presented in the inset of Figure 1, where a clear reduction wave is visible at ca. -100 mV (vs the Ag/AgCl, KCl 3 M reference). Electrode regeneration was performed by immersion in a 200 mM NaOH solution for two minutes. Following the regeneration step the DPV voltammetry was repeated in order to record the background response, due to the immobilised probes.

Fluorescence measurements were performed using a Cary Eclipse Spectrofluorimeter equipped with Cary temperature controller (Varian, Spain). All measurements were performed at constant temperature (25 ºC). Black quartz cuvettes with 1 cm path length with a total volume of 250 µl (Hellma) were used. The excitation wavelength was set to 665 nm and emission spectrum recorded from 670 up to 800 nm. Slits of 5 nm were used for both excitation and emission. All the experiments were performed using a photomultiplier tube Voltage of 600 V. In further detail, 200 µl of freshly prepared solutions were used in this study. In the studies of the DNA quenching effect on the MB the solutions contained 2µM of the investigated amplicon (Mutant or control) in the presence of 5µM of MB in the appropriate buffer (20mM Trizma, pH 7.4 with 20, 200 or 500 mM of NaCl). Background detection experiments were performed by monitoring the fluorescence of a solution 5 µM MB in the appropriate buffer. Spectrophotometric curves were recorded after incubating the DNA with methylene blue for 5 minutes.

3. Results and discussion

In the inset of Figure 1-B a typical result of the differential pulse voltammogramic measurement is presented where the electrochemical responses following hybridisation between the immobilised probe and the single stranded synthetic analogue of the PCR product with 1 µM of the fully complementary synthetic oligonucleotide target and after sensor regeneration. As a result of the hybridisation a large electrochemical response was recorded; on the other hand, when voltammetric measurement was performed after sensor regeneration a much smaller response was recorded. These results confirmed that the electrochemical response is associated to the hybridisation event.

UNIVERSITAT ROVIRA I VIRGILI
TEMPERATURE MODULATED GENOSENSOR FOR DETECTION OF CYSTIC FIBROSIS MUTATIONS
Hany Abdel Hady Abdel Rahman Nasef
ISBN:978-84-693-3386-0/DL:T.1002-2010

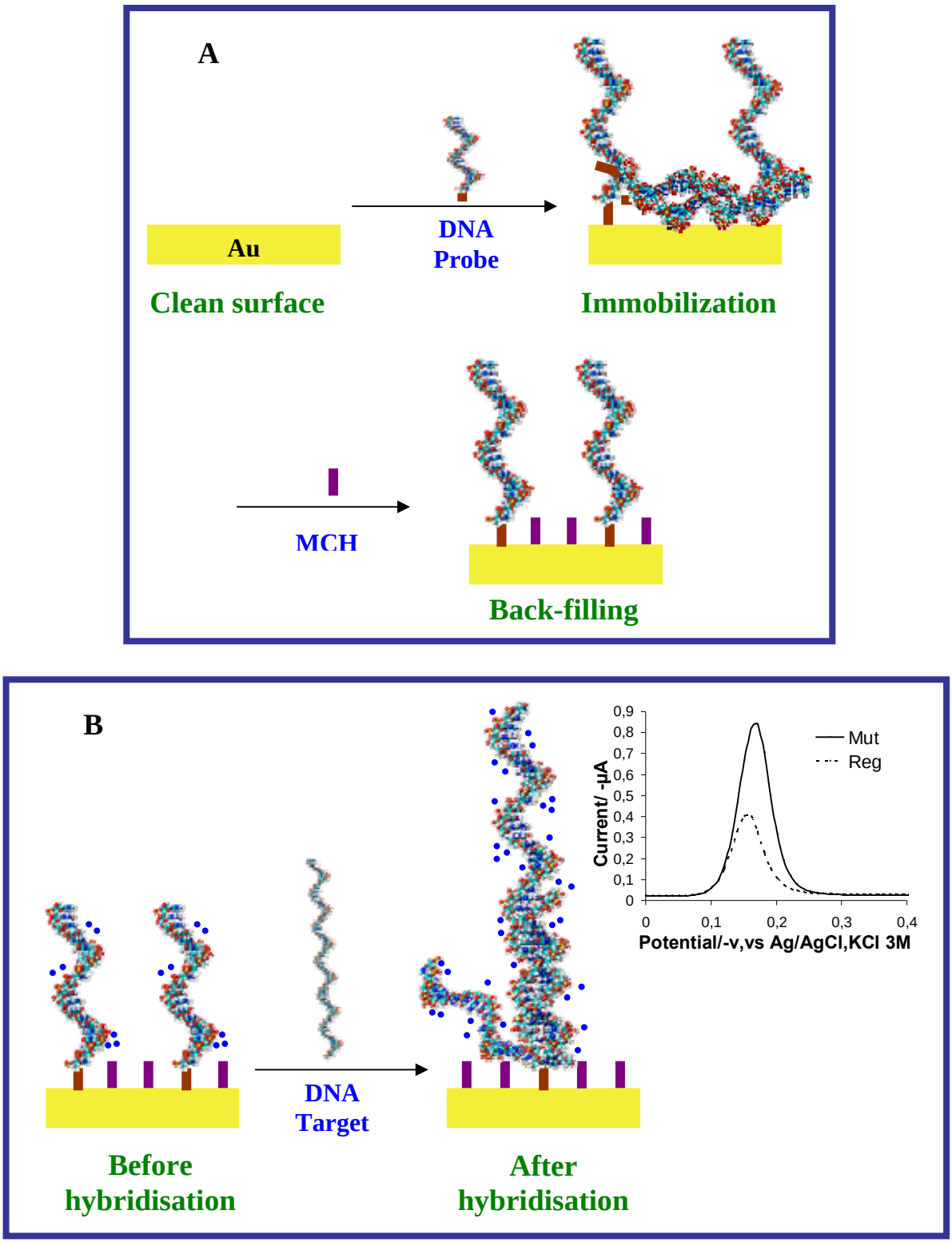

Figure 1: Schematic representation of sensor preparation (A) and target dermination according to the proposed detection protocol (B). Inset: Differential pulse voltammograms of Mutant amplicon captured on the electrode surface. Hybridisation performed from a solution of 1µM target amplicons. Measurement solution: 20 µM MB in 0.5M NaCl and 20 mM Trizma, pH 7.4. Regeneration solution: 0.2 M NaOH for 60 seconds.

ISBN:978-84-693-3386-0/DL:T.1002-2010

3.1. Ionic strength influence on MB signal intensity and the hybridisation stability:

High NaCl concentrations are known to stabilise the DNA duplex; for this reason it is important to work in a solution containing high concentrations of NaCl. In this work the understanding of the MB/DNA interaction mechanism at high salt concentrations was considered important due to the fact that in the detection protocol adopted, inspired by those recently proposed by Henry et al.[38], MB accumulation and electrochemical measurements were performed in the same solution. Several studies on the MB/DNA interaction, especially via spectroscopic techniques, can be found in literature [41]-[42]. The different reports agree on the complexity of the nature of this interaction demonstrating its dependency on (i) MB/DNA ratio and (ii) ionic strength of the interaction buffer. Moreover experimental [43, 44] and static modelling [45] has highlighted the existence of several interaction sites between DNA and MB mainly via: GC and AT alternating sequences and electrostatic interaction with the negatively charged backbone. Kara et al. [46] investigated, by mean of electrochemical measurements, the interaction of MB with dsDNA and ssDNA as a function of the ionic strength reporting a progressive loss of the electrostatic component with increasing ionic strength until a NaCl concentration of 10 mM is reached; for higher NaCl concentrations no further losses in signal were reported due to an exclusive G specific interaction. According to these results most reports detail the use of a concentration of NaCl of 20 mM [38]. More recently, Nafisi et al. [43] reported, using FTIR measurements, that at high ionic strength (NaCl concentration in the measurement solution of 100 mM) MB-DNA interaction occurred mainly via electrostatic interaction with the backbone and with the G base. The author also reported that the importance of the G specific interaction grows with the MB-DNA ratio.

In order to gain a better insight into the nature of the MB/DNA interaction at high NaCl concentrations the voltammetric responses, as a function of the NaCl concentration, of three different systems were monitored. The three systems were: Au electrode modified with mercaptohexanol only (system A), Au electrode modified with 1 μM of the mutant specific probe after hybridisation with 1 μM of the mutant target (System B) and analogous to system B but this time hybridised was performed with a control sequence (system C). This control sequence was designed around the mutant sequence by randomly replacing the guanine, in the region non-involved in the hybridisation with the

ISBN:978-84-693-3386-0/DL:T.1002-2010

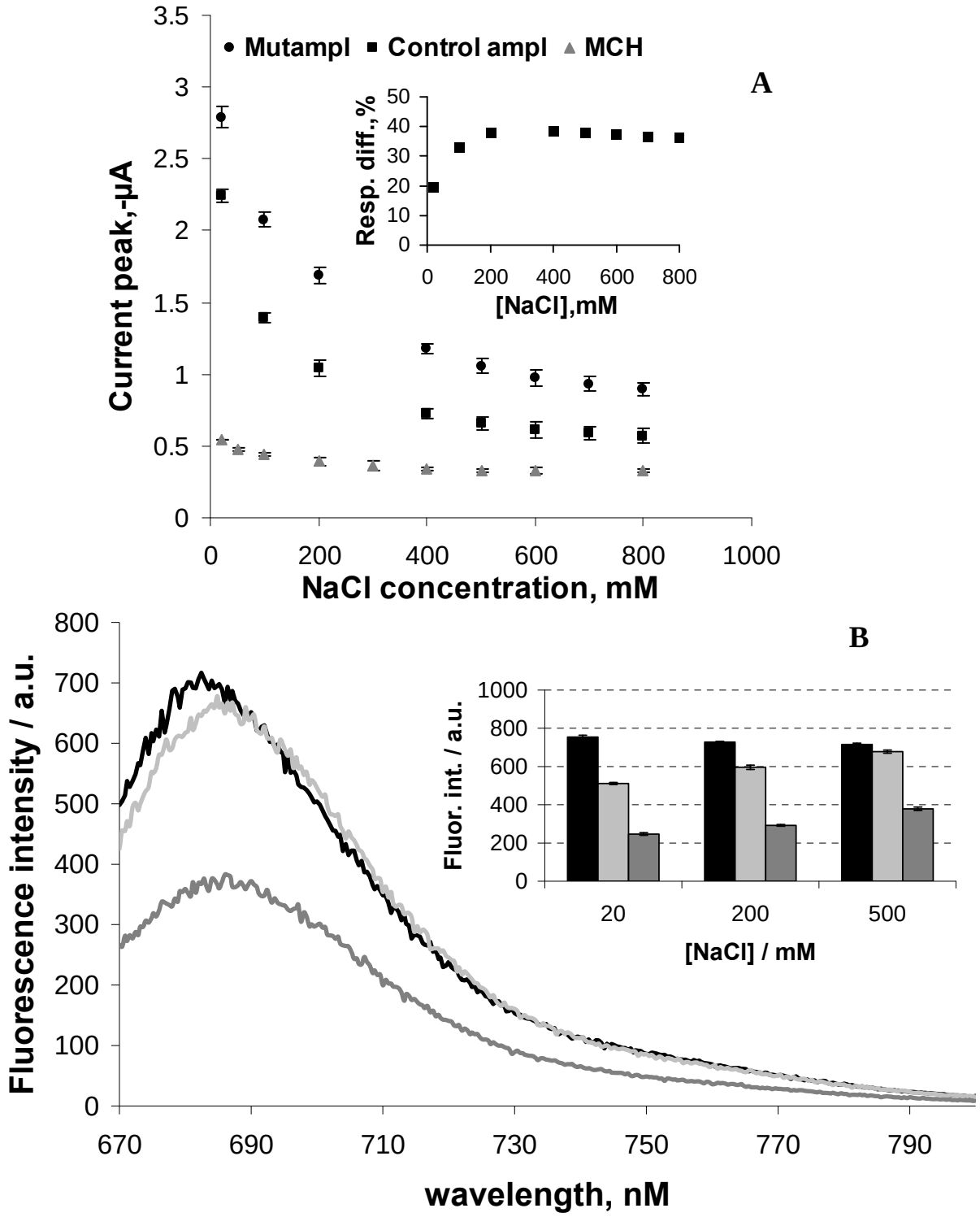

Figure 2.A**:** The effect of sodium chloride concentrations on the MB Differential pulse voltammogram response for the DF508 Mutant and Control amplicon hybridised on the gold electrode surface and for electrode surface modified with MCH. Inset: the response difference percentage between mutant and control targets. B: Fluorescence spectra of MB in absence of DNA and in presence of DF508 Mutant and control amplicons, in 0.5M NaCl and 10mM Trizma (pH 7.4). Inset effect of NaCl concentration on the fluorescence spectra of MB in absence of DNA and in presence of DF508 Mutant and Control amplicon, in 10mM Trizma (pH 7.4).

ISBN:978-84-693-3386-0/DL:T.1002-2010

Mut probe, with adenine or thymine (control sequence from Table 1). System A was designed to acquire information about the trend of the background with the ionic strength, whilst system C sequence was selected in order to minimise the contribution of the G specific interaction to the electrochemical response allowing the evaluation of other possible contributions such as electrostatic interaction or the role of the AT bases. In Figure 2-A the peak current values, recorded for the three different systems, as a function of NaCl concentrations (between 0.02 and 0.7 M) in the incubation/measurement solution, are presented. In the case of the mercaptohexanol modified electrode (System A) a progressive decrease in the electrochemical response was recorded with the increase of the NaCl concentration; this result seems to be consistent with the presence of an electrostatic accumulation of the MB at the mercaptohexanol surface [47] progressively shielded by the increase of the NaCl concentration. When the evaluation was performed using systems B and C much higher responses were recorded confirming the MB accumulation at the oligonucleotide modified electrodes. Higher response was recorded at the G containing sequence strongly confirming the contribution of the MB guanine interaction. The two systems presented very similar behaviour; in both cases the voltammetric responses exponentially decreased, with the increase of salt concentration. In order to elucidate the origin of the differences in responses recorded with the two amplicons the weight of the difference in response (ΔResp.%) on the Mut sequence response was evaluated.

Signal difference was defined as:

$$\text{Response difference (\%)} = 100 \times [(I_{Mut} - I_{cont})/I_{Mut}] \qquad \text{eq. (1)}$$

Where:

I_{Mut} is the current peak obtained at the sensor hybridised with the mutant sequence

I_{cont} is the current peak obtained at the sensor hybridised with the control sequence

The ΔResp.% (Inset in Figure 2-A) was observed to augment with the increase in NaCl concentration until a concentration of ca. 0.2 M was reached; for higher salt concentrations (up to 1 M) no further variations were recorded. This result seems to indicate that the electrostatic or weak base interaction contributions were present and important at NaCl concentrations lower than 0.2 M. For NaCl concentrations higher

ISBN:978-84-693-3386-0/DL:T.1002-2010

than this value the response difference levelled off becoming more or less constant; this is consistent with the presence of a second contribution, independent from the electrostatic properties of the DNA. This contribution can be associated with the presence of the 14 free guanine bases in the mutant sequence. Notably a residual electrostatic contribution can be still identified even at very high NaCl concentrations.

In Figure 2-B the fluorescence spectra of a 5 μM solution of MB, before and after interaction with the mutant sequence and the control sequence, are presented. Two main features can be recognised from these spectra: the red-shift of the fluorescence spectra, due to the DNA-MB interaction [44] and the quenching of the fluorescence [42], [43]. Quenching efficiency was recorded to be a function of the presence of the G in the sequences and of the NaCl concentration (inset of Figure 2-B) [42], [44]; with an increase in quenching observed with decreasing NaCl concentration, indicating higher levels of MB/DNA interaction. This could be explained by the fact that in low ionic strength conditions the MB molecules tends to accumulate onto the negatively charged back bone of the DNA and hence the quenching is higher than in the case of higher ionic strength levels in which only the DNA bases, specifically guanine, bases are responsible for the quenching of MB signal.

3.2. Influence of ionic strength on the discrimination between Mutant and Wild type:

An evaluation of the stringency conditions, in the form of NaCl concentration, of the hybridisation buffer was also performed with the aim of optimising discrimination between the fully complementary (mutant) and interfering sequence (wild type). Hybridisation was performed, according to the protocol described in the experimental section, in the presence of different NaCl concentrations. Following a washing step (performed using the same buffer used in the hybridisation step) the sensor was transferred to the incubation/measurement solution, containing 0.5 M NaCl for duplex stability and DPV experiment recorded. Following each measurement, sensor regeneration was performed and background response (response due to probes) recorded.

The analytical response used in this study was the signal variation normalised versus the background response according to equation 2.

ISBN:978-84-693-3386-0/DL:T.1002-2010

$$\text{Signal variation (\%)} = 100 \times [(i_{amp} - i_{reg}) / i_{reg}] \qquad \text{eq. (2)}$$

Where:

i_{amp} Peak current recorded with hybridised target

i_{reg} Peak currents after regeneration i.e. denaturation of formed duplex

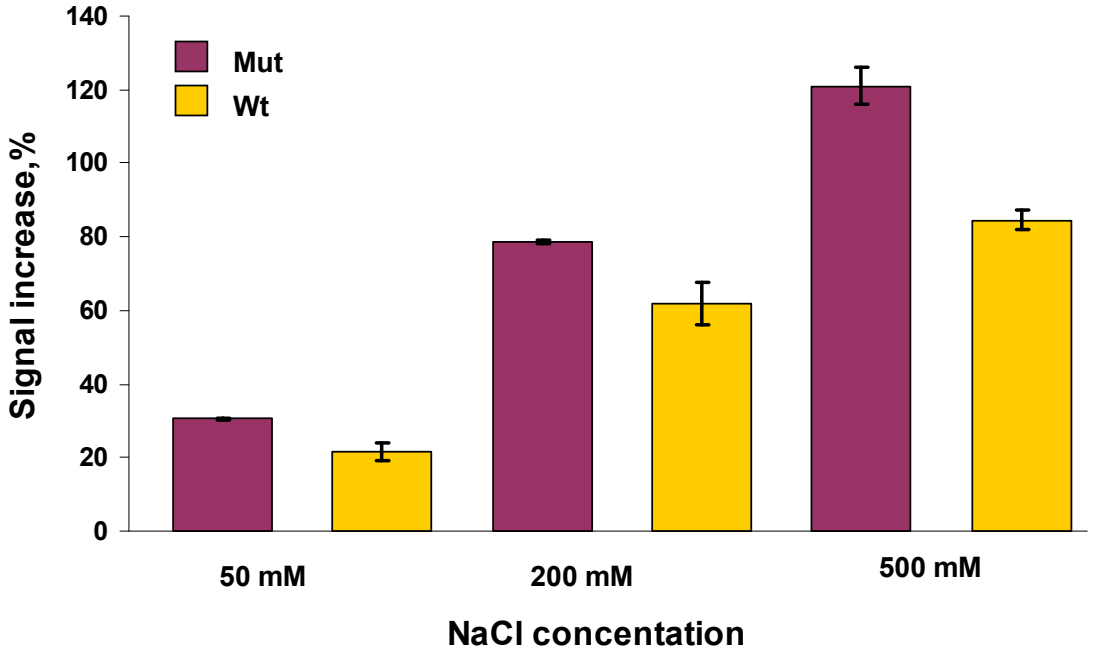

Figure 3: Signal increase % for 1µM DF508 Mutant and/or Wild Type targets, at a Mutant specific sensor, as a function of NaCl concentration in the hybridisation buffer. Measuring solution: 20 µM MB in 0.5 M NaCl and 20 mM Trizma (pH 7.4)

In Figure 3 the signal variations recorded for the hybridisation of the fully complementary target (Mut) and those recorded for the three mis-matches target (Wt), as a function of three different salt concentrations, is reported. As expected the increase in NaCl concentration in the hybridisation buffer resulted in an increase of the efficiency of the hybridisation process; for example by increasing the NaCl concentration from 0.05 M to 0.5 M an increase in analytical response, from about 9 to 36%, was recorded. Moreover the increase in the Na^+ concentration in the hybridisation buffer allowed a better discrimination between the Mut and Wt synthetic targets. From the mechanism studies and the hybridisation efficiency study it was decided to carry out

ISBN:978-84-693-3386-0/DL:T.1002-2010

further experiments in the presence of 0.5 M NaCl in the hybridisation buffer in order to reduce the possible alteration to the duplex during the incubation/measurement step and to work at a NaCl concentration where the guanine MB interaction was more important.

3.3. Quantitative detection

Quantitative analysis of DF508 synthetic PCR analogue was performed by monitoring the signal variation as a function of the oligonucleotide concentration in the hybridisation buffer. Solutions containing different concentration of the synthetic analogues of a typical PCR product (between 10 and 1000 nM) were prepared by dilution, using the hybridisation buffer, of a 100 μM stock solution of the synthetic oligonucleotide (prepared according to the indication of the supplier). The calibration curve was performed by putting an aliquot of the hybridisation buffer containing 500 mM of NaCl and the desired concentration of the synthetic target in contact with the sensor surface followed by 1 hour incubation at room temperature (ca. 23 ºC). Following a thorough wash in the hybridisation buffer, the sensor was transferred to the measurement solution (20mM Trizma buffer containing 0.5 M NaCl, pH 7.4, containing 20 μM MB), and allowed to interact for 5 minutes, after which the DPV response were recorded. Following the DPV measurements the sensor surface was regenerated (immersion for 2 minutes in a 200 mM NaOH solution) and the baseline signal recorded. In Figure 4-A the calibration curve, between 10 and 1000 nM of the synthetic Mut target is presented. Two well-defined regions can be recognised in this calibration: a linear region and a plateau region. For target concentrations below 100 nM a linear response of the sensor with the target concentration was recorded. For concentrations higher than 100 nM the calibration curve started to level off clearly indicating the saturation of the sensor. In the inset of Figure 4-A the calibration curve recorded for concentrations between 10 nM and 50 nM is presented**.** This concentration range was chosen due to its analytical relevance and a good linearity was observed (R^2 = 0.991) with a sensitivity of 1.842 signal increase (%) nM^{-1}. The reproducibility between electrodes (three electrodes) was calculated to be 6.7% and the repeatability obtained for each electrode was calculated to be 5.6%. The limit of detection (LOD) was calculated to be 2.64 nM, an improvement on the detection limits reported in recent publications of 10nM [48, 49] up to a few micromolar [50].

ISBN:978-84-693-3386-0/DL:T.1002-2010

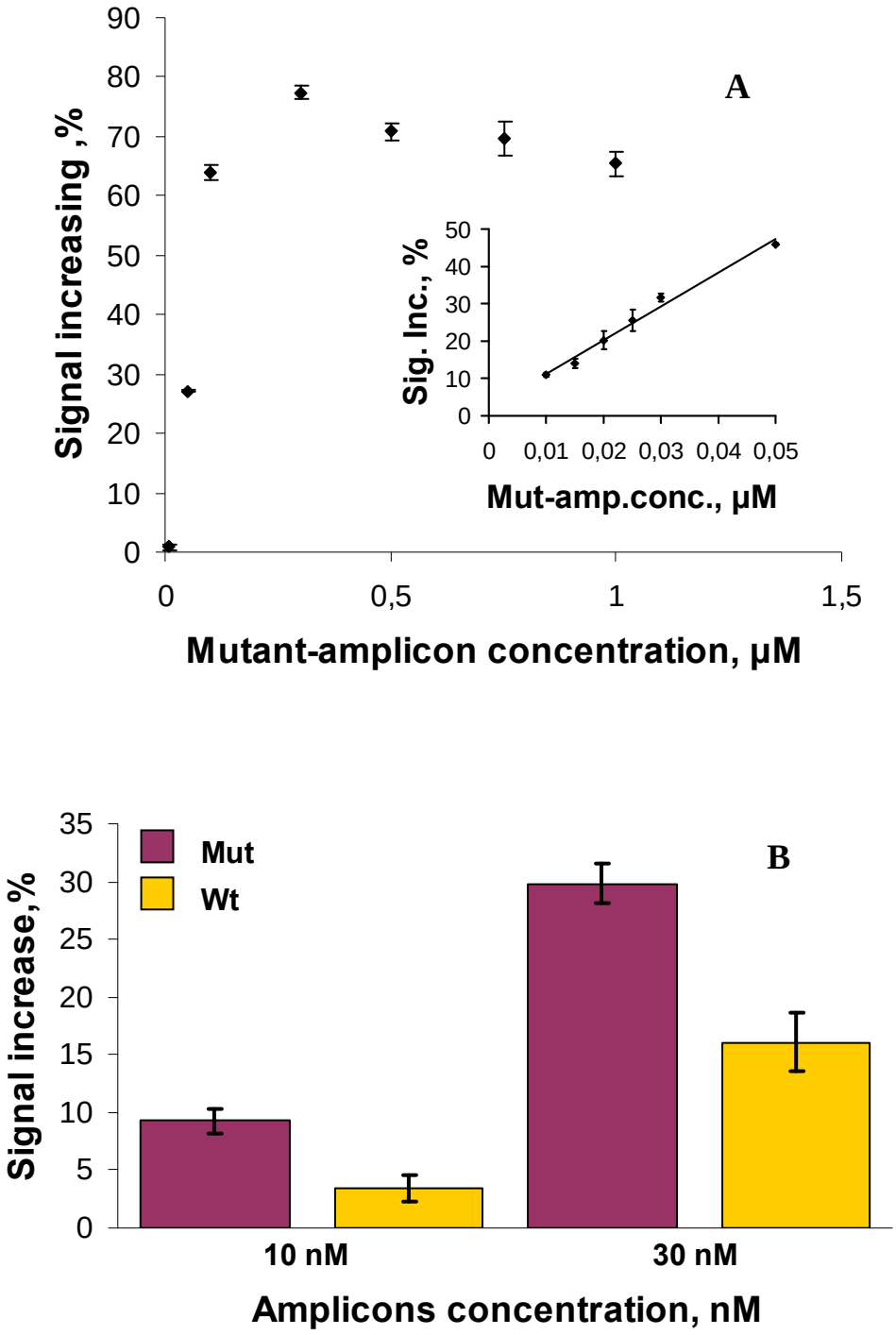

Figure 4: A: Signal increase (%) recorded for different concentration (between 10 and 1000 nM) of DF508 Mutant synthetic PCR analogue. Inset: Calibration of the Mutant syntetic PCR analogue in the concentration range between 10 and 50 nM. B: Comparison of the sensor performances when put in contact with 10 and 30 nM of the Mut and Wt synthetic PCR analogues. Response reported as signal variation (%) according to definition of section 4.1. Measurement solution: 20 µM MB in 0.5 M NaCl and 20 mM Trizma (pH 7.4).

ISBN:978-84-693-3386-0/DL:T.1002-2010

3.4. Effect of Formamide on Hybridisation Stability

In order to enhance the discrimination between mutant and wild type targets, and to suppress or even to fully eliminate the non-specific response, the use of formamide to destabilise the Wt/probe duplex was explored, as formamide has been reported [46] to have the ability to denature DNA duplexes. This denaturation ability is related to ion-solvating power and to its ability to increase the solubility of free bases concomitantly decreasing the hydrophobic character of the solvent, the activity coefficients and free energies of the bases [52-54]. Indeed, the use of formamide in the hybridisation buffer has been reported to improve the discrimination between single-base mismatched sequences [55, 56] in electrochemical genosensors. In these works the authors reported no significant destabilisation of the hybridisation between probe and fully complementary sequence for formamide concentrations up to 25% v/v; whilst a considerable destabilisation of the unspecific duplex was reported [55, 56]. We thus attempted to exploit formamide as a means to improve discrimination between the complementary mutant and the non-fully complementary wild type. Different formamide percentages (v/v) were added to the hybridisation buffer together with 1μM of the desired target (Mut or Wt sequences), and following the hybridisation step the electrode surface was washed for ca. 5 minutes in the hybridisation buffer (without formamide). Following this washing step the sensor was transferred to the incubation/measurement solution and voltammetric detection performed as previously described. In Figure 5-A the signal variations obtained for the hybridisation of the mutant and wild type sequences as a function of the formamide percentage in the hybridisation buffer are presented. In the case of the experiments performed with the Mutant synthetic analogue a progressive loss of the electrochemical response was recorded, and was more evident at formamide concentrations higher than 20% (v/v). On the other hand in the case of the experiments performed using the Wt sequences a more notable decrease in signal was recorded until levelling off at concentrations higher than 30-35% (v/v). These results are consistent with those previously reported [55, 56] where a formamide concentration of 25% (v/v) was demonstrated to facilitate discrimination between the fully complementary sequence and mis-matched sequences. In order to fully evaluate the applicability of the use of formamide in the hybridisation buffer as a means of improving the specificity of the sensor, the influence of formamide on the electrochemical performance of the sensing platform was evaluated, using two different set of experiments. In the first set of experiments the influence of increasing percentages

ISBN:978-84-693-3386-0/DL:T.1002-2010

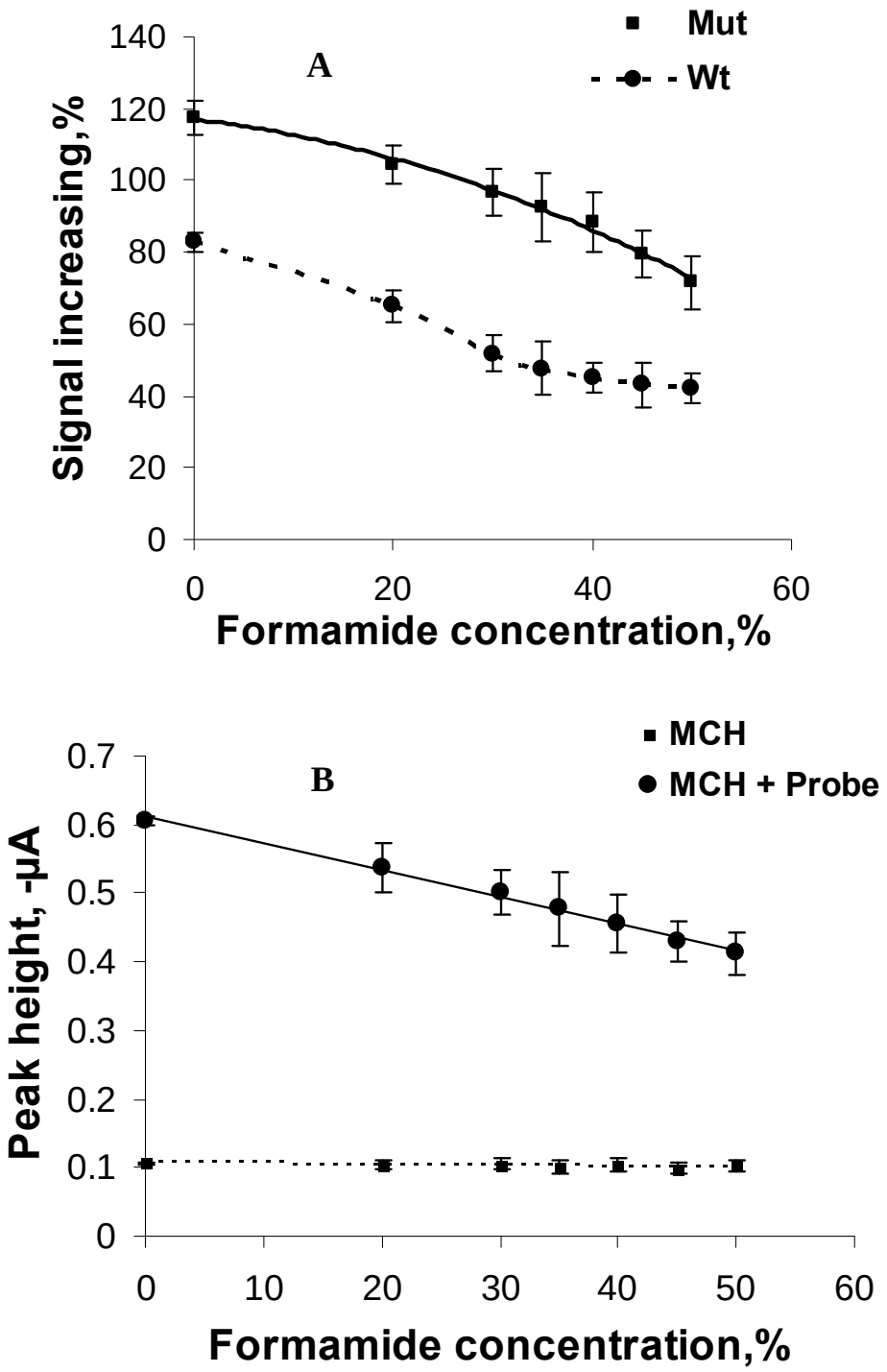

Figure 5: A: Signal increase percentage as a function of the formamide concentration (between 0% and 50% v/v) in the hybridization buffer for Mutant and Wild Type amplicons. B: Peak current recorded at a Mut probe sensor and a MCH modified Au electrode, as a function of formamide concentration (between 0% and 50% v/v) in the buffer solution. The Measurement solution: 20 µM MB in 0.5 M NaCl and 20 mM Trizma (pH 7.4)

ISBN:978-84-693-3386-0/DL:T.1002-2010

of formamide on the sensor background (i.e. due to the immobilised probe MB interaction), was evaluated. In the second set the influence of the formamide on the electrochemical performances of the Au electrode was evaluated by monitoring the response of an electrode modified with mercaptohexanol alone. In both cases the evaluation was performed by contacting the two sensors for 1 hour with aliquots of the hybridisation buffer with increasing concentrations of formamide, followed by thorough washing and voltammetric measurement according to the protocol presented in section 3.3. As can be seen in Figure 5-B (MCH curve) incubation with increasing concentrations of formamide did not affect the mercaptohexanol layer present onto the Au electrode, or the electrochemical properties of the Au itself. This is clearly shown by the fact that no variation of the MB response was recorded in the second set of controls. However as it can be seen in the case in which probes were present on the electrode surface (curve MCH + probe of Figure 5-B) a clear decrease of the MB reduction, as a function of the formamide concentration, was recorded. Three possible explanations for the loss in signal can proposed: (i) the loss of probes from the electrode surface (ii) a change in the electrochemical properties of the Au electrode as a result of the hydrogen bond interaction with the formamide [57] or (iii) due to a reduced MB/DNA interaction due to the formamide solvation of the nucleotides in the oligonucleotides. Formamide has a dielectric constant 40% higher than water and its interaction with the phosphate backbone as well as the bases effectively results in a blocking of the MB-DNA interaction. Experimental results, together with previous reports [55, 56], seem to indicate the third option as the most probable.

Despite the fact that the results obtained in this evaluation confirmed the ability of formamide to destabilise the DNA duplex, due to the poor reproducibility, possible probe loss or the effect of formamide on the MB DNA interaction, this approach was not used in further experiments.

3.5. Multi-electrode array for selective detection of DF508 mutation:

As the use of formamide was demonstrated to be an unfeasible approach for improving discrimination, an alternative strategy for the selective detection of Mut and/or Wt was pursued, based on the simultaneous use of three sensors. In this approach two of the three electrodes were modified with thiolated probes specific for the Mut or for the Wt sequence; whilst the third electrode was modified with mercaptohexanol alone acting as

ISBN:978-84-693-3386-0/DL:T.1002-2010

a control. In this way, by combining the response from the three electrodes, a definitive detection of mutant or wild type can be achieved. The performance of this detection approach was evaluated for the discrimination between Mut and Wt sequences at a concentration value of 10 nM, a concentration analogous to that which could be expected from a polymerase chain reaction (PCR).

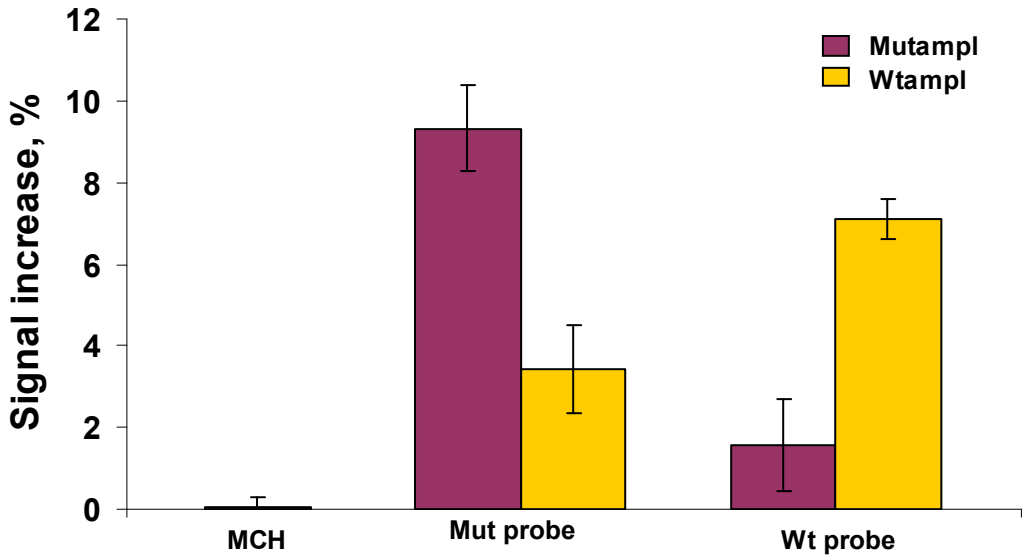

Figure 6: Mutant and Wild type synthetic single stranded PCR product analogues discrimination at low target concentration (10nM) using a mutiparameter detection platform of: Mut specific sensor, Wt specific sensor and control sensor (no probe on it) Measurement solution: 20 μM MB in 0.5 M NaCl and 20 mM Trizma (pH 7.4)

The results of this evaluation are reported in Figure 6 where it can be observed that when hybridisation is performed the sensor carrying the specific probe gave, as expected, a higher response (ca. 2 folds) as compared to those provided by sensor with the mismatched probe. The reported results clearly showed that the proposed sensing approach allows an unambiguous discrimination between mutant/wild types. It is believed that the proposed approach can find large application in clinical analysis.

ISBN:978-84-693-3386-0/DL:T.1002-2010

Conclusions

In the reported work a detection platform exploiting a base specific electroactive marker, for the unambiguous detection of the DF508 mutation of CF has been presented. The assessment of the possibility of discriminating between "wild type" and "mutant" sequences was performed using two synthetic single stranded PCR analogues. Electrochemical and fluorimetric studies facilitated further insight into the MB/DNA interaction mechanisms that are involved in the electrochemical detection, demonstrating that electrostatic interaction and weak bases interaction play a more prominent role at concentrations of NaCl lower than 0.2 M, whilst guanine specific contribution was observed to become predominant for NaCl concentrations higher than 0.2 M. The electrochemical detection of the specific sequences was quantitative for target concentrations between 10 and 50 nM (R^2 = 0.991) with a limit of detection of 2.64 nM. Although the sensitivity of the proposed methods is lower than those achievable using labels, the reported approach offer definitive advantages such as speed and ease-of-use. An attempt to improve sensor selectivity exploiting the use of formamide in the hybridisation buffer was investigated but was not suitable for the reported detection mechanism due to the influence of formamide on the interaction of the methylene blue with DNA. Finally the use of a multisesnor detection platform was demonstrated to achieve a clear and definitive discrimination between the different possible forms of the targeted genomic region.

Acknowledgements

This work has been carried out with financial support from the Commission of the European Communities, specific RTD program 'Isolation of fetal cells from maternal blood, SAFER, NEST-ADVENTURE 04977'. Dr. Valerio Beni kindly acknowledges the European Community's, Seventh framework programme (FP7/2007-2013) under grant agreement nº (PIGF-GA-2008-220928) for the financial support. Hany Nasef wishes to thank Universitat Rovira I Virgili for a BRDI scholarship.

ISBN:978-84-693-3386-0/DL:T.1002-2010

6. References

1 Andersen DH (1938) Cystic fibrosis of the pancreas and its relation to celiac disease: A clinical and pathological study. Am J Dis Child 56:344–399.
2 Kerem BS, Rommens JM, Buchanan JA, Markiewicz D, Cox TK, Chakravarti A (1989) Identification of the cystic fibrosis gene: Genetic analysis. Science 245: 1073–1080.
3 Dodge JA, Marison S, Lewis PA, Coles EC, Geddes D, Russell G (1997) Incidence, population and survival of cystic fibrosis in 1995. Archives of diseases in childhood 77:493-496.
4 Boat T, Welsh M, Beaudet AL (1989) Cystic fibrosis, ed 6. New York, McGraw Hill,.
5 Murphy D, Redmond G (2005) Optical detection and discrimination of cystic fibrosis-related genetic mutations using oligonucleotide–nanoparticle conjugates. Analytical and Bioanalytical Chemistry 381:1122-1129.
6 Schwarz MJ (1998) DNA diagnosis of cystic fibrosis. Ann Clin Biochem 35:584-610.
7 Liu J, Liu J, Yang L, Chen X, Zhang M, Meng F, Luo T, Li M (2009) Nanomaterial-assisted signal enhancement of hybridization for DNA biosensors: A review. Sensors 9:7343-7364.
8 lodes MJ, Suciu D, Wilmoth JL, Ross M, Munro S, Dix K, Bernards K, Stover AG, Quintana M, Iihoshi N, Lyon WJ, Dnaley DL, McShea A (2007) Plos ONE 2 9:e924.
9 Lisdat F, Schäfer D (2008) Anal Bioanal Chem 391:1555–1567.
10 Long Y, Li C, Sutherland T, Kraatz H, Lee J (2004) Anal Chem 76:4059-4065.
11 DeLumley T, Campbell C, Heller A (1996) J Am Chem Soc 118:5504.
12 Alfonta L, Singh AK, Willner I (2001) Anal Chem 73:91.
13 Pividori MI, Merkoci A, Alegret S (2001) Biosensors & Bioelectronics 16 (9-12):1133-1142.
14 Arias P, Ferreyra NF, Rivas GA, Bollo S (2009) Glassy carbon electrodes modified with cnt dispersed in chitosan: Analytical applications for sensing DNA-methylene blue interaction. Journal of Electroanalytical Chemistry 634:123-126.
15 Ihara T, Nakayama M, Murata M, Nakano K, Maeda M (1997) Chem Commun 1609.
16 Kertez V, Whittemore NA, Inamati G, Manoharan M, Cook P, Baker D, Chambers JO (2000) Electroanalysis 12:889.
17 Patolsky F, Lichtenstein A, Willner I (2001) J Am Chem Soc 123 (22):5194–5205.
18 Napier ME, Loomis CR, Sistare MF, Kim J, Eckhardt AE, Thorp HH (1997) Probing biomolecule recognition with electron transfer: Electrochemical sensors for DNA hybridization. Bioconjugate Chemistry 8:906-913.
19 Millan KM, Saraullo A, Mikkelsen SR (1994) Voltammetric DNA biosensor for cystic fibrosis based on a modified carbon paste electrode. Analytical Chemistry 66:2943-2948.
20 Li X-M, Ju H-Q, Du L-P, Zhang S-S (2007) A nucleic acid biosensor for the detection of a short sequence related to the hepatitis b virus using bis(benzimidazole)cadmium(ii) dinitrate as an electrochemical indicator. Journal of Inorganic Biochemistry 101:1165-1171.

21 Petty JT, Bordelon JA, Robertson ME (2000) Thermodynamic characterization of the association of cyanine dyes with DNA. The Journal of Physical Chemistry B 104:7221-7227.
22 Zhao GC, Zhu JJ, Chen HY (1999) Spectrochimica Acta Part A: Molecular and Biomolecular Spectroscopy 55 (5):1109–1117.
23 Nafisi S, Saboury AA, Keramat N, Neault JF, Tajmir-Riahi HA (2007) Journal of Molecular Structure 827 (1–3):35–43.
24 Erdem A, Kerman K, Meric B, Akarca US, Ozsoz M (2000) Analytica Chimica Acta 422 (2):139–149.
25 Yang WR, Ozsoz M, Hibbert DB, Gooding JJ (2002) Electroanalysis 14(18):1299–1302.
26 Boon EM, Ceres DM, Drummond TG, Hill MG, Barton JK (2000) Mutation detection by electrocatalysis at DNA-modified electrodes Nature Biotechnology 18:1096-1100
27 Kelley SO, Barton JK, Jackson NM, Hill MG (1997) Electrochemistry of methylene blue bound to a DNA-modified electrode. Bioconjugate Chemistry 8:31-37.
28 Sismani C, Kousoulidou L, Patsalis PC: Multiplex amplifiable probe hybridization (maph) in Walker JM, Rapley R (2000) Molecular biomethods handbook. Totowa, NJ,, Humana Press, pp 179-193.
29 Zhu N, Zhang A, Wang Q, He P, Fang Y (2004) Electrochemical detection of DNA hybridization using methylene blue and electro-deposited zirconia thin films on gold electrodes. Analytica Chimica Acta 510:163-168.
30 Jin Y, Yao X, Liu Q, Li J (2007) Hairpin DNA probe based electrochemical biosensor using methylene blue as hybridization indicator. Biosensors and Bioelectronics 22:1126-1130.
31 Lin X-H, Wu P, Chen W, Zhang Y-F, Xia X-H (2007) Electrochemical DNA biosensor for the detection of short DNA species of chronic myelogenous leukemia by using methylene blue. Talanta 72:468-471.
32 Óscar AL, Susana C, María P, José MP (2008) Designs of enterobacteriaceae lac z gene DNA gold screen printed biosensors. Electroanalysis 20:1397-1405.
33 Zhu, N, Zhang, A, Wanf, Q, He, P, Fang, Y (2004) Electrochemical detection of DNA hybridization using methylene blue and electro-deposited zirconia thin films on gold electrode. Analytica Chimica Acta 510: 163-168
34 Pänke, O, Kirbs, A., Lisdat, F (2007), Voltammetric detection of single base-pair mismatches and quantification of label-free target ssDNA using a competitive binding assay. Biosensors & Bioelectronics 22: 2656-2662
35 Lin, XH, Wu, P, Chen, W, Zhang, YF, Xia, XH (2007), Electrochemical DNA biosensor for the detection of short DNA species of Chronic Myelogonous Leukemia by using methylene blue. Talanta 72: 468-471
36 Jin, Y, Yao, X, Liu, Q, Li, J (2007) Hairpin DNA probe based electrochemical biosensor using methylene blue as hybridization indicator. Biosensors & Bioelectronics 22: 1126-1130
37 Loiaza, OA, Campuzano, S, Pedrero, M, Pingarron, JM (2008) Designs of Enterobacteriacae Lac Z gene DNA gold screen printed biosensors. Electroanalysis 20: 1397-1405
38 Henry OYF, Acero Sanchez JL, Latta D, O'Sullivan CK (2009) Electrochemical quantification of DNA amplicons via the detection of non-hybridised guanine bases on low-density electrode arrays. Biosens Bioelectron 24:2064-2070.
39 Kelley SO, Jackson NM, Hill MG, Barton JK (1999) Angew Chem 38 941.

40 Riordan JR, Rommens JM, Kerem BS, Alon N, Rozmahel R, Grzelczak Z (1989) Identification of the cystic fibrosis gene: Cloning and characterization of complementary DNA. Science 245 1066–1073.
41 Herne TM, Tarlov MJ (1997) J Am Chem Soc 119:8916-8920.
42 Fujimoto BS, Clendenning JB, Delrow JJ, Heath PJ, Schurr M (2002) Fluorescence and photobleaching studies of methylene blue binding to DNA. The Journal of Physical Chemistry 98:6633-6643.
43 Nafisi S, Saboury AA, Keramat N, Neault J-F, Tajmir-Riahi H-A (2007) Stability and structural features of DNA intercalation with ethidium bromide, acridine orange and methylene blue. Journal of Molecular Structure 827:35-43.
44 Wang Y, Zhou A (2007) Spectroscopic studies on the binding of methylene blue with DNA by means of cyclodextrin supramolecular systems. Journal of Photochemistry and Photobiology A: Chemistry 190:121-127.
45 Rohs R, Sklenar H (2004) Methylene blue binding to DNA with alternating at base sequence: Minor groove binding is favored over intercalation. Journal of biomolecular structure & dynamics 21(5):699-711.
46 Kara P, Kerman K, Ozkan D, Meric B, Erdem A, Ozkan Z, Ozsoz M (2002) Electrochemical genosensor for the detection of interaction between methylene blue and DNA. Electrochemistry Communications 4 705–709.
47 Zhao F, Zeng B, Pang D (2003) Voltammetric study of methylene blue at thiol sams-modified gold electrodes. Electroanalysis 15:1060-1066.
48 Dharuman V, Hahn JH (2007) Sensors and actuators b: Chemical 127:536–544.
49 Dharuman V, Hahn JH (2008) Biosens Bioelectron 23 (8):1250–1258.
50 Yan F, Erdem A, Meric B, Kerman K, Ozsoz M, Sadik OA (2001) Electochemistry Communications 3 (5):224–228.
51 Levine L, Gordon JA, Jencks W (1962) Biochemistry 2:168–175.
52 Herskovitz TT, Singer SJ, Geiduschek EP (1961) Arch Biochem Biophys 94:99–114.
53 Geiduschek EP, Herskovitz TT (1961) Arch Biochem Biophys 95:114–129.
54 Hamaguchi K, Geiduschek P (1962) J Am Chem Soc 84:1329–1338.
55 Abad-Valle P, Fernández-Abedul MT, Costa-García A (2007) DNA single-base mismatch study with an electrochemical enzymatic genosensor. Biosensors and Bioelectronics 22:1642-1650.
56 Hernandez-Santos D, Gonzalez-Garcia MB, Costa-Garcia A (2005) Genosensor based on a platinum(ii) complex as electrocatalytic label. Analytical Chemistry 77:2868-2874.
57 Pyykkö P (2005) Theoretical chemistry of gold. Ii. Inorganica Chimica Acta 358:4113-4130.

UNIVERSITAT ROVIRA I VIRGILI
TEMPERATURE MODULATED GENOSENSOR FOR DETECTION OF CYSTIC FIBROSIS MUTATIONS
Hany Abdel Hady Abdel Rahman Nasef
ISBN:978-84-693-3386-0/DL:T.1002-2010

CHAPTER 4 (Art 3):

Electrochemical molecular beacon based DNA biosensor for the discrimination of Cystic fibrosis mutations

ISBN:978-84-693-3386-0/DL:T.1002-2010

1. Introduction:

Cystic fibrosis (CF) is an inherited chronic disease resulting in lung and pancreatic damage, causing progressive disability, and, for most, early death (1-4). A defective gene and its protein product cause the body to produce unusually thick, sticky mucus. Almost 1,000 mutations have been identified in the CF gene, but a few common mutations cause disease in most patients (5). DF508 is the most common mutation in which there is a deletion of phenylalanine at position 508 in the amino acid sequence of cystic fibrosis transmembrane conductance regulator gene located in chromosome 7. DF508 is frequency varies between ethnic groups, accounting for 70 per cent of mutations in the white populations of Britain and US but fewer than 50 per cent in southern European populations. CFTR mutations are correlated with disease severity (3).Cystic fibrosis ordinary diagnosis is achieved by sweat test as people with cystic fibrosis have an abnormally high salt level in sweat (6) and by screening test to detect a chemical called immunoreactive trypsinogen (7) which is high in babies with cystic fibrosis.

Since the discovery of the DNA structure in 1953 (8), there has been an increasing demand for accurate and rapid genotyping, especially in the last few decades (9-14). Recent reports for detection of cystic fibrosis mutations include the use of surface plasmon resonance (SPR) (15, 16). Surface plasmon resonance imaging SPRI was applied the detection of gene mutations accounting for human cystic fibrosis and specifically some of those localized in Exon 10, with the common three-base-pair deletion ΔF508, as well as several single nucleotide polymorphisms (SNPs). The SPRI system was able to monitor the hybridisation kinetics of unlabelled DNA targets (short oligonucleotides or a 377 pb PCR product) to a 196 spot matrix of ssDNA probes immobilised onto a bio-functionalised surface and to detect in real-time the mutations in a DNA fragment (15). Mannelli et al have studied two different surface chemistries (employing 11-mercaptoundecanoic acid–poly (ethylenimine) and dextran procedures) for the development of surface plasmon resonance imaging (SPRI) based DNA microarray affinity sensors to detect in parallel several mutations causing cystic fibrosis DF508, DI507, M470V, Q493X, V520F and 1716 G>A (16).

ISBN:978-84-693-3386-0/DL:T.1002-2010

Electrochemical methods show great potential in DNA diagnostics (17-28). The advantages of electrochemical transduction are high sensitivity, independence from solution turbidity, compatibility with micro-fabrication, low cost, low power requirements and simple instrumentation which is compatible with small portable devices (9). Hahm and Lieber (29) reported a DNA biosenosr based on the use of silicon nanowire (SiNW) transduction elements. The surface of the SiNW was functionalized with biotin, onto which an avidin layer was immobilized followed by the biotinylated 10-mer peptide nucleic acid (PNA) probe. Hybridization of the immobilized probe with oligonucleotide targets (a complementary 31-mer wild type target and a 28-mer target mimicking a deletion associated with the DF508 mutation) was followed in a label-free capacity. An increase in conductance was observed on association of negatively charged nucleic acids with the SiNW. Recently, a biosensor based on employing of methylene blue as a reporter in the discrimination of synthetic PCR analogue of the DF508 cystic fibrosis mutation (Mut) from the wild type (Wt) was introduced. The methylene blue reduction beak was measured directly after 5 minutes incubation with the gold electrode surface duplexes. At optimum experimental condition a discrimination factor, between mutant and wild type of ca. 1.5 fold was found. The proposed assay was quantitative and linear in the range of 10 – 100 nM, exhibiting a limit of detection (LOD) of 2.64 nM (30).

A fluorescent molecular beacon (MB) is defined as a fluorescent-labelled oligonucleotide chain, typically containing 25–35 nucleotides, and constructed by three parts (31, 32): (1) A loop portion generally consisting of 15–30 nucleotides, which specifically binds with the target sequence (2) A stem portion of 5–8 bases. During the binding process of the MBs and target molecules, this portion is reversibly dissociated. The thermodynamic equilibrium relation between the stem portion and double-stranded structure of loop portion targets hybrid molecular is designed so that the hybridization specificity of MBs is significantly stronger than that of a conventional linear probe. (3) Tyagi first reported the molecular beacons (MBs) technology in 1996 (31), obviating the requirement to separate probe-target hybrids from excess probes in hybridization assays (31, 33) Because of the characteristics of simple operation, high-sensitivity, and specificity, MBs have been used for real-time quantitative determination of nucleic acid (34), for the construction of self-reporting oligonucleotide arrays (35), and even for analysis in vivo (36).

ISBN:978-84-693-3386-0/DL:T.1002-2010

An example of an electrochemical based molecular beacon was first reported by Fan et al (37). Dubbed the E-DNA sensor, the device comprises of electrochemically labelled MB probe oligonucleotides, functionalized at the 3`-terminus with a thiol residue and at the 5`- terminus with a ferrocene moiety. These were attached to a gold electrode surface by the well established gold– thiol interaction. The stem-loop structure of the molecular beacon maintained the electrochemical reporter in close proximity to the electrode surface in the absence of the target nucleic acid. In the presence of the target nucleic acid, the stem-loop structure was dissociated and replaced by a more linearized double-stranded nucleic acid structure. As such, the electrochemical reporters that were associated with linearized hybrids were extended away from the electrode surface and the distancing of the transduction element could be determined as a reduction in peak current in cyclic voltammetry measurements.

Ying et al, (38) presented an impedance-based DNA biosensor using thionine intercalation to amplify the DNA hybridization signal. Beacon single-stranded DNA (ssDNA) probe and mercaptoacetic acid were self-assembled onto an Au electrode by chemisorption. After hybridisation with the DNA target and due to the neutralization of the negative charges of dsDNA by the intercalated thionine, the electronic transfer resistance (Ret) of the DNA modified Au electrode was significantly diminished. An unlabeled hairpin-DNA probe was used for the detection of eight single-nucleotide mismatches by electrochemical impedance spectroscopy (EIS) (39). Upon hybridization of the target strand with the hairpin DNA probe, the stem-loop structure is opened and forms a duplex DNA. Accordingly, the film thickness is increased, which causes differences in the electrical properties of the film before and after hybridization. The differences in the charge-transfer resistance ΔRCT between hairpin DNA (before hybridization) and duplex DNA (after hybridization) results in a large structural rearrangement from hairpin to duplex (39). A recent approach was introduced by Plaxco et al. (40), who describe an electrochemical DNA (E-DNA) sensing platform based on target-induced conformation changes in an electrode-bound DNA pseudo-knot. The pseudo-knot, a DNA structure containing two stem-loops in which the first stem's loop forms part of the second stem, is modified with a methylene blue redox tag at its 3′ terminus and covalently attached to a gold electrode via the 5′ terminus. In the absence of a target, the structure of the pseudo-knot probe minimizes collisions between the redox tag and the electrode, thus reducing faradic current. Target binding disrupts the

ISBN:978-84-693-3386-0/DL:T.1002-2010

pseudo-knot structure, liberating a flexible, single-stranded element that can strike the electrode and efficiently transfer electrons (40).

In the work reported here, we present an electrochemical based genosensor exploiting molecular beacons for the discrimination between synthetic PCR analogue cystic fibrosis DF508 mutant and the corresponding wild type. A 34 bp molecular beacon probe, complementary to the DF508 mutant sequences in 18 bp length in loop region of the beacon, was immobilized on a gold electrode surface. The electrochemical reporter employed in this work is methylene blue which was attached in the 5`-end of the molecular beacon (Table 7.1). The immobilization of the beacon probe on the gold electrode surface was achieved via the thiolated 3`-end to form a S-Au bond. The effect of different buffer types (PBS, PBS-T, SSC, HEPES and Trizma) was investigated. Two immobilization mechanisms were examined in this work namely "backfilling" and "co-immobilization" and the melting temperature was also studied for the immobilized beacon probe. Finally, the hybridisation time for the complementary target and the discrimination between the two targets was examined. The optimum conditions were applied for the discrimination between the mutant and wild type for both the Δ508 mutation as well as another cystic fibrosis mutation, which has only one base mismatch. V520F cystic fibrosis mutant occurs in exon 10 of the cystic fibrosis gene and results from a substation of G by T nucleotide to change the corresponding amino acid from valine to phenylalanine (41).

2. Experimental

2.1. Chemicals, probes and targets

All chemicals and reagents: Trizma base (Sigma), Potassium hexacyanoferrate (III), $K_3Fe(CN)_6$ (Sigma), hydrochloric acid (6M, Scharlau), potassium dihydrogen phosphate KH_2PO_4 (Scharlau), sodium chloride NaCl (Scharlau), sodium hydroxide NaOH pellets (Panreac), sulphuric acid H_2SO_4 (Sigma), 6-mercaptohexanol, MCH (Fluka), potassium hexacyanoferrate (II) $K_4Fe(CN)_6$ (Fluka), phosphate buffer saline, PBS (Sigma), phosphate buffer saline (pH 7.4) with Tween-20, PBS-T (Sigma), saline sodium citrate buffer, SSC (Sigma) and HEPES buffer (Acros organics) were of analytical grade and used without further purification. Alumina powder (1, 0.3, 0.05 micron) was provided by CHI Instruments (USA). All solutions were prepared in ultra

ISBN:978-84-693-3386-0/DL:T.1002-2010

pure water (18 MΩ.cm) obtained using a "Simplicity Water Purification System" (Millipore, France).

Oligonucleotides, listed in Table 7.1, were provided by Biomers (Biomers, Germany).

The oligonucleotides, used in this work, are analogues to the PCR products obtained using an amplification protocol, based on a "Multiplex Amplifiable probe Hybridization (MAPH)" strategy (42). The two primers, specific for the DF508 mutation region and carrying specific MAPH tails, were: 5' GCCGC GAATTCACTAGTGTGGCACCATTAAAGAAAA 3' (forward) and 5' GGCCGCG GGAATTCGATTATATATTC ATCAT AGGAAAC 3' (reverse), where the regions specific for the probe are indicated in bold and those for the MAPH tags are underlined. As a result of the amplification process two possible amplicons could be generated: an 82 bases long amplicon in the case of the mutant and an 85 bases long sequence for the wild type. The full sequences of the synthetic PCR analogues are listed in Table 1.

DF508 Mutant target amplicon (82 mer)	**5' GCC GCG AAT TCA CTA GTG TGG CAC CAT TAA AGA AAA TAT CAT TGG TGT TTC CTA TGA TGA ATA TAA TCG AAT TCC CGC GGC C 3'**
DF508 Wild type target amplicon (85 mer)	**5' GCC GCG AAT TCA CTA GTG TGG CAC CAT TAA AGA AAA TAT CAT <u>CTT</u> TGG TGT TTC CTA TGA TGA ATA TAA TCG AAT TCC CGC GGC C 3'**
DF508 Mutant complementary molecular beacon probe (34 mer)	**5' MB- GCG AGA AAG AAA CAC CAA TGA TAT TTA GCC TCG C – SH 3'**
V520F Mutant target amplicon (29 mer)	**5' MB-GCG AGC TTT GAT GAA GCT TCT GTA CTC GC– SH 3'**
V520F Wild type target amplicon (68 mer)	**5' GTG TTT CCT ATG ATG AAT ATA GAT ACA GAA GC<u>G</u> TCA TCA AAG CAT GCC AAC TAG AAG AGG TAA GAA AC 3'**
V520F Mutant complementary molecular beacon probe (68 mer)	**5' GTG TTT CCT ATG ATG AAT ATA GAT ACA GAA GCT TCA TCA AAG CAT GCC AAC TAG AAG AGG TAA GAA AC 3'**

Table 1: Sequences of the oligonucleotides and synthesised amplicons used in this work, where MB is methylene blue.

ISBN:978-84-693-3386-0/DL:T.1002-2010

2.2. Instrumentation and measurements

The electrochemical studies were carried out using an Autolab model PGSTAT 12 potentiostat/galvanostat controlled with the General Purpose Electrochemical System (GPES) software (Eco Chemie B.V., The Netherlands). A classical three electrode cell was used. A set of commercially available polycrystalline Au disk (2 mm diameter) electrodes (CHI Instruments) were used as working electrode, a Ag/AgCl was used as reference electrode (CHI Instruments) and a Pt wire (Sigma) used as counter electrode. Working electrodes were cleaned using mechanical cleaning followed by electrochemical cleaning. The mechanical cleaning was achieved with alumina (using three different sizes: 1, 0.3, 0.05 micron) aqueous slurry, to a mirror finish. After rinsing with ultra pure water the electrodes were electrochemically cleaned by cycling it ca. 40 times (scan rate 100 mVs-1) between -0.2 and 1.6 V in sulphuric acid 0.5 M. The number of cycles was not fixed: the Au electrodes were considered clean when, in a cyclic voltammetric experiment with a ferro\ferri equimolar solution, a peak to peak separation below 80 mV was recorded.

2.2.1. Molecular beacon probe immobilization:

Following the cleaning step, Thiolated molecular beacon probe (Mut complementary MB, table 7.1) was self assembled, via (1) backfilling procedure: by spotting of 50 µl of a 4 µM solution, freshly prepared in 1 M KH_2PO_4, onto the electrode surface and left to assemble for 3 hours. Following probe self assembling the sensor surface was washed with ultra pure water and subsequently back-filled by spotting 50 µl of a 0.01M aqueous solution of mercaptohexanol onto the electrode surface and let to incubate for 30 minutes. The sensor was then thoroughly washed by sequential immersion in 0.1 M NaOH, MilliQ water, 0.1 M HCl and MilliQ water, leaving an organized mixed SAM of chemisorbed DNA probe and MCH.(2) co-immobilization procedure: where a fixed concentration (1µM) of the molecular beacon probe was prepared with different MCH concentration ratios (1:10, 1:30, 1:50 and 1:100) in the immobilization solutions buffered with 1M KH_2PO_4. Following an immobilization time of 3 hrs, the sensor surface was then washed for 20 minutes with contentious stirring in PBS-Tween buffer followed by 10 minutes in MilliQ water. The signal intensity and stability of the immobilized molecular beacon was examined in different buffered solutions, PBS, PBS-Tween, SSC, Trizma and HEPES, the buffers were prepared to be 10 mM concentrated with 0.5M NaCl.

ISBN:978-84-693-3386-0/DL:T.1002-2010

2.2.2. Hybridization with target amplicons:

Target hybridization was carried out via a 45 min incubation of 50µL of the desired target (Mut or Wt synthetic PCR analogues) in 10 mM PBS-T (pH 7.4) in the presence of 0.5 M NaCl. The sensor was then washed with 10 mM PBS-T buffer (pH 7.4) containing 0.5 M NaCl and the hybridization levels were monitored by evaluating the reduction response of the Methylene Blue (MB) label on the 5` end of the molecular beacon immobilized on the gold electrode surface. The sensor, following hybridisation, was immersed in an aliquot of a 10mM PBS-T (pH 7.4), 0.5M NaCl buffer solution and a differential pulse voltammogram (DPV) was recorded. The parameters employed in the DPV experiments were: potential window between 0 and -0.6 V (vs. Ag/AgCl) , step potential 10 mV, modulation amplitude 10 mV, modulation time 0.015 s and interval time 0.1 s. A typical DPV result is presented in the inset of Figure 1, where a clear reduction wave is visible at ca. -100 mV (vs the Ag/AgCl). Electrode regeneration was performed by Milli-Q water. Following the regeneration step the DPV voltammetry was repeated in order to record the background response, due to the immobilised probes.

Melting temperature studies included the immobilized molecular beacon probes and the electrode formed duplexes was achieved employing a 10 mL electrochemical cell surrounded by built-in jacket. The system was thermostatted via (Grant Instruments, Cambridge, Type GD120) device. The electrode surface was incubated at each temperature for 10 minutes prior to measurement.

3. Results and discussion:

As described in figure 1, the molecular beacon probe was immobilized on a clean gold electrode surface. Before hybridisation with the complementary target, beacon configuration was stable under suitable buffer and temperature conditions, making the electron exchange possible between the methylene blue label and the electrode surface. After hybridisation with the complementary target, a marked change occurs to the beacon probe opening the stem region and orienting the beacon structure to “stand up”. Hence, the methylene blue moieties are moved away from the electrode surface, resulting in a dramatic decrease in the reduction peak height (Figure 1 inset). Through regeneration with Milli-Q water, the formed duplexes on the electrode surface are

ISBN:978-84-693-3386-0/DL:T.1002-2010

denatured, restoring the immobilized probe structure to the previous beacon shape, demonstrated by the methylene blue reduction peak after regeneration, which is almost identical to the original peak (Figure 1 inset).

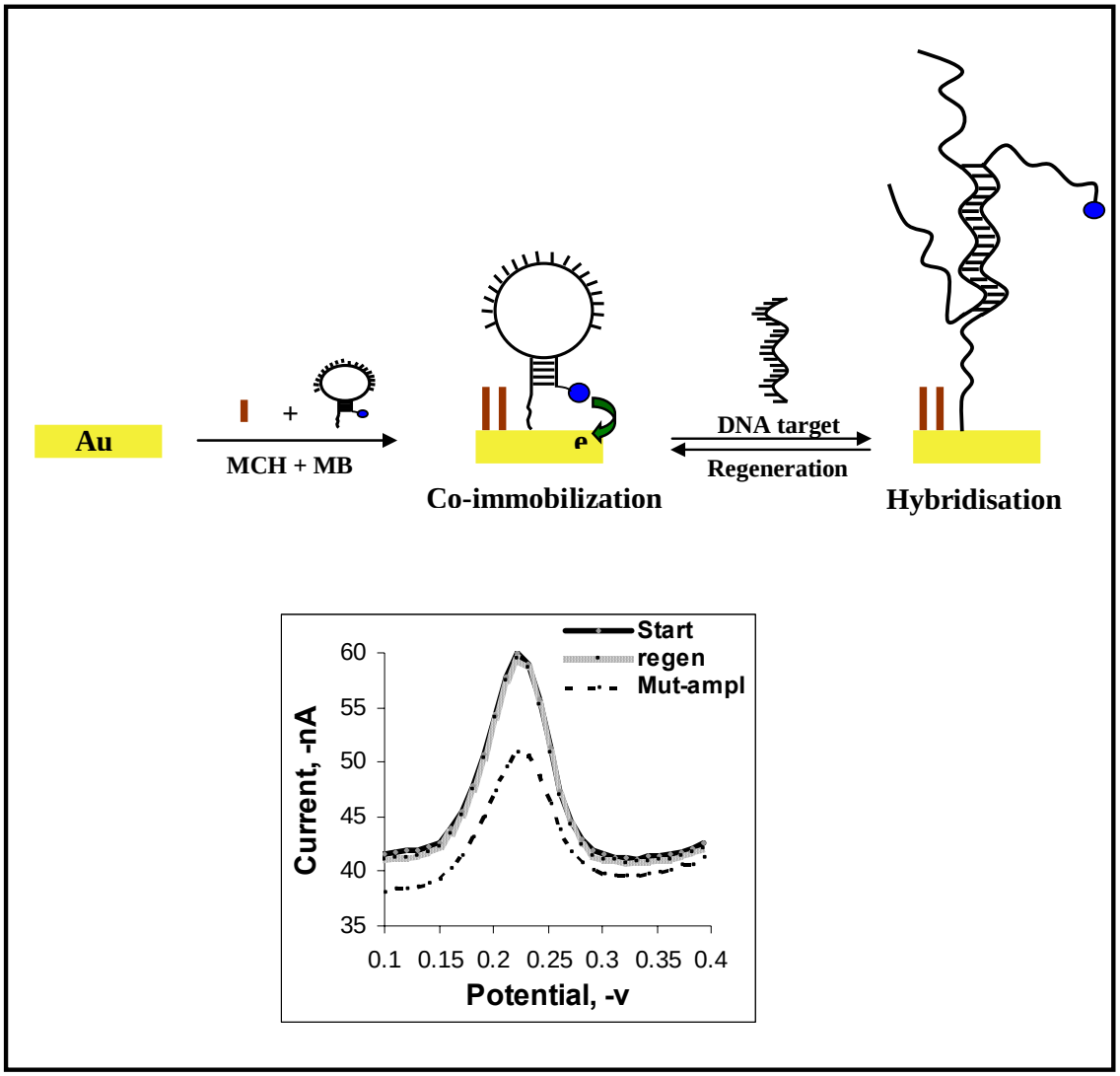

Figure 1: Schematic representation of sensor preparation and hybridisation with the DNA target, the blue sphere represents the methylene blue label. Inset: Differential pulse voltammograms of Mutant amplicon captured on the electrode surface. Hybridisation performed from a solution of 0.5µM target amplicons. Measurement solution: 10 mM PBS-T, pH 7.4, and 0.5M NaCl.

3.1. Beacon probe immobilization stability and buffer solution effect:

After beacon probe immobilization on the cleaned gold electrode via the backfilling procedure, the electrode surface was immersed in different buffer solutions in order to select the optimum buffer corresponding to the higher reduction peak of the labelled beacon probe with methylene blue. The buffer solutions investigated were Trizma, HEPES, PBS, PBS-T and SSC, all of 10mM concentration and 0.5M NaCl at pH 7.4.

ISBN:978-84-693-3386-0/DL:T.1002-2010

Figure 2 depicts the current peak height of the immobilized beacons corresponding to each buffer solution. The optimum peak height obtained was obtained in PBS-T buffer. This could be due to the beacon probe intra-hybridisation in the stem region being more stable in PBS-T buffer solution, which maintains the methylene blue molecules near to the electrode surface, facilitating the electron transfer process.

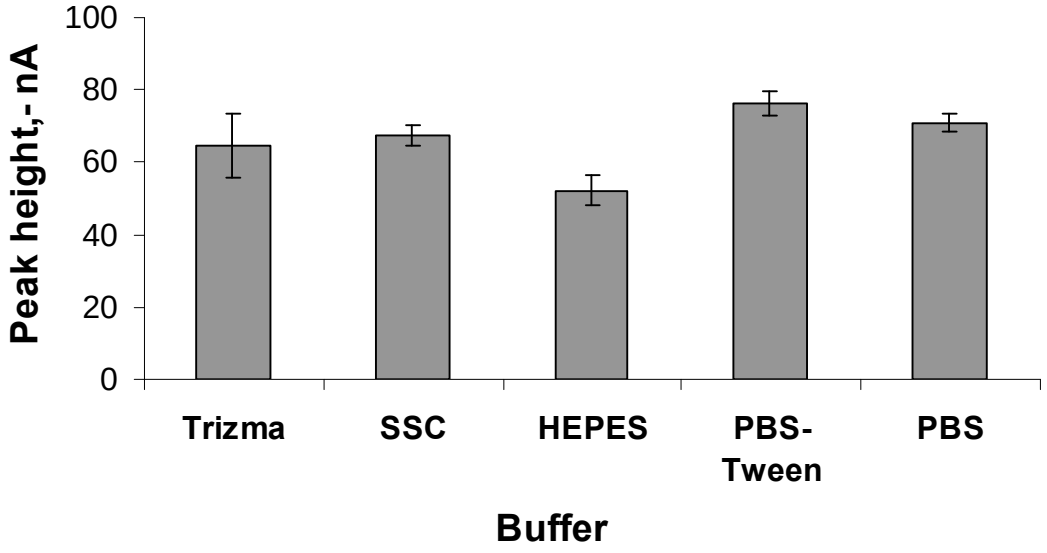

Figure 2: Effect of different buffer solutions on the beacon probe immobilized via backfilling procedure on the gold surface electrode. The concentration of these solutions was 10 mM and all contained 0.5 M NaCl.

The stability of the backfilled immobilization for beacon probes was monitored. As illustrated in figure 3-A, the freshly prepared beacon probes sensors via backfilling procedure exhibits a comparably sharper and higher reduction peak for the methylene blue label. After two days storage in PBS-T buffer the peak was massively decreased as shown in figure 3-A concluding, the sensor could not be reproducible after storage. This result is compatible with data previously reported by Lai et al. (43). Thus, a need for another procedure was necessary in order to assure the reproducibility and repeatability of the employed sensor. The so-called co-immobilization procedure was thus examined for this purpose, in which both the probe and MCH are simultaneously added in the same immobilization buffered solution. Four different concentration ratios were examined as illustrated in figure 3-B inset. The stability of the immobilized probe was checked after two days. The concentration ratio of 1:50 (beacon probe: MCH) showed

ISBN:978-84-693-3386-0/DL:T.1002-2010

the best stability results among the other tested co-immobilized ratios (figure 3-B). Based on these data, further experiments used the co-immobilization procedure with the optimum ratio concentration.

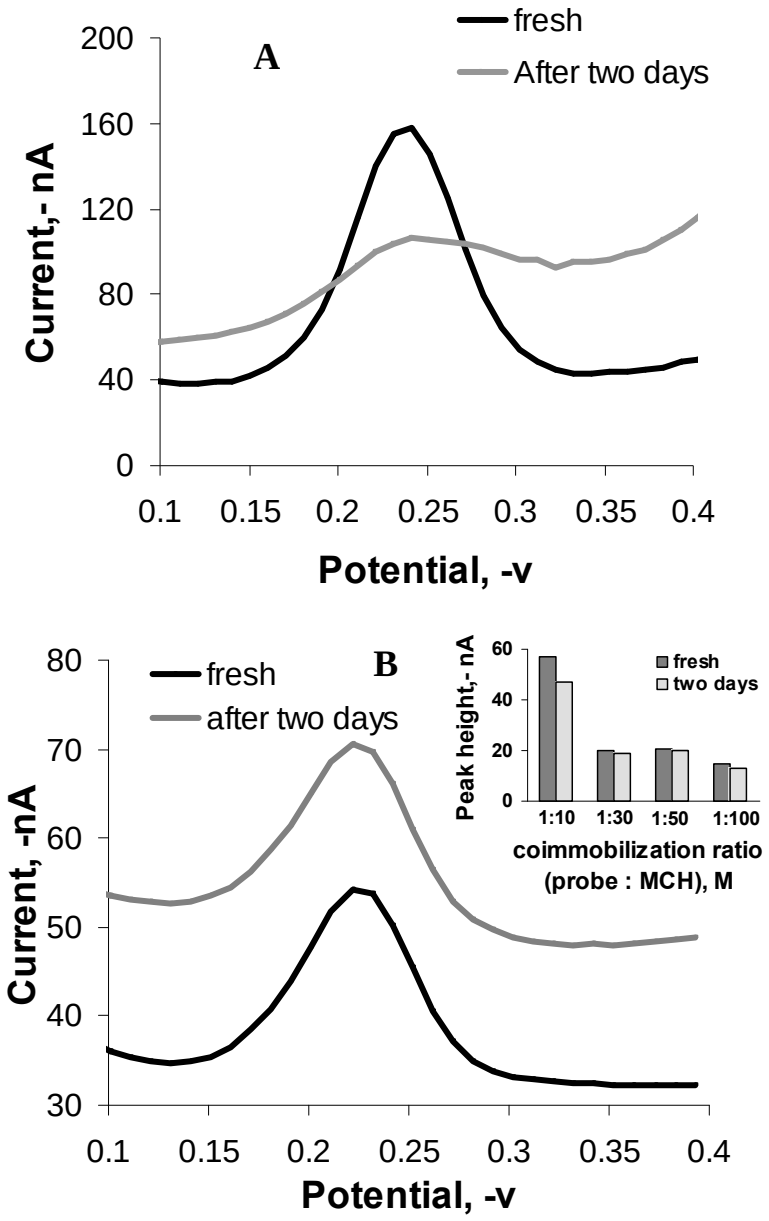

Figure 3: The PBS-T buffer solution storage effect on to electrode surfaces immobilized with beacon probe via backfilling procedure (A) and via co-immobilization procedure (B). Inset: different concentration ration of beacon probe: MCH employed in the co-immobilization solution and the effect of storage in PBS-T buffer solution.

ISBN:978-84-693-3386-0/DL:T.1002-2010

The melting temperature of the immobilized electrochemical molecular beacon in the absence of target DNA was investigated and observed to be 31.5 ºC, indicating good stability at room temperature.

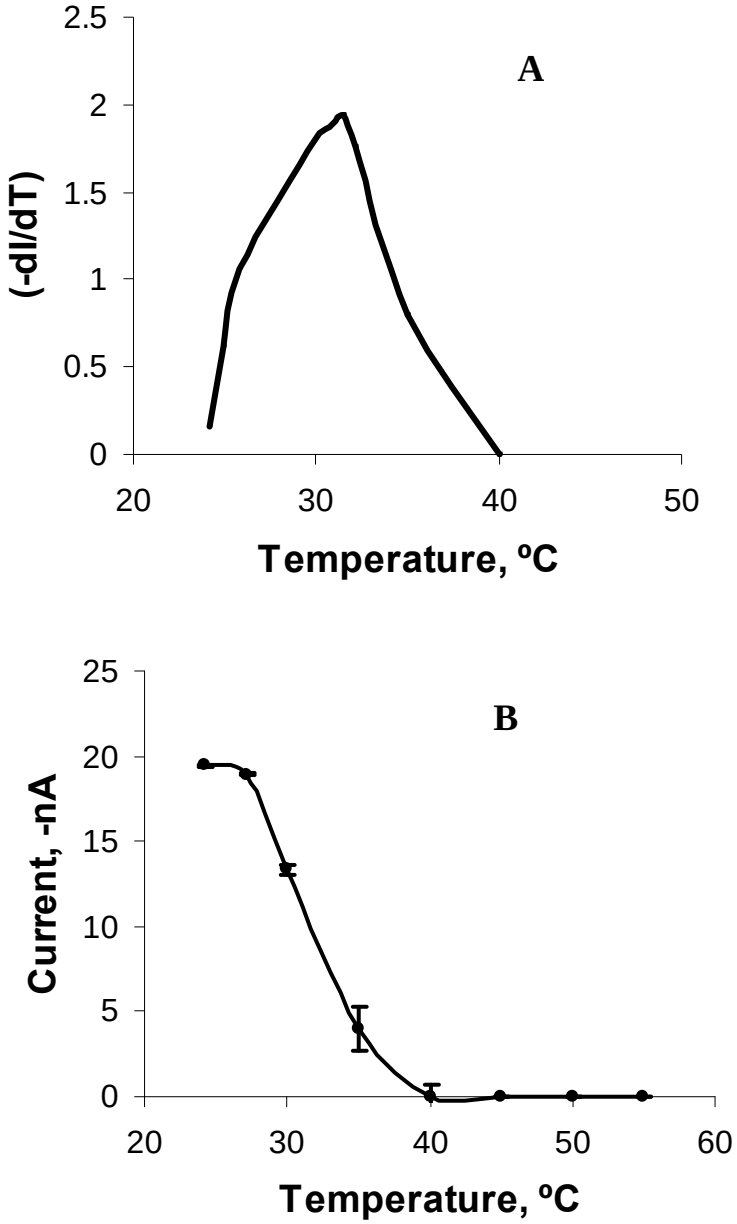

Figure 4: Melting curve of beacon probe immobilized on the electrode surface. Measurement solution: 10mM PBS-T ,pH 7.4 in 0.5M NaCl (A). First derivative of the electrochemical melting curves (shown in fig.4A) Vs temperature (B).

ISBN:978-84-693-3386-0/DL:T.1002-2010

The percentage of cytosine and guanine bases (CG %) is 80 % giving rise to higher stability intra duplex. This could be demonstrated by the melting temperature diagrams in figure 4. The beacon configuration was stable up to 27 ºC (i.e over the room temperature values), hence, the destabilisation process started after increasing the temperature over this value to reach to zero value in which the beacon structure is changed to the "straight and stand up" structure causing the methylene blue to be located away from the electrode surface, thus retarding the electron transfer process (figure 4-A). After cooling the electrode surface the original current value was restored (results not shown). In order to determine the melting temperature value in which half of the immobilized beacons are denatured, the first derivative of the electrochemical melting curve vs. temperature is plotted in figure 4-B.

3.2. Hybridisation time and discrimination between mutant and wild type:

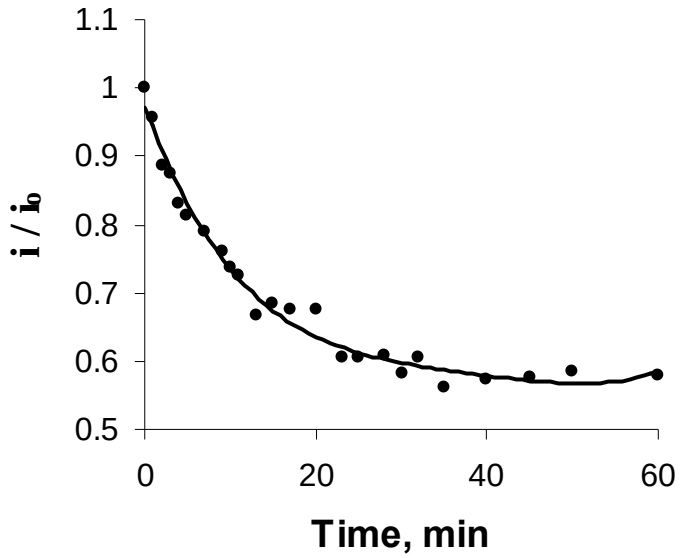

Figure 5: effect of time on the hybridisation between 0.5 μM of cystic fibrosis DF508 mutant and the complementary beacon probe immobilized on the electrode surface. The buffer solution consists of 10mM PBS-T, pH 7.4 in 0.5M NaCl.

An electrochemical cell (3 mL total volume) of 10 mM PBS-T buffer and 0.5 M NaCl was used to study the effect of time on the hybridisation between mutant amplicon target and the immobilized beacon probe on the gold working electrode surface. With similar previously mentioned experimental conditions, a relation between 0.5 μM mutant amplicon and the beacon probe immobilized on the electrode surface

ISBN:978-84-693-3386-0/DL:T.1002-2010

hybridisation vs. time is illustrated in figure 5. The plateau behaviour is reached after 20 minutes of the direct contact with the mutant target, and to ensure complete hybridisation, for further hybridisation experiments, a time of 45 minutes was used.

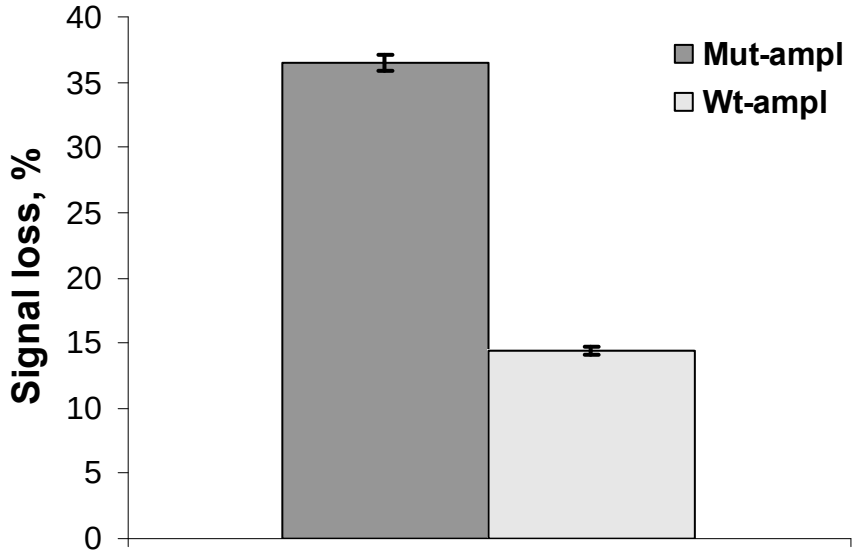

Figure 6: Mutant and Wild type synthetic single stranded PCR product analogues discrimination at 0.5 μM concentration via hybridisation with beacon probe fully complementary to the mutant target and immobilized on the electrode surface. The buffer solution employed was10mM PBS-T, pH 7.4 in 0.5M NaCl. The regeneration took place by washing the electrode surface with Milli-Q water.

The current peak height of the immobilized beacon probe demonstrated a clear signal loss (signal off) after hybridisation with the mutant amplicon complementary (figure 1 inset). The percentage of loss in the original signal was calculated as shown in equation 1:

$$\textbf{Signal loss percentage} = (I_{reg} - I_{hybrid}) \times 100 / (I_{reg}) \qquad (1)$$

Where, I_{reg} is the peak current height after regeneration the electrode surface with Mill-Q water, and I_{Hybrid} is the current peak height after hybridisation with the amplicon targets (mutant or wild type). Figure 6 show the results obtained with different target hybridisation for fully complementary F508 mutant complementary and 3 mismatched wild type complementary. The system shows good reproducibility as illustrated in the

ISBN:978-84-693-3386-0/DL:T.1002-2010

standard deviation values in Figure 6 with a discrimination factor between mutant and wild-type of ca. 2.5.

The detection of the cystic fibrosis V520F mutant, which contains only one base mismatch, was evaluated using similar conditions. Sensor surface preparation and target hybridisations were carried out as described for the DF508 mutation. The discrimination between single base polymorphism is illustrated in figure (7). As expected, a lower discrimination value was obtained as compared to that obtained with the three mismatches DF508 case and unfortunately a clear discrimination between wild type and mutant was not achievable with the assay conditions used.

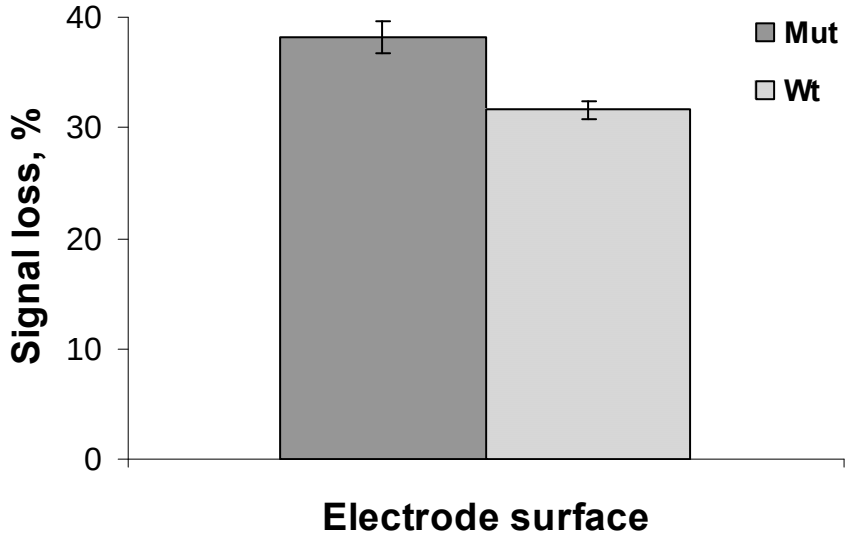

Figure 7: V520F Cystic fibrosis Mutant and Wild type PCR analogues discrimination at 0.5 µM concentration via hybridisation with beacon probe fully complementary to the mutant target and immobilized on the electrode surface. The buffer solution employed was10mM PBS-T, pH 7.4 in 0.5M NaCl. The regeneration took place by washing the electrode surface with Milli-Q water.

3.3. Temperature modulation for the enhancement of discrimination between DF508 mutant and wild type:

Two electrodes were prepared as illustrated before and subjected to hybridisation with either DF508 mutant or the corresponding wild type. These electrodes were immersed in 10 mM PBS-T buffer and 0.5 M NaCl in a thermostatted electrochemical cell and incubated in each examined temperature degree for 10 minutes prior to DPV

ISBN:978-84-693-3386-0/DL:T.1002-2010

measurement. Figure 8 shows the melting behaviour for both mutant and wild type hybrids with the mutant complementary molecular beacon immobilized on the gold electrode surface. Unfortunately, both curves are similar, maintaining a discrimination of just two degrees Celsius. This behaviour could be explained by another hybrid shape represented in the molecular beacon stem region, where a higher CG content could play a role in such an effect.

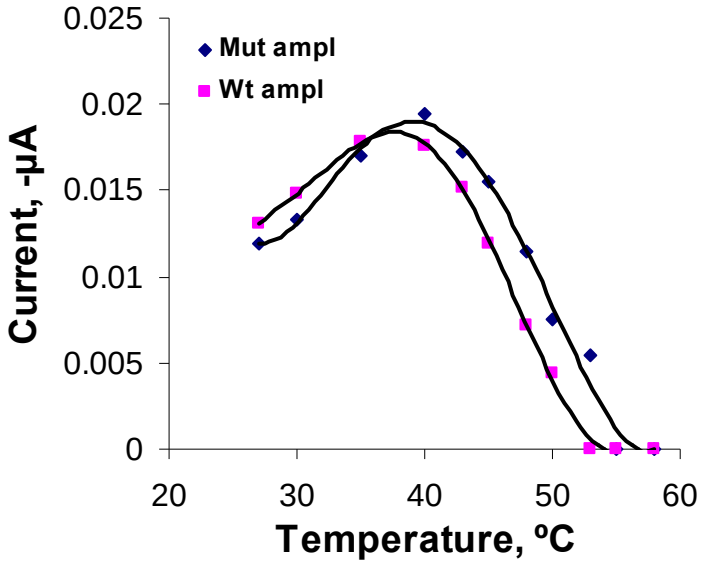

Figure 8: Melting curves of Mutant and Wild type PCR product analogues at 0.5 µM concentration via hybridisation with beacon probe fully complementary to the mutant target and immobilized on the electrode surface. The buffer solution employed was10mM PBS-T, pH 7.4 in 0.5M NaCl.

4. Conclusions:

Electrochemical molecular beacon based biosensor was introduced in this report to discriminate between cystic fibrosis mutations. Different buffer solutions were examined for immobilized molecular beacon better signal expression and 10 mM PBS-T was choose for its higher signal response. The sensor surface was better prepared via co-immobilsation in which molecular beacons and MCH were exists in the same solution, where a ratio of 1:50 (Probe: MCH) was shown to be more stable. The hyrbidisation with the complementary amplicon targets were shown to be completed after 30 minutes. The melting temperature of the immobilized molecular beacon was

ISBN:978-84-693-3386-0/DL:T.1002-2010

over room temperature value assuring the signal stability of the methylene blue at room temperature. A good discrimination factor of ca.2.5 was obtained between DF508 mutant and wild type were this discrimination factor was reasonably decreased in the case of one mismatched mutant namely V520F. It was not possible to enhance the discrimination factor by temperature modulating application; this could be due to the geometry and the interference of the immobilized molecular beacon itself.

ISBN:978-84-693-3386-0/DL:T.1002-2010

5. References:

1. Anderson, D. H. (1938) Am. J. Dis. Child. 56, 344–399.
2. Kerem, B. S., Rommens, J. M., Buchanan, J. A., Markiewicz, D., Cox, T. K., Chakravarti, A., and et. al. (1989) Science 245, 1073–80.
3. Dodge, J. A., Marison, S., Lewis, P. A., Coles, E. C., Geddes, D., and Russell, G. (1997) Archives of diseases in childhood 77, 493-6.
4. Boat, T., Welsh, M., and Beaudet, A. L. (Eds.) ((1989)) Cystic fibrosis, McGraw Hill, McGraw Hill, New York.
5. Ratjen, F., and Doring, G. (2003) The Lancet 361, 681-9.
6. Gibson, L. E., and Cooke, R. E. (1959) Pediatrics 23, 545-9.
7. Davies, J. C., Alton, E. W. F. W., and Bush, A. (2007) BMJ 335, 1255-1259.
8. Watson, J., and Crick, F. (1953) Nature 171, 737.
9. Gooding, J. J. (2002) Electroanalysis 14, 1149-1156.
10. Sassolas, A., Leca-Bouvier, B. D., and Blum, L. J. (2007) Chemical Reviews 108, 109-139.
11. Cheryl, L. B., and David, G. M. (2001) Journal of Molecular Recognition 14, 261-268.
12. Lucarelli, F., Marrazza, G., Turner, A. P. F., and Mascini, M. (2004) Biosensors and Bioelectronics 19, 515-530.
13. Liu, J., Liu, J., Yang, L., Chen, X., Zhang, M., Meng, F., Luo, T., and Li, M. (2009) Sensors 9, 7343-7364.
14. Susan, R. M. (1996) Electroanalysis 8, 15-19.
15. Mannelli, I., Courtois, V., Lecaruyer, P., Roger, G., Millot, M. C., Goossens, M., and Canva, M. (2006) Sensors and Actuators B: Chemical 119, 583-591.
16. Mannelli, I., Lecerf, L., Guerrouache, M., Goossens, M., Millot, M.-C., and Canva, M. (2007) Biosensors and Bioelectronics 22, 803-809.
17. Drummond, T. G., Hill, M. G., and Barton, J. K. (2003) Nat Biotech 21, 1192-1199.
18. DeLumley, T., Campbell, C., and Heller, A. (1996) J. Am. Chem. Soc. 118, 5504.
19. Alfonta, L., Singh, A. K., and Willner, I. (2001) Anal. Chem. 73, 91.
20. Pividori, M. I., Merkoci, A., and Alegret, S. (2001) Biosensors & Bioelectronics 16 (9-12), 1133-1142.
21. Arias, P., Ferreyra, N. F., Rivas, G. A., and Bollo, S. (2009) Journal of Electroanalytical Chemistry 634, 123-126.
22. Ihara, T., Nakayama, M., Murata, M., Nakano, K., and Maeda, M. (1997) Chem. Commun., 1609.
23. Kertez, V., Whittemore, N. A., Inamati, G., Manoharan, M., Cook, P., Baker, D., and Chambers, J. O. (2000) Electroanalysis 12, 889.
24. Patolsky, F., Lichtenstein, A., and Willner, I. (2001) J. Am. Chem. Soc. 123 (22), 5194–5205.

25. Napier, M. E., Loomis, C. R., Sistare, M. F., Kim, J., Eckhardt, A. E., and Thorp, H. H. (1997) Bioconjugate Chemistry 8, 906-913.
26. Millan, K., Saraullo, A., and Mikkelsen, S. (1994) Anal. Chem. 66(18), 2943-2948.
27. Li, X.-M., Ju, H.-Q., Du, L.-P., and Zhang, S.-S. (2007) Journal of Inorganic Biochemistry 101, 1165-1171.
28. Petty, J. T., Bordelon, J. A., and Robertson, M. E. (2000) The Journal of Physical Chemistry B 104, 7221-7227.
29. Hahm, J., and Lieber, C. M. (2003) Nano Letters 4, 51-54.
30. Nasef, H., Beni, V., and O'Sullivan, C. K. (2009) Analytical and Bioanalytical Chemistry DOI 10.1007/s00216-009-3369-5
31. Tyagi, S., and Kramer, F. R. (1996) Nat Biotech 14, 303-308.
32. Li, Y., Zhou, X., and Ye, D. (2008) Biochemical and Biophysical Research Communications 373, 457-461.
33. Tyagi, S., Bratu, D. P., and Kramer, F. R. (1998) Nat Biotech 16, 49-53.
34. Sandhya, S., Chen, W., and Mulchandani, A. (2008) Analytica Chimica Acta 614, 208-212.
35. Steemers, F. J., Ferguson, J. A., and Walt, D. R. (2000) Nat Biotech 18, 91-94.
36. Sokol, D. L., Zhang, X., Lu, P., and Gewirtz, A. M. (1998) Proceedings of the National Academy of Sciences of the United States of America 95, 11538-11543.
37. Fan, C., Plaxco, K. W., and Heeger, A. J. (2003) Proceedings of the National Academy of Sciences of the United States of America 100, 9134-9137.
38. Ying, X., Lin, Y., Xiaoyan, Y., Pingang, H., and Yuzhi, F. (2006) Electroanalysis 18, 873-881.
39. Wang, Y., Li, C., Li, X., Li, Y., and Kraatz, H.-B. (2008) Analytical Chemistry 80, 2255-2260.
40. Cash, K. J., Heeger, A. J., Plaxco, K. W., and Xiao, Y. (2008) Analytical Chemistry 81, 656-661.
41. Jones, C. T., McLntosh, l., Keston, M., Ferguson, A., and Brock, D. J. H. (1992) Hum. Mol. Genet. 1, 11-17.
42. Sismani, C., Kousoulidou, L., and Patsalis, P. C. (2000) in Molecular Biomethods Handbook (Walker, J. M., and Rapley, R., Eds.), pp. 179-193, Humana Press, Totowa, NJ,.
43. Lai, R. Y., Seferos, D. S., Heeger, A. J., Bazan, G. C., and Plaxco, K. W. (2006) Langmuir 22, 10796-10800.

UNIVERSITAT ROVIRA I VIRGILI
TEMPERATURE MODULATED GENOSENSOR FOR DETECTION OF CYSTIC FIBROSIS MUTATIONS
Hany Abdel Hady Abdel Rahman Nasef
ISBN:978-84-693-3386-0/DL:T.1002-2010

CHAPTER 5 (Art 4):

Melting Temperature of Surface-tethered DNA

UNIVERSITAT ROVIRA I VIRGILI
TEMPERATURE MODULATED GENOSENSOR FOR DETECTION OF CYSTIC FIBROSIS MUTATIONS
Hany Abdel Hady Abdel Rahman Nasef
ISBN:978-84-693-3386-0/DL:T.1002-2010

Melting Temperature of Surface-tethered DNA

Hany Nasef[1], V. Cengiz Ozalp[1], Valerio Beni[1] and Ciara K. O'Sullivan[1,2 *]

[1] Nanobiotechnology & Bioanalysis Group, Departament d'Enginyería Química, Universitat Rovira i Virgili, Avinguda Països Catalans, 26, 43007 Tarragona, Spain
E-mail: ciara.osullivan@urv.cat; Fax: +34 977 55 96 21; Tel.+ 34 977 55 8740
[2] Institucio Catalana de Recerca i Estudis Avançats, Passeig Lluis Companys 23, 08010, Barcelona, Spain

Abstract

A method for the accurate determination of the melting temperature (Tm) of surface immobilised DNA duplexes, which exploits the fluorescence quenching properties of gold, is reported. A thiolated ssDNA probe is chemisorbed onto a gold surface, and then hybridized to a fluorophore labelled complementary sequence. Upon formation of the duplex, the fluorescence of the label is effectively quenched by the gold surface. As the temperature is increased and the duplex dehybridises, the fluorophore label moves away from the gold surface and the fluorescence signal is again observed. The increase in fluorescence is measured as the temperature is ramped and using first derivative plots, the Tm determined. To demonstrate the approach, the Tm of the Cystic Fibrosis DFF508 mutation was determined in three different phases – in solution, in "suspension" immobilized on gold nanoparticles, and immobilized on gold film coated substrate. The technique was further applied to optimize conditions for differentiation between a surface immobilized DF508 mutant probe and mutant/wild type target exploiting increasing stringency varying salt and formamide concentration. The approach has application in optimization of assay conditions for biosensors that use gold substrates as well as for melting curve analysis.

Keywords: Melting temperature; Surface-immobilised DNA; Fluorescence quenching; Gold nanoparticles

ISBN:978-84-693-3386-0/DL:T.1002-2010

Introduction

DNA hybridization on solid surfaces was developed on membranes in 1970s, where surface tethered single stranded DNA (ssDNA) were used to bind complementary DNA(1). Since then a plethora of biosensors and microarrays for the detection of DNA hybridization have been reported. Allele discrimination using surface immobilized probes is based on differences in DNA capture efficiencies dependent on mismatches, where experimental conditions are tuned to maximize the difference in melting temperature (Tm) of wild-type and mutant containing duplexes. Thus, any platform for mutation detection, using surface tethered nucleic acid probes requires a method for the accurate determination of the Tm in order to rationally design experimental conditions.

The hybridization behaviour of surface immobilized probes with target often differs from that in bulk solution, and is case-specific where duplex stability may be greater or weaker than that in solution (2).

Some reports have appeared detailing the accurate determination of melting temperature of surface immobilized or tethered DNA. Peterlinz used a method based on surface plasmon resonance (SPR), reporting a Tm of ≈ 5 ^{o}C less as compared to solution Tm (3). The difference in melting temperature obtained with surface immobilized DNA has also been demonstrated, assembling a (dA)20 probe onto an optical fibre functionalised with fused silica substrate (4). Additionally, epoxy-linked DNA probes were hybridized to biotin labelled PCR amplicons, subsequently linked to streptavidin Cy5 and the fluorescence signal detected using a CCD camera (5). The use of total internal reflection fluorescence has also been reported for the determination of the melting temperature of surface immobilized DNA duplexes, and single-point mutations could be recorded (6). In another approach, dynamic light scattering was used to detect duplex melting by measuring a decrease in hydrodynamic radius of DNA-functionalized and hybridized colloidal gold nanoparticles (2). Dynamic allele specific hybridization, DASH, has been used for single nucleotide polymorphism detection where target DNA is immobilized on a microtitre plate and hybridized with a probe specific for one allele, with hybridization and melting being monitored using a double-stranded DNA-specific dye. They observed that melting temperatures were lower for sequences containing a SNP than for fully hybridized strands, with temperature differences of 6-12 ^{o}C for 15- and 21-mer probes (6). Similar values for in situ surface plasmon imaging of DNA hybridization surfaces were observed (7). Reflectometric interference spectroscopy has been successfully applied for the determination of melting temperature, where melting curves of surface immobilized 15-mer LNA/PNA/DNA probes with their complementary 15-mer DNA were calculated (8). Finally, the use of the intercalating dye, SYBR Green, was used for the determination of the Tm of

ISBN:978-84-693-3386-0/DL:T.1002-2010

immobilized duplexes, monitoring the increase in fluorescence as the dye is released with increasing temperature and dehybridisation of the duplex (6).

Here we report a new method for the determination of the Tm of surface immobilized DNA duplexes, exploiting gold induced fluorescence quenching, as depicted in Figure 1.

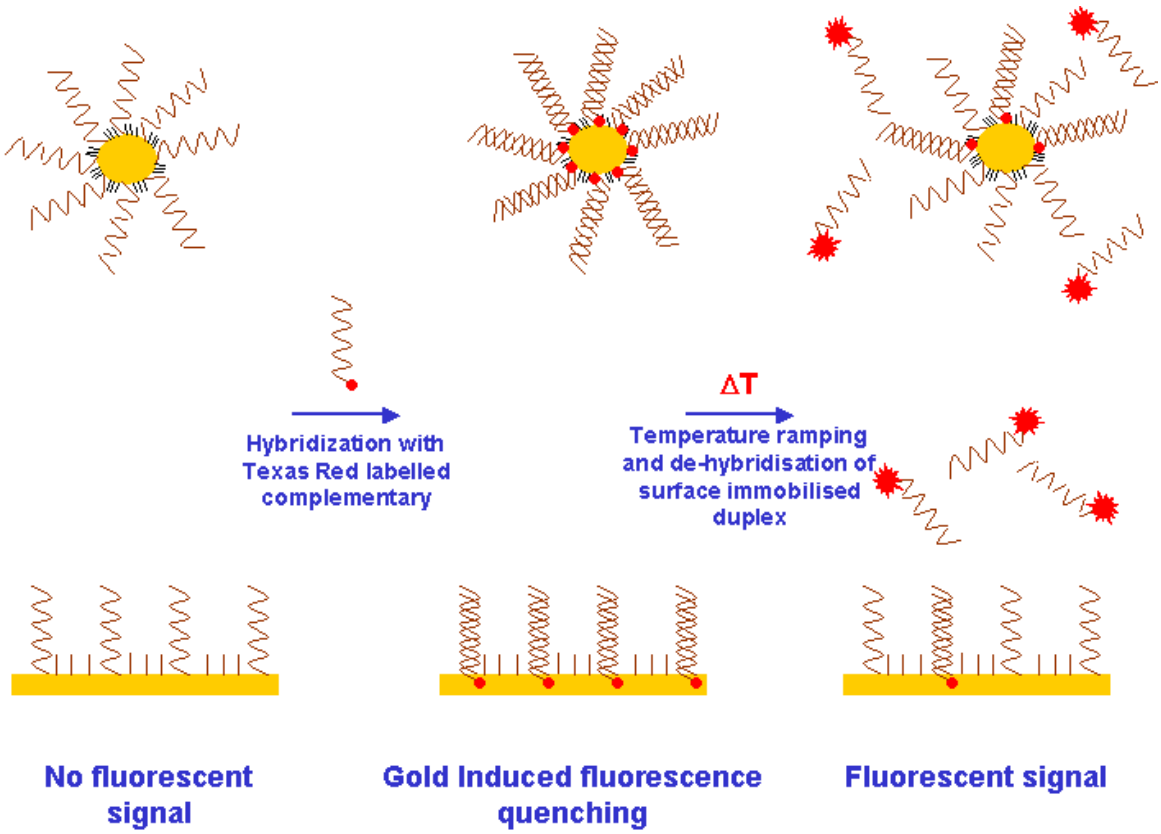

Figure 1 Schematic of reported method for measurement of melting temperature of surface tethered DNA duplexes.

A thiolated ssDNA probe is chemisorbed onto a gold surface, and backfilled with mercaptohexanol as previously reported (10), and then hybridized to a fluorophore labelled complementary sequence. Upon formation of the duplex, the fluorescence label is effectively quenched by the gold surface (9). As the temperature is increased and the duplex dehybridises, the fluorophore label moves away from the gold surface, the increase in fluorescence measured and the Tm determined. To demonstrate the approach, the Tm of the Cystic Fibrosis DFF508 mutation was determined in three different phases – in solution, in "suspension" immobilized on gold nanoparticles, and immobilized on gold film coated substrate. The technique was further applied to optimize conditions for differentiation between a surface immobilized DF508 mutant

ISBN:978-84-693-3386-0/DL:T.1002-2010

probe and mutant/wild type target exploiting increasing stringency varying salt and formamide concentration. The approach has application in optimization of assay conditions for biosensors using gold substrates (e.g. electrochemical, surface plasmon resonance, quartz crystal microbalance, fluorescent etc.) as well as for melting curve analysis.

Materials and methods

All chemicals and reagents used were of analytical grade. Trizma buffer was purchased from Sigma and the pH adjusted to 7.4 by addition of HCl (6M, Scharlau). KH_2PO_4, NaCl and $MgCl_2$ were received from Scharlau. NaCl, formamide and mercaptohexanol were obtained from Panreac, Acros Organics and Fluka, respectively. For the preparation of gold nanoparticles, potassium tetrachloro-aurate (III) (98%, Sigma-Aldrich) and trisodium citrate (Sigma) were used. All oligonucleotides were received from VBC-Biotech Company (Service GmbH Campus Vienna, Biocenter 6/5, A-1030 Wien).

Model DNA system used to demonstrate approach of measuring melting temperature of surface tethered DNA

Cystic fibrosis (CF) is one of the most common life-shortening, childhood-onset inherited diseases. CF is caused by a mutation in a gene called the cystic fibrosis transmembrane conductance regulator (CFTR). The most common mutation of cystic fibrosis is called DF508, because the CFTR protein it encodes is missing a single amino acid at position 508, and this mutation represents 70 per cent of mutations in the white populations of Britain and US and 50 per cent in southern European populations. The DF508 mutation is a 3bp deletion, and this deletion causes loss of the amino acid phenylalanine located at position 508 in the protein.

The following oligos were employed in this study:

5‘-AAT ATC ATT GGT GTT-3´ (Δ508 mutant target)
5‘-TAT CAT **CTT** TGG TGT-3´ (Wild type target)

5’-ACC CTT GGG AGG AAG AGA CG-3’ (Non-complementary target)

The bold underlined letters indicate the 3bp deletion present in the DF508 mutation.

5‘-AAC ACC AAT GAT ATT-(C6)-SH-3´ (thiolated DNA probe complementary to mutant)

The mutant and wild type targets, as well as the non-complementary probe were used in their native state as well as being labelled at the 5’ terminal with Texas Red (synthetic DNA-Texas

ISBN:978-84-693-3386-0/DL:T.1002-2010

Red purchased), which was chosen as the fluorescent label as it has been previously been shown that this fluorophore is the most thermally stable fluorescent label among Fluorescein, Rhodamine Red, Tamra, Cy3, Oregon Green, FITC, FAM and Cy2 (11).

Instrumentation and equipment

A UV-VIS spectrometer (Varian, CARY 100 BIO, EL05023424) was used for the measurement of DNA concentration in solution. Fluorescence spectrometer (Varian, CARY eclipse, EL05083124) was employed for fluorescent measurements. A Varian CARY temperature controller (EL05073367) was employed as a thermal peltier.

Preparation and characterisation of gold nanoparticles and sputtered gold film

Gold film chips Sputtered gold chips were fabricated as follows. A silicon wafer was first insulated with a 150 nm layer of SiO_2 followed by an adhesive layer of 20 nm chromium. A 200 nm gold layer was then sputtered and structured by a lift-off process to shape a gold square of $16mm^2$. The wafer was diced and the surface was cleaned in oxygen plasma (100 W, 5 min). This method allowed the preparation of several dozens of gold chips with a high degree of reproducibility (± 0.1%) of area.

Preparation of Gold nanoparticles The gold nanoparticles (Au-NP) were prepared by refluxing 50 mL of $KAuCl_4$ (0.3 mM) to boiling point, followed by addition of 2.5 mL trisodiumcitrate (1%) and heating until a wine red colour was obtained. The size of the gold nanoparticles was determined from measurement of the maximal wavelength (λmax = 520 nm), to be 20 nm (12).

Immobilisation of probes on gold nanoparticles and gold films

A 15-mer thiolated probe with six carbon spacer at the 3´terminal (5'-AAC ACC AAT GAT ATT-C6-SH-3' probe) complementary to the mutated region of the DF508 mutant was immobilised on each of the gold surfaces via addition of 4μM thiolated DNA in 10mM KH_2PO_4 solution to freshly prepared gold nanoparticles, or freshly cleaned gold films and left to incubate overnight, followed by thorough washing with Milli-Q water. The gold surface was then back-filled with 0.01M mercaptohexanol (MCH) for 30 minutes. The gold films were then thoroughly washed by sequential immersion in 0.1 M NaOH and 0.1 M HCl. In the case of the nanoparticles, they were centrifuged and collected after each washing/modification step. These extensive washing steps in NaOH/HCl were to ensure the complete removal of any physisorbed probe to leave an organized mixed SAM of chemisorbed DNA probe and MCH backfiller. In

ISBN:978-84-693-3386-0/DL:T.1002-2010

order to investigate the effect of different probe concentrations on melting temperature, concentrations of 0.5, 2 and 4μM of the thiolated DNA probe on the gold film were evaluated.

Hybridization of immobilized mutant probe with labelled wild type/mutant target

The 5' terminal of the mutant and wild type targets were labelled with the Texas Red fluorescent molecule, 5'-Texas Red-C6-AAT ATC ATT GGT GTT-3' and 5'-Texas Red-C6-TAT CAT CTT TGG TGT-3′, respectively. Hybridization was carried out using solutions of 1μM WT/MUT-Texas Red in 10mM Trizma (pH 7.4) containing 10 mM $MgCl_2$, which was added to the centrifuged functionalised Au-NP or the sputtered gold film chips. Hybridization was monitored by looking at the quenching of the fluorescence of the Texas Red label as it was brought into close proximity with the gold surface of the nanoparticles or the film, until a constant level of quenching was achieved. Hybridization was allowed to proceed at room temperature for one hour, prior to thorough washing to remove any non-hybridized targets.

Determination of Tm

Free solution Tm Two hundred microliters solutions of 1μM WT/MUT target and 1μM MUT/WT probe in 10mM Trizma (pH 7.4) was added to a cuvette, which was placed in a thermostatted cell with Peltier control in a UV-Vis spectrophotometer. The melting temperature of DNA in solution was determined by UV-Vis at λ= 260nm, over a temperature range from 20 to 80 ºC at a thermal ramping at a rate of 5 ºC/min.

Surface immobilised Tm

Melting determination experiments were performed by using 1 μM concentration of synthetic target oligo in an interaction buffer containing 10 mM Trizma, pH=7.4. As the temperature was ramped, the Texas Red-labelled target strand dissociated and was released into solution, resulting in an increase in fluorescence recorded as a temperature-fluorescence curve for Tm determination. The Texas Red fluorescence (λ_{Ex}=590 nm and λ_{Em}=613 nm) was measured at a ramping rate of 5 ºC/min using a standard fluorimeter equipped with a Peltier heating unit. Experiments were carried out in triplicate.

In the case of the gold film, the large gold surface quenched most of the fluorescence of the dissociated target strand with increasing temperature and produced irreproducible results. The method was thus adjusted, to discontinuously measure the fluorescence of the dissociated target, by heating the cuvette in a Peltier controlled unit, to temperatures at 1ºC intervals and then taking 100 μL of the solution containing the dissociated fluorescent labelled target to a separate

ISBN:978-84-693-3386-0/DL:T.1002-2010

cuvette and measuring the fluorescence at 30^{o}C, then returning the solution to the cuvette containing the gold chip and continuing the procedure from 20 to 80 ºC.

Control Experiments

Control experiments were carried out where a non-complementary sequence labelled with the fluorescent label was added to the immobilized probe on the nanoparticle and sputtered gold film surfaces. Additionally, surfaces with no immobilized probe and simply coated with mercaptohexanol were subjected to immersion with the labelled mutant and wild type targets. The effect of temperature on the Texas Red fluorescent label was also evaluated. The possible effect of the presence of the Texas Red fluorescent label on melting temperature was tested by monitoring melting temperature in solution, using both unlabelled DNA and the Texas Red labelled DNA. Finally, the effect of temperature on buffer pH was established by measuring the pH of Trizma buffer at 5^{o}C intervals over a temperature range between 30^{o}C and 60^{o}C.

RESULTS AND DISCUSSSION

The objective of this work was to develop a method for the measurement of the melting temperature of surface immobilized DNA duplexes. As the Tm may also be dependent on the type of surface on which the probe/duplex is immobilized, it was interesting to measure the Tm on both gold nanoparticles and planar gold films. The approach we detail for melting temperature determination can be applied to both surfaces, and thus can find application not only for biosensors and melting curve analysis, but also for gold nanoparticle immobilized DNA duplexes (13) or molecular beacons (14). As detailed below, in the first part of the work, we demonstrated the applicability of the method for the determination of melting temperature of gold nanoparticle and gold film supported DNA duplexes, and in the second part of the work we apply the technique for the optimization of conditions for differentiation of wild type and mutant targets using a probe complementary to the mutant immobilized on the gold film.

Determination of solution melting temperature

The absorbance at λ =260nm was read as the temperature was ramped at a rate of 5 ºC/min over the temperature range of 20 to 80ºC. Melting Temperature (Tm) by definition is the temperature at which one half of the DNA duplex will dissociate to become single stranded and indicates the duplex stability. Under the conditions of 10mM Trizma buffer, pH 7.4 containing 10mM $MgCl_2$, a Tm of 59^{o}C was obtained, agreeing with a predicted melting temperature as calculated using the nearest neighbour meeting temperature calculation (15).

ISBN:978-84-693-3386-0/DL:T.1002-2010

Determination of melting temperature of surface immobilized mutant-mutant duplex

The proposed method for determination of the melting temperature of surface immobilized duplexes was demonstrated using a thiolated 15-mer probe complementary to the DF508 mutation immobilized on gold nanoparticles, and gold film. The immobilized probe was hybridized to either the labelled mutant target or wild type target, and the fluorescence of the Texas Red was quenched by the gold surface. With increasing temperature, the Texas Red-labelled target strand dissociated and was released into solution, resulting in an increase in fluorescence recorded as a temperature-fluorescence curve for Tm determination (Figure 2).

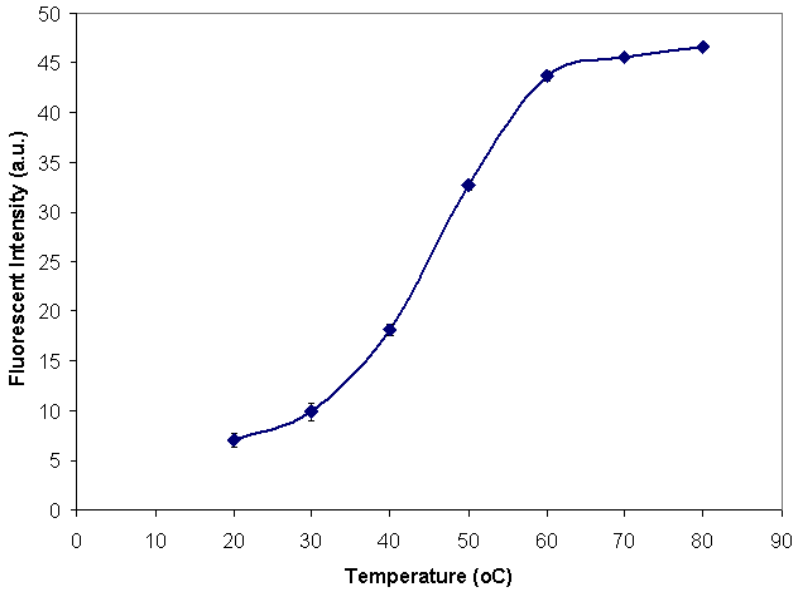

Figure 2 Typical melting curve obtained with planar thin-film gold chip immobilized duplexes. Each melting curve experiment was carried out in triplicate as represented by the error bars

The effect of the concentration of the immobilized probe was evaluated looking at the melting temperatures obtained using 0.5, 2 and 4μM mutant probe and mutant target, and there is a very definite effect of probe concentration and Tm, with the more probe there is on the surface, the more stable the duplex becomes (Table 1). This could be attributed to that fact that the density of ssDNA immobilized will have an effect on charge density due to the ionisable phosphate groups, and the negatively charged surface of immobilized probes will attract positive counter-ions from solution, resulting in local ionic strength pH and dielectric constant on the surface, which is markedly different from that in bulk electrolyte solution. These local conditions influence the thermodynamics of hybridization and results in vastly different melting temperatures as compared to solution Tm (4), and the higher the concentration of the immobilized probe, the disparity in Tm becomes more pronounced.

ISBN:978-84-693-3386-0/DL:T.1002-2010

Probe concentration / µM	Melting temperature, ºC
0.1	28 ± (1.25)
0.5	30 ± (0.98)
1	33 ± (1.14)
2	38 ± (0.76)
4	48 ± (0.85)

Table 1. Effect of the concentration of the immobilized probe on to the Mut-Mut hybrid formed on to the gold surface.

As can be seen in Figure 3, there is a marked difference in the melting temperatures obtained on planar gold surfaces as compared to spherical gold surfaces, with values of 48 and 54 ^{o}C being obtained, respectively. As detailed by Xu and Craig (2), "extrapolating the findings on planar surfaces to small particles is complicated by the relatively high curvature of the DNA-Au surface which relaxes the steric and electrostatic interactions between neighbouring DNA and may also perturb long-rang interactions". It can thus be expected that the duplexes formed with probes immobilized on gold nanoparticles will be different to that of the Tm of planar gold immobilized probes. Moreover, both the surface immobilized duplexes were observed to be less stable that the solution based duplex, with differences of 5 and 11 ^{o}C for the nanoparticles and the gold film, respectively. This is in agreement with some authors, who report similar differences between solution and immobilised Tm (16), whereas other authors report a higher Tm for immobilised DNA duplexes as compared to solution based duplexes (17). However, the surface chemistries and probe densities used are different in each report, and this clearly has a very strong effect on duplex stability.

UNIVERSITAT ROVIRA I VIRGILI
TEMPERATURE MODULATED GENOSENSOR FOR DETECTION OF CYSTIC FIBROSIS MUTATIONS
Hany Abdel Hady Abdel Rahman Nasef
ISBN:978-84-693-3386-0/DL:T.1002-2010

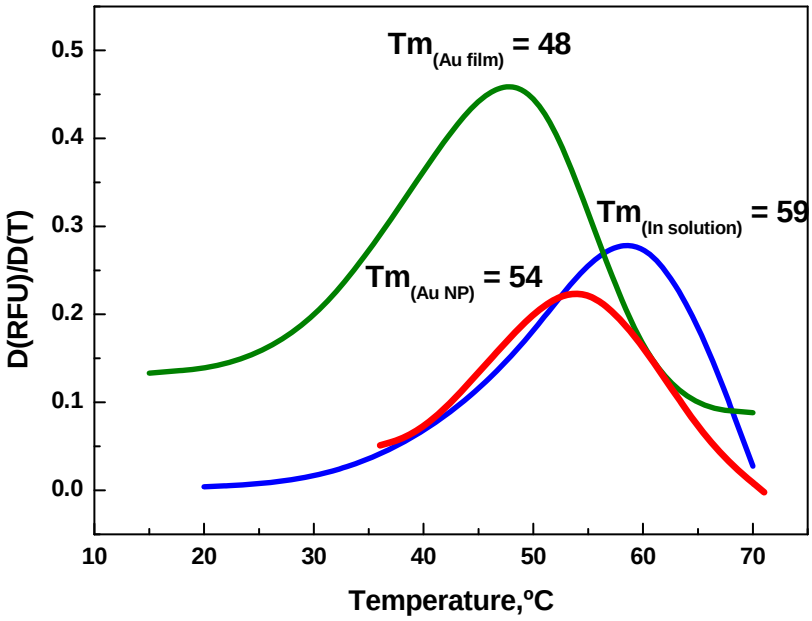

Figure 3 Comparison of Tm values obtained for solution duplex and gold nanoparticle and gold film immobilised duplexes.

Control Experiments Using a non-complementary DNA, apparently no hybridization took place as no quenching nor subsequent increase in fluorescence upon heating was observed. When mercaptohexanol coated surfaces were used, there was a small amount of non-specific binding of the Texas Red labelled targets, but this was immediately removed in the washing step. The melting temperature of the DNA duplex in solution of mutant probe – mutant target and mutant probe – Texas Red labelled mutant target were the same, thus indicating that the presence of the Texas Red label does not have any destabilising effect. Finally, the pH of the Trizma buffer gradually changed from 7.4 to 6.8 over the temperature range of 20 to 80 ^{o}C; however using solution studies and changing the pH from 7.4 to 6.4 no denaturation of the duplex was observed, demonstrating that the effect of temperature on the buffer pH does not effect the melting temperature determination (18).

Elucidation of optimal conditions for differentiation between mutant and wild type targets As a further application of the demonstrated approach to determine the melting temperature of surface tethered DNA duplexes, the technique was used to optimize conditions for differentiation between mutant and wild type targets using a surface immobilized probe complementary to the mutant sequence. Stringency conditions are routinely applied to facilitate hybridization to a complementary target sequence (i.e. in this case, mutant containing) and lesser/no hybridization to a non complementary sequence (i.e. wild type). Optimised

ISBN:978-84-693-3386-0/DL:T.1002-2010

concentrations of formamide and NaCl are commonly used to apply these stringency conditions, and to this end, a series of experiments to study their effect on the Tm of the gold film immobilized duplexes was carried out. Initial studies investigated the effect of NaCl and formamide on melting temperature in solution, monitoring the increase in absorbance at 260 nm upon denaturation of the duplex, as can be seen in Table 2.

Summarising the results obtained with the solution based DNA, the stabilizing effect of NaCl plateaus at about 0.5M, As expected, the 3 bp deletion present in the mutant target results in a considerable decrease in Tm, independent of salt concentration, with a difference of ≈12 ºC observed between fully complementary and non-complementary (MUT-MUT vs WT-MUT). Previous reports have demonstrated the denaturing ability of agents such as formamide, due to their lower ion-solvating power (19, 20), and their ability to increase the solubility of free bases (19). It has been reported that these agents increase the hydrophobic character of the solvent, thereby decreasing the activity coefficients and free energies of the bases, favouring the denatured state (21-24). Independent of the formamide concentration, there is again a difference in Tm of complementary and non-complementary hybrids of ≈12ºC and using a concentration of 25 % v/v formamide, hybridization to complementary targets and no hybridization to the mutated target was observed at room temperature.

NaCl			Formamide		
	Tm / ºC			Tm / ºC	
Conc. / M	Mut	Wt	Conc. / %	Mut	Wt
0	36 (± 0.71)	30 (± 0.53)	1	62 (± 1.13)	46.8 (± 0.71)
0.05	46 (± 0.28)	31.4 (± 0.99)	5	59 (± 1.2)	43.8 (± 1.41)
0.1	50 (± 0.57)	33 (± 0.21)	10	55 (± 1.27)	40.7 (± 1.2)
0.2	54 (± 0.57)	38 (± 0.71)	15	51 (± 0.85)	36.8 (± 1.34)
0.4	58.6 (± 0.42)	43.6 (± 0.78)	20	47 (± 1.26)	34.1 (± 1.13)
0.5	60 (± 0.35)	45 (± 0.46)	25	44 (± 0.57)	28.9 (± 1.06)
0.6	60.5 (± 0.85)	45.7 (± 0.35)			
0.75	61 (± 0.14)	45.8 (± 0.48)			
1	61 (± 0.28)	46 (± 0.03)			

Table 2 Effect of NaCl and Formamide on melting temperature of solution based mutant-mutant (MUT-MUT) and mutant-wild type (MUT-WT) type hybrids. Melting temperature measured using UV-Vis, following DNA concentration at λ = 260nm, over temperature range of 20-80^{o}C, with a ramping rate of 5^{o}C/minute.

UNIVERSITAT ROVIRA I VIRGILI
TEMPERATURE MODULATED GENOSENSOR FOR DETECTION OF CYSTIC FIBROSIS MUTATIONS
Hany Abdel Hady Abdel Rahman Nasef
ISBN:978-84-693-3386-0/DL:T.1002-2010

Similar studies were carried out with the surface immobilized duplexes, using immobilised mutant probe, and fluorophore labelled mutant targets (Figure 4). Analogous trends were observed, and in all cases, a lower Tm was observed for the surface immobilized duplexes.

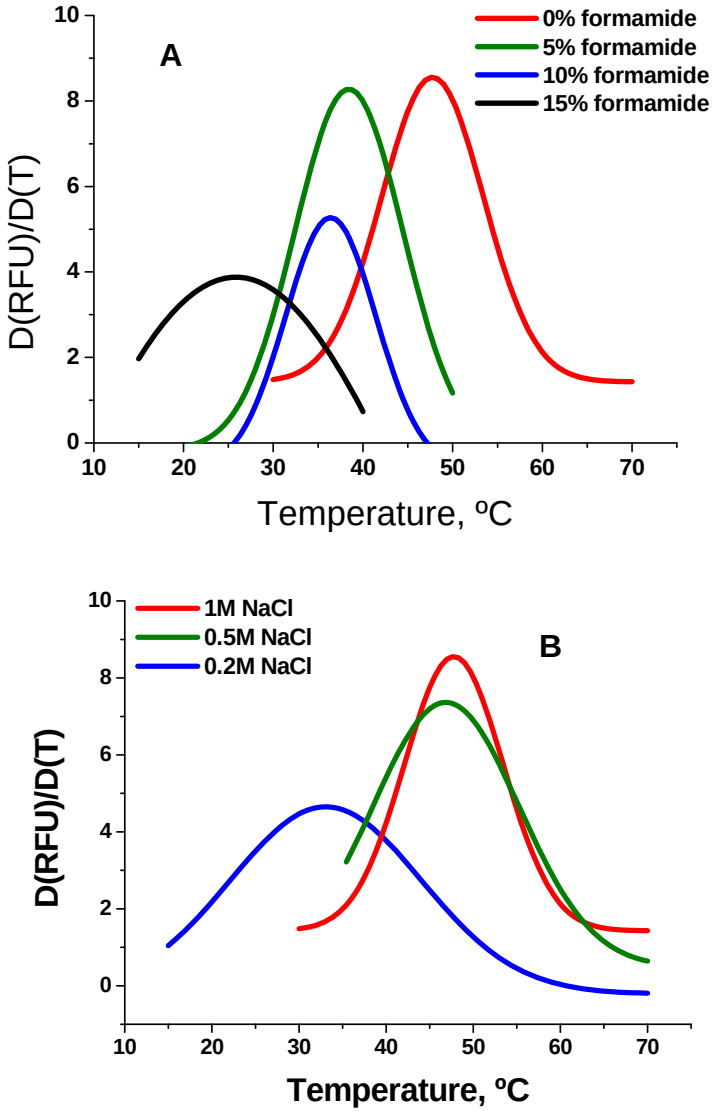

Figure 4 (A) Effect of formamide (0%, 5%, 10% and 15 %) . 30 µl solutions of 1µM Mutant- TR, in 10mM Trizma (pH 7.4) containing 1M NaCl with the different formamide concentrations were incubated with the gold film immobilized probe for 1 hour (B) Effect of NaCl concentration 0.2M, 0.5M and 1M on MutTR:Mut duplex immobilized on planar gold chip. 30 µl solutions of 2µM Mutant- TR, in 10mM Trizma (pH 7.4) and various NaCl concentrations, were incubated with the gold film immobilized probe for 1 hour.

UNIVERSITAT ROVIRA I VIRGILI
TEMPERATURE MODULATED GENOSENSOR FOR DETECTION OF CYSTIC FIBROSIS MUTATIONS
Hany Abdel Hady Abdel Rahman Nasef
ISBN:978-84-693-3386-0/DL:T.1002-2010

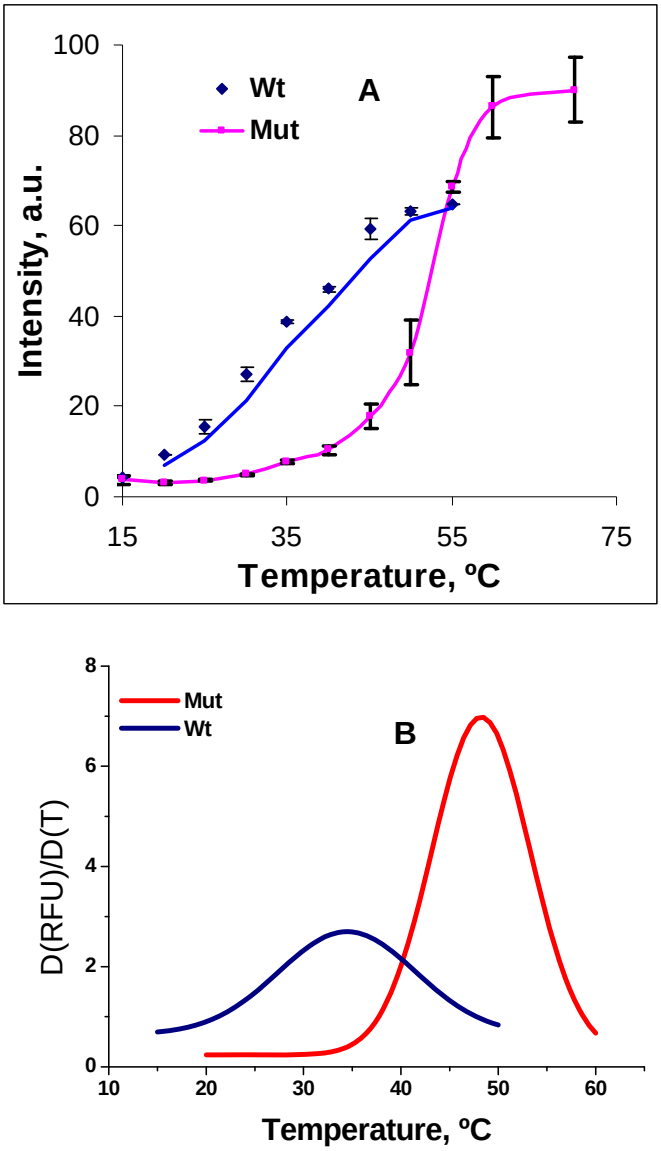

Figure 5 (A) Melting temperature curve for mutant and wild type-TR hybrid with mutant probe immobilised on gold films 10 µl solutions of 1µM MUT or WT-Texas Red, in 10mM Tris HCl (pH 7.4) containing 0.5M NaCl was added to the immobilized probe for 1 hrs. (B) First derivative of the melting curve

Gold films were functionalised with mutant probe and hybridized to mutant and wild type target, respectively. As can be seen in Figure 5, as would be expected for a 3bp deletion, there is considerably less hybridization of the wild type to the immobilized mutant probe, as compared to the mutant-mutant hybrid. Using 0.5M NaCl, a melting temperature of ≈ 46°C and 36°C was obtained for the mutant-mutant and mutant-wild type hybrids, respectively. Incorporating 15% v/v formamide, reduced the melting temperature of the mutant-mutant hybrid dramatically, but completely eliminated any hybridization between the immobilized

ISBN:978-84-693-3386-0/DL:T.1002-2010

probe and wild type target, thus allowing for complete differentiation of mutant and wild type samples as can be seen in Figure 5.

In summary, here we report a facile means of accurately determining the Tm of surface anchored duplexes exploiting the fluorescence quenching effect of gold, which can be applied to planar gold surfaces, or gold spherical structures, such as nanoparticles. Using the method of backfilling with mercaptohexanol, resulted in a surface density of DNA probes, which gave rise to melting temperatures 5^{o}C and 11^{o}C for gold nanoparticles and gold film, respectively, lower than their solution based counterparts. The approach was applied to an elucidation of optimal conditions for detection of the cystic fibrosis associated Δ508 mutation, which is a 3bp deletion. Melting temperatures for a surface immobilized probe complementary to the mutant and its hybrids with complementary mutant and non-complementary wild type under a range of conditions were elucidated, and based on these conditions for complete differentiation between mutant and wild type were established.

Further studies will look at the effect of the surface chemistry (i.e. spacing of DNA probes, types of backfillers used) on the Tm, in order to determine true optimal conditions for gold based biosensors and microarrays for detection of mutations and SNPs.

ACKNOWLEDGMENT

This work was carried out with partial financial support from the Commission of the European Communities, specific RDT programme “Coeliac Disease Management Monitoring and Diagnosis using Biosensors and an Integrated Chip System, CD-MEDICs, FP7-2007-ICT-1-216031”. V.B. acknowledges the European Union’s Seventh Framework Programme (FP7/2007-2013) under grant agreement no. PIGF-GA-2008-220928 for financial support.

ISBN:978-84-693-3386-0/DL:T.1002-2010

References

1. Carauna, D. J. (2004) Hybridization at oligonucleotide sensitive electrodes, Oxford University Press.
2. Xu, J., and Craig, S. L. (2005) *Journal of the American Chemical Society* **127,** 13227-13231.
3. Peterlinz, K. A., Georgiadis, R. M., Herne, T. M., and Tarlov, M. J. (1997) *Journal of the American Chemical Society* **119,** 3401-3402.
4. Piunno, P. A. E., Watterson, J., Wust, C. C., and Krull, U. J. (1999) *Analytica Chimica Acta* **400,** 73-89.
5. Lehr, H. P., Reimann, M., Brandenburg, A., Sulz, G., and Klapproth, H. (2003) *Analytical Chemistry* **75,** 2414-2420.
6. Russom, A., Haasl, S., Brookes, A. J., Andersson, H., and Stemme, G. r. (2006) *Analytical Chemistry* **78,** 2220-2225.
7. Dodge, A., Turcatti, G., Lawrence, I., de Rooij, N. F., and Verpoorte, E. (2004) *Analytical Chemistry* **76,** 1778-1787.
8. Pröll, F., Kumpf, M., Gauglitz, G., and Möhrle, B. (2005) *Analytical and bioanalytical chemistry* **382,** 1889-1894.
9. Dubertret, B., Calame, M., and Libchaber, A. J. (2001) *Nat Biotech* **19,** 365-370.
10. Herne, T. M., and Tarlov, M. J. (1997) *Journal of the American Chemical Society* **119,** 8916-8920.
11. Liu, W.-T., Wu, J.-H., Li, E. S.-Y., and Selamat, E. S. (2005) *Applied Environmental Microbiology* **71,** 6453-6457.
12. Link, S., and El-Sayed, M. A. (1999) *The Journal of Physical Chemistry B* **103,** 4212-4217.
13. Elghanian, R., Storhoff, J. J., Mucic, R. C., Letsinger, R. L., and Mirkin, C. A. (1997) *Science* **277,** 1078-1081.
14. Bonnet, G., Tyagi, S., Libchaber, A., and Kramer, F. R. (1999) *PNAS* **96,** 6171-6176
15. http://www.basic.northwestern.edu/biotools/oligocalc.html.
16. Brewood, G. P., Rangineni, Y., Fish, D. J., Bhandiwad, A. S., Evans, D. R., Solanki, R., and Benight, A. S. (2008) *Nucl. Acids Res.* **36,** e98-.
17. Harris, N. C., and Kiang, C.-H. (2006) *The Journal of Physical Chemistry B* **110,** 16393-16396.
18. Owczarzy, R., Moreira, B. G., You, Y., Behlke, M. A., and Walder, J. A. (2008) *Biochemistry* **47,** 5336-5353.
19. Helmkamp, G. K., and Ts'o, P. O. P. (1961) *Journal of the American Chemical Society* **83,** 138-142.
20. Levine, L., Gordon, J. A., and Jencks, W. P. (1963) *Biochemistry* **2,** 168-175.
21. Herskovits, T. T., Singer, S. J., and Geiduschek, E. P. (1961) *Archives of Biochemistry and Biophysics* **94,** 99-114.
22. Geiduschek, E. P., and Herskovits, T. T. (1961) *Archives of Biochemistry and Biophysics* **95,** 114-129.
23. Hamaguchi, K., and Geiduschek, E. P. (1962) *Journal of the American Chemical Society* **84,** 1329-1338.
24. Ts'o, P. O. P., Helmkamp, G. K., and Sander, C. (1962) *PNAS* **48,** 686–698.

UNIVERSITAT ROVIRA I VIRGILI
TEMPERATURE MODULATED GENOSENSOR FOR DETECTION OF CYSTIC FIBROSIS MUTATIONS
Hany Abdel Hady Abdel Rahman Nasef
ISBN:978-84-693-3386-0/DL:T.1002-2010

CHAPTER 6 (Art.5):

Electrochemical Melting Curve Analysis

UNIVERSITAT ROVIRA I VIRGILI
TEMPERATURE MODULATED GENOSENSOR FOR DETECTION OF CYSTIC FIBROSIS MUTATIONS
Hany Abdel Hady Abdel Rahman Nasef
ISBN:978-84-693-3386-0/DL:T.1002-2010

Electrochemical Melting Curve Analysis

Hany Nasef[1], Valerio Beni[1] and Ciara K. O'Sullivan*[1,2]

[1] *Nanobiotechnology & Bioanalysis Group, Departament d'Enginyería Química, Universitat Rovira i Virgili, Avinguda Països Catalans, 26, 43007 Tarragona, Spain*
E-mail: ciara.osullivan@urv.cat; Fax: +34 977 55 96 21; Tel.+ 34 977 55 8740
[2] *Institucio Catalana de Recerca i Estudis Avançats, Passeig Lluis Companys 23, 08010, Barcelona, Spain*

Abstract

Genotyping technologies need to tackle issues of cost-effectiveness, flexibility, and mutiplexability to meet the ever-increasing demands for detection of mutations and single polynucleotide polymorphisms for clinical diagnostics, addressing the medical paradigm of tomorrow. Here we report on a facile method for the rapid detection of mutations and SNPs using electrochemical melting curve analysis. The concept is based on the use of an immobilised probe hybridised to the mutant/SNP-containing region of a ferrocene labelled PCR amplicon. Following hybridisation, the temperature is ramped and the dissociation of the ferrocene labelled DNA from the electrode surface is monitored using differential pulse voltammetry. Using a model system using short probe and target, the approach was demonstrated to clearly discriminate between complementary and mis-match containing targets. The melting temperature of the surface confined DNA duplex was also observed to markedly lower that that obtained in solution, with melting temperatures of 38 and 59 ºC, observed, respectively. The approach can be extended to array based melting curve analysis, allowing the simultaneous detection of multiple mutations and SNPs, as well as for genosensor design.

ISBN:978-84-693-3386-0/DL:T.1002-2010

1. Introduction:

Since the completion of the Human Genome Project there has been immense progress in the identification of disease associated mutations, and this coupled with the ongoing identification of single nucleotide polymorphisms (SNPs) has spawned the development of a plethora of techniques for rapid detection of these mutants and SNPs, such as minisequencing [1], allele-specific PCR [2], specific ligation assays [3], pyrosequencing [4], and endonuclease cleavage [5]. However, these techniques are lengthy involving several steps, and straightforward DNA hybridisation is being increasingly exploited in the field of DNA diagnostics [6]. The potency of hybridisation for DNA diagnostics is due to the marked change in duplex stability that results from even subtle sequence changes, which can be reliably detected by measurement of the duplex stability. Melting-curve analysis is a well-established technique where a probe is hybridised to a single stranded PCR product and an intercalating dye is incorporated into the duplex. As the temperature is ramped, the duplex starts to dissociate releasing the fluorescent dye and the melting temperature can be determined and the specific mutant/SNP can be detected [7]. This concept forms the basis of dynamic allele-specific hybridisation (DASH)[8], where the duplex under interrogation is attached to a solid surface and has been further developed as a microtitre plate-based version [9] and as a membrane-based macroarray format [10].

Although fluorescence detection has dominated the field of melting curve analysis, electrochemistry-based methods are an attractive alternative due to their low-cost, high-sensitivity, simplicity and compatibility with microfabrication techniques. Meunier-Prest et al. [11] studied the melting behaviour of a synthetic model DNA duplex immobilized onto gold electrodes using methylene blue as an electroactive intercalator; where duplex melting resulted in the liberation of methylene blue and a concomitant reduction in signal. Brewood et al. [12] and Marquette et al. [13] developed impedance based approaches for melting temperature determination. However, whilst these reports have accurately determined the melting temperature of surface tethered DNA duplexes, to date, there are only two reports detailing the electrochemical melting curve analysis. Luo et al. [14], reported on an immobilisation free method for the melting curve analysis of a DNA-PNA duplex , using ferrocene labelled PNA. The negatively charged DNA-PNA-FC duplex is repulsed from the negatively charged ITO electrode, but upon

ISBN:978-84-693-3386-0/DL:T.1002-2010

heat-induced dissociation of the duplex, the neutral PNA-Fc diffuses to the electrode, where it is detected. The authors used the technique to distinguish between fully complementary and one mis-match. Finally, Surkus et al [15] used melting curve analysis to explore the effect of ionic strength and number of mismatches on melting temperature, observing that the melting temperature of the surface immobilised DNA duplex was significantly lower than in homogenous solution.

Here, we report a facile method for electrochemical melting curve analysis exploiting a gold electrode anchored DNA-probe and a ferrocene labelled target. As a model target to demonstrate the approach, we used the cystic fibrosis associated Δ508 mutation, which represents a 3 base mutation at the 508 position of the CFTR gene. A gold electrode was functionalised with thiolated probe and was hybridised with a ferrocene labelled target. Following hybridisation, the electrode was placed in a peltier unit and the temperature ramped, resulting in dissociation of the duplex and removal of the ferrocene label from being in close proximity with the electrode surface, resulting in a decrease in signal. The data was used to produce melting curves for both fully complementary and mis-match duplexes and clear differences observed.

2. Experimental

All chemicals and reagents were of analytical grade and used without further purification. All solutions were prepared in ultra pure water (18 MΩ.cm) obtained using a "Simplicity Water Purification System" (Millipore, France). Oligonucleotides were provided by Eurogentec (Spain). *Mutant sequence specific probe: 5`-AACACCAATGATATT-C6-SH)-3`; Wild type sequence specific probe: 5`-ACACCAAAGATGATA-C6-SH-3`; DF508 mutant sequence: 5`-$NH_2$-C6-AATATC ATT GGT GTT-3`*

Electrochemical measurements were carried out using an Autolab model potentiostat/galvanostat 12 controlled with GPES software (Eco Chemie B.V.,). A classical three electrode configuration was used: Ag/AgCl wire reference electrode, Pt wire counter electrode and thin film Au working electrode prepared as previously described [16]. Working electrodes were cleaned electrochemically, cycling at a scan

ISBN:978-84-693-3386-0/DL:T.1002-2010

rate of 100 mVs^{-1} between -0.2 and 1.6 V in 0.5 M sulphuric acid until a peak-to-peak separation below 80 mV was recorded.

Preparation of DNA-ferrocene conjugate The DNA-ferrocene conjugate was prepared as previously reported [17]. Briefly, the amine-terminated DF508 mutant sequence (22 nmol) was dissolved in 0.5M $NaHCO_3/Na_2CO_3$ buffer (pH 9.0) and added to the N-hydroxysuccinimide ester of ferrocene carboxylic acid (1.3 mmol), and the solution was sonicated for 10 minutes, and then left under stirring conditions at room temperature overnight. Finally the solution was diluted to 1ml with 0.2M of triethyl ammonium acetate (TEAA) pH 7.0. The DNA-ferrocene conjugate was purified using a RP-HPLC column (Agilent Zorbax oligo 5uM, 6.2 x 80 mm). The mobile phase composed of two solutions, 0.1M TEAA, pH 7 and acetonitrile using a gradient of 10 to 40 % v/v acetonitrile for 7 minutes with 0.5 mL/min flow rate; the conjugate having a retention time of 7.6 minutes.

Probe Immobilisation Thiolated probe (Mut or Wt) was self-assembled, via spotting of 10µl of a 4µM solution, freshly prepared in 1M KH_2PO_4, onto the electrode surface and left to assemble for 3 hours, followed by thorough washing with ultra pure water and subsequent back-filling with a 0.01M aqueous solution of mercaptohexanol and left to incubate for 30 minutes. The sensor was extensively washed via sequential immersion in 0.1M NaOH, MilliQ water, 0.1M HCl and MilliQ water, leaving an organized mixed SAM of chemisorbed DNA probe and MCH.

Effect of temperature on buffer pH and probe stability An aliquot of the 10mM Tris buffer (pH 7.5) containing 20mM of magnesium chloride was thermostatted, using a water bath, and allowed to stabilise at fixed temperature intervals (between 30 and 60 ºC with step of 5 ºC) before the pH was measured. Additionally, the probe stability was measured over the same temperature interval, using differential pulse voltammetry and 20 µM methylene blue.

Hybridisation with mutant target Hybridisation was carried by spotting 10µL of 1µM Mut-Fc in 10mM Tris buffer (pH 7.4) in the presence of 20mM $MgCl_2$ onto the functionalised electrode surface. Following a 1 hour incubation, the sensor was washed with 10 mM Tris buffer (pH 7.4) containing 20mM $MgCl_2$ and the hybridization levels

ISBN:978-84-693-3386-0/DL:T.1002-2010

were monitored by evaluating the oxidation response of the ferrocene label. The working electrode was transferred to a thermostatted electrochemical cell and the temperature increased at intervals. Differential pulse measurements were recorded after the electrode had been exposed to each temperature interval for 15 minutes. The parameters employed in the DPV experiments were: potential window between 0 and 0.8 V (vs. Ag/AgCl) , step potential 10 mV, modulation amplitude 10 mV, modulation time 0.015 s and interval time 0.1 s.

Results and discussion:

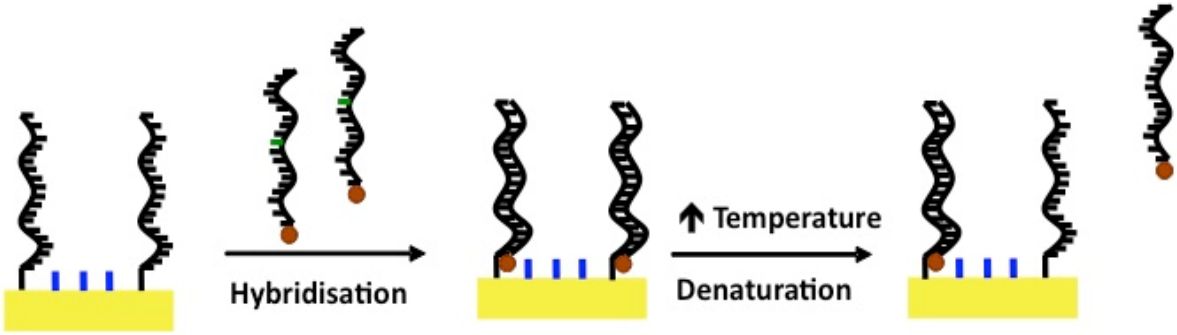

Schematic 1. A Schematic representation of electrochemical melting curve analysis reported

The pH of Tris buffer solution is known to be influenced by the temperature, whilst the melting temperature of DNA is not affected by a change in pH within the range of pH values from 6.5 to 8.0 [18]. In order to ensure that the change in pH under the temperature range used in this work, a study of the variation of the pH of the buffer with the temperature was performed. The pH value of the buffer solution clearly varied with the temperature with a slope of 0.02 pH unit per 1ºC. UV-based melting temperature studies were carried out within this pH range and the change in pH between 6.5 and 8 had no effect on the melting temperature. Additionally, probe layer stability is crucial in melting temperature experiment and there are several reports outlining the thermal stability of alkanethiol and DNA monolayers, reporting desorption from gold surface, ranging from 55°C [19, 20] and 90°C [21], dependent on the surface chemistry. We carried out an evaluation of the thermal stability using a DNA specific electroactive indicator, methylene blue as a means of quantifying the surface immobilised DNA probe and observed the mixed SAM of thiolated DNA and mercaptohexanol to be stable from 30 to 60^{o}C.

ISBN:978-84-693-3386-0/DL:T.1002-2010

Electrochemical melting curve analysis In Figure 1 the electrochemical responses, as a function of the temperature, of two different sensors, modified with Mut-probe and Wt-probe, respectively and hybridized with the ferrocene modified mutant sequence are reported, and the first derivative curves are shown in Figure 2. As can be seen the melting temperature (T_m) for the fully complementary duplex was 38ºC; whilst for mismatched duplex the T_m 30ºC, and the presence of the mutation can be clearly distinguished from the wild type. The T_m of the duplex in homogenous solution was observed to be 59ºC using UV-Vis measurements at λ=260nm. The significantly lower values obtained for the surface immobilised DNA duplex have also been observed using other techniques such as those reported by Majumdar [22], who used microcantilevers and nanomechanical detection of DNA melting, observing lower Tm for surface tethered duplexes, or Surkus [15], who recently reported a difference of more than 30 ºC between surface and solution T_m.

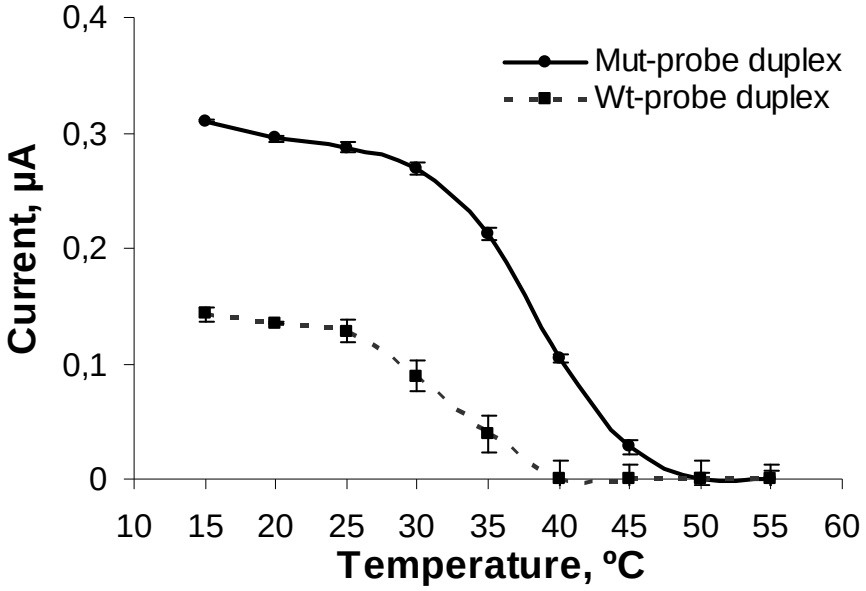

Figure 1. Differential pulse voltammetric (DPV) detection of DF508 Mut-Fc melting curve duplex with immobilized (mutant and wild type complementariness) probes on the gold electrode surface

A marked decrease in the Tm has also been reported by Peterlinz using surface plasmon resonance [21], and both Meunier-Prest [11] and Hartwich, using electrochemical detection [23]. This difference in melting behaviour may be attributed to the effect of the density of the immobilised DNA probes on charge density, due to the ionisable phosphate groups. Furthermore, the negatively charged surface of immobilised probes attracts positive counter-ions from solution, which will result in local ionic strength pH

ISBN:978-84-693-3386-0/DL:T.1002-2010

and dielectric constant on the surface, which is markedly different from that in the bulk electrolyte solution.

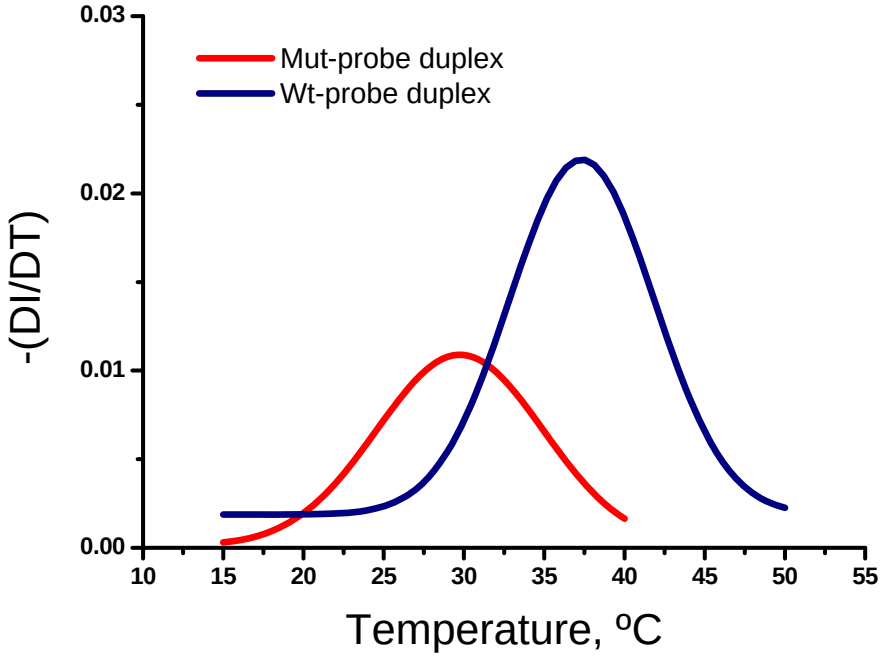

Figure 2. First derivative of the electrochemical melting curves (shown in fig.1) Vs temperature.

The values obtained with those predicted using the approach proposed by Wallace rule [24], where a good approximation of the melting temperature for short DNA oligos of 14-20 base pairs hybridised to membrane bound DNA targets in the presence of 0.9M NaCl can be obtained, using equation 1.

$$T_d = 2\,(A+T) + 4(G+C) \qquad \textbf{(Equation 1)}$$

where:

Td is the temperature at which 50% of the oligonucleotides are in their duplex form. A, G, C, and T are the number of occurrences of each nucleotide. The calculated melting temperature according to equation 1 was 38 ºC in excellent correlation with the values we obtained experimentally.

Using the melting curve analysis, it was also possible to identify optimal experimental conditions for single genosensors designed to detect one specific mutation, or to identify several mutations that could be detected on one platform using similar thermal

ISBN:978-84-693-3386-0/DL:T.1002-2010

conditions. From the melting curve analysis, it is clear that at 40 ºC, there should be no hybridisation whatsoever between the immobilised mutant probe, and the wild type sequence, whereas 50% of the duplexes between the probe and the mutant sequence should still be intact. This is shown in Figure 3, where for the mut-wt no hybridisation has taken place, with no electrochemical signal observed, whereas a good response is obtained for the mut-mut duplex.

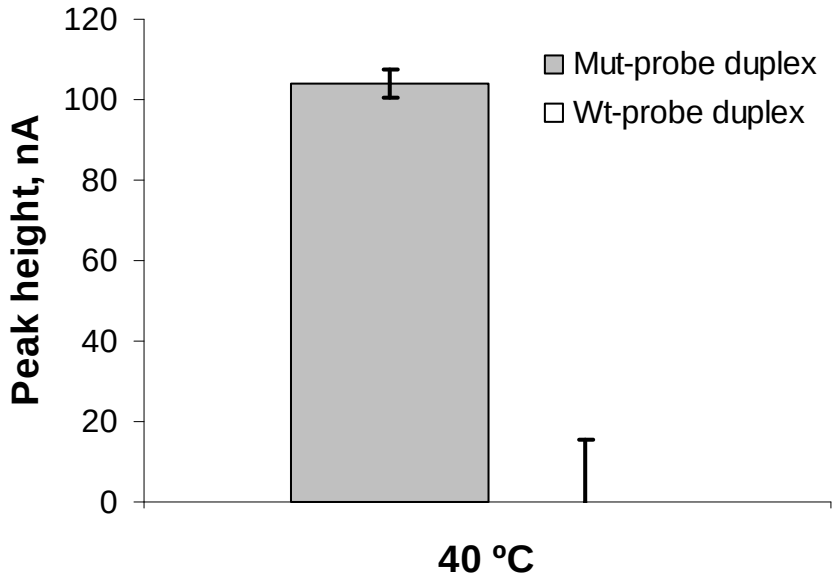

Figure 3. Comparison of the electrochemical response of mut-mut and mut-wt duplexes with applied temperature of 40 ºC

4. Conclusion:

Here we reported on a facile and widely applicable method for electrochemical melting curve analysis. Using a model system based on a cystic fibrosis mutation, the melting curve analysis facilitated a clear discrimination between complementary and non-complementary DNA with an immobilised probe. Previous reports have demonstrated the use of ferrocene as a primer label that can be used in the polymerase chain reaction [25], and a further extension of this work will be the detection of labelled PCR amplicons. The reported approach can be used in array based detection of mutations, where probes against specific target mutants/SNPs would be immobilised on individual electrodes of the array, and the entire array is subject to temperature ramping and the dissociation of the labelled amplicons from the immobilised probes monitored using

ISBN:978-84-693-3386-0/DL:T.1002-2010

multiplex potentiostat. Alternatively, and as reported in this work, the melting curve analysis can be used to optimise conditions for a thermal modulated genosensor targeting one specific mutation, or group of mutations with similar melting behaviour. Further work is focused on the detection of SNPs, as well as array based simultaneous detection of multiple SNPs/mutants using electrochemical melting curve analyses, representing a cost-effective, easy to use approach with far less complicated detection systems than required by i-FRET, or fluorescence analysis.

ISBN:978-84-693-3386-0/DL:T.1002-2010

5. References:

1. Pastinen, T., Kurg, A., Metspalu, A., Peltonen, L., Syvanen, A.C., Genome Res., 7, (1997), 606.
2. Newton, C.R., Graham, A., Heptinstall, L.E., Powell, S.J., Summers, C., Kalsheker, N., Smith, J.C. et al Nucleic Acids Research, 17, (1989), 2503.
3. Landegren, U., Kaiser, R., Sanders, J., Hood, L., Science, 241, (1988), 1077.
4. Ronaghi, M., Uhlen, M., Nyren, P., Science, 281, (1998,) 363.
5. Lyamichev, V., Mast, A.L., Hall, J.G., Prudent, J.R., Kaiser, M.W., Takova, T., Kwiatkowski, R.W. , Nat. Biotechnol, 17, (1999), 292-296
6. Strömqvist Meuzelaar, L.,Hopkins, K., Liebana, E., and Brookes, A.J., J. Mol. Diag., 9, (2007), 30.
7. Ririe KM, Rasmussen RP, Wittwer CT, Anal Biochem., 245, (1997), 154.
8. Howell, W.M., Jobs, M., Gyllensten, U., Brookes, A.J.,.Nat. Biotech, 17, (1999), 87.
9. Prince, JA, Feuk L, Howell WM, Jobs, M, Emahazion T., Blennow, K., Brookes, AJ, Genome Res.,, 11, (2001), 152.
10. Jobs, M., Howell, WM, Strömqvist, L., Mayr, T., Brookes, AJ., Genome Res., 13, (2003), 916.
11. R. Meunier-Prest, S. Raveau, E. Finot, G. Legay, M. Cherkaoui-Malki, N. Latruffe, Nucl. Acids Res., 31 (2003) e150.
12. G.P. Brewood, Y. Rangineni, D.J. Fish, A.S. Bhandiwad, D.R. Evans, R. Solanki, A.S. Benight, Nucleic Acid Research, 26 (2008) e98.
13. C.A. Marquette, I. Lawrence, C. Polychronakos, M.F. Lawrence, Talanta, 56 (2002) 763.
14. L. Xiaoteng, I.M. Hsing, Electroanalysis, 21 (2009) 1557.
15. A.-E. Surkus, G.-U. Flechsig, Electroanalysis, 21 (2009) 1119.
16. O.Y.F. Henry, J.L. Acero Sanchez, D. Latta, C.K. O'Sullivan, Biosens. Bioelectron., 24 (2009) 2064.
17. S. Takenaka, Y. Uto, H. Kondo, T. Ihara, M. Takagi, Analytical Biochemistry, 218 (1994) 436.
18. Durst, RA and Staples, BR, Clin. Chem., 18, (1972) 206.
19. S.O. Kelley, N.M. Jackson, M.G. Hill, J.K. Barton, Angew Chem., 38 (1999) 941.
20. J.J. Storhoff, C.A. Mirkin, Chemical Reviews, 99 (1999) 1849.
21. K.A. Peterlinz, R.M. Georgiadis, T.M. Herne, M.J. Tarlov, Journal of the American Chemical Society, 119, (1997), 3401.
22. Biswal, S.L., Raorane, D., Chaiken, A., Birecki, H., and Majumdar, A., Anal. Chem., 78, (2006) 7104.
23. Liepold, P., Kratzmüller, Persike, N., Bandilla, M., Hinz, M., Wieder, H., Hillebrandt, H., Ferrer, E., Hartwich, G., Anal. Bioanal. Chem, 391, (2008) 1759.
24. R.B. Wallace, J. Shaffer, R.F. Murphy, J. Bonner, T. Hirose, K. Itakura, Nucl. Acids Res., 6, (1979) 3543.
25. Takenaka, S., Bulletin of the Chem. Soc. Japan, 74, (2001) 217.

UNIVERSITAT ROVIRA I VIRGILI
TEMPERATURE MODULATED GENOSENSOR FOR DETECTION OF CYSTIC FIBROSIS MUTATIONS
Hany Abdel Hady Abdel Rahman Nasef
ISBN:978-84-693-3386-0/DL:T.1002-2010

CHAPTER 7 (Art.6):

Labelless Electrochemical Melting Curve Analysis for Rapid Detection of Mutations

UNIVERSITAT ROVIRA I VIRGILI
TEMPERATURE MODULATED GENOSENSOR FOR DETECTION OF CYSTIC FIBROSIS MUTATIONS
Hany Abdel Hady Abdel Rahman Nasef
ISBN:978-84-693-3386-0/DL:T.1002-2010

Labelless Electrochemical Melting Curve Analysis for Rapid Detection of Mutations

Hany Nasef[1], Valerio Beni[1] and Ciara K. O'Sullivan*[1,2]

[1] *Nanobiotechnology & Bioanalysis Group, Department of Chemical Engineering, Universitat Rovira i Virgili, Avinguda Països Catalans, 26, 43007 Tarragona, Spain*

[2] *Institucio Catalana de Recerca i Estudis Avançats, Passeig Lluis Companys 23, 08010, Barcelona, Spain*

Abstract

The completion of the Human Genome Project has resulted in the continuous identification of mutations associated with genetic diseases or disease predispositions and the ability to simultaneously analyse many mutations in a gene in a simple, fast, and inexpensive way is critical. Here we report on a straightforward method for the rapid detection of mutations exploiting labelless electrochemical melting curve analysis, using the detection of the cystic fibrosis associated DF508 mutant as a model. A thiolated probe complementary to the region of Exon 10 of the cystic fibrosis transmembrane regulatory gene where the Δ508 mutation lies was immobilised on a gold electrode and hybridised to a synthetic analogue of a single stranded PCR product for each of the mutant (85 bases) and wild type (83 bases) targets. Conditions were optimised to exploit the guanine-specific interaction of the electroactive indicator, methylene blue. Upon hybridisation of the immobilised probe to the target, the number of guanine bases present increased from 3 to 14, resulting in a significant increase in signal. Ramping the temperature caused dentauration of the surface immobilised duplex, and a concomitant reduction in signal, and using first derivative curves a clear differentiation between the mutant and wild-type target could be observed. The approach can be extended to array based melting curve analysis, allowing the simultaneous detection of multiple mutations and SNPs, and the melting properties observed can also be used to design genosensors for single target detection.

ISBN:978-84-693-3386-0/DL:T.1002-2010

1. Introduction:

The completion of the Human Genome Project has resulted in the continuous identification of mutations associated with genetic diseases or disease predispositions and the ability to simultaneously analyse many mutations in a gene in a simple, fast, and inexpensive way is essential and this requirement has ushered the development of many techniques and technologies for genotyping [1]. DNA duplex stability can be used to identify mutations; for example, single-stranded conformation polymorphism [2], denaturing gradient gel electrophoresis [3] and temperature gradient gel electrophoresis [4], separate PCR products based on the stability of different conformations [5]. Hybridisation stability can also be monitored using fluorescence resonance energy transfer [6], and monitoring of melting curves has been reported as been used as an additional discriminating dimension in sequencing by hybridisation techniques [7]. PCR product melting analysis was first introduced in 1997 [8] and is simple, rapid and inexpensive but dependents strongly on the dyes and instruments used [9]. There have been advances in DNA melting techniques, e.g. improvements in instrumentation and data collection [10]; more precise data analysis and fluorescent DNA binding dyes with improved properties [11], which have led to the development of high-resolution melting curve analysis [12], which has demonstrated several advantages and capabilities for genotyping and/or mutation scanning [13]. It uses the fact that each double-stranded DNA fragment has its own characteristic melting behaviour, which is dependent on GC content, length, and sequence of the product, among other factors [5]. Sequence alterations lead to changes in duplex stability, and thus to changed melting behaviour [14], which can be easily detected using the most-common first derivative method, or by means of the shape of the generated melting curves [11]. Straight forward melting curve analysis has been used for genotyping of sequence changes such as single-nucleotide polymorphisms [15], insertion/deletion polymorphisms [16], deletions of varying lengths [17] and internal tandem duplications [12, 18]. Melting curve analysis has some limitations, such as the effect of the concentration of the fluorescent dye concentration and temperature transition rates on the absolute position and width of melting curves [5], and the addition of intercalators such as ethidium bromide increases the melting temperature and broadens the melting transition [19]. In this article, we report on a labelless approach for electrochemical melting curve analysis. Electrochemistry-based methods are an attractive alternative due to their low-cost, high-sensitivity, simplicity, compatibility

ISBN:978-84-693-3386-0/DL:T.1002-2010

with microfabrication techniques and their miniaturisability. There have been reports of the electrochemical detection of melting temperature have appeared. Brewood et al. [20] and Marquette et al. [21] developed impedance based approaches for the detection of the melting temperature. Luo et al. [22], reported on an immobilisation free method for the melting curve analysis of a DNA-PNA duplex and Surkus et al [23] used melting curve analysis to explore the effect of ionic strength and number of mismatches on melting temperature, observing that the melting temperature of the surface immobilised DNA duplex was significantly lower than in homogenous solution.

Methylene blue (MB), an organic dye belonging to the phenothiazine family, is an example of a redox active non-metal molecule characterised by having a high affinity for nucleic acids. Three different mechanisms of MB-DNA interaction have been recognised: (i) electrostatic interaction with the negatively charged DNA backbone [24], (ii) intercalation within the DNA double helix [25] and (iii) preferential binding to free guanine bases present on single stranded DNA (ss DNA) [26, 27]. Several reports on the use of MB as a reporting element in electrochemical genosensors can be found in the literature [26-30]. Meunier-Prest et al. [31] studied the melting behaviour of a synthetic model DNA duplex immobilized onto gold electrodes using methylene blue as an electroactive intercalator; where duplex melting resulted in the liberation of methylene blue and a concomitant reduction in signal.

Here, we report on a facile method for labelless electrochemical melting curve analysis using methylene blue as an electroactive indicator of hybridisation and denaturation. As a model target to demonstrate the approach, we used the cystic fibrosis associated Δ508 mutation, which represents a 3 base mutation at the 508 position of the cystic fibrosis transmembrane regulator gene, resulting in deletion of a phenylalanine. A gold electrode was functionalised with thiolated probe complementary to either the wild type, or the mutant form, and was hybridised with single stranded synthetic analogues of PCR products being 83 and 85 bases in length for mutant and wild type target, respectively. The stability of the immobilised probes at elevated temperatures was evaluated and the melting curves obtained showed a clear differentiation between wild type and mutant targets.

ISBN:978-84-693-3386-0/DL:T.1002-2010

2. Experimental

2.1. Materials and methods

All chemicals and reagents were of analytical grade and used without further purification. All solutions were prepared in ultra pure water (18 MΩ.cm) obtained using a "Simplicity Water Purification System" (Millipore, France). The oligonucleotides used in the study were obtained from Biomers (Germany) and are detailed in Table 1.

Mutant target amplicon (83 mer)	**5' GCC GCG AAT TCA CTA GTG TGG CAC CAT TAA AGA AAA TAT CAT TGG TGT TTC CTA TGA TGA ATA TAA TCG AAT TCC CGC GGC C 3'**
Wild type target amplicon (85 mer)	**5' GCC GCG AAT TCA CTA GTG TGG CAC CAT TAA AGA AAA TAT CAT CTT TGG TGT TTC CTA TGA TGA ATA TAA TCG AAT TCC CGC GGC C 3'**
Mutant-MB (21 mer)	**5' MB-C6-GAA AAT ATC ATT GGT GTT TCC 3'**
Mutant probe (21 mer)	**5' GGA AAC ACC AAT GAT ATT TTC-C6-SH 3'**
Wt type probe (21 mer)	**5' AAC ACC AAA GAT GAT ATT TTC-C6-SH 3'**

Table 1. Details of oligonucleotides used in this study. The long sequences represent synthetic analogues of single stranded PCR amplicons

Electrochemical measurements were carried out using an Autolab model PGSTAT 12 potentiostat/galvanostat controlled with the General Purpose Electrochemical System (GPES) software (Eco Chemie B.V., The Netherlands). A classical three electrode configuration was used: a Ag/AgCl wire reference electrode, a Pt wire counter electrode and a thin film Au working electrode prepared as previously described. Working electrodes were cleaned electrochemically by cycling them (scan rate 100 mVs^{-1}) between -0.2 and 1.6 V in 0.5 M sulphuric acid until a peak to peak separation below 80 mV was recorded.

Thiolated probe (Mut or Wt) was self assembled, via spotting of 10 µl of a 4 µM solution, freshly prepared in 1 M KH_2PO_4, onto the electrode surface and left to assemble for 3 hours, followed by thorough washing with ultra pure water and subsequent back-filled by spotting of 10 µl of a 0.01M aqueous solution of mercaptohexanol onto the electrode surface, which was hen left to incubate for 30 minutes. The sensor was then again extensively washed via sequential immersion in

ISBN:978-84-693-3386-0/DL:T.1002-2010

0.1 M NaOH, MilliQ water, 0.1 M HCl and MilliQ water, leaving an organized mixed SAM of chemisorbed DNA probe and MCH.

Effect of temperature on buffer pH and probe stability

An aliquot of the 10 mM Tris buffer (pH 7.5) containing 20 mM of magnesium chloride was thermostatted, using a water bath, and allowed to stabilise at fixed temperature intervals (between 30 and 60 ºC with step of 5 ºC) before the pH was measured. Additionally, the probe stability was measured over the same temperature interval, using differential pulse voltammetry and methylene blue.

Hybridisation with target sequences and electrochemical melting curve analysis

Target hybridisation was carried out via 1 hour incubation of a 1 μM solution of the desired target (Mut or WT synthetic PCR analogues) in 20 mM Trizma buffer (pH 7.4) in the presence of 0.5 M NaCl. Following hybridisation the sensor was washed with 20 mM Trizma buffer (pH 7.4) containing 0.5 M NaCl. Estimation of the hybridisation level was performed by monitoring the electrochemical reduction of the MB via immersion of the sensor in an aliquot of a 20mM Trizma (pH 7.4), 0.5 M NaCl buffer containing 20 μM methylene blue and left to interact for 5 minutes. A differential pulse voltammogram (DPV) was recorded; as a result a clear reduction wave was visible, in at ca. -100 mV (vs the Ag/AgCl). Electrode regeneration was performed by immersion in a 200 mM NaOH solution for two minutes.

It is known that the electrochemical behaviour of methylene blue is influenced by temperature [31]. In order to overcome this, all electrochemical measurements were performed at a fixed temperature of 21 ºC. The heating of the sensors were performed using a Thermomixer compact (Eppendorf Iberica, Spain). This was performed by immersing the sensor in an Eppendorf containing 500 μl of 20 mM Trizma buffer (pH 7.4) and 0.5 M NaCl buffer previously stabilised to the desired temperature. The incubation time in the desired temperature was 10 minutes, and then the sensor was washed within the same temperature by immersing in a thermostatted eppendorf containing the same buffer solution. Finally, the electrode was transferred to the measurement solution and let to cool to the room temperature before starting the measurement.

ISBN:978-84-693-3386-0/DL:T.1002-2010

Optimisation of salt concentration for maximal discrimination

In order to optimize the salt concentration for maximal discrimination between mutant and wild type targets, a range of salt concentrations were studied by varying the salt concentration in the hybridization, wash and measurement buffers, between 0.05M and 0.5M.

Results and discussion:

Previously, we have developed techniques for measuring the melting temperature of surface immobilised duplexes using a gold film immobilised probe and a fluorophore labelled complementary. The gold film quenches the fluorescence upon hybridisation and when heated the duplex dissociates, with the fluorophore moving away from the gold film, thus giving an increase in fluorescent signal [32]. The melting temperatures obtained indicated a significant difference in melting temperature as compared to solution based studies, with the surface immobilised duplex being markedly less stable. This was further demonstrated in an extension of this work where the fluorescent label was replaced by either ferrocene or methylene blue and electrochemical melting curve analysis was carried out to differentiate between the cystic fibrosis Δ508 mutant and wild type [33]. Whilst both these approaches have extensive application for melting curve analysis of surface tethered DNA duplexes, they require labelling (e.g. labelling of forward/reverse primer) and have not yet been demonstrated with full length amplicons. In the work we report here, we carry out labelless electrochemical melting curve analysis using an immobilised probe that is complementary to the DF508 region of Exon 10 of the cystic fibrosis transmembrane regulator. The probe is hybridised to a synthetic analogue of single stranded PCR product of the complementary mutant target (85 bases) or non-complementary wild type target (83 bases), and the electrochemical indicator, methylene blue is used to measure the levels of hybridisation. Three different mechanisms of MB-DNA interaction have been recognised: (i) electrostatic interaction with the negatively charged DNA backbone, (ii) intercalation within the DNA double helix and (iii) preferential binding to free guanine bases present on single stranded DNA (ss DNA).

UNIVERSITAT ROVIRA I VIRGILI
TEMPERATURE MODULATED GENOSENSOR FOR DETECTION OF CYSTIC FIBROSIS MUTATIONS
Hany Abdel Hady Abdel Rahman Nasef
ISBN:978-84-693-3386-0/DL:T.1002-2010

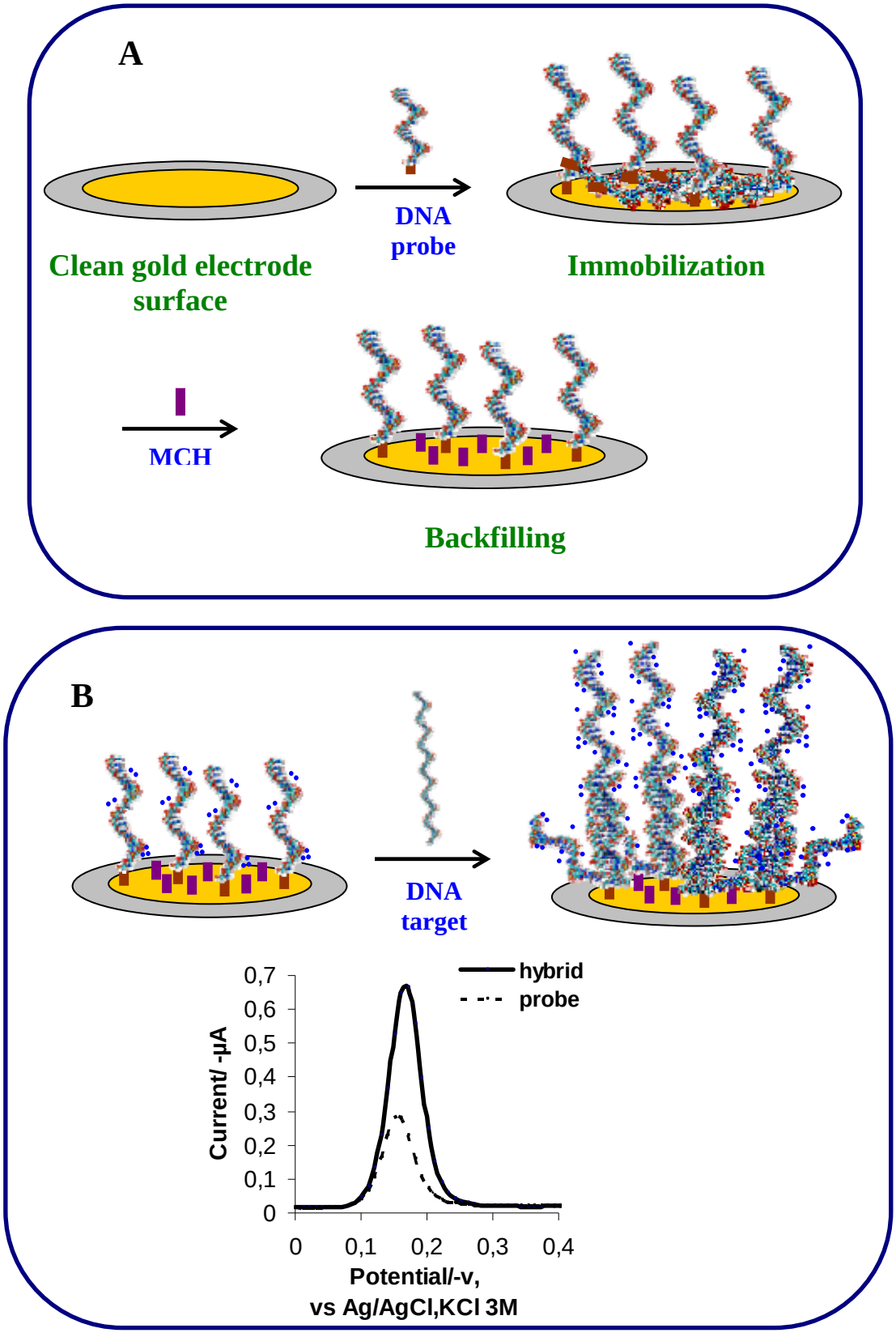

Figure 1. Schematic representation of sensor preparation (A) and duplex determination via methylene blue represented as small blue spheres (B). Inset: Differential pulse voltammograms of Mutant amplicon captured on the electrode surface. Hybridisation performed from a solution of 1µM target amplicons. Measurement solution: 20 µM MB in 0.5M NaCl and 20 mM Trizma, pH 7.4.

ISBN:978-84-693-3386-0/DL:T.1002-2010

In previous work, we elucidated optimal conditions to minimise methylene blue-DNA electrostatic interactions so that guanine-specific interactions would predominate [34], The hybridisation with the targets add free guanine bases to the electrode surface duplex through the lateral sides of the amplicon which are not participating in hybridisation, increasing the number of guanines from 3 present in the immobilised probe to 14 present in the duplex formed upon hybridisation, resulting in significant increase in signal. Typical DPV results obtained upon hybridisation are presented in the inset of Figure 1B, where a clear reduction wave is visible at ca. -100 mV (vs the Ag/AgCl).

Prior to carrying out the temperature ramping experiments, the probe stability over the temperature range to be studied was determined. There are several reports outlining the thermal stability of alkanethiol and DNA monolayers, reporting desorption from gold surface, ranging from 55 °C [35, 36] and 90 °C [37], dependent on the surface chemistry. We carried out an evaluation of the thermal stability using a DNA specific electroactive indicator, methylene blue as a means of quantifying the surface immobilised DNA probe and observed the mixed SAM of thiolated DNA and mercaptohexanol to be stable from 30 to 60^{o}C, as can be seen in Figure 2.

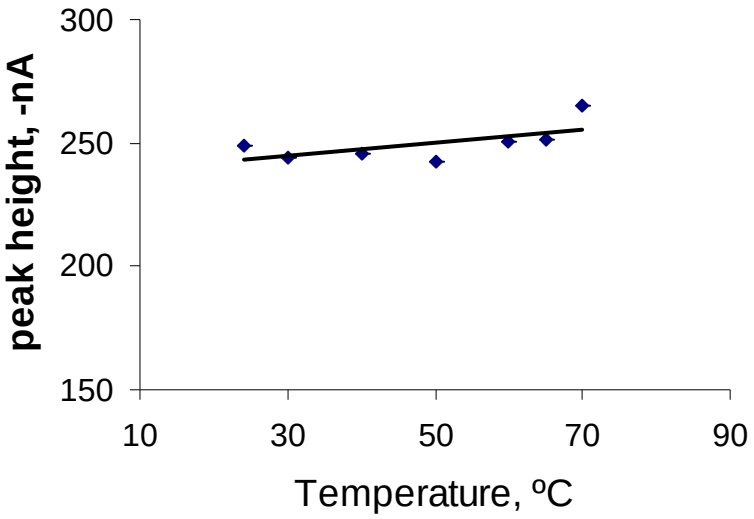

Figure 2. The temperature influence on the 21 bp mutant complementary probe immobilized on the gold electrode surface. The immobilized electrode was heated in buffer solution (0.5M NaCl and 20 mM Trizma, pH 7.4) and the electrochemical detection via methylene blue was achieved in constant temperature, room temperature. Measurement solution: 20 μM MB in 0.5M NaCl and 20 mM Trizma, pH 7.4.

ISBN:978-84-693-3386-0/DL:T.1002-2010

Additionally, the pH of Tris buffer solution is known to be influenced by the temperature, whilst the melting temperature of the DNA is not affected by a change in pH within the range of pH values from 6.5 to 8.0 [38]. In order to ensure that the change in pH under the temperature range used in this work, a study of the variation of the pH of the buffer with the temperature was performed. The pH value of the buffer solution clearly varied with the temperature with a slope of 0.02 pH unit per 1 ºC. UV-based melting temperature studies were carried out within this pH range and the change in pH between 6.5 and 8 had no effect on the melting temperature.

Effect of ionic strength

The ionic strength is critical in the stabilisation of DNA duplexes. In order to optimize the ionic strength employed for the labelless electrochemical melting analysis, as well as the ionic strength for a maximal differentiation between wild type and mutant targets, a study of the effect of the concentration of NaCl in the hybridisation buffer and washing buffer was carried out (the concentration in the measurement buffer was maintained at 0.5M in order to minimise electrostatic interactions).

The results are presented as percentage increase in signal as compared to base signal as detailed below and the results can be clearly seen in Figure 2.

$$\textbf{Signal variation (\%)} = 100 \times [(i_{amp} - i_{reg}) / i_{reg}] \qquad (1)$$

Where:

i_{amp} Peak current recorded with hybridised target

i_{reg} Peak currents after regeneration i.e. denaturation of formed duplex

In Table 2 the signal variations recorded for the hybridisation of the fully complementary target (Mut) and those recorded for the three mismatches target (WT), as a function of three different salt concentrations, is reported. The increase in NaCl concentration in the hybridisation buffer resulted in an increase of the efficiency of the hybridisation process; for example by increasing the NaCl concentration from 0.05 M to 0.5 M an increase in analytical response, from about 9 to 36%, was recorded. Moreover the increase in the Na^+ concentration in the hybridisation buffer allowed a better

ISBN:978-84-693-3386-0/DL:T.1002-2010

discrimination between the Mut and WT synthetic targets. From the above studies, it was decided to carry out the melting curve analysis in the presence of 0.5 M NaCl.

[NaCl], mM	Mut amplicon , signal variation, %	WT amplicon , signal variation, %	signal variation difference , %
50	30,5 (± 0.314)	21,584 (± 2.455)	8,916
200	78,74 (± 0.554	62,01(± 5.695)	16,73
500	121,01(± 4.93)	84,59 (± 2.514)	36,42

Table 2. Effect of ionic strength on discrimination factor between mutant and wild type targets.

Labelless electrochemical melting curve analysis

The effect of temperature on the fully matched DF508 mutant amplicon and three mismatched wild type amplicon duplexes with the immobilised mutant probe is shown in Figure 3a. The melting behaviour of the two different electrode surface duplexes shows a clear discrimination between the DF508 mutant amplicon and the corresponding wild type amplicon. To pinpoint the exact melting temperature (i.e. the inflection point of an electrochemical melting curve), the first derivative of the electrochemical melting curve vs temperature is plotted in Figure 3b for fully and 3 mismatches complementary cases. The melting temperature for the fully complementary duplex is 57 ºC and for the three-mismatched case is 35 ºC.

Using the melting curve analysis, it was also possible to identify optimal experimental conditions for single genosensors designed to detect one specific mutation, or to identify several mutations that could be detected on one platform using similar thermal conditions. An enhancement in discrimination between DF508 mutant and wild type amplicons was achieved via increasing temperature. The discrimination ratio is based on the increasing percentage ratios of obtained signal, comparing mutant and wild type amplicons. By increasing the temperature from 27ºC to 55ºC, the discrimination factor increased from 1.1 to 4.3, demonstrating the usefulness of temperature modulation for genosensors.

ISBN:978-84-693-3386-0/DL:T.1002-2010

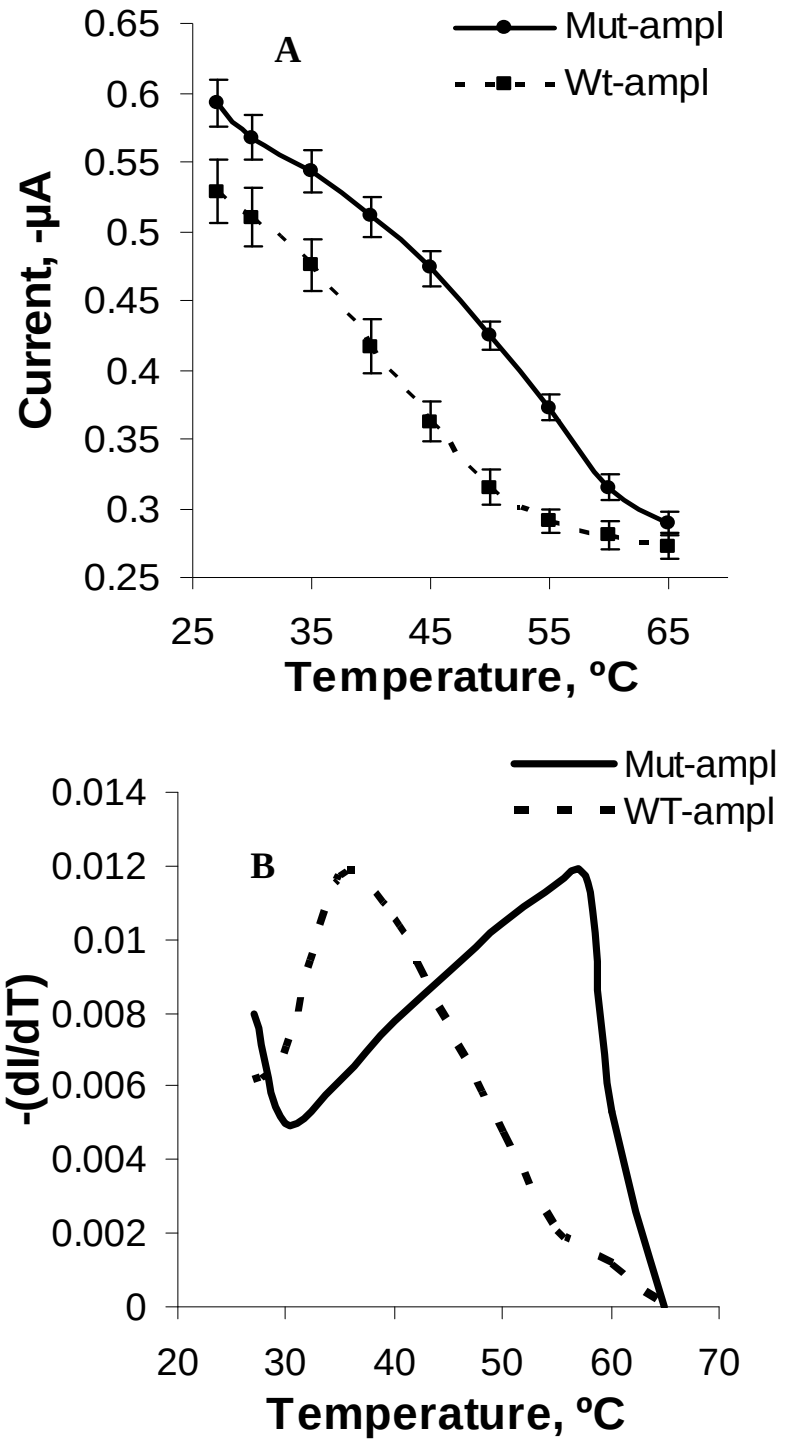

Figure 3. Melting curves of the mutant and wild type amplicon duplexes with mutant complementary probe immobilized on the electrode surface. The methylene blue voltammograms represented at each temperature is a result of the measurement of the pre-heated electrode surface separately in a buffer solution (0.5M NaCl and 20 mM Trizma, pH 7.4) and then cooled to the room temperature. Measurement solution: 20 µM MB in 0.5M NaCl and 20 mM Trizma, pH 7.4 (A). First derivative of the electrochemical melting curves (shown in Fig. 4A) Vs temperature (B).

ISBN:978-84-693-3386-0/DL:T.1002-2010

Conclusion:

Here we reported on a facile and widely applicable method for labelless electrochemical melting curve analysis. Using a model system based on the cystic fibrosis mutation, the melting curve analysis of synthetic analogues of single stranded PCR amplicons, facilitated a clear discrimination between complementary and non-complementary DNA with an immobilised probe. The approach does not require labelling and the melting curve analysis can be carried out at low concentrations of target DNA. The reported approach can be used in array based detection of mutations, where probes against specific target mutants/SNPs would be immobilised on individual electrodes of the array, and the entire array is subject to temperature ramping and the dissociation of the amplicons from the immobilised probes monitored using a multiplex potentiostat. Alternatively, and as also reported in this work, the melting curve analysis can be used to optimise conditions for a thermal modulated genosensor targeting one specific mutation, or group of mutations with similar melting behaviour. Further work is focused on moving to detection of SNPs, as well as array based simultaneous detection of multiple SNPs/mutants using electrochemical melting curve analyses, representing a cost-effective, easy to use approach with far less complicated detection systems than required by i-FRET, or fluorescence analysis.

ISBN:978-84-693-3386-0/DL:T.1002-2010

References

(1) Drobyshev, A.; Mologina, N.; Shik, V.; Pobedimskaya, D.; Yershov, G.; Mirzabekov, A. *Gene* 1997, *188*, 45-52.
(2) Orita, M.; Iwahana, H.; Kanazawa, H.; Hayashi, K.; Sekiya, T. *Proceedings of the National Academy of Sciences of the United States of America* 1989, *86*, 2766-2770.
(3) Fischer, S. G.; Lerman, L. S. *Proceedings of the National Academy of Sciences of the United States of America* 1983, *80*, 1579-1583.
(4) Ke, S. H.; Wartell, R. M. *Nucleic Acids Res.* 1993, *21*, 5137–5143.
(5) Ririe, K. M.; Rasmussen, R. P.; Wittwer, C. T. *Analytical Biochemistry* 1997, *245*, 154-160.
(6) Hiyoshi, M.; Hosoi, S. *Analytical Biochemistry* 1994, *221*, 306-311.
(7) Stimpson, D. I.; Hoijer, J. V.; Hsieh, W. T.; Jou, C.; Gordon, J.; Theriault, T.; Gamble, R.; Baldeschwieler, J. D. *Proceedings of the National Academy of Sciences of the United States of America* 1995, *92*, 6379-6383.
(8) Wittwer, C. T.; Herrmann, M. G.; Moss, A. A.; Rasmussen, R. P.; . *Biotechniques* 1997, *22*, 130-131, 134-138.
(9) Carl, T. W. *Human Mutation* 2009, *30*, 857-859.
(10) Herrmann, M. G.; Durtschi, J. D.; Bromley, L. K.; Wittwer, C. T.; Voelkerding, K. V. *Clin Chem* 2006, *52*, 494-503.
(11) Wittwer, C. T.; Reed, G. H.; Gundry, C. N.; Vandersteen, J. G.; Pryor, R. J. *Clin Chem* 2003, *49*, 853-860.
(12) Radvansky, J.; Resko, P.; Surovy, M.; Minarik, G.; Ficek, A.; Kadasi, L. *Analytical Biochemistry* 2010, *398*, 126-128.
(13) Vorkas, P. A.; Christopoulos, K.; Kroupis, C.; Lianidou, E. S. *Clinical Biochemistry*, *43*, 178-185.
(14) Montgomery, J.; Wittwer, C. T.; Palais, R.; Zhou, L. *Nat. Protocols* 2007, *2*, 59-66.
(15) Liew, M.; Pryor, R.; Palais, R.; Meadows, C.; Erali, M.; Lyon, E.; Wittwer, C. *Clin Chem* 2004, *50*, 1156-1164.
(16) Lin, M.-H.; Tseng, C.-H.; Tseng, C.-C.; Huang, C.-H.; Chong, C.-K.; Tseng, C.-P. *Clinical Biochemistry* 2001, *34*, 661-666.
(17) Liu, J.; Yan, M.; Wang, Z.; Wang, L.; Zhou, Y.; Xiao, B. *Translational Research* 2006, *148*, 6-12.
(18) Vaughn, C. P.; Elenitoba-Johnson, K. S. J. *Journal of Molecular Diagnostics* 2004, *6*, 211-216.
(19) Maeda, Y.; Nunomura, K.; Ohtsubo, E. *Journal of Molecular Biology* 1990, *215*, 321-329.
(20) Brewood, G. P.; Rangineni, Y.; Fish, D. J.; Bhandiwad, A. S.; Evans, D. R.; Solanki, R.; Benight, A. S. *Nucleic Acid Research* 2008, *26*, e98.
(21) Marquette, C. A.; Lawrence, I.; Polychronakos, C.; Lawrence, M. F. *Talanta* 2002, *56*, 763-768.
(22) Xiaoteng, L.; Hsing, I. M. *Electroanalysis* 2009, *21*, 1557-1561.
(23) Surkus, A.-E.; Flechsig, G.-U. *Electroanalysis* 2009, *21*, 1119-1123.
(24) Zhao, G. C.; Zhu, J. J.; Chen, H. Y. *Spectrochimica Acta Part A: Molecular and Biomolecular Spectroscopy* 1999, *55 (5)*, 1109–1117.
(25) Nafisi, S.; Saboury, A. A.; Keramat, N.; Neault, J. F.; Tajmir-Riahi, H. A. *Journal of Molecular Structure* 2007, *827 (1–3)*, 35–43.

(26) Erdem, A.; Kerman, K.; Meric, B.; Akarca, U. S.; Ozsoz, M. *Analytica Chimica Acta* 2000, *422 (2)*, 139–149.
(27) Yang, W. R.; Ozsoz, M.; Hibbert, D. B.; Gooding, J. J. *Electroanalysis* 2002, *14(18)*, 1299–1302.
(28) Boon, E. M.; Ceres, D. M.; Drummond, T. G.; Hill, M. G.; Barton, J. K. *Nature Biotechnology* 2000, *18*, 1096-1100
(29) Kelley, S. O.; Barton, J. K.; Jackson, N. M.; Hill, M. G. *Bioconjugate Chemistry* 1997, *8*, 31-37.
(30) Sismani, C.; Kousoulidou, L.; Patsalis, P. C. In *Molecular Biomethods Handbook*; Walker, J. M., Rapley, R., Eds.; Humana Press: Totowa, NJ,, 2000, pp 179-193.
(31) Meunier-Prest, R.; Raveau, S.; Finot, E.; Legay, G.; Cherkaoui-Malki, M.; Latruffe, N. *Nucl. Acids Res.* 2003, *31*, e150-.
(32) Nasef, H.; Ozlap, V. C.; Beni, V.; O'Sullivan, C. K. *Analytical Biochemistry, , submitted*.
(33) Nasef, H.; Beni, V.; O'Sullivan, C. K. *Analytical letters*, *Submitted.*
(34) Nasef, H.; Beni, V.; O'Sullivan, C. K. *Analytical and Bioanalytical Chemistry* 2009, *DOI 10.1007/s00216-009-3369-5*
(35) Storhoff, J. J.; Mirkin, C. A. *Chemical Reviews* 1999, *99*, 1849-1862.
(36) Peterlinz, K. A.; Georgiadis, R. M.; Herne, T. M.; Tarlov, M. J. *Journal of the American Chemical Society* 1997, *119*, 3401-3402.
(37) Kelley, S. O.; Jackson, N. M.; Hill, M. G.; Barton, J. K. *Angew Chem.* 1999, *38* 941-945.
(38) Owczarzy, R.; Moreira, B. G.; You, Y.; Behlke, M. A.; Walder, J. A. *Biochemistry* 2008, *47*, 5336-5353.

UNIVERSITAT ROVIRA I VIRGILI
TEMPERATURE MODULATED GENOSENSOR FOR DETECTION OF CYSTIC FIBROSIS MUTATIONS
Hany Abdel Hady Abdel Rahman Nasef
ISBN:978-84-693-3386-0/DL:T.1002-2010

CHAPTER 8:

Conclusions and future work

ISBN:978-84-693-3386-0/DL:T.1002-2010

8. Conclusions and future work

8.1. Conclusions

This PhD had a vision to evaluate different electrochemical based genosensors for the detection of cystic fibrosis mutations.

Using electrochemical impedance spectroscopy, the assessment of the possibility of discriminating between “wild type” and “mutant” sequences was performed using short models and synthetic PCR analogues. It was clearly illustrated that despite the fact that the 15 bases long probe was able to provide good selectivity for the short model, a longer probe was required for the longer oligonucleotides chains representing PCR product analogues. Additionally, the increase in probe length resulted in higher stability of the target-probe duplex reducing the selectivity of the assay. A discrimination factor of ca. 1.5 was obtained.

An alternative approach was investigated with the objective of achieving a better discrimination factor exploiting a DNA specific electroactive indicator. To this end, a detection platform exploiting the base specific electroactive marker (methylene blue), for the unambiguous detection of the DF508 mutation of CF was explored. The assessment of the possibility of discriminating between “wild type” and “mutant” sequences was performed using two synthetic single stranded PCR analogues. Electrochemical and fluorescence studies facilitated further insight into the MB/DNA interaction mechanisms that are involved in the electrochemical detection, demonstrating that electrostatic interaction and weak bases interaction play a more prominent role at concentrations of NaCl lower than 0.2 M, whilst guanine specific contribution was observed to become predominant for NaCl concentrations higher than 0.2 M. The electrochemical detection of the specific sequences was quantitative for target concentrations between 10 and 50 nM (R^2 = 0.991) with a limit of detection of 2.64 nM, and a discrimination factor of ca. 1.5 was obtained.

As no improvement in discrimination was obtained using the specific DNA electroactive indicator methylene blue, electrochemical molecular beacon were investigated as another alternative for the differentiation between cystic fibrosis DF508

ISBN:978-84-693-3386-0/DL:T.1002-2010

mutant and the corresponding wild type. The immobilised beacon probe was complementary in its loop region for DF508 mutant target with 18 base length. The effect of different buffer solutions was examined and PBS-T was selected to be optimum. Both backfilling and co-immobilisation procedures for the immobilization of the beacon probe were investigated, and the latter was found to be more stable and reproducible. A melting temperature value of 31.5 ºC was obtained for the immobilised beacon probe, assuring its stability at room temperature in which the discrimination experiments were carried out. A hybridisation time of 20 minutes was sufficient to reach plateau behaviour and 45 minutes was taken as an optimum time to assure complete hybridisation between targets and the immobilised beacon probe on the electrode surface. The discrimination between cystic fibrosis DF508 mutant and the corresponding wild type complementary was achieved. The signal loss percentage was taking as a reference value in which a discrimination factor of ca. 2.5 was obtained. The electrochemical molecular beacon was also applied for the discrimination between one base mismatch mutant and wild type, namely, V520F. The results obtained were reasonable if compared with three base mismatched DF508 case.

In order to improve the discrimination factor between mutant and wild type, an application of stringency conditions were tested. An attempt to improve sensor selectivity exploiting the use of formamide in the hybridisation buffer was investigated but was not suitable for the reported detection mechanism as the presence of formamide affected the probe stability.

As the use of formamide was not suitable, the use f temperature modulation was explored. A facile means of accurately determining the Tm of surface anchored duplexes exploiting the fluorescence quenching effect of gold was illustrated, which can be applied to planar gold surfaces, or gold spherical structures, such as nanoparticles. Using the method of backfilling with mercaptohexanol, resulting in a mixed self-assembled monolayer of DNA probes and mercaptohexanol, which gave rise to melting temperatures 5ºC and 11ºC lower than their solution based counterparts. The approach was applied to an elucidation of optimal conditions for detection of the cystic fibrosis associated DF508 mutation, a 3bp deletion. Melting temperatures for a surface immobilised probe complementary to the mutant and its hybrids with complementary mutant and non-complementary wild type under a range of conditions were elucidated,

ISBN:978-84-693-3386-0/DL:T.1002-2010

and based on these conditions for complete differentiation between mutant and wild type established.

A new approach for an electrochemical based melting temperature methodology for cystic fibrosis DF508 mutant discrimination was also exploited, where the 15 bp mutant target was labelled with a ferrocene redox label achieved via a conjugation preparation method. The labelled target was hybridised with its fully complementary mutant probe as well as with a wild tope probe and a melting curve analysis was carried out for both indicating the optimum discrimination temperature. At 40 ºC there could be fully discrimination between mutant and wild type, where the latter is nearly completely de-hybridised from electrode surface.

In electrochemical impedance spectroscopy, the introduction of a high temperature wash was demonstrated to be an effective route to a discrimination factor enhancement between PCR analogous amplicon targets. On the route to implement thermally modulated approach in EIS measurements the influence of the temperature on the selectivity of the probes was evaluated using SPR showing that 40 ºC allowed the best discrimination. Moreover the stability of the sensor surface chemistry with temperature was investigated. The implementation of the previous results in the EIS measurements, in the form of high temperature post-hybridisation wash clearly resulted in a considerable improvement of the selectivity. Finally in this work the use of a multiple-parameters detection platform was demonstrated to achieve a clear and definitive discrimination between the different possible forms of the targeted genomic region.

Based on the reported methylene blue work, an approach to discriminate the cystic fibrosis DF508 mutation from the Cystic fibrosis wild type sequence based on melting curve analysis employing methylene blue as reporter was investigated. The assessment of the possibility of discriminating between “wild type” and “mutant” sequences was performed using two synthetic single stranded PCR analogues. In order to avoid the methylene blue signal change under temperature effect, all the differential pulse voltammetric measurements were taken at a fixed (room) temperature . The immobilised mutant complementary probe on the gold electrode surface was demonstrated to be stable up to 70 ºC. The ionic strength was also optimized and 0.5M NaCl was found to be the optimum salt concentration. As previously mentioned, the

ISBN:978-84-693-3386-0/DL:T.1002-2010

change in pH of trizma buffer with temperature was also demonstrated not affect the hybridisation efficiency. Using the melting curve analysis, the discrimination factor between mutant and wild type amplicons was improved via rising the temperature to be ca.4.26 at 55ºC which could be the optimum temperature in which the 3 mismatched duplex-MB signal is very near to the regeneration current level.

8.2. Future work

Based on the data and results illustrated in the PhD thesis, our future work is aiming to have a genosensors that can distinguish between more than one mutation of the most common Cystic fibrosis mutations. Melting curve analysis could be utilised in the multiplex detection of several mutations.